sommerfeltia

32

H.Y. Liu, T. Økland, R. Halvorsen, J.X. Gao, Q.R. Liu, O. Eilertsen & H. Bratli

Gradient analyses of forests ground vegetation and its relationships to environmental variables in five subtropical forest areas, S and SW China

2008

ISBN 82-7420-046-2

ISSN 0800-6865

Liu, H.Y., Økland, T., Halvorsen, R., Gao, J.X., Liu, Q.R., Eilertsen, O. & Bratli, H. 2008. Gradients analyses of forests ground vegetation and its relationships to environmental variables in five subtropical forest areas, S and SW China. – Sommerfeltia 32: 1 – 196. Oslo. ISBN 82-7420-046-2. ISSN 0800-6865.

Monitoring of ground vegetation and environmental variables in subtropical forests in China was initiated in 1999 as part of the "Integrated Monitoring Programme of Acidification of Chinese Terrestrial Systems". The study areas were selected to span regional gradients, in deposition of airborne pollutants and climatic conditions. All five study areas are located in the southern and south-western parts of China and consist of subtropical forests. In each study area 50 1-m^2 plots were randomly chosen within each of ten 10×10 m macro plots, each in turn positioned in the centre of 30×30 m extended macro plot. All 250 1-m^2 plots were subjected to vegetation analysis, using frequency in subplots as measure of species abundance. A total of 33 environmental variables were recorded for 1-m^2 plots as well as 10×10 m macro plots. A major objective of this study is to identify the environmental variables that are most strongly related to the species composition of ground vegetation in S and SW Chinese subtropical forests, as a basis for future monitoring.

Comparison among DCA, LNMDS and GNMDS ordination methods, an additional objective of the study, was achieved by using a set of different techniques: calculation of pair-wise correlation coefficients between corresponding ordination axes, Procrustes comparison, assessment of outlier influence, and split-plot GLM analysis between environmental variables and ordination axes. LNMDS and GNMDS consistently produce very similar ordinations. GNMDS ordinations are generally more similar to DCA than LNMDS to DCA. In most cases DCA, LNMDS and GNMDS extract the same main ground vegetation compositional gradients and the choice of LNMDS or GNMDS is therefore hardly decisive for the results. GNMDS was chosen for interpretation and presentation of vegetation-environment relationships. The dimensionality of GNMDS (number of reliable axes) was decided by demanding high correspondence of all axes with DCA and LNMDS axes. Three dimensions were needed to describe the variation in vegetation in two of the areas (TSP and LXH), two dimensions in the other three areas (LCG, LGS and CJT).

Environmental interpretation of ordinations (identification of ecoclines; gradients in species composition and the environment) was made by split-plot GLM analysis and non-parametric correlation analysis. Plexus diagrams and PCA ordination were used to visualize correlations between environmental variables. Several graphical means were used to aid interpretation.

Complex gradients in litter-layer depth, topography, soil pH/soil nutrient, and tree density/crown cover were found to be most strongly related to vegetation gradients. However, the five study areas differed somewhat with respect to which of the environmental variables that were most strongly related to the vegetation gradients (ordination axes). Litter-layer depth was related to vegetation gradients in four areas (TSP, LCG, CJT and LXH); topography in four study areas (TSP, LGS, CJT and LXH); soil pH in three areas (LCG, LGS and CJT); soil nutrients in one area (LGS); and tree density/crown cover in one area (LCG).

The ecological processes involved in relationships between vegetation and main complex-gradients in litter-layer depth, topography, soil pH/soil nutrient, and tree density/crown cover, in subtropical forests, are discussed. We find that gradient relationships of subtropical forests are complex, and that heavy pollution may increase this complexity. Furthermore, our results suggest that better knowledge of vegetation-environment relationships has potential for enhancing our understanding of subtropical forests that occupy vast areas of the S and SW China.

Keywords: China, DCA, Environmental variables, Gradient, GNMDS, LNMDS, Monitoring, Ordination, Subtropical forests, Ground vegetation.

Hai-Ying Liu, Department of Botany, Natural History Museum, University of Oslo, P.O. Box 1172 Blindern, N-0318 Oslo, Norway and Institute of Ecology, Chinese Research Academy of Environmental Science, Beiyuan, Anwai, 100012, Beijing, P.R. China; Tonje Økland, Norwegian Forest and Landscape Institute, P.O. Box 115, N-1431, Ås, Norway; Rune Halvorsen, Department of Botany, Natural History Museum, University of Oslo, P.O. Box 1172 Blindern, N-0318 Oslo, Norway; Ji-Xi Gao, Institute of Ecology, Chinese Research Academy of Environmental Science, Beiyuan, Anwai, 100012, Beijing, P.R. China; Quan-Ru Liu, College of Life Science, Beijing Normal University, No 19, Xinjiekouwai Avenue, 100875, Beijing, P.R. China; Harald Bratli, Norwegian Forest and Landscape Institute, P.O. Box 115, N-1431, Ås, Norway;and Odd Eilertsen, Norwegian Forest and Landscape Institute, P.O. Box 115, N-1431, Ås, Norway and Institute of Ecology, Chinese Research Academy of Environmental Science, Beiyuan, Anwai, 100012, Beijing, P.R. China.

Current address: Hai-Ying Liu
Norweigan Institute for Air Research
P.O.Box 100, NO-2027 Kjeller, Norway
Phone: +47 63898040
E-mail: hyl@nilu.no

CONTENTS

INTRODUCTION

The rapid economic growth in China has been accompanied by a corresponding increase in pollution. During the last decades Chinese energy consumption increased more than 5% annually (Byrne et al. 1996, World Bank 1999). Coal accounts for about 75% of the commercial energy production and it is likely that coal will be the major energy carrier in the coming decades (Seip et al. 1999). Acid rain was recognized as a potential environmental problem in China in the late 1970s and early 1980s (Zhao & Sun 1986, Zhao et al. 1988, Wang et al. 1997), but it was not until mid 1990s Chinese research projects provided relevant information needed for implementing adequate control measures. There are still big gaps in the scientific knowledge of air pollution effects in China, particularly regarding quantification of effects. In order to provide a sound scientific basis for cost-effective control measures to reduce emissions of acidifying substances, China found it beneficial to exploit foreign experience, methodologies and "State of the art" equipment through cooperation with bilateral and multilateral development agencies. One of this activities was the Sino-Norwegian project IMPACTS (The Integrated Monitoring Program on Acidification of Chinese Terrestrial System), launched in 1999 and running for five-year (Larssen et al. 2006). It included five forest monitoring areas that receive significant amounts of long-distance airborne acidifying compounds. Motivated by the sensitivity of ground vegetation to acid rain (Falkengren-Grerup 1986, Nieppola 1992, R. Økland 1995a, R. Økland & Eilertsen 1996, T. Økland et al. 2004) and the high conservation value of ground vegetation in Chinese subtropical forests, a ground vegetation module was included in the IMPACTS project together with monitoring of the quality of air, precipitation, soil water, surface water, and forests health. These forests represent species-rich ecosystems with many important species (endemic species, key stone species, threatened species, etc.), and the forests are also important as resource (biodiversity, food, building material, etc.) for individual residents and thus for local and national economy (Tang et al. 2004). Ground vegetation monitoring in the IMPACTS project is based upon the basic principles of monitoring developed for use in Norway, highlighting detailed studies of ground vegetation and environmental conditions in permanent plots, in ways that facilitate statistical analyses (R. Økland & Eilertsen 1993, T. Økland 1996, Lawesson et al. 2000). Five monitoring areas were selected to span local environmental gradients and regional gradients in air pollution, while other human influences were as far as possible kept at a low level. Acidification pollution has been and continues to be of major concern for management of the region (Tang et al. 2004). In order to control acidification and to better manage the ecosystems of subtropical forests, a better knowledge of relationships between environmental variables and species composition in the region is needed.

The species composition in an area is known to vary along with differences in environmental conditions (Gleason 1926, Whittaker 1967). A gradual change in environmental conditions will most often produce a gradual shift in species composition. The identification of major coenoclines (gradients in species composition; Whittaker 1967) and the complex-gradients responsible for them are fundamental tasks of vegetation ecological research (R. Økland & Eilertsen 1993, Antoine & Niklaus 2000). For more than a century, ecologists have attempted to determine the factors that control plant species distribution and variation in vegetation composition (Glenn et al. 2002). The importance of climate for plant distributions was recognized already in the early 19th century (Humboldt & Bonpland 1807). Later, climate in combination with other environmental factors has been used to explain vegetation patterns around the world (Stott 1981, Woodward 1987, Cook & Irwin 1992). To explain relationships between species composition (variation in species abundances) and the environment on finer scales, large sets of corresponding vegetation and soil data sets (i.e. data recorded for

the same plots) are collected. Knowledge of present gradient relationships is a prerequisite also for understanding possible effects on ground vegetation of environmental changes over time, e.g. by air pollution, soil acidification, etc. There are strong reasons to expect that the forest ground vegetation is more sensitive than trees to environmental change (R. Økland & Eilertsen 1993), making early stages of damage to the forest ecosystem caused by air pollution likely to be reflected in the forest ground vegetation (T. Økland 1990). Monitoring results from boreal forest ecosystems have revealed vegetation changes that may be related to acid deposition (Falkengren-Grerup 1986, R. Økland & Eilertsen 1996, T. Økland et al. 2004), while for most parts of the world, including S and SW China, relevant monitoring programmes were lacking.

Considerable efforts have been made to describe and explain the relationships between environmental variables and vegetation in temperate and boreal regions (Golley et al. 1978, Alban 1982, Gartlan et al. 1986, Haase 1990, R. Økland & Eilertsen 1993, T. Økland 1996, Lawesson et al. 2000). Patterns seem to be valid for restricted regions and forest types and to be hard to generalise. For subtropical and tropical regions our knowledge about relationships between the distribution of vegetation and environmental variables is rather poor. Subtropical forests are characterized by a mild climate but with periods of high temperatures and precipitation. Determination of which variables control the presence and relative abundance of plant species is an important research goal for subtropical and tropical ecosystems (Chen et al. 1997, Yin et al. 2005).

Chinese subtropical forest vegetation has mostly been described by phyto-sociological methods and studied by simulation experiments in laboratories and greenhouses (Wu 1980). Previous botanical studies in these forests have generally focused on trees, while few studies of main ground vegetation gradients and their relationships with environmental variables have been performed. Vegetation-environment relationships, including species distributions along major gradients in S and SW Chinese subtropical forests, therefore still remain insufficiently known. Zhang (2002) used canonical correspondence analysis (CCA) to study the relationships between vegetation, climate and soil on broad regional in north China. The complex-gradients that appeared to be important to the plants in Zhang's (2002) study were, accordingly, broad-scaled, like macroclimatic temperature and soil types. Chen et al. (1997) investigated the distribution of tree species in a rain forest in southern Taiwan, using a wide range of statistical techniques. They found relationships between the distribution of tree species and a complex-gradient in elevation, soil base cations and soil pH, which was related to soil moisture and identified an important complex-gradient related to wind stress.

Investigations of vegetation-environment relationships in Chinese subtropical forests conducted at the scale and with the methods applied in the IMPACTS project have not been performed earlier. A better understanding of vegetation-environment relationships in Chinese forests ecosystems is thus urgently needed, as a platform for further studies of ecology, conservation, sustainable use, and for monitoring vegetation change in a region strongly influenced by acid rain.

Ordination methods are important tools for analysing relationships between vegetation and environmental conditions. The relative performance of the two ordination methods that are currently most often used and that are considered the most reliable, Detrended Correspondence Analysis, DCA (Hill 1979, Hill & Gauch 1980) and Local Non-metric Multi-dimensional Scaling, LNMDS (Kruskal et al. 1973, Minchin 1987), has been discussed since 1980 (Gauch & Whittaker 1981, Kenkel & Orloci 1986, Minchin 1987, T. Økland 1996). DCA ordination of data from the Chinese terrestrial ecosystems has been performed by several authors (Yang & Lu 1981, Zhang 1993), but use of ordination has been restricted to studies of broad-scale patterns and careful studies of fine-scaled vegetation patterns based on parallel use of several ordination methods (R. Økland 1996) appear to be lacking. Also on a world scale, studies in which several ordination methods are compared on several data sets are very few. Notably, hardly any comparison of LNMDS and GNMDS of the same data sets exists,

and which are the generally best options for each method can still not be decided with certainty (R. Økland et al. 2001a).

This study aims at: (1) comparing and evaluating DCA, LNMDS and GNMDS ordination methods by use of extensive field data; (2) identifying patterns of variation in ground vegetation composition in S and SW Chinese subtropical forests by use of multivariate statistical methods; and (3) interpreting vegetation patterns in terms of environmental variation. All of these aims serve the main objective, to understand vegetation-environment relationships of subtropical forests. This first comprehensive investigation of vegetation-environment relationships in the region may contribute to development of the established monitoring system and hence contribute to the maintenance of biodiversity and sustainable use of in Chinese subtropical forests.

THE STUDY AREAS

All background information for the study areas is derived from Tang et al. (2004), to which is referred for more complete descriptions.

This study was performed in five areas, chosen in well defined watersheds in subtropical forests in S and SW China (Tie Shan Ping in Chongqing municipality, TSP; Liu Chong Guan in Guizhou province, LCG; Lei Gong Shan in Guizhou Province, LGS; Cai Jia Tang in Hunan Province, CJT; Liu Xi He in Guangdong Province, LXH; Fig. 1). The climate in all five study areas was monsoonal with dry winters and wet summers. The prevailing wind direction is from northeast in the winter and southwest in the summer. Relative humidity varies with typical values around 80 %. The estimated annual mean temperature and annual mean precipitation at the meteorological stations situated most closely to the study areas for the period 1971–2002 (data from Chinese Meteorological Administration) were in the ranges 15.3–22.0 °C and 1,105–1,736 mm, respectively (Tab.1)

Fig. 1. Map of China showing the position of the five study areas.

In all five study areas except LXH which was dominated by granites, the parent material of the soil was sedimentary bedrock, such as sandstone and shale. Regions with sedimentary bedrock have considerable geological heterogeneity on fine scales, with limestone in the vicinity of the watersheds.

Two soil types predominate, yellow soil and red soil according to the Chinese classification system, corresponding to Haplic Alisol and Acrisol according to the FAO classification system (FAO 1998). These soil types are typical of S and SW China (Tang et al. 2004).

Tree stands in all five study areas were about 40–45 years old. Many of the forests were planted in the 1960s, after most Chinese forests were logged during "the Great Leap Forward" (1958–1962) (Tang et al. 2000). At the time this study was carried out, four (TSP, LCG, LGS, and LXH) of the

five study areas were protected by law. Three areas (TSP, LCG and LXH) have been exposed to pressure by tourism in recent years. However, there is no evidence of large-scale, human-induced, recent disturbances (except for the impact by 'acid rain') in any study area.

All the studied forests were mixed coniferous and broadleaf deciduous forests; in TSP and LCG dominated by Masson pine (*Pinus massoniana*) and Chinese fir (*Cunninghamia lanceolata*); in LGS by Armand pine (*Pinus armandii*) and Chinese fir; in CJT by Masson pine and sweet gum (*Liquidambar formosana*); and in LXH by short-flowered machilus (*Machilus breviflora*) and itea (*Itea chinensis*). Field work for the present study was carried out in 2000 (TSP, LCG), 2001(LGS, CJT) and 2002 (LXH).

All five study areas were located within the target zones for acid rain control in China (Tang et al. 2004). Sulphur dioxide (SO_2) and sulphuric acid (H_2SO_4) have for decades been important long distance airborne pollutants while nitrogen oxides (NO_x) and nitric acid (HNO_3) are of increasing importance in all five study areas. Both S and N are supplied both by dry and by wet deposition which also contains significant amounts of ammonium (NH_4), calcium (Ca) and magnesium (Mg). Deposition data are given in Tab. 1.

TIE SHAN PING

TSP is located in the Sichuan basin about 25 km northeast from the centre of Chongqing City (104°41′E, 29°38′N). The TSP study area (Fig. 2) has since 1988 been protected by law as part of a larger forest reserve. The area is about 16 ha and the elevation ranges from 540 m to 600 m a.s.l.

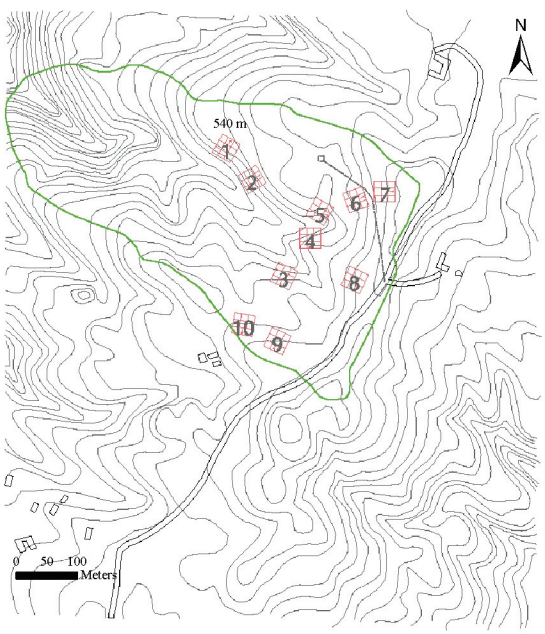

Fig. 2. Tie Shan Ping: Map of the study area with positions of macro plots 1–10. Black double continuous line: road; black single continuous line: path; small rectangle: buildings; green continuous line: ridge; contour interval: 5 m.

TSP has a subtropical, humid climate with little frost and snow, but much fog all year round. Annual mean temperature and precipitation (1971–2002) are 18.2 °C and 1,105 mm, respectively (measurements at Sha Ping Ba outside of Chongqing, five km from the study area). The mean temperature and precipitation (1971–2002) for the dry winters are 10.3 °C and 76 mm, and for the wet summers, 26.7 °C and 437 mm, respectively.

The high mountains surrounding Chongqing City reduce air circulation and increase the air pollutant load. Accordingly the TSP site receives high amounts of deposited sulphur, calcium and reactive nitrogen and the soil and surface water is strongly acidified (pH < 5.0). Compared with the other four study areas TSP is considered as a more polluted area.

According to local old residents, some parts of this area were cultivated as cropland 40–50 years ago.

LIU CHONG GUAN

LCG is located in Guizhou province (106°43′E, 26°38′N) about 10 km northeast of Guiyang City. This area is situated within a so-called 'botanical garden', established in 1963. The area covers about 7 ha and the elevation ranges from 1,260 m to 1,400 m a.s.l. Annual mean temperature and precipi-

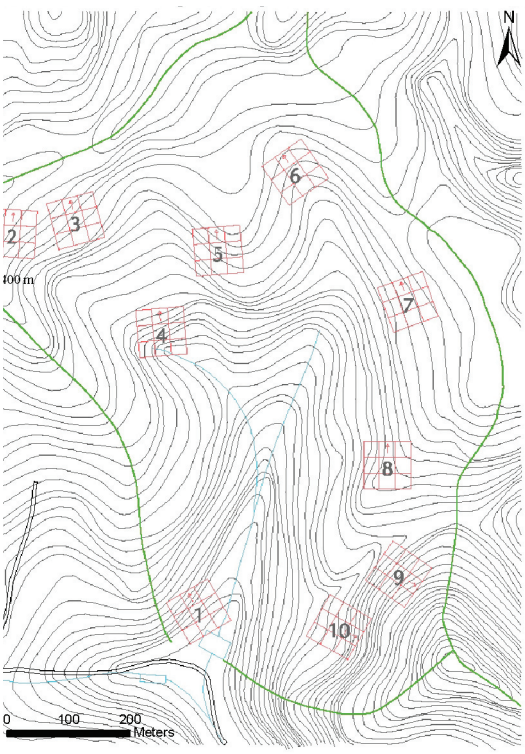

Fig. 3. Liu Chong Guan: Map of the study area with position of macro plots 1–10. Black double continuous line: road; green continuous line: ridge; blue continuous line: valley; blue rectangle: V-notch weir; contour interval: 5 m.

tation (1971–2002) in Guiyang are 15.3 ºC and 1,118 mm, respectively. The mean temperature and precipitation (1971–2002) in the dry winters are 7.6 °C and 73 mm, and in the wet summers, 22.7 °C and 404 mm, respectively. The city has an average of 220 cloudy days per year (Zhao et al. 1988).

The monitoring area is a suburban area located close to large emission sources, resulting in high deposition of sulphur as well as alkaline dust. Sulphate and calcium are important pollutants in precipitation, soil water and surface water. The concentration of nitrate in soil and surface water is low, but the surface water is acidified (pH < 5.0).

LEI GONG SHAN

LGS is located in Guizhou province (108°11′E, 26°22′N), outside Lei Shan county, a small mountain village 40 km southeast of Kaili City and 140 km east of Guiyang. The study area is part of a mountain area that has been protected since 1982. The area is about 6 ha and the elevation ranges from 1,620 m to 1,720 m a.s.l. Annual mean temperature and precipitation (1971–2002) at Kaili are 15.7 °C and 1,225 mm, respectively. The mean temperature and precipitation (1971–2002) in the dry winters are 5.2 °C and 63 mm, and in the wet summers, 20.1 °C and 422 mm, respectively. Fog is omnipresent,

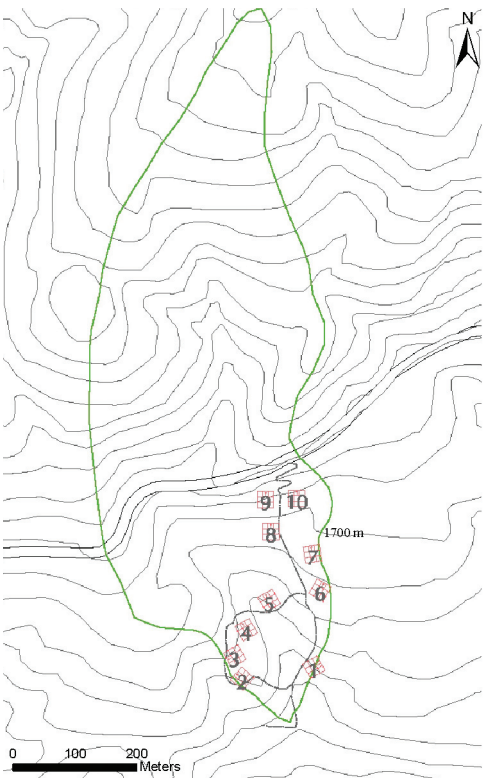

Fig. 4. Lei Gong Shan: Map of the study area with position of macro plots 1–10. Black double continuous line: road; black single continuous line: path; green continuous line: ridge; contour interval: 20 m.

for instance 315 foggy days were recorded in 1987.

The study area is remotely situated, and no large, local emission sources occur. However, the wet deposition of sulphur and nitrogen is relatively high and illustrates the importance of long-range transported air pollutants. So far, however, the study area is not strongly acidified, but the low electric conductivity of surface waters indicates that the area may be sensitive to acidification.

Compared with the other four study areas LGS is considered as a more pristine areas, and the forest stand in this area is relatively old and in a near natural state.

CAI JIA TANG

CJT is located in Hunan province (112º 26′E, 27º 55′N). The study area is situated on the southern side of the Cai Jia Tang Mountain, 10 km west of the small city Shaoshan, and 130 km southwest of Changsha City. The study area is not protected by law, but no evident human impact has taken place in recent years. This area is about 4.2 ha and the elevation of the site ranges from 240 m to 380 m a.s.l. Annual mean temperature and precipitation (1971–2002) at ZhuZhou, close to the site, are 17.0 °C and 1,331 mm, respectively. The mean temperature and precipitation (1971–2002) in the dry winters are 7.4 °C and 333 mm, and in the wet summers, 26.8 °C and 406 mm, respectively.

The study area has relatively high deposition of both sulphur and nitrogen, but also high inputs of alkaline dust. The base saturation in the soil is relatively high. Calcium and sulphate concentrations are high both in soil water and surface water.

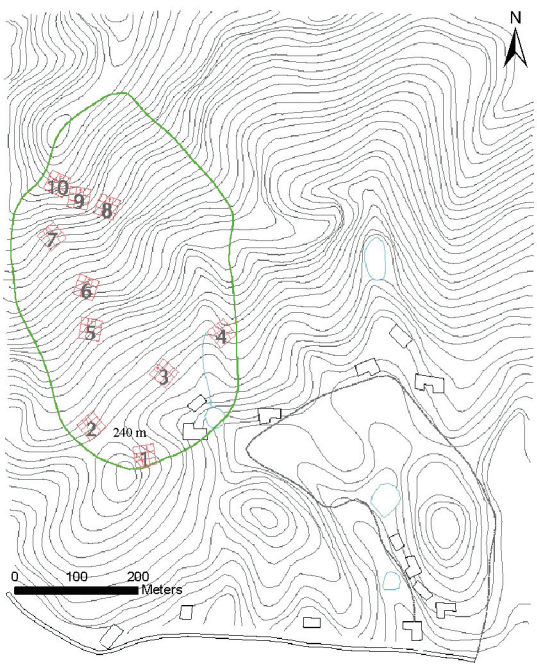

Fig. 5. Cai Jia Tang: Map of the study area with position of macro plots 1–10. Black double continuous line: road; black single continuous line: path; green continuous line: ridge; blue continuous line: valley; blue circle: pond; small rectangle: buildings; contour interval: 5 m.

Compared with the other four areas, there is more bamboo in this area, especially in macro plots number one and two. According to local old residents, macro plots number one and two were cultivated as cropland 40–50 years ago.

LIU XI HE

LXH is located in Guangdong province (133°35′E, 23°33′N), 67 km northeast of Conghua City. The study area is part of a so-called 'forest garden', protected since 1986. This area is about 261 ha and the elevation ranges from 480 m to 510 m a.s.l. Annual mean temperature and precipitation (1971–2002) at Guangzhou (107 km from the study area), are 22.0 °C and 1,736 mm, respectively. The mean temperature and precipitation (1971–2002) in the dry winters are 15.3 °C and 195 mm, and in the wet summers, 28.0 °C and 626 mm, respectively.

This area is part of the catchment of a large drinking water reservoir, supplying Guangzhou with tap water. Both the bedrock (igneous plutonic granite) and the soil composition are quite different from the other four areas.

The study area receives deposition of nitrogen and sulphur of intermediate magnitudes, and relatively low inputs of alkaline dust compared with the other four areas. Since LXH is located relatively close to the sea, the area receives much more sodium and chloride from marine aerosols than the other areas. The acid load is relatively low, but the ratio of aluminium to calcium plus magnesium (Al/Ca+Mg) in the soil is high.

Compared with the other four areas, the forest in this area is relatively young and is mainly dominated by broadleaved evergreen trees.

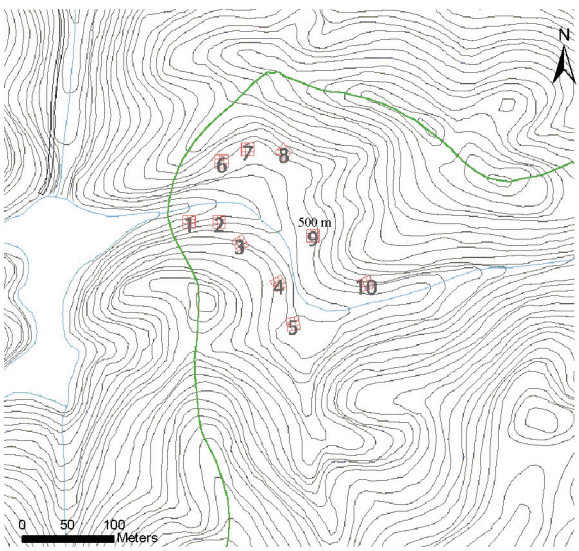

Fig. 6. Liu Xi He: Map of the study area with position of macro plots 1–10. Double black continuous line: road; green continuous line: ridge; blue continuous line: valley; blue circle: reservoir; small rectangle: buildings; contour interval: 5 m.

Tab. 1. Study areas: geographic position, annual precipitation and temperature normal 1971–2002 for meteorological stations close to each area (data from Chinese Meteorological Administration), annual wet deposition 2002 of sulphur (S), nitrogen (N) and calcium (Ca), and soil quality of horizon A of average pH, base saturation (BS) and carbon/nitrogen ratio (C/N) of soils (based upon 50 representative samples from each study area).

Study area	Latitude (°N)	Longitude (°E)	Altitude (m)	Area (ha)	Annual Precipitation (mm)	Temperature (°C/year)	Wet deposition				Soil quality			
							Amount (mm)	S	N	Ca	Bedrock	Soil pH	BS (%)	C/N
								($g\ m^{-2}\ yr^{-1}$)						
Tie Shan Ping	29°38′	104°41′	540–600	16.3	1,105	18.2	1,558	3.9	2.3	1.3	Sand-stone	3.6	33	19
Liu Chong Guan	26°38′	106°43′	1,260–1,400	6.8	1,118	15.3	1,080	3.5	1.1	2.8	Sand-stone	3.5	26	20
Lei Gong Shan	26°22′	108°11′	1,620–1,720	6.0	1,225	15.7	2,209	1.5	1.2	4.0	Shale	3.9	46	15
Cai Jia Tang	27°55′	112°26′	240–380	4.2	1,331	17.0	1,611	2.6	2.0	1.3	Sand-Stone/shale	3.8	38	18
Liu Xi He	23°33′	133°35′	480–510	261	1,736	22.0	1,253	4.5	1.3	2.2	Granite	4.0	17	21

MATERIALS AND METHODS

APPROACH AND SELECTION OF STUDY AREAS

Monitoring of vegetation and the environment was established in the IMPACTS forest study areas according to the basic principles of the Norwegian concept for ground vegetation monitoring (T. Økland 1996, Lawesson et al. 2000). The key principles are summarised below:

(1) Study areas should be selected to represent the regional variation within the entire area of interest (for example a country or parts of a country), the intensity of impact factors (for example airborne pollutants), as well as climatic and other broad-scaled environmental gradients.

(2) Similar ranges of variation along all presumably important vegetation and environmental gradients within the pre-selected habitat type should be sampled from each study area, in similar ways.

(3) Ground vegetation, tree variables, soil variables and other local environmental conditions of importance for the vegetation should be recorded in the same, permanently marked plots.

(4) Identification and understanding of the complex relationships between species distributions, the total species composition and the environmental conditions in each study area form a necessary basis for interpretation of changes in ground vegetation, and for hypothesising relationships between vegetation change and changes in the environment.

(5) Observed changes in nature caused by anthropogenic factors not of primary interest for the monitoring study may interfere with and obscure trends related to the factors of primary interest. The influence of such factors should be kept at a minimum, for example by selecting areas in near- natural state.

(6) The sampling scheme must take into consideration the purpose of the monitoring and meet the requirements for data analyses set by relevant statistical methods which imply constraints on plot placement, plot number and plot size.

(7) All plots should be re-analysed regularly. For most forest ecosystems yearly re-analyses will impose too much trampling impact etc. to be consistent with the purpose of monitoring. The optimal time interval between re-analyses in different ecosystems may vary among ecosystems.

Ideally, the number of monitoring areas should be high and reflect the range of variation in the area of interest (point 1, above). The number of study areas, five, which are included in our study, was determined by available time and resources. Furthermore, our study forms part of an interdisciplinary project, and the study areas were therefore selected as a compromise between requirements set by all partners. Although points (1–7) above were used as a guideline, many compromises were made with respect to points (1), (2) and (5). Furthermore, the wide range of variation within Chinese subtropical forests and the demand for spanning much of this variation resulted in study areas that differed more than ideally prescribed by point (2).

PLACEMENT OF PLOTS WITHIN EACH STUDY AREA

In each of the five study areas “randomisation within selected blocks” was used (T. Økland 1990):

ten macro plots, each 10×10 m, were placed subjectively in order to represent the variation along presumably important ecological gradients [for example in aspect favourability, nutrient conditions, light supply, topographic conditions, soil moisture etc.; see T. Økland (1996)]. Each 10×10 m macro plot was positioned in the centre of one 30×30 m extended macro plot which was used for recording of tree parameters. Five 1-m^2 plots were placed at random within each macro plot, resulting in 50 1-m^2 plots from each study area within ten 10×10 m macro plots. This sampling with two hierarchical levels made possible assessment of vegetation-environment relationships both at between-macro plot and within-macro plot (between-plot) scales.

Positions for 1-m^2 plots were rejected if they (1) included trees and shrubs or other plants that physically prevented placement of the aluminium frame used for vegetation analysis over the plot; (2) were physically disturbed by man (for example by soil scarification, extensive trampling or crossed by a path, included a pit dug by man, etc.); (3) were disturbed by earth slides; or (4) were covered by stones for more than 20 % of their area. In case of rejection, a new position for the 1-m^2 plot was selected randomly according to a predefined set of criteria. All plots were permanently marked by subterranean aluminium tubes as well as with visible plastic sticks.

RECORDING OF ENVIRONMENTAL VARIABLES

A total of 70 environmental variables recorded in or just outside each 1-m^2 plot or in the 10×10 m macro plots, 33 were used in order to interpret ecologically main gradients in species composition in the five sets of 50 plots from each area (T. Økland & Eilertsen 2001). The recorded variables of possible importance for the differentiation of vegetation within each study area were divided into six groups: (1) topography; (2) soil depth; (3) organic layer depth and litter layer depth; (4) soil moisture; (5) tree influence variables; and (6) other soil chemical/physical variables. Detailed information on the environmental variables including the methods used to record and calculated them is given in Tab. 2.

Of 14 topographical variables involved nine were used here: inclination, aspect favourability, heat index, median terrain roughness, concavity/convexity sum index at 1-m^2 scale, variance concavity/convexity at 1-m^2 scale, concavity/convexity sum index at 9-m^2 scale and variance concavity/convexity at 9-m^2 scale, respectively (Tab. 2).

Soil depth was recorded in cm, from measurements of the distance a steel rod can be driven into the soil in fixed position, 10–15 cm outside the sample plots borders. In our monitoring, eight single measurements are made for each plot. Maximum soil depth, minimum soil depth and median soil depth were calculated and median soil depth was used as variable.

Depth of the organic layer was measured in F-layer (fermentation layer) and H-layer (humic layer) just outside the border of each plot in order to avoid damage of vegetation in the plots. Measurements of depth of litter layer were performed in five fixed points within each 1-m^2 plots. Maximum litter layer depth, minimum litter layer depth and median litter layer depth were calculated and median litter layer depth was used as variable (T. Økland & Eilertsen 2001, Tab. 2).

The soil moisture measurements by the Trime-FM instrument, based on the principle of time-domain-reflectometry (Ledieu et al. 1986), should, ideally, be performed after some days without rainfall. In practice this was sometimes impossible because of time constraints (the measurements had to be made during the scheduled field trip to each area regardless of weather conditions in this particular period). Furthermore, some measurements (from the LGS area) are likely to be unreliable because of instability of the instrument shortly after rainfall. Our reason for including the soil moisture

variable despite these sources of unreliability is that soil moisture is likely to be a very important variable for species compositional variation in subtropical forests, and that the measurements may, though, provide some indications of relationships.

All trees that are (1) rooted within the macro plot or (2) covering the plot, should be marked with numbers, in the field and on the sketch map. Of 11 tree influence indices, i.e. indices that quantify the influence of trees on ground vegetation on different scales involved five were used here: litter index, crown cover index, the number of coniferous trees, the number of broadleaved tress, and tree influence index (T. Økland & Eilertsen 2001). Different indices have different requirements for tree characteristics recorded in the field. Relevant tree characteristics and the methods used to record and calculated them are given in Tab. 2.

Chemical soil analysis was restricted to the upper 5 cm of the humus layer where most of the root mass of vascular plants in mixed coniferous and broadleaved forests is concentrated. Humus samples were collected just outside each vegetation plot in end September 2000 in two areas (TSP and LCG), early October 2001 in two areas (LGS and CJT) and early October 2002 in one area (LXH). Each sample was a composite 5–10 sub-samples that from each quadrant in the macro plot. Samples were kept frozen until analysis at central laboratory at Chinese Research Academy of Environmental Sciences, Beijing [procedures according to Vogt & Mulder (pers. comm.); see Tang et al. (2004)], dried at 38 °C, ground and sifted (2 mm mesh width). Of the 32 soil physical and chemical variables involved 16 were used here (Tab. 2): pH_{H_2O} (mixed with 2.5 parts of distilled water); pH_{CaCl_2} (2.5 parts 0.01 M $CaCl_2$); effective exchangeable H, Ca, Mg, K, Fe, Mn, Al (ppm of organic matter); total C (wt % of organic matter); total N (wt % of organic matter); base saturation (the percentage of sum base cations (Ca + Mg + Na + K) relative to the sum of all cations (CEC_E, Al + Fe + H + Mn + Ca + Mg + Na + K)); aluminium saturation (the percentage of aluminium compared with the CEC_E); SO_4 adsorption (extraction with $Ca(H_2PO_4)_2$); dry matter content (WDM, in %); and loss on ignition (LOI, in %).

All variables in this study were collected for describing the growth conditions for, i.e. the environment of, the forest ground vegetation. We therefore refer to these variables collectively by the term “environmental variables” instead of, e.g., “explanatory variables”.

RECORDING OF SPECIES COMPOSITION AND ABUNDANCE

Presence or absence of all vascular plant and bryophyte species that were rooted in or growing over humus was recorded in each of 16 contiguous subplots (each 0.0625 m^2) within each 1-m^2 plot. A species was recorded as present in a subplot if any part of its vertical projection covered the subplot.

Species abundance in 1-m^2 plots was used: frequency in subplots, i.e. the number of subplots in which a species was recorded as present (T. Økland 1988).

STATISTICAL ANALYSES

For each data set, recorded abundances for species with a frequency lower than the median frequency (in the set of all species) were down-weighted by multiplying for each species the recorded abundances with the ratio of this species’ frequency and the median frequency (Eilertsen et al. 1990). All

Tab. 2. Environmental variables recorded in all five study areas: affiliation to group, abbreviated code, unit of measurement, range of values and method used for recording.

Environmental variable name	Code	Unit	Explanation of method and comments
Topography			
Inclination	Inclin	°	Measured in a way that is representative for each 1-m^2 plot by a clinometer compass
Aspect favourability	AspecF	°	The absolute value of the difference between the plot's aspect and NNE (25 ° or 425 °, whichever gives the lowest value for AspecF), NNE is considered to be the most unfavourable aspect at these latitudes (Heikkinen 1991).
Heat index	HeatIn		Calculated according to Parker (1988), as $H_i = \tan \alpha_1 \cos \alpha_2$, where α_1 is the inclination and α_2 is the absolute value of the difference between the plot's aspect and SSW (225 °), considered to be the most favourable aspect (Heikkinen 1991).
Median terrain ruggedness	TerraM	cm	Calculated according to Nellemann & Thomsen (1994) by placing four chains on the ground along the borders between subplots (25 cm from the corners of the plot; two chains in each direction), TerraMed is the median of the four chain lengths after subtraction of the theoretical minimum length, 100 cm, for each chain.
Sum concavity/convexity (1-m^2) Variance concavity/convexity (1-m^2)	ConvS1 ConvV1		An index value for concavity/convexity was assigned to each subplot by use of the following scale: –2 (concave), –1 (slightly concave), 0 (plane), 1 (slightly convex), 2 (convex). ConvS1 and ConvV1 are the mean and variance of the 16 values, respectively.
Sum concavity/convexity (9-m^2) Variance concavity/convexity (9-m^2)	ConvS9 ConvV9		The method for calculating ConvS1 and ConvV1 applied to the set of 9 concavity/convexity index values obtained for 1-m^2 'subplots' in a 3 m × 3 m plot with the 1-m^2 plot in centre
Soil depth			
Median soil depth	SoilDM	cm	The distance a steel rod could be driven into the soil was recorded in eight fixed positions, 10–15 cm outside the border of each plot. SoilDM is the median of these eight values.
Litter layer depth and organic layer depth			
Median litter layer depth	LitLDM	cm	Measured in five fixed positions within each 1-m^2 plot, LitLDM is the median of these five values.
Organic layer depth	OrgaLD	cm	Measured in F-layer (fermentation layer) and H-layer (humic layer) by just outside the border of each plot

Tab. 2 (continued). Environmental variables recorded in all five study areas: affiliation to group, abbreviated code, unit of measurement, range of values and method used for recording.

Environmental variable name	Code	Unit	Explanation of method and comments
Soil moisture			
Median soil moisture	SoiMLM	Vol %	Measured by means of a Trime-FM instrument, which is based on the principle of time-domain-reflectometry (Ledieu et al. 1986). In each plot four measurements in fixed positions were performed at 0–10 cm soil depth with a long probe. (i.e. 4 measurements in each plot). SoiMLM is the median of these 4 measurements. To ensure comparability, all measurements in one study area were performed on the same day. Soil moisture measurements were made after some days without rainfall with the intention of representing 'normal' or median soil moisture conditions (R. Økland & Eilertsen 1993).
Tree influence			
Litter index	LitteI		Relative amounts of litterfall over the 1-m^2 plot were calculated according to T. Økland (1990, 1996) and R. Økland & Eilertsen (1993) as the sum of index values obtained for each tree with phytomass covering the plot, $I_i = (d_i/cr_i) \cdot cc_i \cdot ca_i\,(h_i - ch_i)$, where d_i is the distance from the crown periphery to the proximal plot border (i.e. the side facing the stem) along the line through the plot centre and the stem centre for tree i, cr_i is the crown radius of tree i, measured through the plot centre, cc_i is the crown cover of tree i, ca_i is the crown area of tree i within the 1-m^2 plot, h_i is the tree height, and ch_i is the length along the stem from top to the point of emergence of the lowest-situated green branch whorl (in m), respectively.
Crown cover index	CrowCI		Calculated as the sum-product of canopy cover and crown area for all trees within a 25-m^2 plot with the 1-m^2 plot in the centre, as CrowCI = $\sum$ i $ca_i \cdot cc_i$ /25, where ca_i is crown area, cc_i is crown cover.
Relascope coniferous number Relascope broadleaved number	RelaCN RelaDN		Measured at breast height by use of a relascope from the lower left corner of each 1-m^2 plot as an expression of tree density, Relascope factor 2 (the narrowest slit on the relascope) was used. RelaCN and RelaDN are the numbers of coniferous and broadleaved trees counted, respectively.
Soil physical and chemical variables			
pH_{H_2O} and pH_{CaCl_2}	pH_{H_2O} pH_{CaCl_2}		pH in water extracts of the soil and in $CaCl_2$ extracts (ISO10390)
Effective exchangeable H, Ca, Mg, K, Fe, Mn, Al	Ca, Mg, K, Fe, Mn, Al	ppm	$CaCl_2$ extraction and the extractant analysed for pH, Ca, Mg, K, Fe, Mn and Al by flame-atomic adsorption (FAAS), all element concentrations were recalculated as ppm of organic matter (from mg/kg dry sample to mg/kg organic matter).

Tab. 2 (continued). Environmental variables recorded in all five study areas: affiliation to group, abbreviated code, unit of measurement, range of values and method used for recording.

Environmental variable name	Code	Unit	Explanation of method and comments
Total C	C	%	High temperature combustion of a soil sample to CO_2. Detection by IR adsorption (CHN-analyzer) (ISO 10694)
Total N	N	%	High temperature combustion of a soil sample to NO_2, followed by reduction to N_2. Detection by thermic conductivity (ISO13878)
Base saturation	BS	%	% BS = $\sum$ (Ca^{2+}, Mg^{2+}, Na^{+}, K^{+}) · 100/CEC_E CEC_E = $\sum$ (Al, Fe, H, Mn, Ca^{2+}, Mg^{2+}, Na^{+}, K^{+})
Aluminium saturation	AlS	%	% AlS = $\sum$ (Al^{3+}) · 100/CEC_E
SO_4 adsorption	SO_4	%	Extraction with $Ca(H_2PO_4)_2$
Dry matter content	WDM	%	Gravimetric loss from the fine fraction of an air-dried soil sample (obtained by passing soil through a 2 mm aperture sieve).after drying at 105 °C (ISO11465)
Loss on ignition	LOI	mmol/kg	Gravimetric loss by combustion (ashing) of ca. 1 g of the fine fraction of a sample at 550 °C in a muffle furnace

environmental variables recorded on a continuous scale were transformed to zero skewness according to R. Økland et al. (2001) to allow the use of parametric statistical methods with the implicit assumption that all observations are drawn from the same distribution and have the same mean and homogeneous variances (Sokal & Rohlf 1995, R. Økland 2007).

R freeware (Anonymous 2004a, 2004b) and the *vegan* package (Oksanen 2007, Oksanen et al. 2007), was used for all multivariate analyses unless otherwise is stated.

Relationships between environmental variables

Non-parametric correlation coefficients

Correlations between environmental variables were calculated as Kendall's non-parametric correlation coefficients τ (Kendall 1938, Sokal & Rohlf 1995). Kendall's τ was chosen because this coefficient only takes the ranks of variables into account. The structure of the data, with plots nested within macro plots, makes the assumption of strictly statistical independence of observations at the plot scale questionable and tests of deviation of τ from 0 are used for indication only, interpreted in a conservative manner as recommended by R. Økland (2007).

PCA ordination

PCA (Principal Component Analysis) ordination (Pearson 1901, ter Braak & Prentice 1988) was applied to the sets of 33 environmental variables recorded in 50 plots in each of the five study areas, to summarise main patterns of environmental variability. PCA was run on a correlation matrix of transformed variables that were subsequently centred and standardized to unit variance. Correlation biplot scaling of PCA axes was used to optimise the fit of angles between variable vectors to inter-variable correlations. The cosine of the angle between two variable vectors then approximates the (product-moment) correlation between the variables, and the length of a vector's projection on an axis approximates the correlation between the variable and this axis.

Ordination of species data

Ordination methods

Three different ordination methods representing the two main families of ordination methods were applied in parallel to each of the five species-by-plot data matrices, i.e. matrices of subplot frequencies for all species recorded in all plots in each study area: Detrended Correspondence Analysis (DCA; Hill 1979, Hill & Gauch 1980) and two variants of NMDS (Nonmetric Multidimensional Scaling), including Local Non-metric Multi-dimensional Scaling (LNMDS; Kruskal et al. 1973, Minchin 1987) and Global Non-metric Multidimensional Scaling (GNMDS; Kruskal 1964). Parallel use of ordination methods served two purposes: (1) controlling the reliability of the ordination results [because all ordination methods sometimes produce flawed results for reasons discussed by, for example R. Økland (1990a), similar results obtained by several and different methods serve as a strong indication that the main gradient structure has been identified (T. Økland 1996, R. Økland & Eilertsen 1996)]; and (2) comparing the performance of different methods.

DCA is based upon correspondence analysis (CA; Hill 1979) which arranges plots along main gradients in species composition on the basis of differences in abundances of species with different estimated optima. The NMDS methods on the other hand place plots entirely on the basis of floristic

dissimilarity. The optimality criterion in NMDS (stress) is an expression of the rank-order correspondence between floristic dissimilarities and distances in ordination space. LNMDS and GNMDS differ in the way stress is calculated: in LMNDS by comparing the position of each plot with those of all other plots and combining the plot-specific stress values into an overall measure of stress; in GNMDS by calculating one stress value for all plot pairs at the same time. All three methods intentionally place plots with similar species composition close together in the ordination space and plots with dissimilar species composition further apart. The axes thus extracted express variation in species composition that may subsequently be interpreted in terms of main environmental complex gradients (Hill 1979, Minchin 1987, R. Økland 1990, Pitkänen 2000). In order to enhance comparability with DCA axes, the LNMDS and GNMDS axes were linearly rescaled in S.D units by DCCA (Detrended Canonical Correspondence Analysis) with one LNMDS or GNMDS axis at a time used as the only constraining variable (R. Økland 1990).

LNMDS ordination was performed by using the DECODA software (Minchin 1991). Two-, three- and four-dimensional solutions were obtained. The following options were used: dissimilarity measure = percentage dissimilarity (Bray-Curtis), standardized by division with species maxima as recommended by Faith et al. (1987), at least 100 starting configurations, maximum number of iteration = 1000, stress reduction ratio for stopping iteration procedure = 0.99999 (T. Økland 1996). Solutions were not accepted unless reached from at least two different starting configurations.

Both DCA and GNMDS were run using R Version 2.3.1 (Anonymous 2004a), including packages *vegan* Version 1.9–13 (Oksanen 2007, Oksanen et al. 2007) and *MASS*, the latter included in package cluster *stats* (Anonymous 2004b). DCA was run using function *decorana* with detrending by segments, non-linear rescaling of axes, and no downweighting of rare species; GNMDS was run using functions *vegdist*, *initMDS*, *isoMDS* and *postMDS*, with options like those used in the LNMDS. Two-, three- and four-dimensional solutions were obtained.

Comparison of ordination methods

Comparison of the three ordination methods, DCA, LNMDS and GNMDS, was made in terms of differences and similarities as well as 'optimality' with respect to explicit criteria. Evaluation of ordination methods by use of field data has the advantage that the data are real and their properties therefore realistic and the disadvantage that the underlying 'true' gradient structure is unknown so that goodness-of-fit cannot be assessed by use of a 'target configuration' (Minchin 1987, R. Økland 1990). We used four indicators to compare ordination methods, of which only the fourth is an 'optimality criterion':

(1) Pair-wise correlation coefficients (Kendall's correlation τ), calculated between axes obtained by different ordination methods applied to the same data set was used to identify 'corresponding axes', i.e. axes that represent the same compositional gradient. Three ordination axes were considered corresponding when two pairs had $\tau > 0.4$ and the third had $\tau > 0.2$. The choice of τ values was based upon a general judgement. The τ values vary continuously and any criterion of this kind will be arbitrary. An ordination was considered verified if and only if all of its axes corresponded to axes of other ordinations.

(2) Procrustes comparison, by which one ordination in a specified number of dimensions is fit to another ordination by uniform scaling (expansion or contraction) and rotation of axes so that the squared difference between the two ordinations is minimised (Oksanen 2007). The overall fit between ordinations is quantified by the Procrustes correlation r, for which statistical inference was obtained by a permutation test (command *protest* in *vegan*; Oksanen 2007). Procrustes analyses were made for fifteen sets of ordinations; two-, three- and four-dimensional NMDS solutions for each of the five study areas, compared with the first two, three and four DCA axes, respectively. Each pair of corresponding ordination axes in each data set was assigned a rank in each pair (1 = highest r, 2 =

medium *r*, 3 = lowest *r* in each pair). Ranks were summed for the five ordinations of given dimensionality to assess overall similarity.

(3) The tendency to identify outliers, here in the context of ordinations defined as plots which occupy isolated positions along an axis (Gauch 1982, R. Økland 1990). Outliers in ordinations may represent plots with relationships to other plots poorly defined by the data, for example few species in common or species-poor plots (R. Økland 1990). Good ability of an ordination method to identify real outliers may therefore be advantageous because these can then be removed before a new ordination analysis is carried out, the results of which are subjected to environmental interpretation. However, a strong tendency to treat as outliers plots without poor relationships to other plots is no advantage. As a measure of outlier influence, the relative length of the 'core' of an axis, i.e. the length of the shortest interval along an ordination axis containing 90 % of the plots (R. Økland et al. 2001a), was used. The higher the core length of the axis is, the lower the outlier influence. The core length index measures the tendency for outlier influence without indicating the reason why plots act as outliers. For each set of corresponding ordination axes in each data set, DCA, LNMDS and GNMDS were assigned ranks (1 = highest core length, 2 = medium, 3 = lowest) that were summed for all corresponding axes in the five ordinations of given dimensionality to assess overall similarity in outlier influence.

(4) Split-plot GLM (Generalized Linear Model; Crawley 2002) analysis by which relationships were evaluated both at macro-plot and plot scales (see below) was used to rank the methods according to: (*i*) total number of environmental variables strongly correlated ($P < 0.1$) with the axis in question, and (*ii*) the strength of the correlation between each ordination axis and the most strongly correlated environmental variable. For each set of corresponding ordination axes in each data set, DCA, LNMDS and GNMDS were assigned ranks (1 = highest, 2 = medium, 3 = lowest) for each of the two criteria. Ranks were summed for all axes to assess overall performance.

Selection of GNMDS for interpretation of vegetation environment relationships

Initial ordination analyses by DCA and LNMDS revealed one plot in CJT (plot number 5 with four species in total) and four plots in LXH (plots number 38, 47, 48 and 49, with total species numbers of 11, 8, 3 and 5, respectively) that acted as clear outliers. After re-running ordinations on the remaining 49 and 46 plots in the above-mentioned two study areas, the comparison of ordination methods revealed that the maximum number of axes that corresponded to axes in other ordinations was three for the TSP and LXH areas and two in LCG, LGS and CJT. The correspondence between the ordination methods was generally good and GNMDS was chosen for interpretation of vegetation-environment relationships.

Environmental interpretation of vegetation gradients

Ordination axes are interpered as vegetation gradients. In order to elucidate the complex relationships between species composition and environmental conditions, these gradients were interpreted for each study area by means of the measured environmental variables. Biplots of plot scores and the most significant environmental variables were made by the *plot* command of R to visualise vegetation-environment relationships at macro-plot and plot scales. The fit of environmental variables was evaluated using R package *vegan* (Oksanen 2007), the *envfit* function which provides a squared correlation coefficient the significance which indicating the strength of the relationship between an ordination axis and an environmental variable. Only variables with $P < 0.1$ were included in biplots.

The interpretation of GNMDS ordinations was split-plot GLM analysis (Crawley 2002) combined with Kendall's rank correlation coefficient τ calculated between plot scores along GNMDS

axes and environmental variables. The two methods more or less consistently identified the same environmental variables as strongly related with ordination axes. Cases of apparent inconsistency, i.e. opposite signs for *r* coefficients for the between-plot level by the split-plot GLM and correlation coefficients τ, as found for some environmental variables weakly related to the axes in question, occurred when relationships between plot scores and the environmental variable had different signs at the macro-plot and the plot scales. Parallel use of these two methods thus proved useful for resolving scale-dependent relationships between vegetation and environment.

GLM was chosen because it allows flexible handling of data over a wide range of statistical properties (Venables & Ripley 2002). For each axis, the GNMDS plots score was used as response variable and one or more environmental variables were used as predictors in a split-plot GLM (Crawley 2002), using the *aov* function of R. Identity link function and normal errors were used (Anonymous 2004b). Statistical inference was obtained by considering species (plot) as nested within macro plot. The parameters of $SS_{expl}/SS_{macro\ plot}$ (fraction of variation explained by variable at the macro plot), model coefficient *r*, *F* (measurement of fit between predictor and response variables at a given hierarchical level) and *P* value for *F* (for a test of no relationship against the two-tailed alternative) were used to determine the contributions of the measured environmental variables to explaining variation in species composition.

Split-plot GLM analyses with plot scores for each GNMDS axis as response variables and recorded species number of vascular plants and bryophytes, respectively, as predictors, were made to elucidate species number patterns along interpreted GNMDS ordination axes.

Isoline diagram of significant environmental variables and variables of species number

For environmental variables (and species number variables) with significant *P* value in the split-plot GLM analyses and/or high Kendall's rank correlation coefficient τ with GNMDS axes, isoline diagrams were constructed by fitting surfaces to variable values plotted onto plot positions in two-dimensional GNMDS ordination diagrams. The multiple coefficient of determination, R^2, calculated between the original and predicted values for the variable, was used as a measure of goodness-of-fit of the isolines. Isoline plots were made for variables with $P < 0.05$ (at least one hierarchical level) in the split-plot GLM and/or Kendall's correlation coefficient $|\tau| \geq 0.3$ with at least one of the relevant GNMDS axes.

Function *ordisurf* of package *mgcv* (Wood 2000) was used to fit the surfaces. The R^2 values were obtained by use of the *lm* function in the R package *nlme* (Venables & Ripley 2002).

The distribution of species abundance in the GNMDS ordination

For species that occurred in five or more plots, subplot frequencies were plotted onto plot positions in GNMDS ordinations in order to illustrate, for each study area, the species' responses to environmentally interpreted ordination axes.

NOMENCLATURE AND TAXONOMIC NOTES

The nomenclature of vascular plants follows Wu et al. (1959–2005); bryophyte species follows Gao (1994–2004), P.C. Wu (2000) and Z.Y. Wu (2000–2002).

RESULTS

GENERAL COMPARISON OF STUDY AREAS

The variation in environmental conditions between the areas was high (Tab. 3). For instance, compared with the other study areas, the surface was relatively flat and the soil was rather deep in TSP; the

Tab. 3. Raw data for the 33 environmental variables in all five study areas. Min, Med and Max are abbreviation of minimum, medium and maximum. The units and names of environmental variables are abbreviated in accordance with Tab. 2.

Environmental variables	Study area														
	TSP			LCG			LGS			CJT			LXH		
	Min	Med	Max	Min	Med	Max	Min	Med	Max	Min	Med	Max	Min	Med	Max
01 Inclin	0	12	37	8	20	36	4	21	41	12	30	48	17	30.5	49
02 AspecF	0.5	63	177.5	32.5	136	176.5	34.5	144.5	178.5	55.5	145.5	178.5	10.5	100.5	171.5
03 HeatIn	–0.59	0.05	0.34	–0.53	0.2	0.67	–0.72	0.22	0.67	–0.3	0.36	1.1	–0.71	0.06	0.94
04 TerraM	1	6	11	2.5	5.5	13	1.5	7	14.5	2	7.25	14.5	4	9.5	50
05 ConvS1	–8	1	8	–11	1	8	–14	–1	7	–9	–1	7	–20	1	12
06 ConvV1	0	0.12	0.78	0	0.25	0.9	0	0.41	1.26	0.06	0.36	1.6	0	0.27	4.3
07 ConvS9	–7	2	7	–7	2	7	–11	2	12	–5	0.5	12	–7	5	11
08 ConvV9	0	0.28	2	0.11	0.32	1.19	0.11	0.75	2.25	0	0.53	1.78	0	0.65	5.53
09 SoilDM	10.5	34	105	9.5	31.5	79.5	2	37	57.5	5	17	35	18.6	27.98	41.1
10 LitLDM	0	1	5	0	4	8	0	3	5	0	1	4	0	1.69	9.48
11 OrgaLD	0.5	2	4	1	2	9	0.3	2	6	0	0.5	1.5	0.2	0.55	2
12 SoilMLM	16.75	27.25	32.4	16.35	33.23	43.9	9.4	24.7	35.1	3.6	10.43	28.35	0	29.5	80
13 LitteI	0	2.56	6.74	0	1.5	15.75	0	2.45	13.52	0	0.53	6.34	0.5	2	6
14 CrowCI	0	0.04	0.23	0	0.02	0.1	0	0.03	0.06	0	0.02	0.09	0	0.05	0.16
15 RelaCN	1	7.5	17	1	7	17	0	17	24	0	1	8	0	0	2
16 RelaDN	0	1	5	0	2	7	0	0	10	0	7.5	18	2	7.5	14
17 pH_{H_2O}	2.98	3.51	4.5	3.29	3.56	4.28	3.27	3.9	6.3	3.11	3.78	5.48	3.11	4.05	4.64
18 pH_{CaCl_2}	2.73	3.13	4.72	2.81	3.09	3.92	2.83	3.49	5.51	2.82	3.41	5.19	2.83	3.52	4.27
19 Al	1.81	4.91	10.55	4.66	9.65	19.46	0.02	5.41	7.79	0.62	4.92	15.95	0.59	1.69	2.56
20 Fe	0.01	0.61	1.37	0.05	1.2	2.12	0	0.1	0.71	0	0.11	0.44	0	0.02	0.14
21 H	0.1	2.38	7.44	0.57	2.68	7.22	0	1.17	2.1	0.07	1.06	3.74	0.13	0.23	0.39
22 Mn	0.01	0.14	0.8	0.01	0.09	3.31	0.13	0.51	1.21	0.13	0.82	6.13	0.01	0.07	0.25
23 Ca	0.47	2.15	5.51	0.62	4.98	25.61	1.42	4.71	27.95	1.18	3.05	9.67	0.05	0.13	0.49
24 Mg	0.06	0.35	0.86	0.21	0.93	2	0.28	1.07	2.25	0.35	0.72	2.16	0.06	0.1	0.18
25 Na	0.01	0.11	0.23	0.02	0.07	0.18	0.02	0.05	0.18	0.22	0.27	0.79	0.01	0.02	0.04
26 K	0.09	0.38	0.6	0.11	0.48	1.16	0.16	0.42	0.98	0.26	0.5	1.58	0.09	0.15	0.2
27 C	2.36	10.57	32.39	10.81	33.2	73.68	5.81	11.22	21.81	4.43	7.65	15.3	1.14	2.94	7.55
28 N	0.12	0.53	1.46	16.22	44.29	78.11	0.41	0.73	1.34	0.22	0.42	0.96	0.07	0.14	0.36
29 BS	13.3	25.56	54.85	3.1	18.43	38.14	19.92	45.67	99.18	15.96	38.43	79.66	10.32	17.2	27.57
30 AlS	23.12	44.47	73.58	0.19	0.96	1.84	0.09	39.46	63.66	5.65	43.37	72.45	52.62	69.04	78.8
31 SO_4	0.2	0.54	2.13	0.07	0.91	2.77	0	0.59	1.33	0.14	0.54	1.27	0.19	0.54	1.55
32 WDM	94.61	97.07	98.71	92.51	95.08	98.02	92.91	95.63	97.71	94.19	96.78	98.18	96.01	98.49	99.19
33 LOI	5.45	21.61	41.84	9.88	35.72	61.26	13.74	23.52	29.71	9.17	14.93	27.8	5.24	9.71	17.26

number of broadleaved trees was relatively high and the forest denser in LXH while light conditions at ground level were good in CJT. Vascular plants, bryophyte species and in total species number (Tab. 4) recorded in the included plots varied a lot between areas. While the total species number was only 65 in TSP and the number was low also in LCG and CJT, high numbers were recorded from LGS. The maximum, 147 species, was recorded in LXH. Only 47 vascular plant species were recorded in LCG, low numbers also in TSP and CJT, high in LGS, and a maximum of 117 species in LXH. Only 12 bryophytes species were recorded in TSP, low numbers also in LCG and CJT, higher in LXH and a maximum of 41 species was recorded in LGS. Also the vascular plant, bryophyte and total species numbers recorded in ten 10×10 m macro plots varied much between areas, but the ranking of areas remained the same as obtained for the plot scale; number was high in LXH and LGS and low in TSP, LCG and CJT.

Species composition (Appendix 1) varied strongly among the areas. None of the 373 vascular plant species recorded (in total) were found in all five areas, and only very few species were found in three or four areas; for example *Woodwardia japonica*, *Lophatherum gracile* and *Miscanthus sinensis* in TSP, LCG, CJT and LXH; *Symplocos lancifolia* in TSP, LCG, LGS and LXH; *Cunninghamia lanceolata*, *Pteridium aquilinum*, *Rubus corchorifolius* and *Smilax china* in TSP, LCG and CJT; *Dicranopteris pedata* in TSP, LCG and LXH; *Liriope spicata* in LCG, CJT and LXH; *Parathelypteris glanduligera* and *Symplocos sumuntia* in TSP, LGS and CJT; and *Viburnum satigerum* in TSP, LCG and LGS. None of the 119 bryophyte species (in total) were found in all five areas, and only very few species were found in three or four areas, for example *Calypogeia muellerana*, *Cephaloziella microphylla* and *Dicranodentium denudatum* in TSP, LCG, CJT and LXH; *Hypnum plumaeforme* in TSP, LCG, LGS and CJT; *Calypogeia arguta* and *Leucobryum bowringii* in TSP, LCG and LXH; and *Taxiphyllum subarcuatum* in TSP, LCG and CJT.

Tab. 4. Species number at macro plot (10×10 m macro plots) and plot (1-m^2 plots) levels in all five study areas. The number of macro plots was 10 in all five study areas, the number of plots 50 in TSP, LCG and LGS, 49 (plot number 5 omitted) in CJT and 46 (plots number 38, 46, 47 and 48 omitted) in LXH. Min, Med and Max are abbreviation of minimum, medium and maximum.

Species number	Study area														
	TSP			LCG			LGS			CJT			LXH		
	Min	Med	Max	Min	Med	Max	Min	Med	Max	Min	Med	Max	Min	Med	Max
Total		65			67			137			76			147	
Vascular		53			47			96			60			117	
Bryophyte		12			20			41			16			30	
Macro plot															
Total	16	25	30	7	21.5	25	31	34.5	44	16	23	29	25	39	68
Vascular	13	19.5	23	7	13	20	20	24.5	32	15	21	28	23	34	50
Bryophyte	1	5.5	9	0	6	12	6	12	17	0	1	4	2	5.5	18
Plot															
Total	3	10	18	1	8	15	9	14	26	3	8.5	16	3	13	29
Vascular	2	7	13	1	5	10	4	9	19	2	5	11	3	10	20
Bryophyte	0	3	7	0	2	8	2	5	10	0	3	6	0	3	10

COMPARISON OF ORDINATION METHODS

Pair-wise correlation coefficients and identification of corresponding ordination axes

Kendall's non-parametric correlation coefficient τ between corresponding plot scores along DCA and LNMDS and GNMDS axes was fairly strong for two-dimensional ordinations in all five study areas, although the strength of correlations differed somewhat among the areas (Tab. 5). The ranking of axes was less clear in LNMDS and GNMDS as compared to DCA, in which axes are ranked by their eigenvalues (the first axis having the highest eigenvalue, the second axis the second highest eigenvalue, etc.). Thus, many 'corresponding axes' were made up of DCA 1 or DCA 3 and NMDS2, or *vice versa* (Tab. 5)

The axes of two-dimensional ordinations were always corresponding (two $\tau > 0.4$, one $\tau > 0.2$); although in two areas (CJT and LXH) DCA 3 corresponded to GNMDS 2 and LNMDS 2. The first LNMDS/GNMDS axes and the corresponding DCA axis always corresponded strongly ($\tau > 0.6$), while correspondence was weaker for the second (and eventually, the third) axes.

With one exception, axes 1 and 2 of the three-dimensional NMDS solutions corresponded to axes 1 and 2, respectively, of the two-dimensional NMDS ordinations. The exception was LXH, in which the variation in species composition expressed on axes two and three in the three-dimensional GNMDS and LNMDS ordinations were combined to a new set of corresponding axes in the two-dimensional solutions.

The four-dimensional solutions identified the same set of 3 or 2 corresponding axes as the three-dimensional solutions, except that for CJT GNMDS 4 corresponded weakly to DCA 2. As NMDS 3 did not have a counterpart in DCA, the four-dimensional NMDS solutions were not verified and only two axes were identified as truly corresponding for this area.

The maximum numbers of dimensions in verified NMDS ordinations were three for TSP and LXH and two for LCG, LGS and CJT.

Procrustes comparison

Procrustes correlation coefficients r between DCA, LNMDS and GNMDS ordinations were fairly strong for two-, three- and four-dimensional ordinations in all five study areas ($r > 0.5080$). LNMDS and GNMDS ordinations were more closely similar to each other than was any other pair of methods (Tab. 6). For two-dimensional ordinations the similarity between GNMDS and DCA was somewhat higher than between DCA and LNMDS, while in three- and four-dimensional ordinations the converse was true (Tab. 6).

Outlier influence

The order of rank of average core length was GNMDS > LNMDS > DCA in all two-, three- and four-dimensional ordinations. In all dimensions, the difference between LNMDS and GNMDS with respect to core length was negligible; both having higher core lengths than DCA and thus being less prone to influence by outliers. Exceptions to this pattern did, however, occur (Tab. 7).

Tab. 5. Kendall's nonparametric correlation coefficient τ between DCA, LNMDS and GNMDS axes in each of all five study areas. Only axes that are corresponding were included. A, B and C mean the main gradients, A: first gradient, B: second gradient and C: third gradient.

Study area	Dimension	Main gradient		Correlation between DCA, LNMDS and GNMDS		
				DCA-LNMDS	LNMDS-GNMDS	GNMDS-DCA
TSP	2	A	DCA 2, LNMDS 1, GNMDS 1	0.719	0.742	0.631
		B	DCA 1, LNMDS 2, GNMDS 2	0.330	0.606	0.512
LCG	2	A	DCA 1, LNMDS 1, GNMDS 1	0.810	0.814	0.843
		B	DCA 2, LNMDS 2, GNMDS 2	0.538	0.722	0.613
LGS	2	A	DCA 1, LNMDS 1, GNMDS 1	0.854	0.819	0.840
		B	DCA 2, LNMDS 2, GNMDS 2	0.654	0.825	0.639
CJT	2	A	DCA 1, LNMDS 1, GNMDS 1	0.650	0.787	0.662
		B	DCA 3, LNMDS 2, GNMDS 2	0.532	0.602	0.393
LXH	2	A	DCA 1, LNMDS 1, GNMDS 1	0.619	0.693	0.729
		B	DCA 3, LNMDS 2, GNMDS 2	0.449	0.588	0.575
TSP	3	A	DCA 2, LNMDS 1, GNMDS 1	0.768	0.763	0.616
		B	DCA 1, LNMDS 2, GNMDS 2	0.688	0.714	0.510
		C	DCA 3, LNMDS 3, GNMDS 3	0.619	0.709	0.638
LCG	3	A	DCA 1, LNMDS 1, GNMDS 1	0.848	0.816	0.843
		B	DCA 2, LNMDS 2, GNMDS 2	0.509	0.706	0.541
LGS	3	A	DCA 1, LNMDS 1, GNMDS 1	0.833	0.894	0.812
		B	DCA 2, LNMDS 2, GNMDS 2	0.626	0.830	0.577
CJT	3	A	DCA 1, LNMDS 1, GNMDS 1	0.636	0.757	0.723
		B	DCA 3, LNMDS 2, GNMDS 2	0.432	0.604	0.454
LXH	3	A	DCA 1, LNMDS 1, GNMDS 1	0.677	0.648	0.778
		B	DCA 3, LNMDS 3, GNMDS 2	0.360	0.416	0.660
		C	DCA 2, LNMDS 2, GNMDS 3	0.484	0.229	0.513
TSP	4	A	DCA 2, LNMDS 1, GNMDS 1	0.700	0.738	0.515
		B	DCA 1, LNMDS 2, GNMDS 2	0.624	0.737	0.251
		C	DCA 3, LNMDS 3, GNMDS 3	0.652	0.709	0.577
LCG	4	A	DCA 1, LNMDS 1, GNMDS 1	0.849	0.802	0.815
		B	DCA 2, LNMDS 2, GNMDS 2	0.518	0.736	0.531
LGS	4	A	DCA 1, LNMDS 1, GNMDS 1	0.836	0.879	0.817
		B	DCA 2, LNMDS 2, GNMDS 2	0.620	0.798	0.638
CJT	4	A	DCA 1, LNMDS 1, GNMDS 1	0.730	0.820	0.760
		B	DCA 3, LNMDS 2, GNMDS 2	0.425	0.668	0.505
		C	DCA 2, LNMDS 4, GNMDS 4	0.223	0.580	0.469
LXH	4	A	DCA 1, LNMDS 1, GNMDS 1	0.708	0.696	0.697
		B	DCA 2, LNMDS 2, GNMDS 3	0.527	0.521	0.469
		C	DCA 3, LNMDS 3, GNMDS 2	0.438	0.451	0.565

Pair-wise correlation coefficients between ordination axes and the environmental variables

Based on the results of the split-plot GLM analysis, the total number and significance of variables strongly related to DCA, LNMDS and GNMDS were ranked. No consistent differences between methods were found for the number of significant variables (Tab. 8). The *P*-value for the variable

Tab. 6. Procrustes comparison between DCA, LNMDS and GNMDS ordinations in all five study areas. Procrustes correlation *r* is derived from the symmetric Procrustes residual m^2. For each set of corresponding ordination axes in each data set, DCA, LNMDS and GNMDS were assigned ranks (1 = highest *r*, 2 = medium *r*, 3 = lowest *r*) that were summed for each of the five ordinations of given dimensionality to assess overall similarity based on Procrustes comparison. The highest *r* and the total lowest ranked value are indicated by bold-face types.

		Corresponding axes			Ranked corresponding axes		
Study area	Dimension	DCA-LNMDS	LNMDS-GNMDS	GNMDS-DCA	DCA-LNMDS	LNMDS-GNMDS	GNMDS-DCA
TSP	2	0.7604	0.8669	0.9183	3	2	1
LCG	2	0.8793	0.9888	0.8853	3	1	2
LGS	2	0.9376	0.9763	0.9237	2	1	3
CJT	2	0.6593	0.8437	0.7191	3	1	2
LXH	2	0.5080	0.8751	0.6185	3	1	2
Total					14	6	10
TSP	3	0.9183	0.9667	0.8934	2	1	3
LCG	3	0.7699	0.9838	0.7689	2	1	3
LGS	3	0.8550	0.8454	0.7843	1	2	3
CJT	3	0.8182	0.8156	0.6716	1	2	3
LXH	3	0.6835	0.8612	0.8171	3	1	2
Total					9	7	14
TSP	4	0.8277	0.9252	0.8127	2	1	3
LCG	4	0.8056	0.9323	0.7883	2	1	3
LGS	4	0.7973	0.8352	0.7481	2	1	3
CJT	4	0.7794	0.9552	0.7688	2	1	3
LXH	4	0.8086	0.8405	0.7981	2	1	3
Total					10	5	15

most strongly related to each axis at each scale (macro plot or plot) showed disparate results among scales (macro-plot scale: GNMDS generally the best; plot scale: LNMDS the best; DCA intermediate in both respects; Tab. 9) and no reliable difference was found.

In total, DCA, LNMDS and GNMDS ordinations to a large extent produced similar results and the comparison can be summarised as follows:

- No coincident performance difference can be shown between the three methods, except that DCA has a generally stronger tendency to identify outliers.
- LNMDS and GNMDS generally give very similar results.
- Parallel use of NMDS and DCA makes possible identification of corresponding axes and provides an efficient means of verifying and deciding dimensionality of ordinations.
- For verified ordinations, the choice of results obtained by one ordination method (DCA or NMDS) above the others, e.g. for environmental interpretation, is more or less arbitrary.

Tab. 7. Ranking of core length (length of the shortest interval containing 90 % of the plots relative to the gradient length) for each ordination axes by each method in each of the five study areas (highest rank = 1, medium rank = 2, lowest rank = 3). Gradient lengths of LNMDS and GNMDS axes are calculated for the corresponding DCCA axis. The lowest total rank is indicated by bold-face types. The identification of axes as A, B and C follows Tab. 5.

Study area	Dimension	Corresponding axis	Core length			Ranked core length		
			DCA	LNMDS	GNMDS	DCA	LNMDS	GNMDS
TSP	2	A	0.641	0.781	0.793	3	2	1
		B	0.776	0.737	0.755	1	3	2
LCG	2	A	0.670	0.674	0.797	3	2	1
		B	0.435	0.676	0.764	3	2	1
LGS	2	A	0.664	0.744	0.594	2	1	3
		B	0.700	0.626	0.592	1	2	3
CJT	2	A	0.509	0.743	0.765	3	2	1
		B	0.508	0.789	0.780	3	1	2
LXH	2	A	0.689	0.777	0.826	3	2	1
		B	0.611	0.757	0.726	3	1	2
Total	2					25	18	17
TSP	3	A	0.641	0.734	0.817	3	2	1
		B	0.776	0.766	0.801	2	3	1
		C	0.621	0.696	0.738	3	2	1
LCG	3	A	0.557	0.683	0.720	3	2	1
		B	0.563	0.705	0.793	3	2	1
LGS	3	A	0.664	0.752	0.594	2	1	3
		B	0.700	0.628	0.586	1	2	3
CJT	3	A	0.509	0.734	0.808	3	2	1
		B	0.508	0.758	0.721	3	1	2
LXH		A	0.689	0.844	0.807	3	1	2
		B	0.711	0.789	0.857	3	2	1
		C	0.611	0.759	0.789	3	2	1
Total	3					32	22	18
TSP	4	A	0.776	0.821	0.841	3	2	1
		B	0.641	0.802	0. 796	3	1	2
		C	0.621	0.485	0.755	2	3	1
LCG	4	A	0.670	0.751	0.816	3	2	1
		B	0.563	0.847	0.826	3	1	2
LGS	4	A	0.664	0.772	0.635	2	1	3
		B	0.700	0.723	0.634	2	1	3
CJT	4	A	0.509	0.668	0.783	3	2	1
		B	0.508	0.674	0.771	3	2	1
		C	0.555	0.812	0.573	3	1	2
LXH	4	A	0.689	0.812	0.826	3	2	1
		B	0.711	0.725	0.797	3	2	1
		C	0.611	0.753	0.880	3	2	1
Total	4					36	22	20

Tab. 8. Rank for total number of environmental variables which were strongly related to corresponding axes by split-plot GLM analysis ($P < 0.1$) at the scales of macro plot and plot within macro plot in all five study areas. The total number was assigned ranks (highest = 1, medium = 2, lowest = 3). The average lowest value is indicated by bold-face types. The identification of axes as A, B and C follows Tab. 5.

Study area	Dimensions	Main gradients	Macro plot						Plot within macro plot					
			Total number of environmental variables			Ranks			Total number of environmental variables			Ranks		
			DCA	LNMDS	GNMDS	DCA	LNMDS	GNMDS	DCA	LNMDS	GNMDS	DCA	LNMDS	GNMDS
TSP	3	A	5	4	3	1	2	3	4	3	4	1	2	1
		B	6	7	8	3	2	1	7	5	9	2	3	1
		C	0	1	0	2	1	2	4	9	8	3	1	2
	Total		11	12	11	6	5	6	15	17	21	6	6	4
LCG	2	A	5	5	5	1	1	1	4	5	5	2	1	1
		B	6	8	6	2	1	2	3	5	3	2	1	2
	Total		11	13	11	3	2	3	7	10	8	4	2	3
LGS	2	A	19	20	18	2	1	3	7	9	8	3	1	2
		B	3	3	3	1	1	1	2	2	2	1	1	1
	Total		22	23	21	3	2	4	9	11	10	4	2	3
CJT	2	A	10	7	9	1	3	2	4	5	1	2	1	3
		B	8	4	5	1	3	2	2	6	1	2	1	3
	Total		18	11	14	2	6	4	6	11	2	4	2	6
LXH	3	A	3	6	4	3	1	2	7	6	7	1	2	1
		B	7	6	6	1	2	2	9	3	7	1	3	2
		C	6	3	6	1	2	1	7	6	7	1	2	1
	Total		16	15	16	5	5	5	22	15	21	3	7	4
Total						19	20	22				21	19	20

Tab. 9. Rank for significance of most strongly related environmental variable to corresponding axes by split-plot GLM analysis at the scales of macro plot and plot within macro plot in all five study areas. The significance was assigned ranks (maximum = 1, medium = 2, lowest = 3). A, B and C mean the main gradient axes. A: first gradient axis, B: second gradient axis and C: third gradient axis. The average lowest value is indicated by bold-face types.

Study area	Dimensions	Main gradients	Macro plot						Plot within macro plot					
			Significance of most strongly related environmental variable			Ranks			Significance of most strongly related environmental variable			Ranks		
			DCA	LNMDS	GNMDS	DCA	LNMDS	GNMDS	DCA	LNMDS	GNMDS	DCA	LNMDS	GNMDS
TSP	3	A	0.0214	0.0320	0.0502	1	2	3	0.0368	0.0214	0.0387	2	1	3
		B	0.0108	0.0125	0.0121	1	3	2	0.0019	0.0019	0.0099	1	1	2
		C	0.1484	0.0686	0.1242	3	1	2	0.0248	0.0037	0.0069	3	1	2
	Total					5	6	7				6	3	7
LCG	2	A	0.0037	0.0056	0.0012	2	3	1	0.0324	0.0282	0.0380	2	1	3
		B	0.0214	0.0104	0.0004	3	2	1	0.0283	0.0097	0.0226	3	1	2
	Total					5	5	2				5	2	5
LGS	2	A	0.0006	0.0008	0.0010	1	2	3	0.0047	0.0066	0.0183	1	2	3
		B	0.0300	0.0104	0.0067	3	2	1	0.0047	0.0399	0.0441	1	2	3
	Total					4	4	4				2	4	6
CJT	2	A	0.0092	0.0167	0.0049	2	3	1	0.0292	0.0206	0.0909	2	1	3
		B	0.0228	0.0263	0.0057	2	3	1	0.0064	0.0001	0.0083	2	1	3
	Total					4	6	2				4	2	6
LXH	3	A	0.0092	0.0022	0.0215	2	1	3	0.0067	0.0023	0.0004	3	2	1
		B	0.0140	0.0226	0.0102	2	3	1	0.0019	0.0101	0.0029	1	3	2
		C	0.0003	0.0777	0.0001	2	3	1	0.0072	0.0005	0.0097	2	1	3
	Total					6	7	5				6	6	6
Total						24	28	20				23	17	30

Correlations between environmental variables

Concentrations of Al and K, contents of total C and N and organic matter content were pairwise more or less strongly positively correlated ($\tau > 0.35$; see Tab. 10, Fig. 7). The content of soil dry matter was negatively correlated with all elements in this subgroup of correlated variables. Soil pH, SO_4 adsorption, aluminium saturation and concentrations of Fe and H made up another subgroup of more or less strongly correlated variables: soil pH, SO_4 adsorption and aluminium saturation were all positively correlated while the concentrations of Fe and H were negatively correlated with all the others ($|\tau| > 0.6$ for H with pH_{CaCl_2}). These two subgroups of correlated variables were connected via the concentration of Ca, which was positively correlated with the concentration of K in the first subgroup and negatively correlated with the aluminium saturation in the other. The concentration of Ca was also positively correlated with base saturation. Inclination was positively correlated with the content of total C, and negatively correlated with the soil depth.

The first subgroup of correlated variables was connected to another group of pairwise correlated tree influence variables via the concentration of Mg, which was positively correlated with the organic matter content in the first subgroup and the litter index in the other. The litter index was positively correlated with the crown cover index ($\tau > 0.6$). The concentration of Mg was also positively correlated with the concentration of Na.

The second subgroup of correlated variables was connected to another group of pairwise correlated topographic variables via the concentration of Mn, which was positively correlated with the soil pH_{CaCl_2} in the first subgroup and the heat index in the other. The heat index was positively correlated with the aspect favourability ($\tau > 0.6$).

PCA ordination of environmental variables

Eigenvalues of the first two PCA axes were 0.190 and 0.149, thus 33.9 % of the variation in measured environmental variables was explained by the first two PCA axes (Fig. 8).

Soil dry matter content and aluminium saturation obtained high loadings on PCA 1, while concentrations of H, Ca, Mg, Fe, Na and K, total C and N in soil and soil organic matter content obtained low (high negative) loadings on this axis. Inclination and Al concentration in soil obtained high loadings on PCA 2, while the lowest (highest negative) loadings were obtained by the heat index and aspect favourability (Fig. 8).

PCA ordination results thus summarised major features of correlations between environmental variables in fewer dimensions (Tab. 10, Figs 7–8). Apparently, the components of soil nutrients that were comprised of cconcentrations of K, Ca, Mg and Na, contents of total C and N and organic matter content were all more or less strongly negatively correlated with the indicators of soil acidity and alkalinity that included soil pH, SO_4 adsorption and aluminium saturation. The soil moisture was negatively correlated with the heat index and aspect favourability. The inclination and varied topography were negatively correlated with the soil depth and the content of soil dry matter.

Tab. 10. Tie Shan Ping: Kendall's rank correlation coefficients τ between 33 environmental variable in the 50 plots (lower triangle), with significant probabilities (upper triangle). Very strong correlations ($|\tau| \geq 4.0$, $P < 0.0001$) are indicated by bold face. n.s means significance probability $P > 0.1$. Numbers and abbreviations for names of environmental variables in accordance with Tab. 2.

	1	2	3	4	5	6	7	8	9	10	11	12	13	14	15	16	17
01 Inclin	*	n.s	.0986	n.s	.0360	n.s	.0031	.0449	.0001	n.s	n.s	.0887	n.s	n.s	n.s	.0141	n.s
02 AspecF	–.0612	*	**.0000**	n.s	n.s	n.s	n.s	n.s	.0033	.0599	n.s	n.s	n.s	n.s	037	n.s	.0905
03 HeatIn	–.1639	**.7364**	*	n.s	n.s	n.s	n.s	n.s	.0025	.0871	n.s	.0543	n.s	n.s	077	n.s	.0178
04 TerraM	.0953	–.0706	–.0903	*	n.s	.0802	n.s	n.s	n.s	n.s	n.s	n.s	n.s	n.s	n.s	n.s	n.s
05 ConvS1	.2184	–.1366	–.1529	.0843	*	.0951	.0131	n.s	.0078	n.s	n.s	n.s	n.s	n.s	n.s	n.s	n.s
06 ConvV1	.1693	–.1346	–.1533	.1832	.1786	*	n.s	.0009	.0023	.0074	n.s	n.s	n.s	n.s	n.s	n.s	n.s
07 ConvS9	.3046	–.0707	–.1009	–.0344	.2645	.0324	*	n.s	.0104	n.s	n.s	n.s	n.s	n.s	n.s	n.s	n.s
08 ConvV9	.2050	–.1169	–.1481	–.0210	–.0189	.3497	–.0637	*	n.s	n.s	n.s	n.s	n.s	n.s	n.s	n.s	n.s
09 SoilDM	–.3873	.2908	.2966	–.1154	–.2743	–.3128	–.2614	–.1064	*	.0064	n.s	n.s	n.s	n.s	n.s	n.s	n.s
10 LitLDM	–.1294	.2084	.1881	.0534	–.0879	–.3073	–.1535	–.1766	.3014	*	n.s	n.s	n.s	n.s	011	n.s	n.s
11 OrgaLD	–.0641	–.1522	–.0936	.0383	.0286	.0205	–.0611	–.0528	–.1509	.1137	*	n.s	n.s	n.s	n.s	n.s	n.s
12 SoilMLM	.1692	–.1568	–.1883	.0676	.0513	.1554	.0694	.1518	–.0922	–.0072	–.0278	*	*	n.s	n.s	.0922	n.s
13 LitteI	.0784	.1016	.0450	–.1049	.0827	.1062	–.0129	–.0925	–.0404	.0062	–.0984	.0000	*	**.0000**	n.s	.0679	n.s
14 CrowCI	.1155	.0489	.0370	–.1223	.0551	.1405	–.0404	.0426	–.1315	–.0385	–.0233	.0099	**.6298**	*	n.s	.0245	n.s
15 RelaCN	–.0352	–.2935	–.2674	–.0017	–.0538	.1112	.0132	–.0358	–.1213	–.3692	–.0143	–.0482	–.0660	–.0543	*	.0594	.0667
16 RelaDN	.2674	.0724	.0624	–.0293	.0974	.0169	.1750	.0959	–.0998	–.0072	–.1768	.1809	.1961	.2425	2078	*	.0471
17 pH_{H_2O}	–.0109	.1678	.2331	.0400	.1603	.0573	.0190	.0717	.1400	.0354	–.0635	–.0677	–.0157	–.0638	1854	.2144	*
18 pH_{CaCl_2}	.0210	–.0017	–.0149	.0648	.2905	.0644	.0631	.0787	.0515	.0773	–.1385	.0819	.0364	–.0116	0886	.2616	.4128
19 Al	.3234	–.0692	–.1029	.0438	.2474	.1421	.2239	.1700	–.2234	.0506	.0074	.1792	.0950	.1430	2395	.1577	.0527
20 Fe	.0790	–.0461	–.0555	.1029	–.1502	.0732	.0427	–.1074	–.1248	–.1932	.1556	.0237	–.0508	–.0526	383	–.3296	–.3145
21 H	–.0274	.0494	.0702	.0573	–.1988	.0336	–.0239	–.1210	–.0312	–.1395	.1926	–.0581	–.1310	–.0773	860	–.3126	–.2207
22 Mn	–.0441	.2454	.3495	.0270	.1155	–.0095	–.0137	–.0888	.0772	.1890	–.0704	–.1792	–.1277	–.0559	2682	.1030	.3541
23 Ca	.1821	–.0115	.0768	.0810	–.0425	.1438	.0752	–.0025	–.2333	–.1704	.0259	–.0925	–.1097	–.0329	771	–.1653	–.1910
24 Mg	–.0141	.0560	.1225	–.0320	–.1624	.0611	–.0308	.0584	.0838	–.1188	.0722	–.0761	–.3078	–.2696	506	–.1483	.1564
25 Na	.0757	.1350	.1209	–.0101	.0026	.1111	.0923	.0228	.0526	–.2014	–.0074	–.1252	–.1424	–.0871	0354	.0368	.1054
26 K	.3001	–.0511	.0327	.0017	.0252	.1731	.1436	.0550	–.2546	–.1291	.0833	–.0254	–.0131	.1299	320	.0444	–.0214
27 C	.3700	.0132	.0196	.1181	.0460	.1386	.2563	–.0093	–.2316	–.0733	–.0963	.1318	–.0770	–.0279	0978	.1351	.0263
28 N	.3053	.0611	.0901	.1235	.0226	.1339	.2118	.0000	–.1846	–.0404	–.0966	.1371	–.1051	–.0099	1701	.1611	.0942
29 BS	.0457	.0478	.1731	–.0371	–.1363	.0267	.0171	–.0093	–.0131	–.1932	–.1056	–.1121	–.1343	–.0855	024	–.0368	–.0478
30 AlS	.1156	–.0395	–.1601	–.0405	.2474	–.0336	.0889	.1362	–.0181	.2035	–.1019	.1694	.1817	.1315	2429	.3013	.1581
31 SO_4	.0524	.0049	–.0588	.0067	.0860	–.0801	.0854	–.0110	.0131	.1704	–.1370	.0450	–.0033	–.0329	0911	.2087	.0725
32 WDM	–.2918	.0329	.0653	–.0691	–.0946	–.2643	–.0820	–.0753	.2234	.0465	.0167	–.0990	–.0262	–.0986	607	–.1011	–.0840
33 LOI	.2286	.0428	.0212	.1214	.0738	.1920	.1179	.0584	–.1363	–.0031	.0204	.1170	–.0508	–.0099	1181	.0746	.1762

Tab. 10 (continued). Tie Shan Ping: Kendall's rank correlation coefficients τ between 33 environmental variable in the 50 plots (lower triangle), with significant probabilities (upper triangle). Very strong correlations ($|\tau| \geq 4.0$, $P < 0.0001$) are indicated by bold face. n.s means significance probability $P > 0.1$. Numbers and abbreviations for names of environmental variables in accordance with Tab. 2.

	18	19	20	21	22	23	24	25	26	27	28	29	30	31	32	33
01 Inclin	n.s	.0011	n.s	n.s	n.s	.0664	n.s	n.s	.0025	.0002	.0021	n.s	n.s	n.s	.0033	.0212
02 AspecF	n.s	n.s	n.s	n.s	.0126	n.s	n.s	n.s	n.s	n.s	n.s	n.s	n.s	n.s	n.s	n.s
03 HeatIn	n.s	n.s	n.s	n.s	.0003	n.s	n.s	n.s	n.s	n.s	n.s	.0762	n.s	n.s	n.s	n.s
04 TerraM	n.s	n.s	n.s	n.s	n.s	n.s	n.s	n.s	n.s	n.s	n.s	n.s	n.s	n.s	n.s	n.s
05 ConvS1	.0050	.0158	n.s	.0524	n.s	n.s	n.s	n.s	n.s	n.s	n.s	n.s	.0158	n.s	n.s	n.s
06 ConvV1	n.s	n.s	n.s	n.s	n.s	n.s	n.s	n.s	.0893	n.s	n.s	n.s	n.s	n.s	.0094	.0594
07 ConvS9	n.s	.0273	n.s	n.s	n.s	n.s	n.s	n.s	n.s	n.s	.0374	n.s	n.s	n.s	n.s	n.s
08 ConvV9	n.s	.0909	n.s	n.s	n.s	n.s	n.s	n.s	n.s	n.s	*	n.s	n.s	n.s	n.s	n.s
09 SoilDM	n.s	.0228	n.s	n.s	n.s	.0174	n.s	n.s	.0095	.0183	.0607	n.s	n.s	n.s	.0228	n.s
10 LitLDM	n.s	n.s	.0787	n.s	.0853	n.s	n.s	.0668	n.s	n.s	n.s	.0787	.0640	n.s	n.s	n.s
11 OrgaLD	n.s	n.s	n.s	.0701	n.s	n.s	n.s	n.s	n.s	n.s	n.s	n.s	n.s	n.s	n.s	n.s
12 SoilMLM	n.s	.0669	n.s	n.s	.0669	n.s	n.s	n.s	n.s	n.s	n.s	n.s	.0833	n.s	n.s	n.s
13 LitteI	n.s	n.s	n.s	n.s	n.s	n.s	.0017	n.s	n.s	n.s	n.s	n.s	.0632	n.s	n.s	n.s
14 CrowCI	n.s	n.s	n.s	n.s	n.s	n.s	.0060	n.s	n.s	n.s	n.s	n.s	n.s	n.s	n.s	n.s
15 RelaCN	n.s	.0170	n.s	n.s	.0075	.0776	n.s	n.s	n.s	n.s	.0911	.0437	.0155	n.s	n.s	n.s
16 RelaDN	.0156	n.s	.0021	.0035	n.s	n.s	n.s	n.s	n.s	n.s	n.s	n.s	.0049	.0514	n.s	n.s
17 pH_{H_2O}	**.0000**	n.s	.0014	.0248	.0003	.0521	n.s	n.s	n.s	n.s	n.s	n.s	n.s	n.s	n.s	n.s
18 pH_{CaCl_2}	*	n.s	**.0000**	**.0000**	.0072	.0141	.0370	n.s	.0990	n.s	n.s	n.s	**.0000**	.0002	n.s	n.s
19 Al	.1246	*	n.s	n.s	n.s	n.s	n.s	n.s	**.0000**	**.0000**	**.0000**	.0011	**.0000**	n.s	**.0000**	**.0000**
20 Fe	**–.5768**	.1020	*	**.0000**	.0053	.0051	.0053	.0179	.0046	.0102	.0302	n.s	**.0000**	.0005	n.s	.0048
21 H	**–.6230**	–.0433	**.7502**	*	n.s	.0039	.0001	.0023	.0080	.0224	.0278	n.s	**.0000**	.0002	n.s	.0041
22 Mn	.2649	.0547	–.2718	–.1167	*	n.s	n.s	n.s	n.s	n.s	.0163	n.s	n.s	n.s	.0205	.0278
23 Ca	–.2418	.0024	.2735	.2816	.1020	*	.0834	n.s	.0001	.0513	.0533	**.0000**	**.0000**	.6099	.0031	.0721
24 Mg	–.2055	.0171	.2718	.3812	.1592	.1690	*	**.0000**	.0136	.0621	.0107	n.s	.0008	.0316	.0113	.0001
25 Na	–.1328	.1298	.2310	.2980	.1935	.1347	**.4824**	*	.0171	.0142	.0088	n.s	.0278	.0834	.0059	.0001
26 K	–.1626	**.4008**	.2767	.2588	.1510	.3763	.2408	.2327	*	**.0000**	**.0000**	n.s	n.s	n.s	**.0000**	**.0000**
27 C	–.0998	**.4073**	.2506	.2229	.1380	.1902	.1820	.2392	**.4547**	*	**.0000**	n.s	n.s	n.s	**.0000**	**.0000**
28 N	–.0646	**.4349**	.2121	.2154	.2351	.1892	.2498	.2563	**.4840**	**.8346**	*	n.s	n.s	n.s	**.0000**	**.0000**
29 BS	–.0734	–.3192	–.0024	.0580	.0971	**.5967**	.1478	.0939	.1135	–.0302	–.0581	*	**.0000**	n.s	n.s	n.s
30 AlS	**.4546**	**.4041**	**–.4057**	**–.5673**	.0041	–.4106	–.3273	–.2147	–.0939	–.0057	.0025	**–.4318**	*	.0107	n.s	n.s
31 SO_4	.3688	.0514	–.3404	–.3682	.1151	.0498	–.2098	–.1690	–.1233	–.1363	–.1384	.1363	.2490	*	n.s	n.s
32 WDM	–.0256	**–.4857**	–.1331	–.1151	–.2261	–.2882	–.2473	–.2686	**–.5233**	**–.4318**	**–.4660**	–.0057	–.0498	–.0433	*	**.0000**
33 LOI	–.0602	**.5102**	.2751	.2800	.2147	.1755	.3861	.3845	**.5053**	**.5314**	**.6200**	–.1069	.0024	–.0955	**–.6653**	*

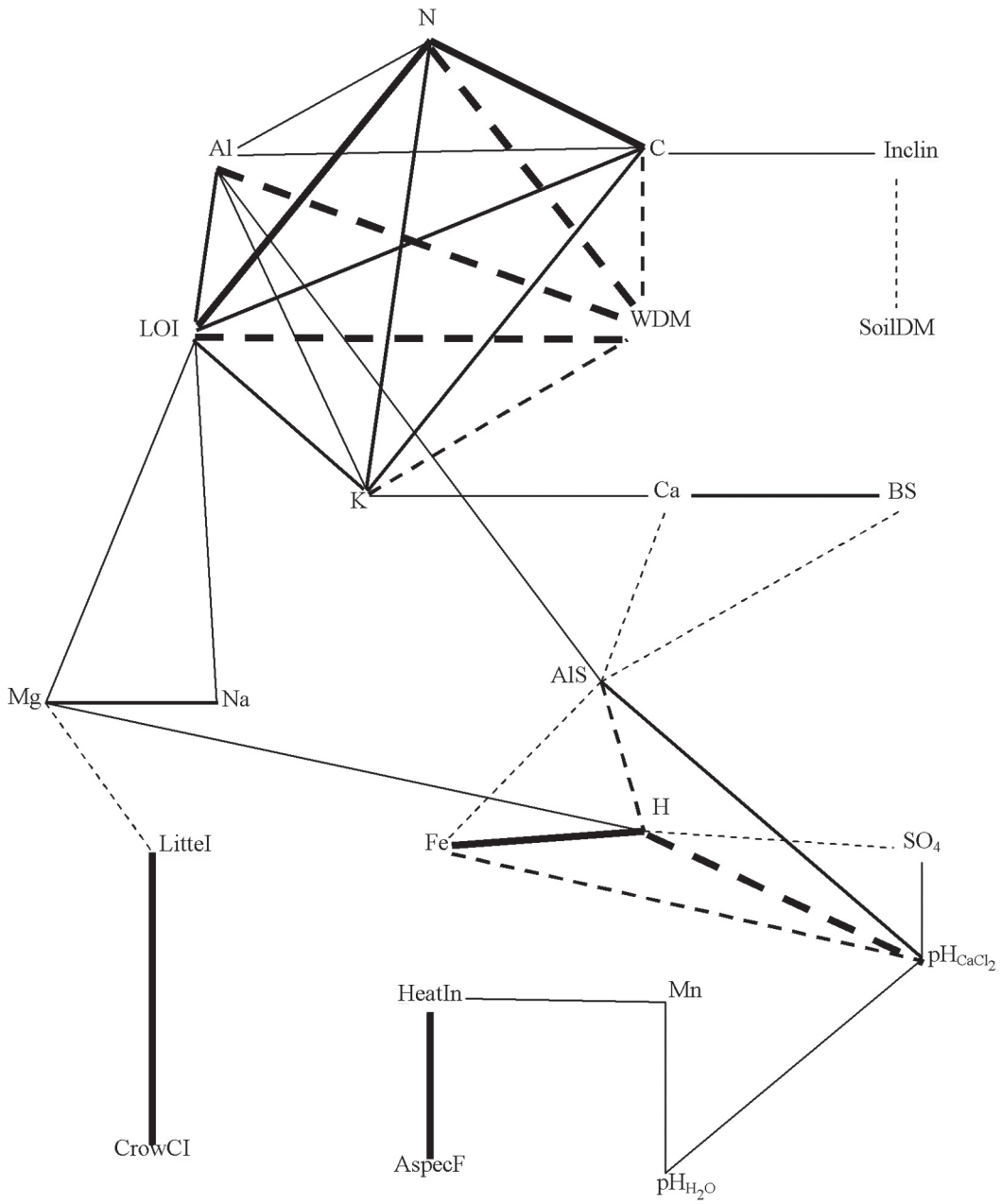

Fig. 7. Tie Shan Ping: Plexus diagram visualizing Kendall's τ between pairs of environmental variables. Significance probabilities for τ are indicated by lines with different thickness (in order of decreasing thickness): $|\tau| \geq 0.60$, $0.45 \leq |\tau| < 0.60$, and $0.35 \leq |\tau| < 0.45$. Continuous lines refer to positive correlations, broken lines to negative.

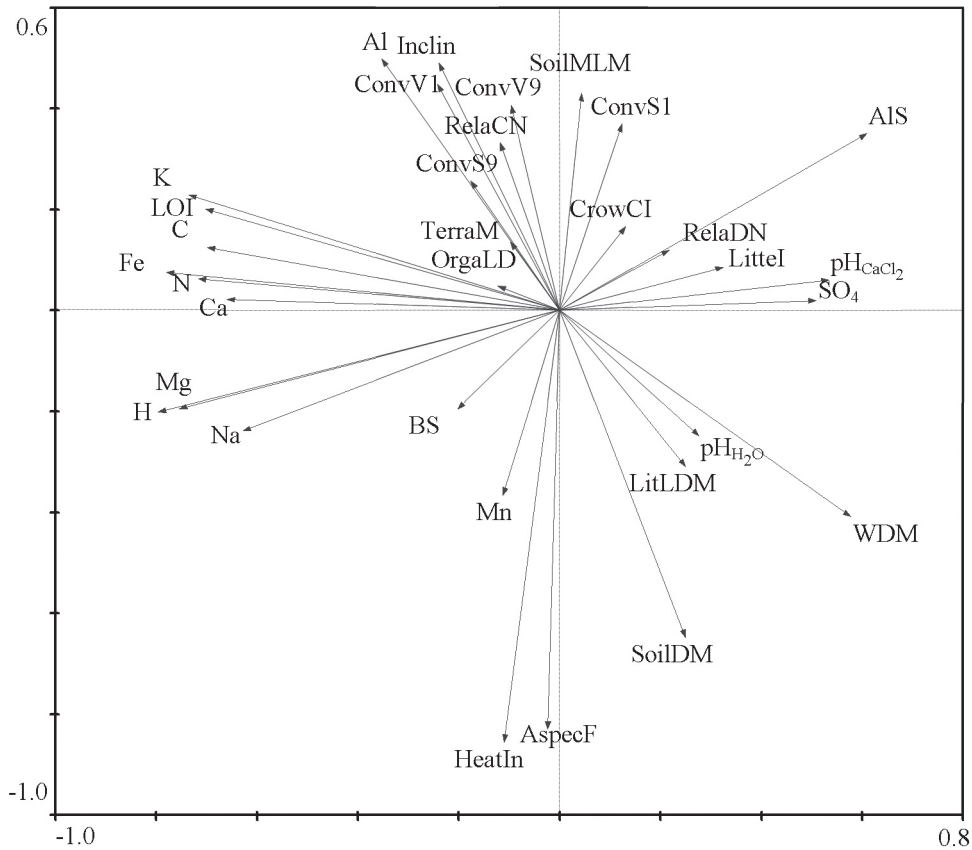

Fig. 8. Tie Shan Ping: PCA ordination of 33 environmental variables (the units and names abbreviated in accordance with Tab. 2), axes 1 (horizontal) and 2 (vertical). Loadings of variables on the ordination axes are shown by heads of variable vectors.

GNMDS ordination

Good correspondence with respect to gradient length, core length and eigenvalues was found between GNMDS 1 and DCA 2, GNMDS 2 and DCA 1, and GNMDS 3 and DCA 3, respectively. There was no marked difference in eigenvalues between GNMDS 1 (DCA 2) and GNMDS 2 (DCA 1), but a marked drop in eigenvalue occurred from GNMDS 2 (DCA 1) to GNMDS 3 (DCA 3), indicating that the first two axes were the major compositional gradients.

The first two axes of the GNMDS ordination of the 50 1-m^2 plots had high eigenvalues (2.6878 and 2.5670, respectively) and gradient lengths of 2.8420 and 2.5140 S.D. units, respectively. Plots number 31, 33 and 34 made up a somewhat isolated group in the space spanned by the first two GNMDS ordination axes while the remaining plots were relatively evenly distributed in the GNMDS ordination (Fig. 9). No plot acted as outliers, as judged by core length (Tab. 11).

The plots were also relatively evenly distributed in space spanned by the first and third GNMDS ordination axes (Fig. 10).

Tab. 11. Ordination of vegetation in the 50 plots in TSP: summary of properties for GNMDS and DCA axes 1–3. Core length means length of the shortest interval containing 90 % of the plots relative to gradient length.

Corresponding axis		Unit	A	B	C
Axis No			GNMDS 1, DCA 2	GNMDS 2, DCA 1	GNMDS 3, DCA 3
GNMDS	Gradient length	HC	1.086	0.984	0.967
		S. D	2.842	2.514	2.440
	Core length	%	0.817	0.801	0.738
	Eigenvalue		2.688	2.567	1.874
DCA	Gradient length	S.D	3.453	2.938	2.527
	Core length	%	0.641	0.776	0.621
	Eigenvalue		0.341	0.429	0.280

Relationships between ordination axes and environmental variables

GNMDS ordination biplots of 50 plots and significant environmental variables

Positions of plot scores in the GNMDS ordination space were related to variation in environmental variables, as indicated by a several environmental variable vectors with significantly directed variation patterns in the ordination space (Figs 9–10). Along the first two axes the following patterns appeared: (1) vectors for concentrations of Fe and H in soil pointed to the right (representing a gradient of increasing concentrations); (2) the soil pH_{CaCl_2} vector pointed leftwards, almost directly in the opposite direction of vectors for Fe and H; (3) the soil and litter-layer depth vectors pointed upwards; and (4) vectors for the topographic variables inclination, concavity/convexity sum at 9-m^2 scale and variance at 1-m^2 scale, concentrations of K and Ca and base saturation in soil, and the number of coniferous trees pointed downwards in the biplots. Thus, plots with relatively high soil pH occurred to the left in the biplots, plots with relatively high concentrations of Fe and H to the right. Plots with a relatively thicker litter layer and deeper soil were situated in the upper part of the biplots, while plots with relatively rougher topography, higher concentrations of Ca and K and higher base saturation in soil, high coniferous tree density were situated in the lower part.

Along the third axis, vectors for total C and N in soil, the crown cover index, and soil moisture pointed towards lower GNMDS 3 scores.

Split-plot GLM analysis of relationships between ordination axes and environmental variables

Variation (in plot scores) along GNMDS axis 1 was partitioned with 71.58 % at the macro-plot scale (i.e. between macro plots) and 28.42 % at the plot scale (i.e. between plots). For the other two ordination axes variation was evenly distributed on the two scales (GNMDS axis 2: 53.11 % at the macro-plot scale and 46.89 % at the plot scale; GNMDS axis 3: 49.64 % at the macro-plot scale and 50.36 % at the plot scale; Tabs 12–14).

At the macro-plot scale, one environmental variable was significantly ($P < 0.05$) and two were indicatively significantly ($P < 0.1$) related to GNMDS axis 1, three and four variables (at the $P < 0.05$ and $P < 0.1$ levels, respectively) were related to GNMDS axis 2, and no variable was related to GNMDS

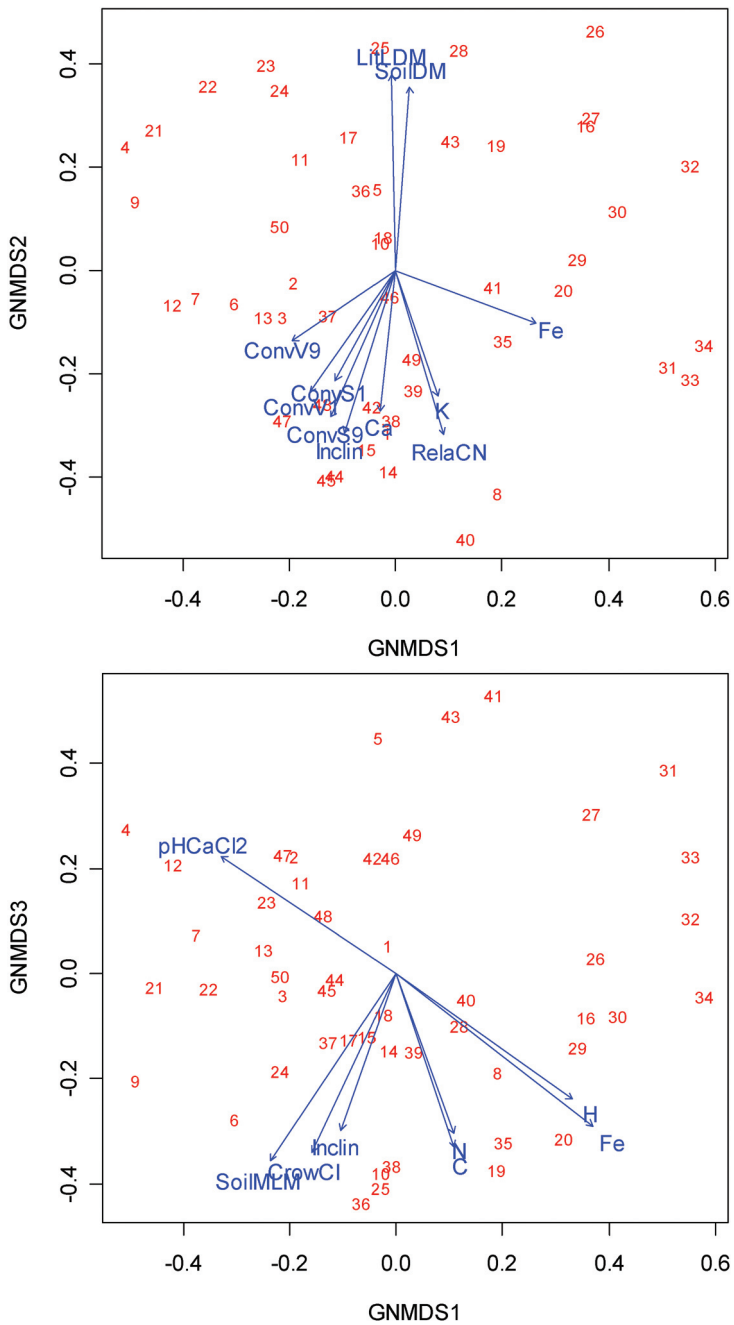

Figs 9–10. Tie Shan Ping: GNMDS ordination biplots of 50 plots (indicated by their number) and significant environmental variables (i.e. with $P < 0.1$ according to goodness-of-fit test; see Tab. 18). Names of variables are abbreviated in accordance with Tab. 2. For each environmental variable the direction of maximum increase and the relative magnitude of increase in this direction are indicated by the direction and length of the vector arrows. Fig. 9. Axes 1 (horizontal) and 2 (vertical). Fig. 10. Axes 1 (horizontal) and 3 (vertical).

axis 3 even at the $P < 0.1$ level. At the plot scale, one environmental variable was significantly and three were indicatively significantly related to GNMDS axis 1, four variables were significantly and four were indicatively significantly related to GNMDS axis 2, and four variables were significantly and four were indicatively significantly related to GNMDS axis 3, respectively (Tabs 12–14)

At the macro-plot scale, the variance of concavity/convexity at the 1-m^2 scale increased significantly along GNMDS axis 1 while indicatively significantly increasing concentrations of soil H, and decreasing soil SO_4 adsorption were observed. At the plot scale, litter-layer depth decreased significantly ($P < 0.05$) while heat index and concentrations of Fe and Na in soil increased ($P < 0.1$) along GNMDS axis 1 (Tab. 12).

At the macro-plot scale, GNMDS axis 2 was strongly positively related to soil depth and litter-layer depth, and negatively related to the variance of concavity/convexity at 9-m^2 scale and the concentration of Ca in soil; while indicatively significantly positively related to litter index, negatively related to the number of coniferous trees and soil base saturation. At the plot scale, GNMDS axis 2 was strongly negatively related to inclination and aspect favourability, and positively related to litter-layer depth and the number of broadleaved trees; while indicatively significantly negatively related to litter index, positively related to soil depth, soil pH_{H_2O} and the concentration of Mn in soil (Tab. 13)

At the macro-plot scale, no variable was related to GNMDS axis 3. At the plot scale, GNMDS axis 3 was strongly related to decreasing the concavity/convexity sum index at 1-m^2 scale, the variance of concavity/convexity at 1-m^2 scale and the concentration of H in soil, increasing soil depth and aluminium saturation in soil, while indicatively significantly related to increasing litter-layer depth and soil dry matter, and decreasing the concentration of Fe and Ca in soil (Tab. 14).

Kendall's rank correlation between ordination axes and environmental variables

GNMDS axis 1 was not strongly correlated ($|\tau| > 0.30$) with any variable. The highest absolute values for τ were observed for soil pH (PH_{CaCl_2}, $\tau = -0.291$) which decreased, and the concentrations of Fe ($\tau = 0.285$) and H ($\tau = 0.238$) in soil, both increasing along this axis (Fig. 9, Tab. 12).

GNMDS axis 2 was most strongly negatively correlated with topography (inclination, $\tau = -0.3030$), tree density (the number of conifer trees, $\tau = -0.315$), and positively correlated with soil depth ($\tau = 0.355$) and litter-layer depth ($\tau = 0.4080$). The variables indicatively significantly negatively correlated with this axis were topography (the variance of concavity/convexity at the 1-m^2 scale, $\tau = -0.2010$; the sum of concavity/convexity at the 9-m^2 scale, $\tau = -0.2940$) and the concentration of K and Ca (K, $\tau = -0.2160$; Ca, $\tau = -0.2390$) and soil base saturation ($\tau = -0.2050$) (Tab. 13) in soil.

The content of total C in soil was most significantly negatively correlated with GNMDS axis 3 (C, $\tau = -0.3010$). The variables indicatively significantly positively correlated with this axis were soil depth ($\tau = 0.2070$) and the content of soil dry matter ($\tau = 0.2230$), and negatively correlated with this axis were topography (inclination, $\tau = -0.2640$), soil moisture ($\tau = -0.2590$) and the content of total N in soil (N, $\tau = -0.2600$) (Tab. 14).

Relationships between ordination axes and species number variables

Split-plot GLM analysis of relationships between ordination axes and species number variables

No variable was related to GNMDS axis 1 (Tab. 15) and GNMDS axis 3 (Tab. 17). At both macro-plot and plot scales, the number of bryophyte species was strongly negatively related to GNMDS axis 2 (Tab. 16).

Tab. 12. Tie Shan Ping: Split-plot GLM analysis and Kendall's nonparametric correlation coefficient τ between GNMDS axis 1 and 33 environmental variables (predictor) in the 50 plots. df_{resid}: degrees of freedom for the residuals; *SS*: total variation; *FVE*: fraction of total variation attributable to a given scale (macro plot or plot); SS_{expl}/SS: fraction of the variation attributable to the scale in question, explained by a variable; *r*: model coefficient (only given when significant at the α = 0.1 level, otherwise blank); *F*: *F* statistic for test of the hypothesis that *r* = 0 against the two-tailed alternative. Split-plot GLM relationships significant at level α = 0.05, *P*, *F*, *r* and SS_{expl}/SS, and Kendall's nonparametric correlation coefficient $|\tau| \geq 0.30$ are given in bold face. Numbers and abbreviations for names of environmental variables are in accordance with Tab. 2.

Predictor	Dependent variable = GNMDS 1 (*SS* = 26.4784)								Correlation between predictor and GNMDS 1
	Error level								
	Macro plot df_{resid} = 8 $SS_{macro\ plot}$ = 18.9544 *FVE* = 0.7158 of *SS*				Plot within macro plot df_{resid} = 39 SS_{plot} = 7.5240 *FVE* = 0.2842 of *SS*				Total
	$SS_{expl}/SS_{macro\ plot}$	*r*	*F*	*P*	SS_{expl}/SS_{plot}	*r*	*F*	*P*	τ
Inclin	0.0117		0.0943	0.7666	0.0338		1.3640	0.2499	-0.092
AspecF	0.0226		0.1846	0.6788	0.0151		0.5975	0.4442	0.049
HeatIn	0.0044		0.0354	0.8555	0.0782	1.6364	3.3066	0.0767	0.043
TerraM	0.0000		0.0001	0.9915	0.0192		0.7614	0.3882	-0.110
ConvS1	0.0309		0.2554	0.6269	0.0362		1.4667	0.2332	-0.175
ConvV1	**0.4099**	**–2.8336**	**5.5577**	**0.0461**	0.0436		1.7792	0.1900	-0.165
ConvS9	0.1374		1.2745	0.2916	0.0023		0.0888	0.7672	-0.147
ConvV9	0.2155		2.1981	0.1765	0.0017		0.0655	0.7994	-0.162
SoilDM	0.0158		0.1285	0.7293	0.0430		1.7502	0.1936	0.043
LitLDM	0.0478		0.4013	0.5441	**0.1103**	**–0.7718**	**4.8360**	**0.0339**	-0.094
OrgaLD	0.1023		0.9118	0.3676	0.0092		0.3605	0.5517	0.046
SoilMLM	0.2193		2.2478	0.1722	0.0003		0.0132	0.9092	-0.194
LitteI	0.0782		0.6790	0.4338	0.0026		0.1007	0.7526	-0.056
CrowCI	0.2201		2.2572	0.1714	0.0077		0.3009	0.5865	-0.072
RelaCN	0.0216		0.1767	0.6853	0.0245		0.9783	0.3287	0.115
RelaDN	0.2325		2.4230	0.1582	0.0163		0.6445	0.4269	-0.179
pH_{H_2O}	0.0220		0.1799	0.6826	0.0664		2.7744	0.1038	-0.152
pH_{CaCl_2}	0.2797		3.1060	0.1160	0.0529		2.1789	0.1479	-0.291
Al	0.0242		0.1985	0.6677	0.0002		0.0078	0.9301	-0.107
Fe	0.2858		3.2009	0.1114	0.0787	0.6181	3.3339	0.0755	0.285
H	0.3305	2.6171	3.9491	0.0821	0.0362		1.4629	0.2338	0.238
Mn	0.0224		0.1835	0.6796	0.0349		1.4116	0.2420	-0.096
Ca	0.0011		0.0086	0.9282	0.0001		0.0058	0.9399	-0.007
Mg	0.0536		0.4530	0.5199	0.0351		1.4205	0.2405	0.109
Na	0.0004		0.0031	0.9571	0.0942	0.4287	4.0572	0.0509	0.071
K	0.0066		0.0535	0.8229	0.0527		2.1696	0.1488	0.123
C	0.0159		0.1296	0.7282	0.0129		0.5095	0.4796	0.081
N	0.0090		0.0723	0.7948	0.0212		0.8434	0.3641	0.032
BS	0.0169		0.1376	0.7203	0.0050		0.1968	0.6598	-0.048
AlS	0.0967		0.8562	0.3819	0.0215		0.8573	0.3602	-0.145
SO_4	0.3401	–5.8347	4.1232	0.0768	0.0332		1.3408	0.2539	-0.184
WDM	0.0673		0.5777	0.4690	0.0005		0.0184	0.8929	0.082
LOI	0.0124		0.1001	0.7598	0.0040		0.1560	0.6950	-0.042

Tab. 13. Tie Shan Ping: Split-plot GLM analysis and Kendall's nonparametric correlation coefficient τ between GNMDS axis 2 and 33 environmental variables (predictor) in the 50 plots. df_{resid}: degrees of freedom for the residuals; *SS*: total variation; *FVE*: fraction of total variation attributable to a given scale (macro plot or plot); SS_{expl}/SS: fraction of the variation attributable to the scale in question, explained by a variable; *r*: model coefficient (only given when significant at the α = 0.1 level, otherwise blank); *F*: *F* statistic for test of the hypothesis that *r* = 0 against the two-tailed alternative. Split-plot GLM relationships significant at level α = 0.05, *P*, *F*, *r* and SS_{expl}/SS, and Kendall's nonparametric correlation coefficient $|\tau| \geq 0.30$ are given in bold face. Numbers and abbreviations for names of environmental variables are in accordance with Tab. 2.

Predictor	Dependent variable = GNMDS 2 (*SS* = 23.0375)								Correlation between predictor and GNMDS 2
	Error level								
	Macro plot df_{resid} = 8 $SS_{macro\ plot}$ = 12.2357 *FVE* = 0.5311 of *SS*				Plot within macro plot df_{resid} = 39 SS_{plot} = 10.8018 *FVE* = 0.4689 of *SS*				Total
	$SS_{expl}/SS_{macro\ plot}$	*r*	*F*	*P*	SS_{expl}/SS_{plot}	*r*	*F*	*P*	τ
Inclin	0.2571		2.7683	0.1347	**0.1484**	**–1.4610**	**6.7967**	**0.0129**	**-0.303**
AspecF	0.1497		1.4087	0.2693	**0.0973**	**–2.1884**	**4.2034**	**0.0471**	0.135
HeatIn	0.0495		0.4165	0.5367	0.0379		1.5373	0.2224	0.139
TerraM	0.1436		1.3419	0.2801	0.0588		2.4356	0.1267	0.047
ConvS1	0.1640		1.5688	0.2457	0.0468		1.9163	0.1741	-0.149
ConvV1	0.2417		2.5501	0.1490	0.0248		0.9909	0.3257	-0.201
ConvS9	**0.4916**	**–3.2596**	**7.7360**	**0.0239**	0.0886	–0.7074	3.7925	0.0587	-0.294
ConvV9	0.1015		0.9035	0.3697	0.0002		0.0068	0.9346	-0.168
SoilDM	**0.4661**	**2.4232**	**6.9842**	**0.0296**	0.0717	1.1431	3.0128	0.0905	**0.355**
LitLDM	**0.5368**	**3.0487**	**9.2719**	**0.0159**	**0.1533**	**1.0902**	**7.0629**	**0.0114**	**0.408**
OrgaLD	0.0069		0.0555	0.8197	0.0578		2.3910	0.1301	0.083
SoilMLM	0.0548		0.4635	0.5152	0.0023		0.0914	0.7640	0.104
LitteI	0.3250	1.7508	3.8511	0.0853	0.0669		2.7947	0.1026	0.054
CrowCI	0.1268		1.1612	0.3126	0.0100		0.3954	0.5331	0.049
RelaCN	0.3258	–1.3257	3.8650	0.0849	0.0654		2.7285	0.1066	**-0.315**
RelaDN	0.0158		0.1283	0.7295	**0.1441**	**0.8742**	**6.5661**	**0.0144**	0.077
pH_{H_2O}	0.0269		0.2215	0.6505	0.0861	0.7641	3.6724	0.0627	0.073
pH_{CaCl_2}	0.0163		0.1323	0.7255	0.0150		0.5937	0.4456	-0.022
Al	0.0178		0.1448	0.7134	0.0106		0.4194	0.5210	-0.048
Fe	0.0096		0.0774	0.7880	0.0453		1.8508	0.1815	-0.091
H	0.0023		0.0183	0.8958	0.0075		0.2951	0.5901	-0.027
Mn	0.0010		0.0077	0.9322	0.0821	0.9160	3.4904	0.0693	0.055
Ca	0.3808	–1.9342	4.9196	0.0574	0.0135		0.5329	0.4697	-0.239
Mg	0.1435		1.3407	0.2803	0.0199		0.7919	0.3790	-0.042
Na	0.1433		1.3386	0.2807	0.0056		0.2210	0.6409	-0.056
K	0.2884		3.2419	0.1095	0.0356		1.4378	0.2377	-0.216
C	0.1751		1.6983	0.2288	0.0054		0.2109	0.6486	-0.161
N	0.1134		1.0234	0.3413	0.0002		0.0098	0.9217	-0.096
BS	0.3433	–2.0693	4.1819	0.0751	0.0007		0.0259	0.8729	-0.205
AlS	0.1032		0.9205	0.3654	0.0009		0.0339	0.8550	0.091
SO_4	0.1658		1.5895	0.2429	0.0025		0.0971	0.7570	-0.007
WDM	0.1132		1.0208	0.3419	0.0004		0.0136	0.9077	0.063
LOI	0.0686		0.5895	0.4647	0.0058		0.2280	0.6357	0.007

Tab. 14. Tie Shan Ping: Split-plot GLM analysis and Kendall's nonparametric correlation coefficient τ between GNMDS axis 3 and 33 environmental variables (predictor) in the 50 plots. df_{resid}: degrees of freedom for the residuals; *SS*: total variation; *FVE*: fraction of total variation attributable to a given scale (macro plot or plot); SS_{expl}/SS: fraction of the variation attributable to the scale in question, explained by a variable; *r*: model coefficient (only given when significant at the α = 0.1 level, otherwise blank); *F*: *F* statistic for test of the hypothesis that *r* = 0 against the two-tailed alternative. Split-plot GLM relationships significant at level α = 0.05, *P*, *F*, *r* and SS_{expl}/SS, and Kendall's nonparametric correlation coefficient $|\tau| \geq 0.30$ are given in bold face. Numbers and abbreviations for names of environmental variables are in accordance with Tab. 2.

Predictor	Dependent variable = GNMDS 3 (*SS* = 17.5299)								Correlation between predictor and GNMDS 3
	Error level								
	Macro plot df_{resid} = 8 $SS_{macro\ plot}$ = 8.7015 *FVE* = 0.4964 of *SS*				Plot within macro plot df_{resid} = 39 SS_{plot} = 8.8284 *FVE* = 0.5036 of *SS*				Total
	$SS_{expl}/SS_{macro\ plot}$	*r*	*F*	*P*	SS_{expl}/SS_{plot}	*r*	*F*	*P*	τ
Inclin	0.1785		1.7380	0.2239	0.0342		1.3792	0.2474	-0.264
AspecF	0.0070		0.0566	0.8179	0.0045		0.1776	0.6757	0.046
HeatIn	0.0175		0.1425	0.7156	0.0046		0.1817	0.6723	0.060
TerraM	0.0269		0.2214	0.6506	0.0084		0.3305	0.5687	-0.083
ConvS1	0.0084		0.0678	0.8011	0.0817	–0.7794	3.4718	0.0700	-0.102
ConvV1	0.0023		0.0186	0.8949	**0.1914**	**–0.9587**	**9.2341**	**0.0042**	-0.196
ConvS9	0.0935		0.8256	0.3901	0.0289		1.1620	0.2877	-0.147
ConvV9	0.0635		0.5425	0.4824	0.0207		0.8241	0.3696	0.011
SoilDM	0.0309		0.2552	0.6270	**0.1129**	**1.2965**	**4.9627**	**0.0317**	0.207
LitLDM	0.1394		1.2958	0.2879	0.0913	0.7606	3.9193	0.0548	0.016
OrgaLD	0.0282		0.2318	0.6431	0.0157		0.6216	0.4352	-0.011
SoilMLM	0.2492		2.6551	0.1419	0.0449		1.8325	0.1836	-0.259
LitteI	0.1601		1.5248	0.2519	0.0074		0.2893	0.5938	-0.175
CrowCI	0.2963		3.3688	0.1038	0.0409		1.6637	0.2047	-0.148
RelaCN	0.1893		1.8678	0.2089	0.0046		0.1788	0.6747	0.162
RelaDN	0.1223		1.1148	0.3219	0.0103		0.4061	0.5277	-0.069
pH_{H_2O}	0.0747		0.6461	0.4447	0.0023		0.0894	0.7666	0.069
pH_{CaCl_2}	0.0810		0.7052	0.4254	0.0017		0.0669	0.7972	0.036
Al	0.2414		2.5457	0.1493	0.0215		0.8560	0.3605	-0.176
Fe	0.0247		0.2022	0.6649	0.0641		2.6702	0.1103	-0.136
H	0.0039		0.0311	0.8644	**0.1003**	**–0.6246**	**4.3497**	**0.0436**	-0.118
Mn	0.0000		0.0000	0.9954	0.0022		0.0879	0.7685	0.022
Ca	0.0068		0.0545	0.8213	0.0755	–0.6691	3.1842	0.0821	-0.109
Mg	0.2665		2.9066	0.1266	0.0480		1.9686	0.1685	0.102
Na	0.0878		0.7698	0.4059	0.0020		0.0781	0.7813	0.029
K	0.1602		1.5267	0.2517	0.0068		0.2656	0.6092	-0.151
C	0.2477		2.6335	0.1433	0.0409		1.6612	0.2050	**-0.301**
N	0.2046		2.0575	0.1894	0.0374		1.5156	0.2257	-0.260
BS	0.1069		0.9572	0.3566	0.0285		1.1450	0.2912	0.063
AlS	0.1595		1.5180	0.2529	**0.1493**	**0.8417**	**6.8422**	**0.0126**	-0.004
SO_4	0.0121		0.0977	0.7626	0.0001		0.0024	0.9614	0.025
WDM	0.0969		0.8584	0.3813	0.0875	0.7588	3.7409	0.0604	0.223
LOI	0.0656		0.5612	0.4752	0.0353		1.4264	0.2396	-0.162

Tab. 15. Tie Shan Ping: Split-plot GLM analysis and Kendall's nonparametric correlation coefficient τ between GNMDS axis 1 and two species number variables (predictor) in the 50 plots. df_{resid}: degrees of freedom for the residuals; *SS*: total variation; *FVE*: fraction of total variation attributable to a given scale (macro plot or plot); SS_{expl}/SS: fraction of the variation attributable to the scale in question, explained by a variable; *r*: model coefficient (only given when significant at the α = 0.1 level, otherwise blank); *F*: *F* statistic for test of the hypothesis that *r* = 0 against the two-tailed alternative. Split-plot GLM relationships significant at level α = 0.05, *P*, *F*, *r* and SS_{expl}/SS, and Kendall's nonparametric correlation coefficient $|\tau| \geq 0.30$ are given in bold face.

Predictor (number of species)	Dependent variable = GNMDS 1 (*SS* = 26.4784)								Correlation between predictor and GNMDS 1
	Error level								
	Macro plot df_{resid} = 8 $SS_{macro\ plot}$ = 18.9544 *FVE* = 0.7158 of *SS*				Plot within macro plot df_{resid} = 39 SS_{plot} = 7.5240 *FVE* = 0.2842 of *SS*				Total
	$SS_{expl}/SS_{macro\ plot}$	*r*	*F*	*P*	SS_{expl}/SS_{plot}	*r*	*F*	*P*	τ
Vascular plants	0.0002		0.0014	0.9712	0.0004		0.0138	0.9070	0.028
Bryophyte species	0.0162		0.1316	0.7261	0.0509		2.0934	0.1559	–0.003

Tab. 16. Tie Shan Ping: Split-plot GLM analysis and Kendall's nonparametric correlation coefficient τ between GNMDS axis 2 and two species number variables (predictor) in the 50 plots. df_{resid}: degrees of freedom for the residuals; *SS*: total variation; *FVE*: fraction of total variation attributable to a given scale (macro plot or plot); SS_{expl}/SS: fraction of the variation attributable to the scale in question, explained by a variable; *r*: model coefficient (only given when significant at the α = 0.1 level, otherwise blank); *F*: *F* statistic for test of the hypothesis that r = 0 against the two-tailed alternative. Split-plot GLM relationships significant at level α = 0.05, *P*, *F*, *r* and SS_{expl}/SS, and Kendall's nonparametric correlation coefficient $|\tau| \geq 0.30$ are given in bold face.

Predictor (number of species)	Dependent variable = GNMDS 2 (*SS* = 23.0375)								Correlation between predictor and GNMDS 2
	Error level								
	Macro plot df_{resid} = 8 $SS_{macro\ plot}$ = 12.2357 *FVE* = 0.5311 of *SS*				Plot within macro plot df_{resid} = 39 SS_{plot} = 10.8018 *FVE* = 0.4689 of *SS*				Total
	$SS_{expl}/SS_{macro\ plot}$	*r*	*F*	*P*	SS_{expl}/SS_{plot}	*r*	*F*	*P*	τ
Vascular plants	0.0931		0.8212	0.3913	0.0022		0.0878	0.7686	–0.098
Bryophyte species	**0.5503**	**–0.3167**	**9.7903**	**0.0140**	**0.2645**	**–0.2292**	**14.0290**	**0.0006**	**–0.498**

Kendall's rank correlation between ordination axes and species number variables

The only strong correlation observed between an ordination axis and species number variables was the negative one between GNMDS axis 2 and bryophyte number (Tabs 15–17).

Isoline diagrams for environmental and species number variables

A total of 14 environmental variables and one species number variables satisfied the criteria for making two-dimensional isoline diagrams (Tab. 18, Figs 11–24).

The distribution of species abundance in the GNMDS ordination

Out of a total of 65 species, 31 were found in at least 5 of the 50 plots (Tab. 19, Figs 24–54).

Taxiphyllum subarcuatum (Fig. 54) and *Leucobryum bowringii* (Fig. 53), typical examples of bryophyte species with wide ecological amplitude, were abundant in most plots, but were absent from plots with high GNMDS 2 scores (i.e. on sites with low inclination and with thick litter layer).

Smilax china (Fig. 45) and *Symplocos sumunita* (Fig. 48), typical examples of vascular plants with wide ecological amplitude, were abundant in most plots.

Miscanthus sinensis (Fig. 36) was abundant in most plots (notably those with high GNMDS 2 scores in the middle part of GNMDS 1; negatively related to bare soil and low and high soil pH, respectively).

Tab. 17. Tie Shan Ping: Split-plot GLM analysis and Kendall's nonparametric correlation coefficient τ between GNMDS axis 3 and two species number variables (predictor) in the 50 plots. df_{resid}: degrees of freedom for the residuals; *SS*: total variation; *FVE*: fraction of total variation attributable to a given scale (macro plot or plot); SS_{expl}/SS: fraction of the variation attributable to the scale in question, explained by a variable; *r*: model coefficient (only given when significant at the α = 0.1 level, otherwise blank); *F*: *F* statistic for test of the hypothesis that $r = 0$ against the two-tailed alternative. Split-plot GLM relationships significant at level α = 0.05, *P*, *F*, *r* and SS_{expl}/SS, and Kendall's nonparametric correlation coefficient $|\tau| \geq 0.30$ are given in bold face.

Predictor (number of species)	Dependent variable = GNMDS 3 (*SS* = 17.5299)								Correlation between predictor and GNMDS 3
	Error level								
	Macro plot $df_{resid} = 8$ $SS_{macro\ plot} = 8.7015$ *FVE* = 0.4964 of *SS*				Plot within macro plot $df_{resid} = 39$ $SS_{plot} = 8.8284$ *FVE* = 0.5036 of *SS*				Total
	$SS_{expl}/SS_{macro\ plot}$	*r*	*F*	*P*	SS_{expl}/SS_{plot}	*r*	*F*	*P*	τ
Vascular plants	0.0064		0.0518	0.8257	0.0529		2.1793	0.1479	0.090
Bryophyte species	0.0039		0.0312	0.8642	0.0351		1.4167	0.2411	–0.081

Tab. 18. Tie Shan Ping. Environmental and species number variables for which two-dimensional isoline diagrams were made: *P* value for relationship with GNMDS axis assessed by split-plot GLM (two scales = error levels), Kendall's correlation coefficient τ with axis, and R^2 between the original and predicted values (according to the isoline diagrams for the variable), used as a measure of goodness-of-fit of the isolines. Isoline diagrams were made for variables with split-plot GLM $P < 0.05$ at the macro plot or the plot scale and/or Kendall's correlation coefficient $|\tau| \geq 0.3$ with one GNMDS axis. *P* values < 0.05 and/or $|\tau| \geq 0.30$ in bold face. Numbers and abbreviations for names of environmental variables in accordance with Tab. 2 (NBS = number of bryophyte species).

Ordination axis	Variable names	The split plot GLM Error level		Kendall's ccorrelation between variable and ordination axis	Goodness-of-fit of the isolines
		$P_{\text{macro plot}}$	P_{plot}	τ_{total}	R^2
GNMDS 1	ConvV1	**0.0461**	0.1900	–0.165	0.1766
	LitLDM	0.5441	**0.0339**	–0.094	0.3490
GNMDS 2	Inclin	0.1347	**0.0129**	**–0.303**	0.1924
	AspecF	0.2693	**0.0471**	0.135	0.0334
	ConvS9	**0.0239**	0.0587	–0.294	0.1783
	SoilDM	**0.0296**	0.0905	**0.355**	0.4147
	LitLDM	**0.0159**	**0.0114**	**0.408**	0.3490
	RelaCN	0.0849	0.1066	**–0.315**	0.2960
	RelaDN	0.7295	**0.0144**	0.077	0.2933
	NBS	**0.0140**	**0.0006**	**–0.498**	0.6570
GNMDS 3	ConvV1	0.8949	**0.0042**	–0.196	0.1934
	SoilDM	0.6270	**0.0317**	0.207	0.4267
	H	0.8644	**0.0436**	–0.118	0.1955
	C	0.1433	0.2050	**–0.301**	0.1301
	AlS	0.2529	**0.0126**	–0.004	0.0893

Examples of species restricted to plots in right part of the GNMDS ordination diagram (related to a more plane surface and a thicker litter layer) were *Ardisia pussilla* (Fig. 25), *Dicranopteris pedata* (Fig. 29) and *Pteridium aquilinum* (Fig. 40).

Examples of species restricted to plots in left part of the GNMDS ordination diagram (related to a higher soil pH and a more varied surface) were *Dryopteris erythrosora* (Fig. 30) and *Woodwardia japonica* (Fig. 49).

Dryopeteris fuscipes (Fig. 31) and *Lophatherum gracille* (Fig. 34) were abundant in most plots (over most of the GNMDS ordination diagram except the uppermost part; positively related to inclination).

Examples of species restricted to plots in lower left part of the GNMDS ordination diagram (related to high inclination, a varied surface and favourable light conditions) were *Setaria palmifolia* (Fig. 44) and *Stenoloma chusanum* (Fig. 46).

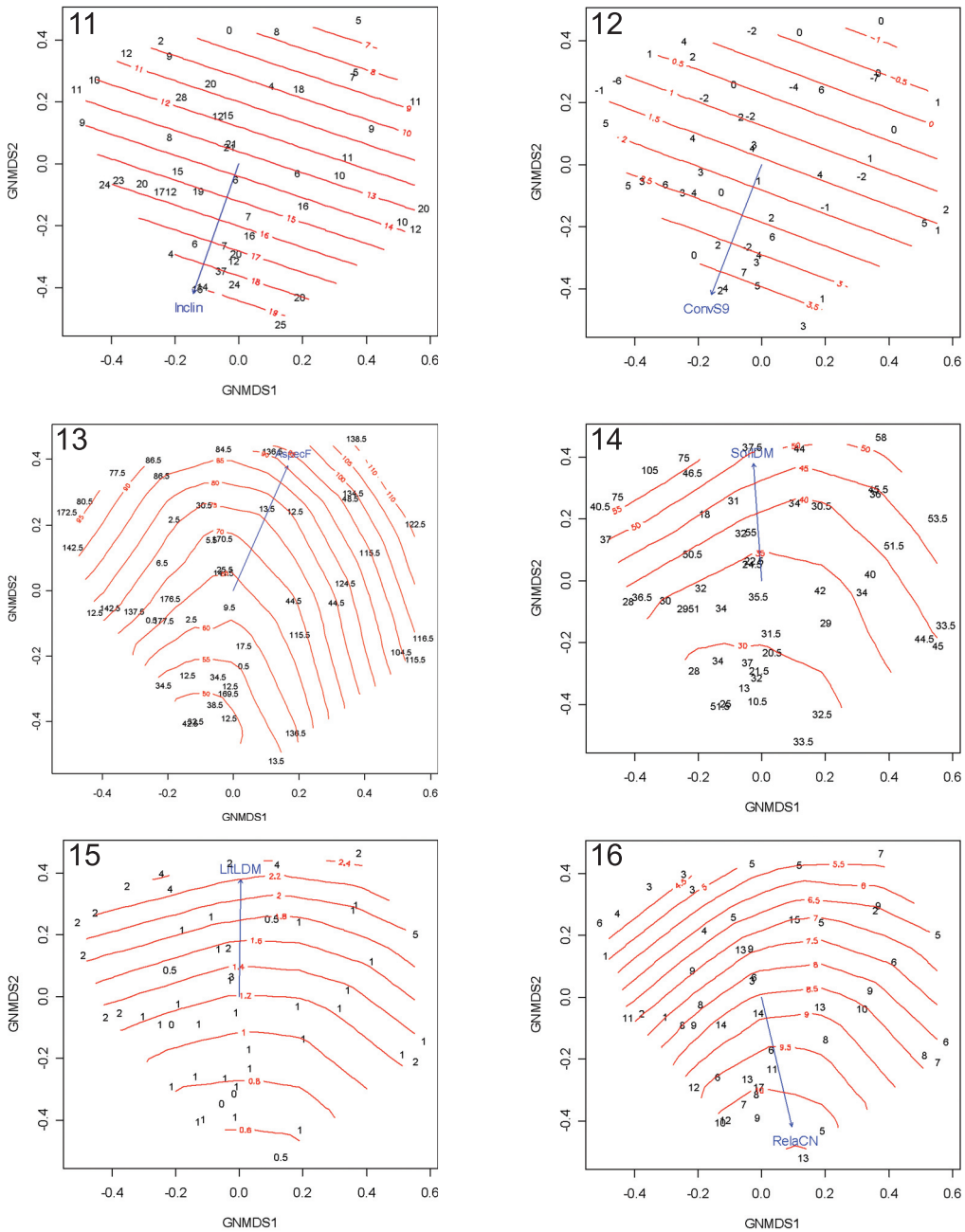

Figs 11–16. Tie Shan Ping: Isolines for environmental variables in the GNMDS ordination of 50 plots, axes 1 (horizontal) and 2 (vertical). Values for the environmental variables are plotted onto plots' positions. Fig. 11. Inclin (R^2 = 0.1924). Fig. 12. ConvS9 (R^2 = 0.1783). Fig. 13. AspecF (R^2 = 0.0334). Fig. 14. SoilDM (R^2 = 0.4147). Fig. 15. LitLDM (R^2 = 0.3490). Fig. 16. RelaCN (R^2 = 0.2960). R^2 refers to the coefficient of determination between original and smoothened values as interpolated from the isolines. Numbers and abbreviations for names of environmental variables are in accordance with Tab. 2.

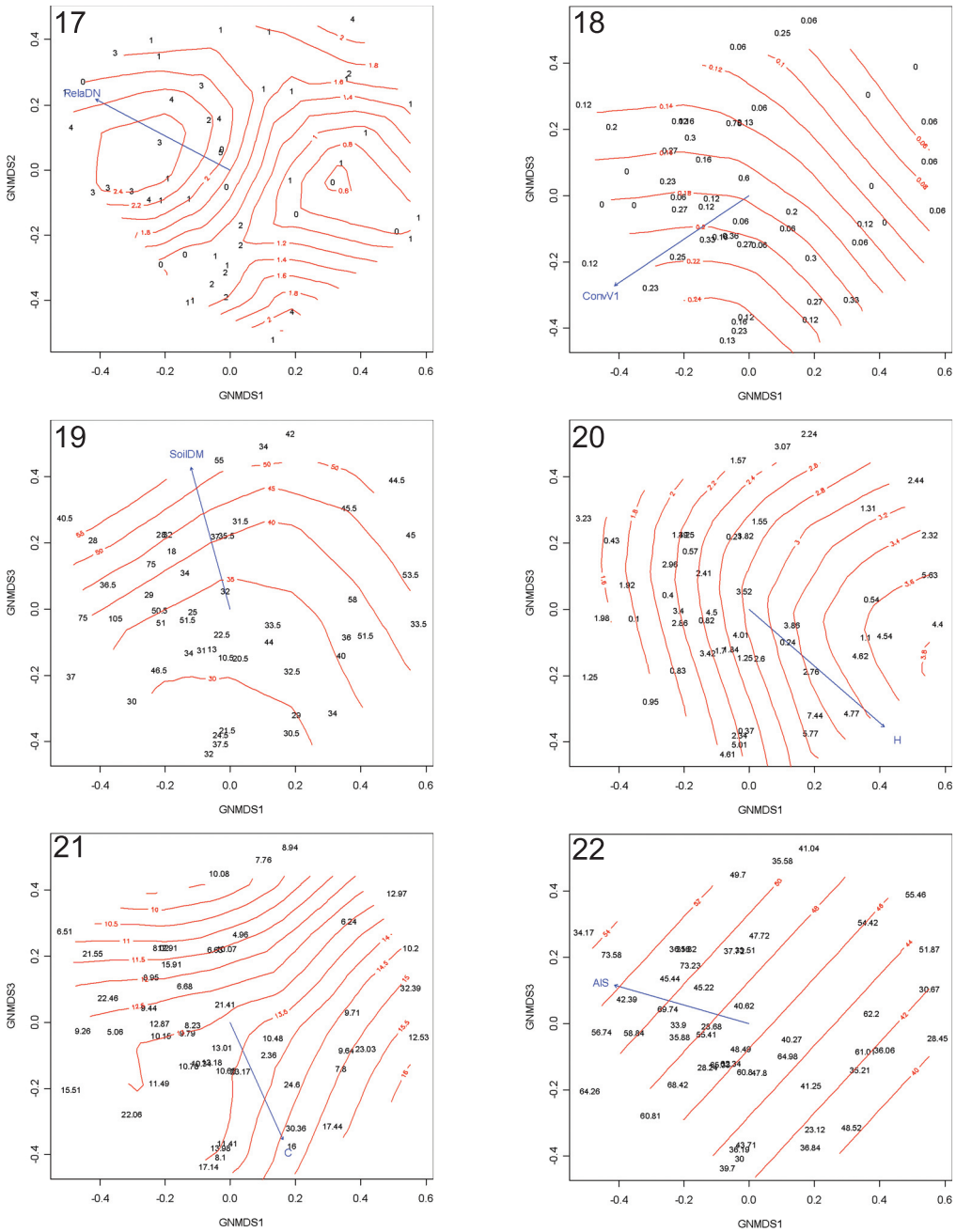

Figs 17–22. Tie Shan Ping: Isolines for environmental variables in the GNMDS ordination of 50 plots. Values for the environmental variables are plotted onto plots' positions. Fig. 17. RelaDN (R^2 = 0.2933), axes 1 (horizontal) and 2 (vertical). Fig. 18. ConvV1 (R^2 = 0.1934), axes 1 (horizontal) and 3 (vertical). Fig. 19. SoilDM (R^2 = 0.4267), axes 1 (horizontal) and 3 (vertical). Fig. 20. H (R^2 = 0.1787). Fig. 21. C (R^2 = 0.1301). Fig. 22. AlS (R^2 = 0.0893). R^2 refers to the coefficient of determination between original and smoothened values as interpolated from the isolines. Numbers and abbreviations for names of environmental variables are in accordance with Tab. 2.

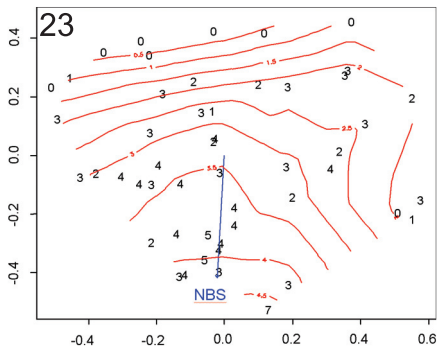

Fig. 23. TSP: Isolines for variables of species number in the GNMDS ordination of 50 plots, axes 1 (horizontal) and 2 (vertical). Values for the variables of species number are plotted onto plots' positions. NBS (the number of bryophyte species) (R^2 = 0.6570). R^2 refers to the coefficient of determination between original and smoothened values as interpolated from the isolines.

Tab. 19. Tie Shan Ping: Occurrence (number of plots in which the species was present) and local abundance (abundant = subplot frequency ≥ 8) of species recorded in five or more of the 50 plots.

Species	The total number of plots	
	Present	Abundant
Aralia chinensis	8	1
Ardisia pusilla	20	12
Camellia oleifera	7	1
Cinnamomum camphora	5	0
Cunninghamia lanceolata	7	3
Dicranopteris pedata	20	10
Dryopteris erythrosora	24	11
Dryopteris fuscipes	11	5
Embelia rudis	6	1
Eurya loquiana	6	1
Lophatherum gracile	17	7
Maesa japonica	8	2
Miscanthus sinensis	15	8
Myrsine afriana	6	1
Parathelypteris japonica	9	4
Phylostachis heteroclada	8	5
Pteridium aquilinum	14	9
Quercus fabric	10	0
Randia cochichinensis	11	0
Rubus corchorifolius	6	2
Setaria palmifolia	5	3
Smilax china	27	3
Stenoloma chusanum	5	1
Symplocos lancifolia	5	0
Symplocos sumuntia	21	5
Woodwardia japonica	31	21
Bazzania semiopaca	11	0
Calypogeia arguta	26	7
Heteroscyphus planus	7	0
Leucobryum bowringii	37	17
Taxiphyllum subarcuatum	40	20

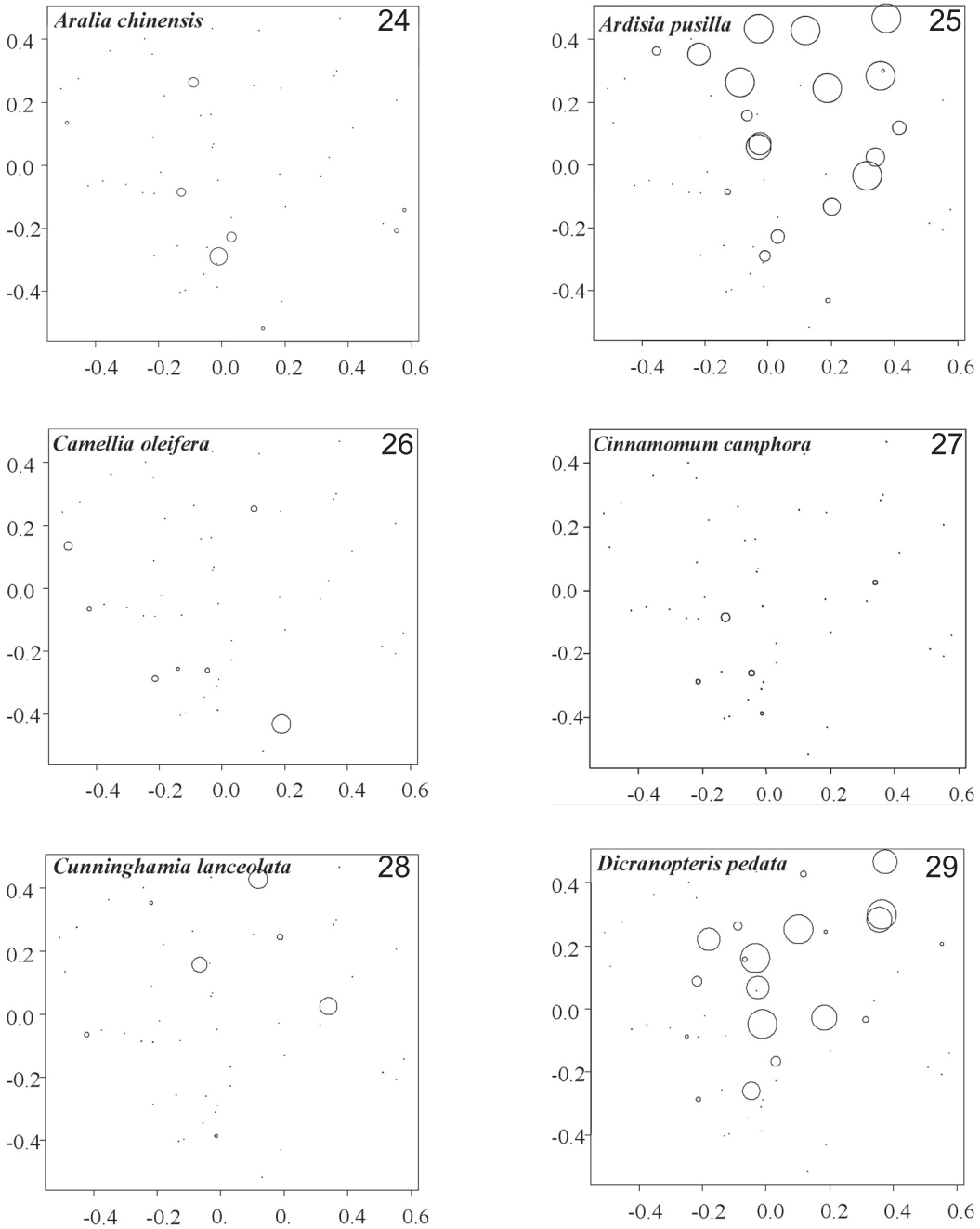

Figs 24–29. Tie Shan Ping: Distribution of species abundances in the GNMDS ordination of 50 plots, axes 1 (horizontal) and 2 (vertical). Frequency in subplots for each species in each plot proportional to circle size. Fig. 24. *Aralia chinensis*. Fig. 25. *Ardisia pusilla*. Fig. 26. *Camellia oleifera*. Fig. 27. *Cinnamomum camphora*. Fig. 28. *Cunninghamia lanceolata*. Fig. 29. *Dicranopteris pedata*. Small dots indicate absence; circles indicate presence, diameter proportional with subplot frequency.

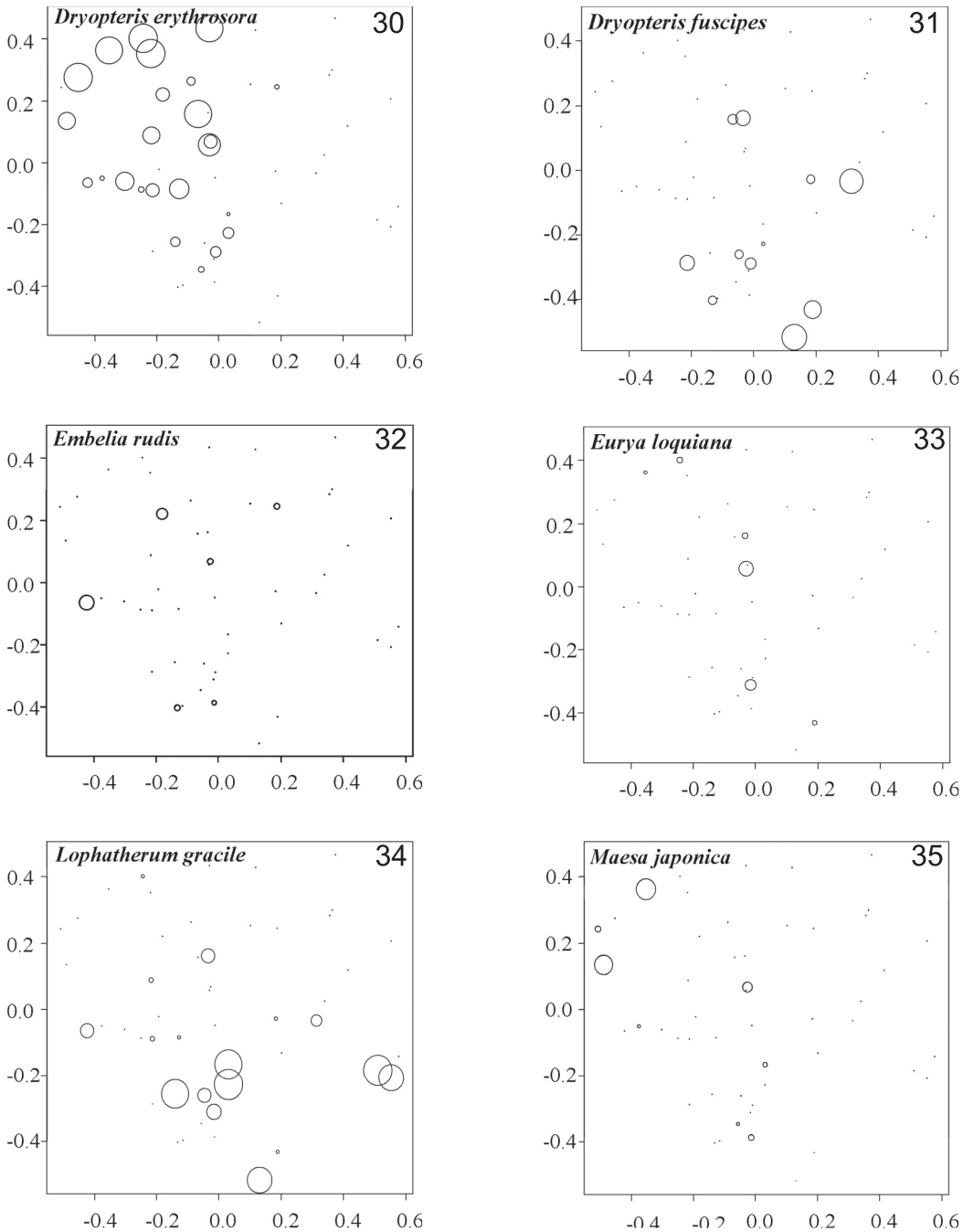

Figs 30–35. Tie Shan Ping: Distribution of species abundances in the GNMDS ordination of 50 plots, axes 1 (horizontal) and 2 (vertical). Frequency in subplots for each species in each plot proportional to circle size. Fig. 30. *Dryopteris erythrosora*. Fig. 31. *Dryopteris fuscipes*. Fig. 32. *Embelia rudis*. Fig. 33. *Eurya loquiana*. Fig. 34. *Lophatherum gracile*. Fig. 35. *Maesa japonica*. Small dots indicate absence; circles indicate presence, diameter proportional with subplot frequency.

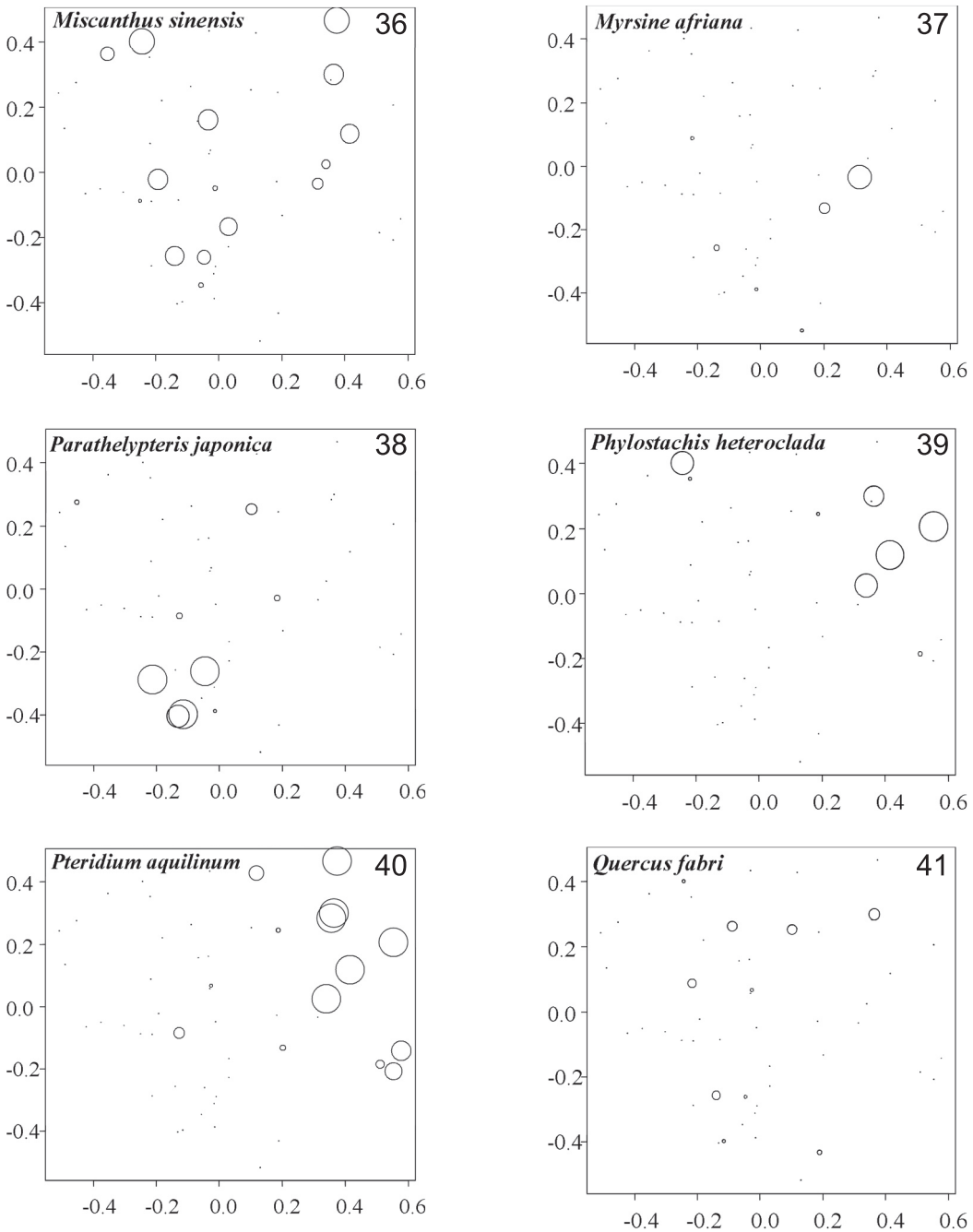

Figs 36–41. Tie Shan Ping: Distribution of species abundances in the GNMDS ordination of 50 plots, axes 1 (horizontal) and 2 (vertical). Frequency in subplots for each species in each plot proportional to circle size. Fig. 36. *Miscanthus sinensis*. Fig. 37. *Myrsine afriana*. Fig. 38. *Parathelypteris japonica*. Fig. 39. *Phylostachis heteroclada*. Fig. 40. *Pteridium aquilinum*. Fig. 41. *Quercus fabri*. Small dots indicate absence; circles indicate presence, diameter proportional with subplot frequency.

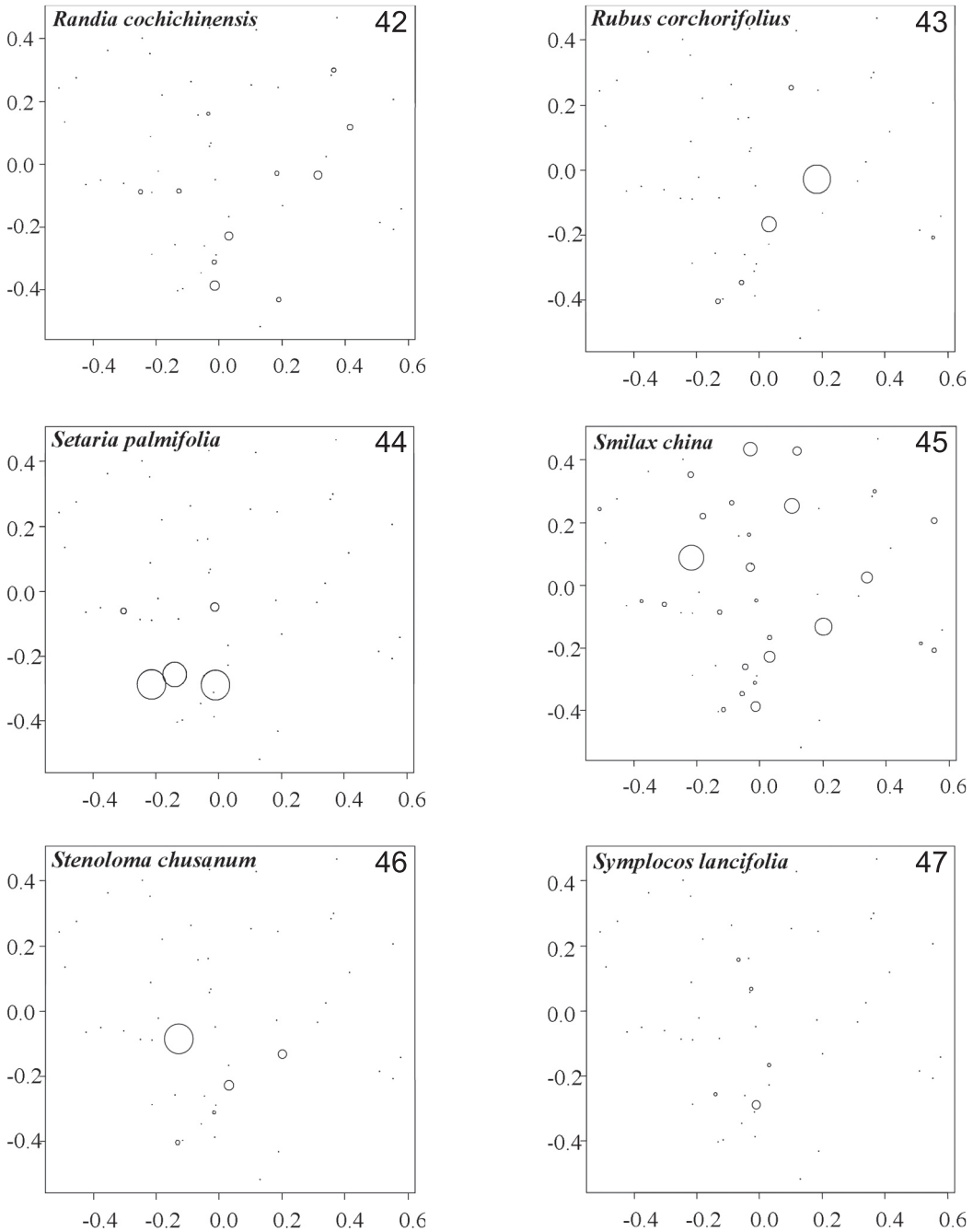

Figs 42–47. Tie Shan Ping: Distribution of species abundances in the GNMDS ordination of 50 plots, axes 1 (horizontal) and 2 (vertical). Frequency in subplots for each species in each plot proportional to circle size. Fig. 42. *Randia cochichinensis*. Fig. 43. *Rubus corchorifolius*. Fig. 44. *Setaria palmifolia*. Fig. 45. *Smilax china*. Fig. 46. *Stenoloma chusanum*. Fig. 47. *Symplocos lanceifolia*. Small dots indicate absence; circles indicate presence, diameter proportional with subplot frequency.

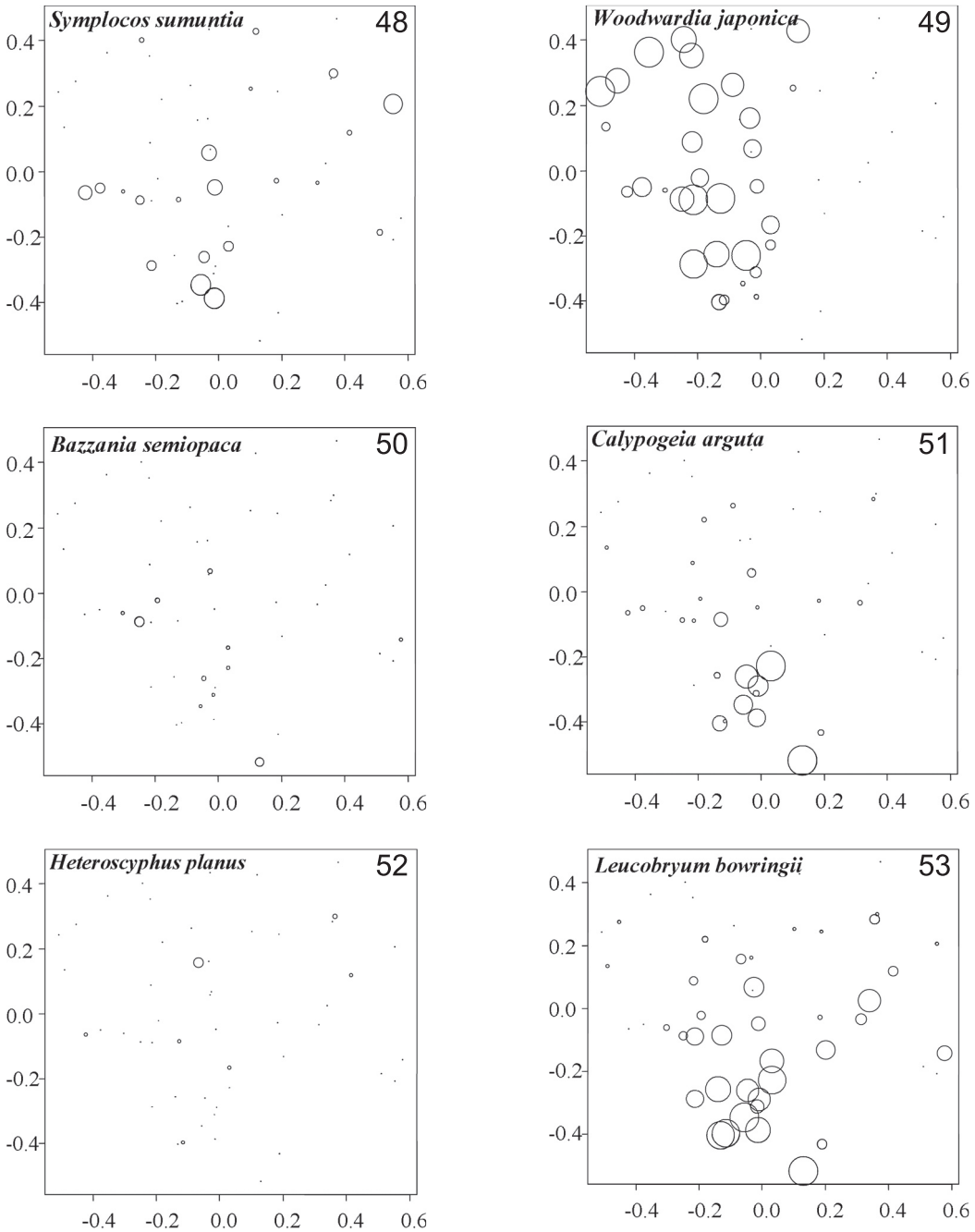

Figs 48–53. Tie Shan Ping: Distribution of species abundances in the GNMDS ordination of 50 plots, axes 1 (horizontal) and 2 (vertical). Frequency in subplots for each species in each plot proportional to circle size. Fig. 48. *Symplocos sumuntia*. Fig. 49. *Woodwardia japonica*. Fig. 50. *Bazzania semiopaca*. Fig. 51. *Calypogeia arguta*. Fig. 52. *Heteroscyphus planus*. Fig. 53. *Leucobryum bowringii*. Small dots indicate absence; circles indicate presence, diameter proportional with subplot frequency.

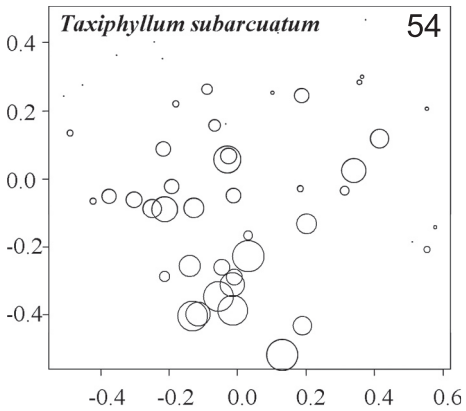

Fig. 54. Tie Shan Ping: Distribution of species abundances (*Taxiphyllum subarcuatum*) in the GNMDS ordination of 50 plots, axes 1 (horizontal) and 2 (vertical). Frequency in subplots for each species in each plot proportional to circle size. Small dots indicate absence; circles indicate presence, diameter proportional with subplot frequency.

LIU CHONG GUAN

Correlations between environmental variables

A total of 11 variables made up a large group of pairwise more or less strongly correlated variables ($|\tau| > 0.35$ for all pairs): concentrations of Mn, Ca, Mg, Na and K, contents of total C and N, soil base saturation and the organic matter content were all positively correlated ($\tau > 0.5$; see Tab. 20, Fig. 55), while the aluminium saturation and the content of dry matter were negatively correlated with all the others. Other variable associated with the large group was the concentration of Al which was negatively correlated with the organic matter content.

Concentrations of Fe and H (positively correlated; $\tau > 0.6$), soil pH_{H_2O} and soil pH_{CaCl_2} (negatively correlated with others; $|\tau| > 0.6$ for H with pH_{CaCl_2}) made up a another group of paiwise more or less strongly correlated variables, and associated with the large group via concentrations of Fe and H, which were positively correlated with the organic matter content and the content of total C, and negative correlated with the content of soil dry matter.

The tree influence variables were connected to the large group via the concentration of Mn, which was positively correlated with the number of broadleaved trees. The group of three tree influence variables and the group of concentrations of Fe and H, soil pH_{H_2O} and soil pH_{CaCl_2} made up one group of correlated variables, as variables in one group were correlated, both positively and negatively, with variables in the other (Fig. 55).

Aspect favourability was positively correlated with the heat index ($\tau > 0.6$). These two topographic variables were connected to the large group via the correlations with concentrations of Mg and Ca and soil base saturation (the heat index positively correlated), and the aluminium saturation (the heat index negatively correlated). Aspect favourability was positively correlated the concentration of H.

Tab. 20. Liu Chong Guan: Kendall's rank correlation coefficients τ between 33 environmental variable in the 50 plots (lower triangle), with significant probabilities (upper triangle). Very strong correlations ($|\tau| \geq 4.0$, $P < 0.0001$) are indicated by bold face. n.s means significance probability $P > 0.1$. Numbers and abbreviations for names of environmental variables in accordance with Tab. 2.

	1	2	3	4	5	6	7	8	9	10	11	12	13	14	15	16	17
01 Inclin	*	n.s	.0042	n.s	n.s	.0390	n.s	n.s	.0005	n.s	n.s	.0013	n.s	n.s	.0140	.0308	n.s
02 AspecF	.0194	*	**.0000**	n.s	n.s	n.s	n.s	.0039	n.s	n.s	n.s	n.s	n.s	n.s	.0774	.0027	n.s
03 HeatIn	.2872	**.7248**	*	n.s	n.s	n.s	n.s	.0642	n.s	n.s	n.s	n.s	n.s	n.s	n.s	n.s	n.s
04 TerraM	.0105	–.0314	–.0025	*	n.s	.0600	n.s	n.s	n.s	n.s	n.s	n.s	n.s	n.s	n.s	n.s	n.s
05 ConvS1	.1259	.1664	.1453	–.0018	*	n.s	n.s	n.s	n.s	n.s	n.s	n.s	.0803	n.s	n.s	n.s	n.s
06 ConvV1	.2106	–.1638	–.0183	.1927	.1026	*	.0350	.0411	n.s	n.s	n.s	n.s	n.s	n.s	.0145	.0178	n.s
07 ConvS9	–.0186	.1520	.1360	.0669	.1577	–.2187	*	n.s	n.s	n.s	.0854	n.s	n.s	n.s	n.s	n.s	n.s
08 ConvV9	.1276	–.2971	–.1899	.0533	–.1550	.2134	–.1047	*	n.s	n.s	n.s	n.s	n.s	n.s	n.s	n.s	n.s
09 SoilDM	–.3491	.0049	–.1035	–.1090	.0484	–.1048	–.1247	–.0578	*	n.s	.0558	.0209	n.s	n.s	n.s	.0050	n.s
10 LitLDM	–.0423	.0726	–.0157	–.1076	.0321	–.0774	.1112	–.0633	–.0044	*	n.s	n.s	n.s	n.s	.0172	.0754	.0483
11 OrgaLD	–.1077	–.0401	–.1453	–.0876	.1262	.0955	–.1896	.1095	.2028	.1183	*	n.s	n.s	n.s	n.s	.0330	n.s
12 SoilMLM	–.3228	–.1352	–.1528	.0381	–.0628	–.0967	.0396	.0157	.2269	–.1187	.0127	*	n.s	n.s	.0128	n.s	n.s
13 LitteI	.0998	.1185	.1148	.0111	.1787	.1113	.0138	–.0630	–.0371	.0893	.1377	–.1264	*	**.0000**	n.s	n.s	n.s
14 CrowCI	.0350	.1244	.0992	–.0480	.1349	.0532	–.0209	–.0265	–.0116	.1263	.1288	–.1456	**.5939**	*	n.s	n.s	n.s
15 RelaCN	–.2543	.1784	.0813	–.0132	.1507	–.2507	.0920	–.1392	.1338	.2533	.0377	.2509	–.0034	.0944	*	.0001	n.s
16 RelaDN	.2314	–.3135	–.1424	.0000	–.1715	.2517	–.1577	.0978	–.2947	–.1959	–.2406	–.1176	–.0537	–.0938	–.4184	*	.0221
17 pH_{H_2O}	.0136	–.1198	–.0881	–.1068	–.0130	.1118	–.1424	.0246	–.0796	–.2050	–.0614	–.0033	.0414	.0960	–.1137	.2408	*
18 pH_{CaCl_2}	.0611	–.2229	–.1448	–.1536	–.0511	.2301	–.2411	.0044	–.1333	–.3295	–.0622	–.0091	.0711	.0683	–.3662	.3795	**.5662**
19 Al	–.2737	–.0123	–.1167	–.0737	.0817	–.1233	.2358	.0087	.1610	.0296	.1271	**.4387**	–.0361	–.0810	.1033	–.1994	–.1343
20 Fe	–.1541	.3284	.2637	.0008	.1315	–.2016	.2961	–.1481	.1610	.2825	.0799	.2181	–.0410	–.0347	.3523	–.3864	–.3221
21 H	–.0312	**.4005**	.3208	.0398	.0456	–.2350	.2324	–.1359	.1051	.2441	–.0073	.0989	–.0705	–.0943	.3676	–.3614	**–.4292**
22 Mn	.2181	.0663	.2196	.1075	–.0696	.1283	.0379	–.0331	–.3220	–.2615	–.3287	.0302	–.1164	–.1323	–.1931	**.4255**	.1442
23 Ca	.1827	.3284	**.4073**	.0669	.1246	.0417	.0155	–.1115	–.1265	–.0558	–.1362	–.0792	–.0033	–.0678	.0322	.1050	.0255
24 Mg	.1811	.3137	**.4073**	.0872	.0490	.0317	.0413	–.0645	–.1856	–.0942	–.1961	–.0368	–.0820	–.1125	–.0068	.1175	.0124
25 Na	–.0379	.2416	.2735	.0483	.0765	–.0816	.2169	–.0592	–.0427	–.0593	–.1217	.1446	–.1181	–.1389	.0881	–.0036	–.0239
26 K	.1457	.2514	.3371	.0533	.0662	.0383	.0293	–.0453	–.0953	–.1761	–.1489	.1168	–.1509	–.1803	–.0525	.1068	.0832
27 C	–.0143	.2711	.2555	.0550	.0902	–.0050	.0430	–.0314	–.0066	–.0314	–.1344	.1789	–.1296	–.1406	.1016	–.0125	–.0684
28 N	.0971	.2553	.2889	.0484	.0560	.0426	.0397	–.0201	–.0774	–.1180	–.1575	.1433	–.1291	–.1732	–.0433	.0571	–.0025
29 BS	.2990	.2858	.3747	.0669	.1401	.1166	–.0448	–.0871	–.1561	–.1099	–.1126	–.1969	.0295	.0066	–.0356	.1887	.1178
30 AlS	–.2771	–.3333	**–.4367**	–.1041	–.0713	–.0633	.0465	.0732	.1708	.0105	.1090	.2377	.0164	.0496	–.0576	–.0837	.0568
31 SO_4	–.0118	–.0699	–.0189	–.1284	.0872	–.0368	.1357	–.1670	.0280	.2259	–.1122	.0730	.0873	–.0008	–.0034	–.0179	–.0637
32 WDM	–.0109	–.2596	–.2718	–.0601	–.1315	.1050	–.1067	.0557	–.0115	.0296	.0908	–.2361	.1132	.1538	–.1050	.0801	.0980
33 LOI	.0430	.3071	.3159	.0483	.1401	–.0633	.1291	–.0627	–.0131	–.0174	–.1017	.1789	–.1476	–.1786	.1220	–.0427	–.0816

Tab. 20 (continued). Liu Chong Guan: Kendall's rank correlation coefficients τ between 33 environmental variable in the 50 plots (lower triangle), with significant probabilities (upper triangle). Very strong correlations ($|\tau| \geq 4.0$, $P < 0.0001$) are indicated by bold face. n.s means significance probability $P > 0.1$. Numbers and abbreviations for names of environmental variables in accordance with Tab. 2.

	18	19	20	21	22	23	24	25	26	27	28	29	30	31	32	33
01 Inclin	n.s	.0063	n.s	n.s	.0295	.0682	.0707	n.s	n.s	n.s	n.s	.0028	.0057	n.s	n.s	n.s
02 AspecF	.0238	n.s	.0008	**.0000**	n.s	.0008	.0014	.0136	.0102	.0056	.0092	.0035	.0007	n.s	.0080	.0017
03 HeatIn	n.s	n.s	.0069	.0010	.0244	**.0000**	**.0000**	.0051	.0006	.0088	.0031	.0001	.0000	n.s	.0053	.0012
04 TerraM	n.s	n.s	n.s	n.s	n.s	n.s	n.s	n.s	n.s	n.s	n.s	n.s	n.s	n.s	n.s	n.s
05 ConvS1	n.s	n.s	n.s	n.s	n.s	n.s	n.s	n.s	n.s	n.s	n.s	n.s	n.s	n.s	n.s	n.s
06 ConvV1	.0215	n.s	.0424	.0180	n.s	n.s	n.s	n.s	n.s	n.s	n.s	n.s	n.s	n.s	n.s	n.s
07 ConvS9	.0188	.0207	.0037	.0226	n.s	n.s	n.s	.0333	n.s	n.s	n.s	n.s	n.s	n.s	n.s	n.s
08 ConvV9	n.s	n.s	n.s	n.s	n.s	n.s	n.s	n.s	n.s	n.s	n.s	n.s	n.s	n.s	n.s	n.s
09 SoilDM	n.s	n.s	n.s	n.s	.0010	n.s	.0586	n.s	n.s	n.s	n.s	n.s	.0817	n.s	n.s	n.s
10 LitLDM	.0015	n.s	.0061	.0177	.0111	n.s	n.s	n.s	.0872	n.s	n.s	n.s	n.s	.0289	n.s	n.s
11 OrgaLD	n.s	n.s	n.s	n.s	.0018	n.s	.0629	n.s	n.s	n.s	n.s	n.s	n.s	n.s	n.s	n.s
12 SoilMLM	n.s	**.0000**	.0255	n.s	n.s	n.s	n.s	n.s	n.s	.0669	n.s	.0438	.0149	n.s	.0156	.0669
13 LitteI	n.s	n.s	n.s	n.s	n.s	n.s	n.s	n.s	n.s	n.s	n.s	n.s	n.s	n.s	n.s	n.s
14 CrowCI	n.s	n.s	n.s	n.s	n.s	n.s	n.s	n.s	.0678	n.s	.0799	n.s	n.s	n.s	n.s	.0703
15 RelaCN	.0003	.3050	.0005	.0003	.0552	n.s	n.s	n.s	n.s	n.s	n.s	n.s	n.s	n.s	n.s	n.s
16 RelaDN	.0003	.0560	.0002	.0005	**.0000**	n.s	n.s	n.s	n.s	n.s	n.s	.0705	n.s	n.s	n.s	n.s
17 pH_{H_2O}	**.0000**	n.s	.0011	**.0000**	n.s	n.s	n.s	n.s	n.s	n.s	n.s	n.s	n.s	n.s	n.s	n.s
18 pH_{CaCl_2}	*	n.s	**.0000**	**.0000**	n.s	n.s	n.s	n.s	n.s	.0759	n.s	n.s	.0463	n.s	.0394	.0182
19 Al	–.1102	*	.0002	.0598	n.s	n.s	n.s	.0062	.0290	.0016	.0196	.0994	.0224	.0894	.0001	.0010
20 Fe	**–.5101**	.3616	*	**.0000**	n.s	.0066	.0048	.0018	.0102	**.0000**	.0028	n.s	.0373	n.s	**.0000**	**.0000**
21 H	**–.6648**	**.1837**	.6359	*	n.s	.0030	.0010	.0084	.0343	.0001	.0025	n.s	.0004	n.s	**.0000**	**.0000**
22 Mn	.1415	.0531	.0220	.0531	*	**.0000**	**.0000**	.0037	**.0000**	**.0000**	**.0000**	**.0000**	.0001	n.s	.0001	**.0000**
23 Ca	–.0839	–.0073	.2653	.2898	**.4792**	*	**.0000**	.0007	**.0000**	**.0000**	**.0000**	**.0000**	**.0000**	n.s	**.0000**	**.0000**
24 Mg	–.0658	.0906	.2751	.3224	**.6163**	**.7061**	*	**.0000**	**.0000**	**.0000**	**.0000**	**.0000**	**.0000**	n.s	**.0000**	**.0000**
25 Na	–.0658	.2669	.3045	.2571	.2833	.3306	**.4318**	*	**.0000**	**.0000**	**.0000**	.0156	.0130	n.s	**.0000**	**.0000**
26 K	.0099	.2131	.2506	.2065	**.5788**	**.6229**	**.7012**	**.4139**	*	**.0000**	**.0000**	**.0000**	**.0000**	n.s	**.0000**	**.0000**
27 C	–.1744	.3078	**.4400**	.3894	**.4416**	**.5118**	**.6196**	**.4367**	**.6376**	*	**.0000**	.0003	.0001	n.s	**.0000**	**.0000**
28 N	–.0652	.2283	.2921	.2954	**.5016**	**.4755**	**.5949**	**.4001**	**.6637**	**.7930**	*	.0002	.0004	n.s	**.0000**	**.0000**
29 BS	.0181	–.1608	.0988	.1559	**.4498**	**.8041**	**.6082**	.2359	**.5216**	.3551	.3609	*	**.0000**	n.s	.0004	.0001
30 AlS	.1958	.2229	–.2033	–.3486	–.3910	**–.7224**	**–.6278**	–.2424	**–.4498**	–.3780	–.3478	**–.7584**	*	n.s	.0003	**.0000**
31 SO_4	–.0066	.1664	.1352	.0795	.0041	.0713	.0500	–.0025	–.0369	.0025	–.0731	.0025	.0221	*	n.s	n.s
32 WDM	.2024	–.3731	**–.4302**	**–.4024**	–.3763	**–.5086**	**–.6196**	**–.4433**	**–.6669**	**–.7192**	**–.6588**	–.3453	.3518	–.0762	*	**.0000**
33 LOI	–.2320	.3224	**.4710**	**.4498**	**.4367**	**.5429**	**.6604**	**.4808**	**.6947**	**.7894**	**.7340**	.3829	**–.4024**	.0369	**–.8384**	*

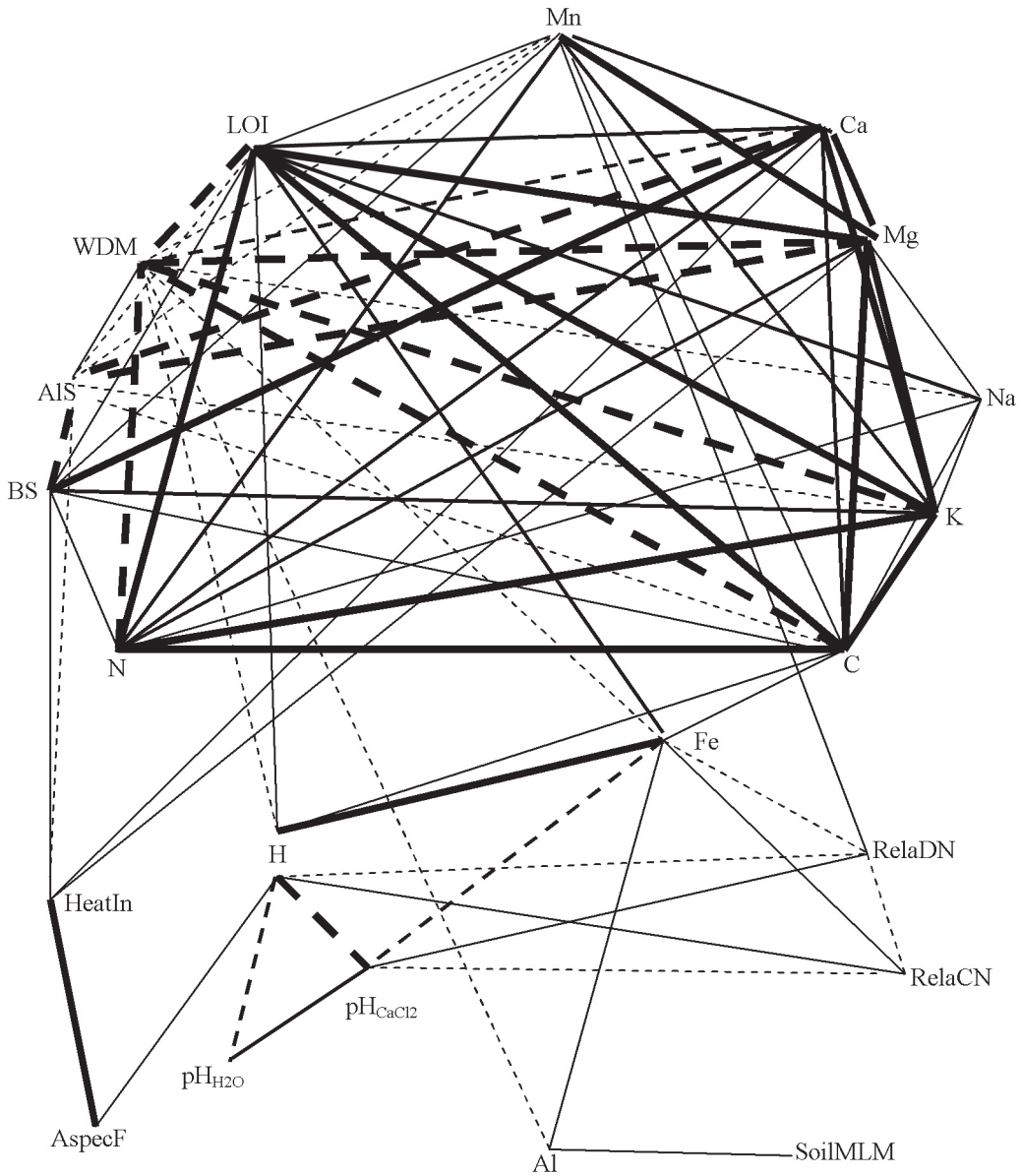

Fig. 55. Liu Chong Guan: Plexus diagram visualizing Kendall's τ between pairs of environmental variables. Significance probabilities for τ are indicated by lines with different thickness (in order of decreasing thickness): $|\tau| \geq 0.60$, $0.45 \leq |\tau| < 0.60$, and $0.35 \leq |\tau| < 0.45$. Continuous lines refer to positive correlations, broken lines to negative.

PCA ordination of environmental variables

Eigenvalues of the first two PCA axes were 0.244 and 0.188, thus 43.10 % of the variation in measured environmental variables was explained by the first two PCA axes.

Soil dry matter content and aluminium saturation obtained high loadings on PCA 1, while concentrations of Fe and H, total C in soil and soil organic matter content obtained low loadings on this axis. Mn Concentration in soil and the number of broadleaved trees obtained high loadings on PCA 2, while low loading was obtained by the number of coniferous trees.

PCA ordination results thus summarised major features of correlations between environmental variables in fewer dimensions (Tab. 20, Figs 55–56). For instance, the topographic variables of aspect favourability and heat index were more or less positively correlated with the soil nutrients variables of concentrations of Mn, Ca, Mg, Na and K, contents of total C and N, soil base saturation and the organic matter content, and negatively correlated with the aluminium saturation and the content of dry matter; the concentrations of Fe and H were strongly negatively correlated with the soil pH_{H_2O} and soil pH_{CaCl_2}; and the variables of concentration of Mn and inclination were negatively correlated with the number of coniferous trees, and positively correlated with the number of broadleaved trees.

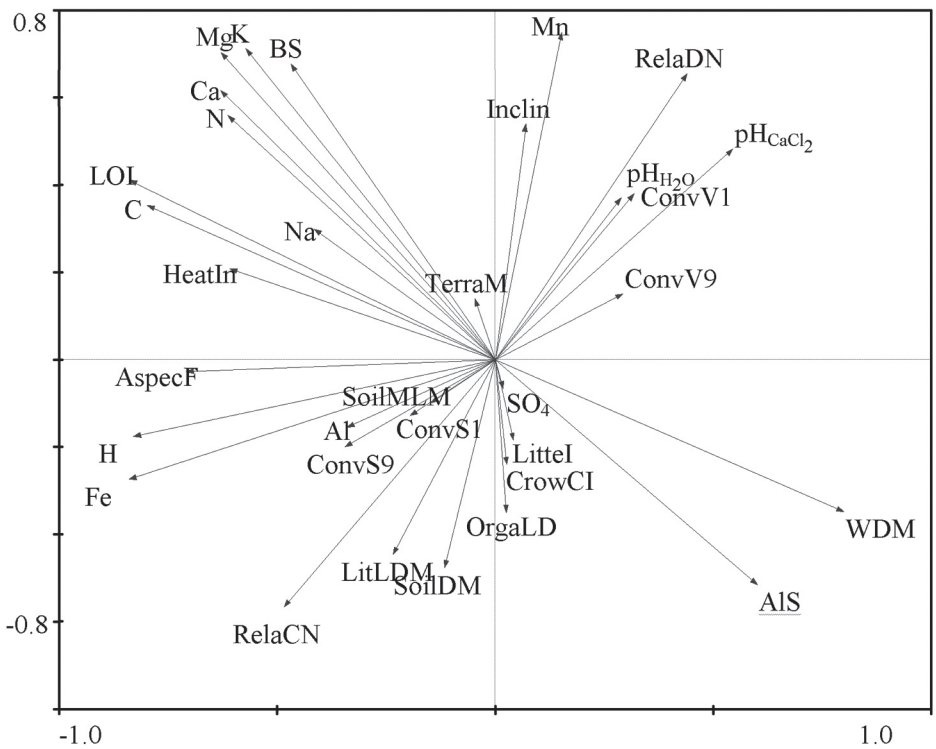

Fig. 56. Liu Chong Guan: PCA ordination of 33 environmental variables (names abbreviated in accordance with Tab.2), axes 1 (horizontal) and 2 (vertical). Loadings of variables on the ordination axes are shown by heads of variable vectors.

GNMDS ordination

Good correspondence with respect to gradient length, core length and eigenvalues was found between GNMDS 1 and DCA 1, and GNMDS 2 and DCA 2, respectively. There was a strongly drop in eigenvalues occurred from GNMDS 1 (DCA 1) to GNMDS 2 (DCA 2), indicating that the first axis was the major compositional gradients.

The first axis of the GNMDS ordination of the 50 1-m^2 plots had high eigenvalue (3.8172) and gradient length of 4.3750 S.D. units, respectively. Plot number 13 was somewhat isolated plot in the space spanned by the first two GNMDS ordination axes, while the remaining plots were relatively evenly distributed in the GNMDS ordination (Fig. 57). No plot acted as outliers, as judged by core length (Tab. 21).

Tab. 21. Ordination of vegetation in the 50 plots in LCG: summary of properties for GNMDS and DCA axes 1–2 properties. Core length means length of the shortest interval containing 90% of the plots relative to gradient length.

Corresponding axis		Unit	A	B
Axis No			GNMDS 1, DCA 1	GNMDS 2, DCA 2
GNMDS	Gradient length	HC	1.240	1.236
		S. D	4.375	2.962
	Core length	%	0.797	0.764
	Eigenvalue		3.817	2.222
DCA	Gradient length	S.D	4.936	3.479
	Core length	%	0.670	0.435
	Eigenvalue		0.667	0.416

Relationships between ordination axes and environmental variables

GNMDS ordination biplots of 50 plots and significant environmental variables

Positions of plot scores in the GNMDS ordination space were related to variation in environmental variables, as indicated by a several environmental variable vectors with significantly directed variation patterns in the ordination space (Fig. 57). Along the first two axes the following patterns appeared: (1) vectors for concentrations of Fe and H in soil, topographic variables of aspect favourability and concavity/convexity sum index at 1-m^2 scale, the number of coniferous trees and litter-layer depth pointed to the upper-left of the biplots (representing a complex gradient of increasing variables above mentioned); (2) vectors for soil pH_{CaCl_2}, soil pH_{H_2O}, the concentration of Mn in soil and the number of broadleaved trees extended to the lower-right, almost directly in the opposite direction of vectors for (1); and (3) Soil Al concentration and concavity/convexity sum index at 9-m^2 scale vectors pointed to the upper-right. Thus, plots with relatively higher soil pH, higher concentration of Mn in soil and higher broadleaved trees density occurred to the lower-right in the biplots, while plots with relatively higher concentrations of Fe and H in soil, thicker litter layer, higher coniferous trees density and favourable light conditions were situated in the converse direction.

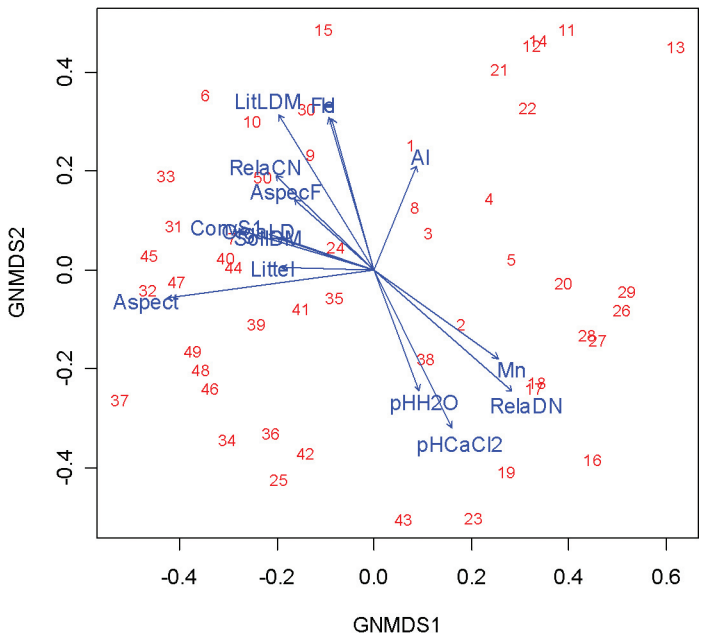

Fig. 57. Liu Chong Guan: GNMDS ordination biplots of 50 plots (indicated by their number) and significant environmental variables (i.e. with $P < 0.1$ according to goodness-of-fit test; see Tab. 26). Names of variables are abbreviated in accordance with Tab. 2. For each environmental variable the direction of maximum increase and the relative magnitude of increase in this direction is indicated by the direction and length of the vector arrows, axes 1 (horizontal) and 2 (vertical).

Split-plot GLM analysis of relationships between ordination axes and environmental variables

Variation (in plot scores) along GNMDS axis 1 was partitioned with 69.82 % at the macro-plot scale (i.e. between macro plots) and 30.18 % at the plot scale (i.e. between plots). Variation along GNMDS axis 2 was evenly distributed on the two scales (49.50 % at the macro-plot and 50.50 % at the plot scale, Tabs 22–23).

At the macro-plot scale, a total of four environmental variables were significantly ($P < 0.05$) related to GNMDS axis 1, and two and four variables (at the $P < 0.05$ and $P < 0.1$ levels, respectively) were related to GNMDS axis 2. At the plot scale, a total of four environmental variables were indicatively significantly related to GNMDS axis 1 ($P < 0.1$), and three and one variables (at the $P < 0.05$ and $P < 0.1$ levels, respectively) were related to GNMDS axis 3.

At the macro-plot scale, the variables significantly negatively related to GNMDS axis 1 were concavity/convexity sum index at 1-m^2 scale, organic-layer depth, litter index and crown cover index. At the plot scale, the variables indicatively significantly related to GNMDS axis 1 were heat index and the number of coniferous trees (negatively), and positively related to this axis were crown cover index and soil aluminium saturation (Tab. 22)

Tab. 22. Liu Chong Guan: Split-plot GLM analysis and Kendall's nonparametric correlation coefficient τ between GNMDS axis 1 and 33 environmental variables (predictor) in the 50 plots. df_{resid}: degrees of freedom for the residuals; *SS*: total variation; *FVE*: fraction of total variation attributable to a given scale (macro plot or plot); SS_{expl}/SS: fraction of the variation attributable to the scale in question, explained by a variable; *r*: model coefficient (only given when significant at the α = 0.1 level, otherwise blank); *F*: *F* statistic for test of the hypothesis that *r* = 0 against the two-tailed alternative. Split-plot GLM relationships significant at level α = 0.05, *P*, *F*, *r* and SS_{expl}/SS, and Kendall's nonparametric correlation coefficient $|\tau| \geq 0.30$ are given in bold face. Numbers and abbreviations for names of environmental variables are in accordance with Tab. 2.

Predictor	Dependent variable = GNMDS 1 (*SS* = 58.7590)								Correlation between predictor and GNMDS 1
	Error level								
	Macro plot df_{resid} = 8 $SS_{macro\ plot}$ = 41.0280 *FVE* = 0.698 of *SS*				Plot within macro plot df_{resid} = 39 SS_{plot} = 17.7310 *FVE* = 0.3018 of *SS*				Total
	$SS_{expl}/SS_{macro\ plot}$	*r*	*F*	*P*	SS_{expl}/SS_{plot}	*r*	*F*	*P*	τ
Inclin	0.0000		0.0000	0.9990	0.0507		2.0832	0.1569	-0.112
AspecF	0.1121		10.0097	0.3444	0.0174		0.6894	0.4114	-0.165
HeatIn	0.0731		0.6313	0.4498	0.0772	–1.0972	3.2614	0.0787	-0.179
TerraM	0.0831		0.7248	0.4193	0.0000		0.0016	0.9680	0.052
ConvS1	**0.7482**	**–7.9434**	**23.7660**	**0.0012**	0.0006		0.0233	0.8794	**-0.300**
ConvV1	0.0213		0.1743	0.6873	0.0061		0.2411	0.6262	-0.085
ConvS9	0.0693		0.5958	0.4624	0.0071		0.2777	0.6012	0.098
ConvV9	0.0667		0.5722	0.4711	0.0066		0.2588	0.6138	0.089
SoilDM	0.3001		3.4301	0.1012	0.0069		0.2712	0.6055	-0.176
LitLDM	0.1465		1.3731	0.2750	0.0642		2.6757	0.1099	-0.221
OrgaLD	**0.6209**	**–5.4786**	**13.1020**	**0.0068**	0.0072		0.2833	0.5976	-0.272
SoilMLM	0.2452		2.5985	0.1456	0.0002		0.0071	0.9333	0.184
LitteI	**0.6303**	**–4.3183**	**13.6390**	**0.0061**	0.0460		1.8825	0.1779	-0.218
CrowCI	**0.6688**	**–4.9731**	**16.1520**	**0.0038**	0.0700	0.7022	2.9346	0.0946	-0.184
RelaCN	0.0801		0.6965	0.4282	0.0741	–1.1786	3.1223	0.0851	-0.208
RelaDN	0.2888		3.2494	0.1091	0.0560		2.3135	0.1363	**0.331**
pH_{H_2O}	0.0164		0.1332	0.7246	0.0084		0.3316	0.5680	0.073
pH_{CaCl_2}	0.0360		0.2989	0.5995	0.0491		2.0139	0.1638	0.094
Al	0.0782		0.6787	0.4339	0.0337		1.3586	0.2509	0.197
Fe	0.0007		0.0059	0.9407	0.0160		0.6332	0.4310	-0.073
H	0.0000		0.0000	0.9960	0.0625		2.6014	0.1148	-0.032
Mn	0.2600		2.8109	0.1322	0.0027		0.1066	0.7458	**0.350**
Ca	0.0174		0.1413	0.7167	0.0376		1.5244	0.2243	0.045
Mg	0.1124		1.0129	0.3437	0.0132		0.5230	0.4739	0.114
Na	0.0523		0.4417	0.5250	0.0037		0.1458	0.7047	0.087
K	0.1822		1.7828	0.2186	0.0561		2.3159	0.1361	0.135
C	0.0906		0.7968	0.3981	0.0001		0.0041	0.9494	0.128
N	0.1253		1.1460	0.3156	0.0000		0.0001	0.9931	0.130
BS	0.0097		0.0784	0.7865	0.0405		1.6468	0.2070	-0.007
AlS	0.0008		0.0064	0.9380	0.0761	1.1881	3.2137	0.0808	0.056
SO_4	0.0068		0.0544	0.8214	0.0293		1.1757	0.2849	0.001
WDM	0.0728		0.6283	0.4509	0.0019		0.0754	0.7851	-0.131
LOI	0.0866		0.7583	0.4092	0.0118		0.4647	0.4995	0.130

Tab. 23. Liu Chong Guan: Split-plot GLM analysis and Kendall's nonparametric correlation coefficient τ between GNMDS axis 2 and 33 environmental variables (predictor) in the 50 plots. df_{resid}: degrees of freedom for the residuals; *SS*: total variation; *FVE*: fraction of total variation attributable to a given scale (macro plot or plot); SS_{expl}/SS: fraction of the variation attributable to the scale in question, explained by a variable; *r*: model coefficient (only given when significant at the α = 0.1 level, otherwise blank); *F*: *F* statistic for test of the hypothesis that *r* = 0 against the two-tailed alternative. Split-plot GLM relationships significant at level α = 0.05, *P*, *F*, *r* and SS_{expl}/SS, and Kendall's nonparametric correlation coefficient $|\tau| \geq 0.30$ are given in bold face. Numbers and abbreviations for names of environmental variables are in accordance with Tab. 2.

Predictor	Dependent variable = GNMDS 2 (*SS* = 24.7447)								Correlation between predictor and GNMDS 2
	Error level								
	Macro plot df_{resid} = 8 $SS_{macro\ plot}$ = 12.2491 *FVE* = 0.4950 of *SS*				Plot within macro plot df_{resid} = 39 SS_{plot} = 12.4956 *FVE* = 0.5050 of *SS*				Total
	$SS_{expl}/SS_{macro\ plot}$	*r*	*F*	*P*	SS_{expl}/SS_{plot}	*r*	*F*	*P*	τ
Inclin	0.0250		0.2053	0.6625	0.0050		0.1952	0.6611	-0.095
AspecF	0.0637		0.5444	0.4817	0.0065		0.2562	0.6156	0.093
HeatIn	0.0541		0.4576	0.5178	0.0025		0.0971	0.7570	0.042
TerraM	0.1417		1.3204	0.2837	0.0229		0.9153	0.3446	0.014
ConvS1	0.0063		0.0504	0.8279	0.0034		0.1332	0.7171	0.001
ConvV1	0.1827		1.7879	0.2179	0.0134		0.5289	0.4714	-0.125
ConvS9	**0.8105**	**4.0985**	**34.2170**	**0.0004**	0.0011		0.0448	0.8335	0.210
ConvV9	0.0057		0.0456	0.8362	0.0100		0.3940	0.5339	0.033
SoilDM	0.0019		0.0154	0.9044	0.0090		0.3532	0.5557	-0.041
LitLDM	0.2520		2.6951	0.1393	**0.1263**	**0.8491**	**5.6380**	**0.0226**	**0.349**
OrgaLD	0.0544		0.4604	0.5166	0.0008		0.0320	0.8590	-0.053
SoilMLM	0.0716		0.6168	0.4549	**0.1238**	**–1.1280**	**5.5093**	**0.0241**	0.048
LitteI	0.0110		0.0891	0.7730	0.0315		1.2685	0.2669	-0.080
CrowCI	0.0032		0.0253	0.8776	0.0063		0.2484	0.6210	-0.060
RelaCN	0.1066		0.9543	0.3572	0.0079		0.3109	0.5803	0.171
RelaDN	0.2092		2.1157	0.1839	0.0000		0.0001	0.9941	-0.198
pH_{H_2O}	0.3304	–6.2282	3.9480	0.0822	0.0532		2.1918	0.1468	-0.284
pH_{CaCl_2}	0.3514	–3.5687	4.3338	0.0709	0.0855	–2.2782	3.6471	0.0635	**-0.326**
Al	0.3640	2.7119	4.5795	0.0648	0.0005		0.0203	0.8874	0.221
Fe	**0.4073**	**1.6717**	**5.4975**	**0.0471**	0.0244		0.9769	0.3291	**0.344**
H	0.3745	1.7031	4.7894	0.0601	0.0618		2.5697	0.1170	**0.319**
Mn	0.1220		1.1114	0.3226	0.0060		0.2352	0.6304	-0.011
Ca	0.0031		0.0250	0.8783	0.0299		1.2020	0.2796	-0.012
Mg	0.0215		0.1755	0.6863	0.0018		0.0684	0.7950	0.063
Na	0.0127		0.1032	0.7563	0.0281		1.1264	0.2951	0.004
K	0.0115		0.0927	0.7685	0.0645		2.6886	0.1091	-0.004
C	0.1626		1.5529	0.2480	0.0003		0.0124	0.9118	0.091
N	0.0247		0.2023	0.6648	0.0112		0.4429	0.5096	0.003
BS	0.0386		0.3208	0.5867	0.0222		0.8844	0.3528	-0.114
AlS	0.0021		0.0168	0.9001	0.0000		0.0014	0.9708	0.002
SO_4	0.1644		1.5735	0.2451	0.0345		1.3923	0.2452	0.243
WDM	0.1874		1.8455	0.2114	0.0008		0.0319	0.8591	-0.153
LOI	0.1668		1.6016	0.2413	0.0003		0.0106	0.9186	0.151

At the macro-plot scale, the variables significantly positively related to GNMDS axis 2 were concavity/convexity sum index at 9-m^2 scale and the concentration of Fe in soil, while indicatively significantly related to this axis were soil pH_{H_2O} and soil pH_{CaCl_2} (negatively), and concentrations of Al and H in soil (positively). At the plot scale, the variable significantly negatively related to GNMDS 2 was soil moisture, while the variables of litter-layer depth was significantly positively related to this axis, and soil pH_{CaCl_2} was indicatively significantly related to this axis (negatively) (Tab. 23).

Kendall's rank correlation between ordination axes and environmental variables

Along GNMDS axis 1, the highest absolute values for τ were observed for concavity/convexity sum index at 1-m^2 scale which decreased, and the number of broadleaved trees and concentration of Mn in soil, both increasing along the axis ($0.30 \leq |\tau| \leq 0.35$). The variables more or less strongly negatively correlated with GNMDS axis 1 were organic-layer depth, litter-layer depth, and litter index and the number of coniferous trees ($0.20 \leq |\tau| \leq 0.30$) (Tab. 22).

The variables most strongly positively correlated with GNMDS axis 2 were litter-layer depth, concentrations of Fe and H, and the variable most strongly negatively correlated with this axis was soil pH (pH_{CaCl_2}) ($0.30 \leq |\tau| \leq 0.35$). The variables more or less strongly positively correlated with GNMDS axis 2 were concavity/convexity sum index at 9-m^2 scale, the concentration of Al and SO_4 adsorption in soil, and the variable negatively correlated with this axis was the soil pH_{H_2O} ($0.20 \leq |\tau| \leq 0.30$) (Tab. 23).

Relationships between ordination axes and species number variables

Split-plot GLM analysis of relationships between ordination axes and species number variables

At both macro-plot and plot scales, the number of bryophyte species was strongly negatively related to GNMDS axis 2. The number of vascular plants was strongly negatively related to GNMDS axis 2 at the macro-plot scale (Tab. 25). No variable of species number was strongly related to GNMDS axis 1 (Tab. 24).

Kendall's rank correlation between ordination axes and species number variables

The number of bryophyte species was most strongly negatively correlated with GNMDS axis 2 ($0.49 < |\tau| < 0.54$), and the number of vascular plants was lightly strongly negatively correlated with this axis ($\tau = -0.2670$) (Tab. 25). No variable of species number was strongly correlated with the GNMDS 1 (Tab. 24).

Isoline diagrams for significant environmental and species number variables

A total of 12 environmental variables and two species number variables satisfied the criteria for making two-dimensional isoline diagrams (Tab. 26, Figs 58–71).

The distribution of species abundance in the GNMDS ordination

Out of a total of 67 species, 24 were found in at least 5 of the 50 plots (Figs 72–95).

Brotherella henonii (Fig. 89) and *Taxiphyllum subarcuatum* (Fig. 95), typical examples of bryophyte species with wide ecological amplitude, were abundant in most plots, but were absent

Tab. 24. Liu Chong Guan: Split-plot GLM analysis and Kendall's nonparametric correlation coefficient τ between GNMDS axis 1 and two species number variables (predictor) in the 50 plots. df_{resid}: degrees of freedom for the residuals; *SS*: total variation; *FVE*: fraction of total variation attributable to a given scale (macro plot or plot); SS_{expl}/SS: fraction of the variation attributable to the scale in question, explained by a variable; *r*: model coefficient (only given when significant at the α = 0.1 level, otherwise blank); *F*: *F* statistic for test of the hypothesis that *r* = 0 against the two-tailed alternative. Split-plot GLM relationships significant at level α = 0.05, *P*, *F*, *r* and SS_{expl}/SS, and Kendall's nonparametric correlation coefficient $|\tau| \geq 0.30$ are given in bold face.

Predictor (number of species)	Dependent variable = GNMDS 1 (*SS* = 58.7590) Error level								Correlation between predictor and GNMDS 1
	Macro plot df_{resid} = 8 $SS_{macro\ plot}$ = 41.0280 *FVE* = 0.6982 of *SS*				Plot within macro plot df_{resid} = 39 SS_{plot} = 17.7310 *FVE* = 0.3018 of *SS*				Total
	$SS_{expl}/SS_{macro\ plot}$	*r*	*F*	*P*	SS_{expl}/SS_{plot}	*r*	*F*	*P*	τ
Vascular plants	0.1724		1.6666	0.2328	0.0035		0.1368	0.7135	–0.125
Bryophyte species	0.0099		0.0802	0.7843	0.0006		0.0227	0.8810	0.032

Tab. 25. Liu Chong Guan: Split-plot GLM analysis and Kendall's nonparametric correlation coefficient τ between GNMDS axis 2 and two species number variables (predictor) in the 50 plots. df_{resid}: degrees of freedom for the residuals; *SS*: total variation; *FVE*: fraction of total variation attributable to a given scale (macro plot or plot); SS_{expl}/SS: fraction of the variation attributable to the scale in question, explained by a variable; *r*: model coefficient (only given when significant at the α = 0.1 level, otherwise blank); *F*: *F* statistic for test of the hypothesis that r = 0 against the two-tailed alternative. Split-plot GLM relationships significant at level α = 0.05, *P*, *F*, *r* and SS_{expl}/SS, and Kendall's nonparametric correlation coefficient $|\tau| \geq 0.30$ are given in bold face.

Predictor (number of species)	Dependent variable = GNMDS 2 (*SS* = 24.7447) Error level								Correlation between predictor and GNMDS 2
	Macro plot df_{resid} = 8 $SS_{macro\ plot}$ = 12.2491 *FVE* = 0.4950 of *SS*				Plot within macro plot df_{resid} = 39 SS_{plot} = 12.4956 *FVE* = 0.5050 of *SS*				Total
	$SS_{expl}/SS_{macro\ plot}$	*r*	*F*	*P*	SS_{expl}/SS_{plot}	*r*	*F*	*P*	τ
Vascular plants	**0.7080**	**–0.1235**	**19.4030**	**0.0023**	0.0029	0.0070	0.1134	0.7382	–0.267
Bryophyte species	**0.4112**	**–0.0720**	**5.5874**	**0.0457**	**0.3263**	**–0.0727**	**18.8860**	**0.0001**	**–0.533**

Tab. 26. Liu Chong Guan: Environmental and species number variables for which two-dimensional isoline diagrams were made: P value for relationship with GNMDS axis assessed by split-plot GLM (two scales = error levels), Kendall's correlation coefficient τ with axis, and R^2 between the original and predicted values (according to the isoline diagrams for the variable), used as a measure of goodness-of-fit of the isolines. Isoline diagrams were made for variables with split-plot GLM $P < 0.05$ at the macro plot or the plot scale and/or Kendall's correlation coefficient $|\tau| \geq 0.3$ with one GNMDS axis. P values < 0.05 and/or $|\tau| \geq 0.30$ in bold face. Numbers and abbreviations for names of environmental variables in accordance with Tab. 2 (NVP = number of vascular plants species; and NBS = number of bryophyte species).

Ordination axis	Variable names	The split plot GLM Error level		Kendall's ccorrelation between variable and ordination axis	Goodness-of-fit of the isolines
		$P_{\text{macro plot}}$	P_{plot}	τ_{total}	R^2
GNMDS 1	ConvS1	**0.0012**	0.8794	**–0.300**	0.1963
	OrgaLD	**0.0068**	0.5976	–0.272	0.1459
	LitteI	**0.0061**	0.1779	–0.218	0.0721
	CrowCI	**0.0038**	0.0946	–0.184	0.0950
	RelaDN	0.1091	0.1363	**0.331**	0.5117
	Mn	0.1322	0.7458	**0.350**	0.3335
GNMDS 2	ConvS9	**0.0004**	0.8335	0.210	0.1581
	LitLDM	0.1393	**0.0226**	**0.349**	0.5460
	SoilMLM	0.4549	**0.0241**	0.048	0.0688
	pH_{CaCl_2}	0.0709	0.0635	**–0.326**	0.5898
	Fe	**0.0471**	0.3291	**0.344**	0.3948
	H	0.0618	0.1170	**0.319**	0.3333
	NVP	**0.0023**	0.7382	–0.267	0.1342
	NBS	**0.0457**	**0.0001**	**–0.533**	0.5545

from plots with high GNMDS 2 scores (i.e. on sites with thick litter layer).

Example of species restricted to plots in upper right part of the GNMDS ordination diagram (related to a low soil pH, and a convex surface at 9-m^2 scale was *Camellia brevistyla* (Fig. 73).

Examples of species restricted to plots in left part of the GNMDS ordination diagram (related to a thick organic layer, a high coniferous trees density, and a relatively dry soil) were *Miscanthus sinensis* (Fig. 78), *Pteridium aquilinum* (Fig. 82) and *Smilax davidiana* (Fig. 85).

Dryopteris erythrosora (Fig. 76), *Hydrangea davidi* (Fig. 77), *Calypogeia arguta* (Fig. 90), and *Cephalozia macounii* (Fig. 91) were restricted to plots in lower right part of the GNMDS ordination diagram (related to a relatively high broadleaved trees density and a high concentration of Mn in the soil).

Example of species restricted to plots in lower left part of GNMDS ordination diagram (related to a drier soil and a convex surface) were *Castanea sequinii* (Fig. 74), *Rhododendron simsii* (Fig. 83), *Symplocos lancifolia* (Fig. 86), *Dicranum japonicum* (Fig. 92) and *Hypnum plumaeforme* (Fig. 95).

Woodwardia japonica (Fig. 88) was restricted to plots with high GNMDS 2 scores (related to a thick litter layer, a low soil pH, and a high concentration of Fe in soil).

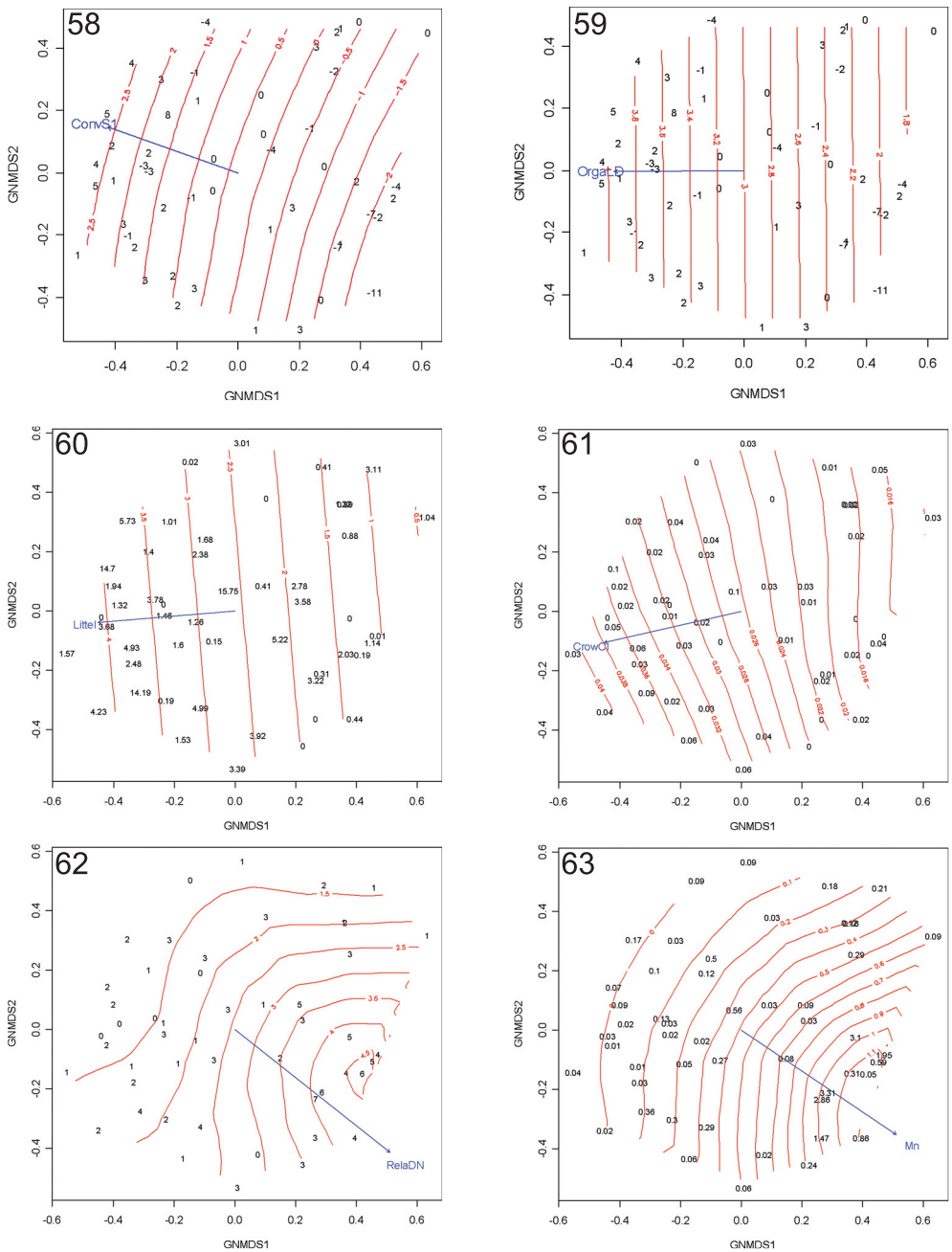

Figs 58–63. Liu Chong Guan: Isolines for environmental variables in the GNMDS ordination of 50 plots, axes 1 (horizontal) and 2 (vertical). Values for the environmental variables are plotted onto plots' position. Fig. 58. ConvS1 (R^2 = 0.1963). Fig. 59. OrgaLD (R^2 = 0.1459). Fig. 60. LitteI (R^2 = 0.0721). Fig. 61. CrowCI (R^2 = 0.0950). Fig. 62. RelaDN R^2 = 0.5117). Fig. 63. Mn (R^2 = 0.3335). R^2 refers to the coefficient of determination between original and smoothened values as interpolated from the isolines. Numbers and abbreviations for names of environmental variables are in accordance with Tab. 2.

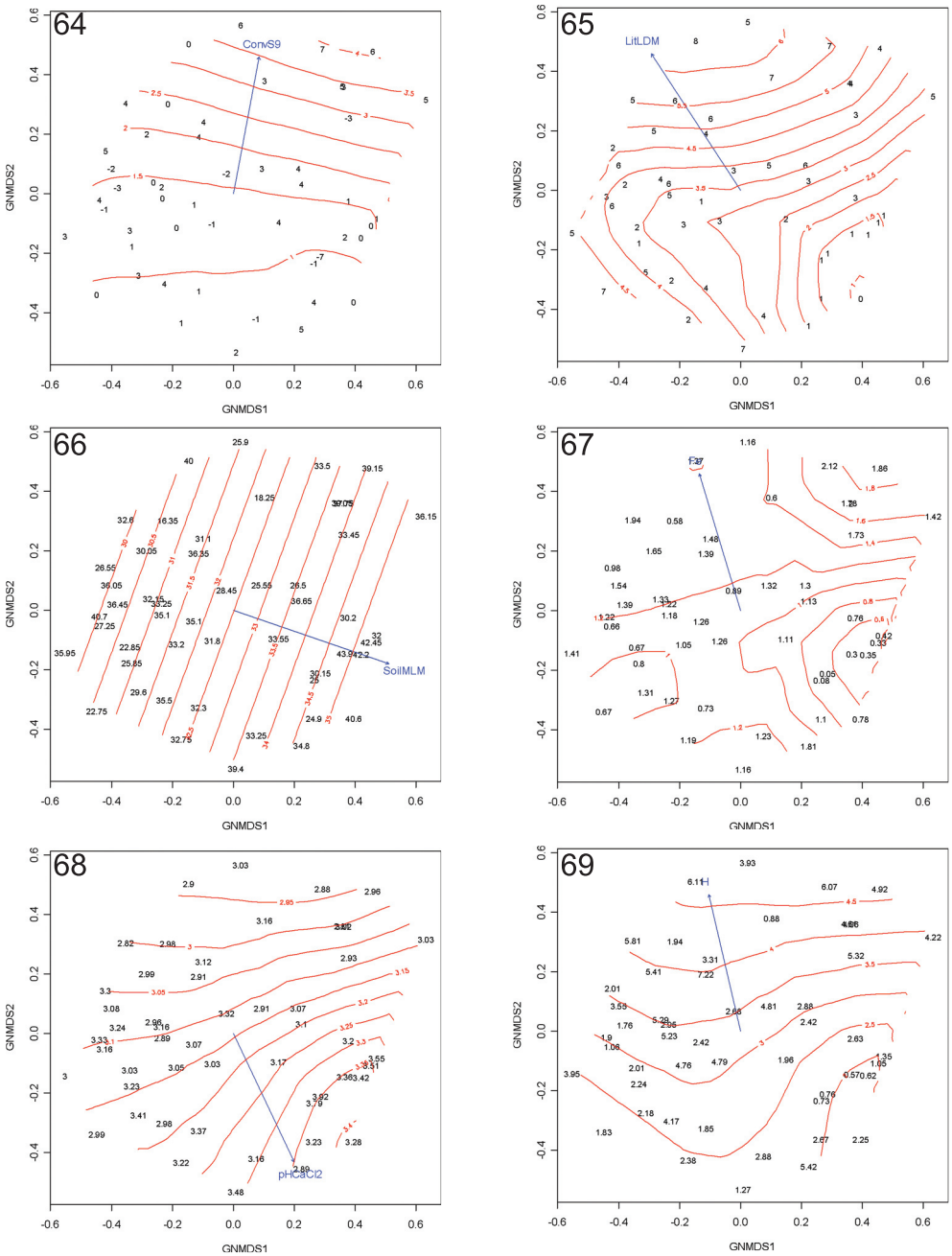

Figs 64–69. Liu Chong Guan: Isolines for environmental variables in the GNMDS ordination of 50 plots, axes 1 (horizontal) and 2 (vertical). Values for the environmental variables are plotted onto plots' position. Fig. 64. ConvS9 (R^2 = 0.1581). Fig. 65. LitLDM (R^2 = 0.5460). Fig. 66. SoilMLM (R^2 = 0.0688). Fig. 67. Fe (R^2 = 0.5898). Fig. 68. pH_{CaCl_2} (R^2 = 0.3948). Fig. 69. H (R^2 = 0.3333). R^2 refers to the coefficient of determination between original and smoothened values as interpolated from the isolines. Numbers and abbreviations for names of environmental variables are in accordance with Tab. 2.

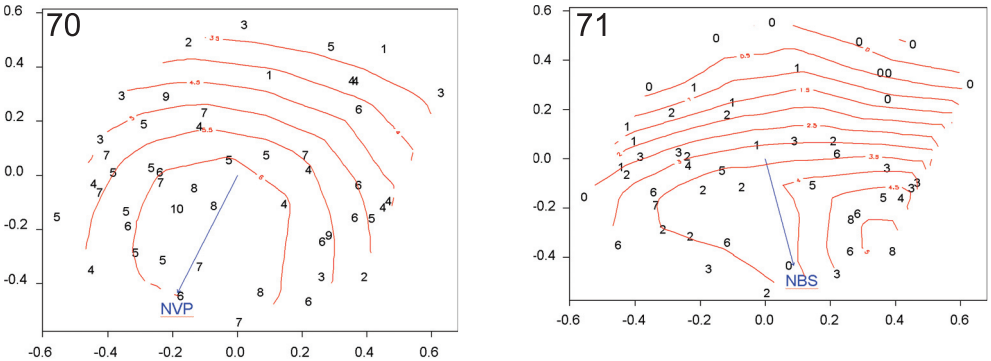

Figs 70–71. Liu Chong Guan: Isolines for species number variables in the GNMDS ordination of 50 plots, axes 1 (horizontal) and 2 (vertical). Values for the species number variables are plotted onto plots' position. Fig. 70. NVP (the number of vascular plants species) ($R^2 = 0.1342$). Fig. 71. NBS (the number of bryophyte species) ($R^2 = 0.5545$). R^2 refers to the coefficient of determination between original and smoothened values as interpolated from the isolines.

Tab. 27. Liu Chong Guan: Occurrence (number of plots in which the species was present) and local abundance (abundant = subplot frequency ≥ 8) of species recorded in five or more of the 50 plots.

Species	The total number of plots	
	Present	Abundant
Ardisia japonica	7	2
Camellia brevistyla	21	6
Castanea sequinii	9	4
Cayratia japonica	5	1
Dryopteris erythrosora	18	7
Hydrangea davidii	5	0
Miscanthus sinensis	15	6
Oplismenus compositus	10	4
Parathelypteris japonica	9	1
Parthenocissus himalayana	5	2
Lophatherum gracile	17	7
Pteridium aquilinum	25	12
Rhododendron simsii	15	4
Rubus buergeri	6	3
Smilax davidiana	14	2
Symplocos lancifolia	21	6
Woodwardia japonica	18	9
Viburnum setigerum	6	0
Brotherella henonii	28	7
Calypogeia arguta	14	2
Cephalozia macounii	5	1
Dicranum japonicum	10	3
Hypnum plumaeforme	10	2
Leucobryum chlorophyllosum	12	1
Taxiphyllum subarcuatum	27	11

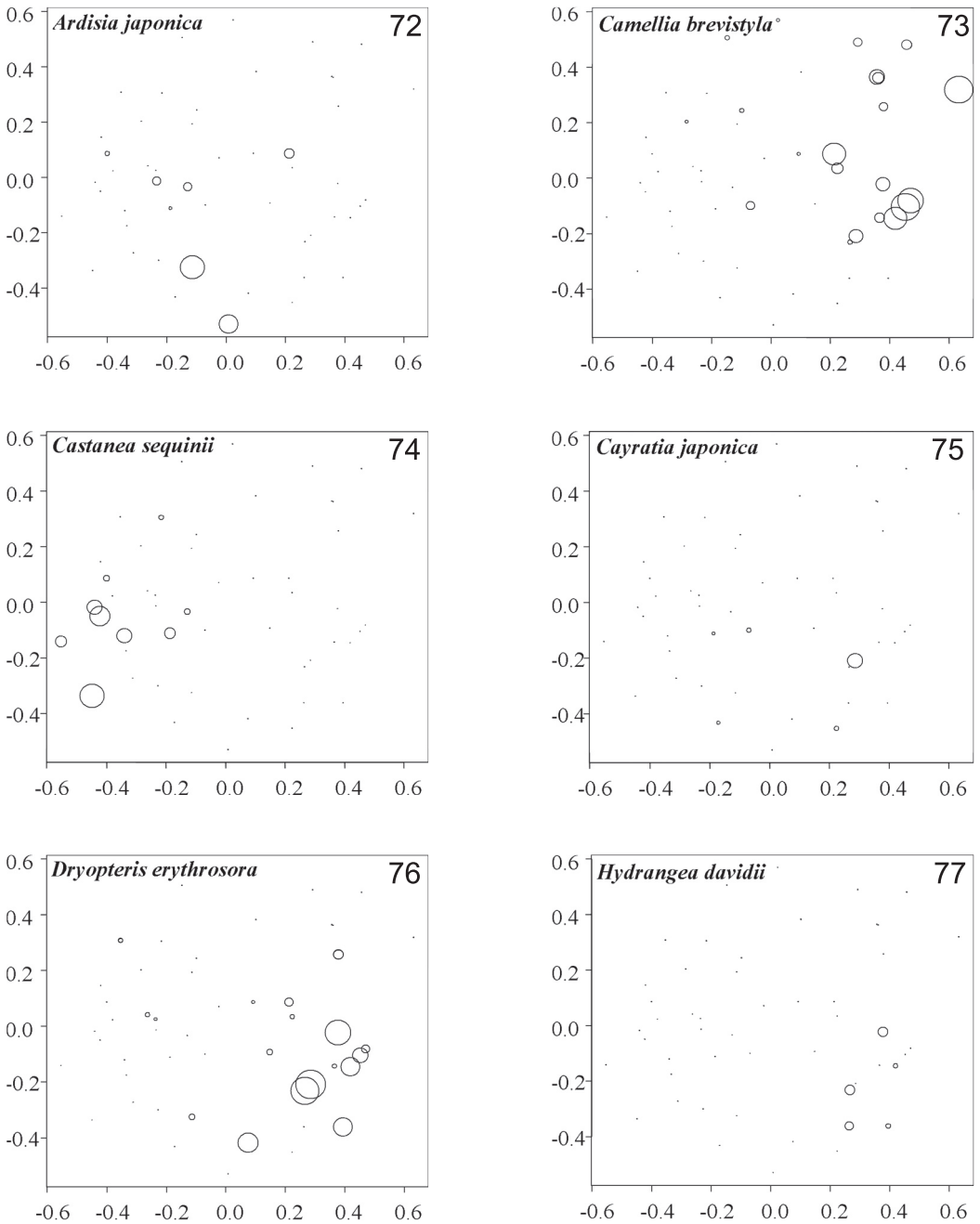

Figs 72–77. Liu Chong Guan: Distribution of species abundances in the GNMDS ordination of 50 plots, axes 1 (horizontal) and 2 (vertical). Frequency in subplots for each species in each plot proportional to circle size. Fig. 72. *Ardisia japonica*. Fig. 73. *Camellia brevistyla*. Fig. 74. *Castanea sequinii*. Fig. 75. *Cayratia japonica*. Fig. 76. *Dryopteris erythrosora*. Fig. 77. *Hydrangea davidii*. Small dots indicate absence; circles indicate presence, diameter proportional with subplot frequency.

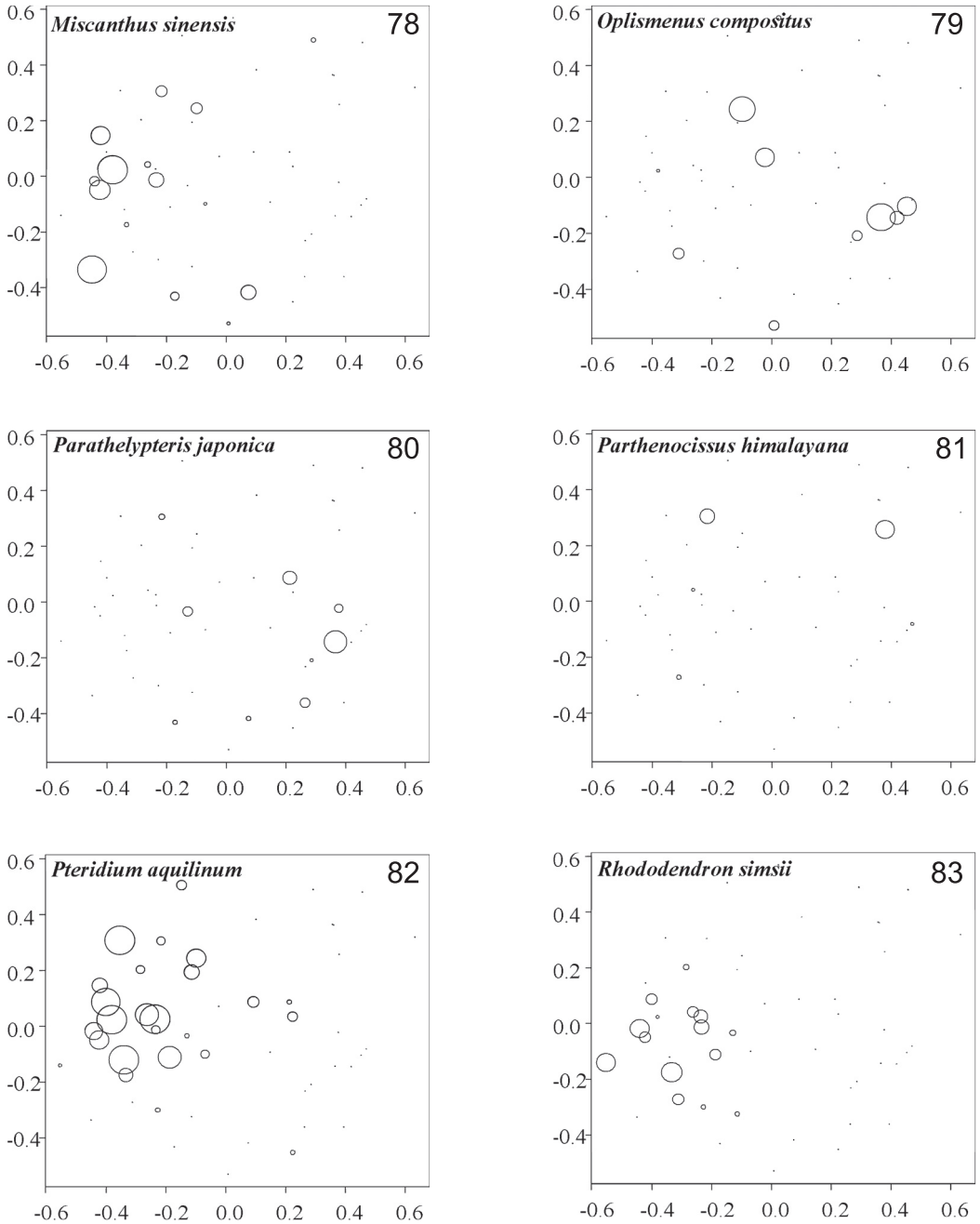

Figs 78–83. Liu Chong Guan: Distribution of species abundances in the GNMDS ordination of 50 plots, axes 1 (horizontal) and 2 (vertical). Frequency in subplots for each species in each plot proportional to circle size. Fig. 78. *Miscanthus sinensis*. Fig. 79. *Oplismenus compositus*. Fig. 80. *Parathelypteris japonica*. Fig. 81. *Parthenocissus himalayana*. Fig. 82. *Pteridium aquilinum*. Fig. 83. *Rhododendron simsii*. Small dots indicate absence; circles indicate presence, diameter proportional with subplot frequency.

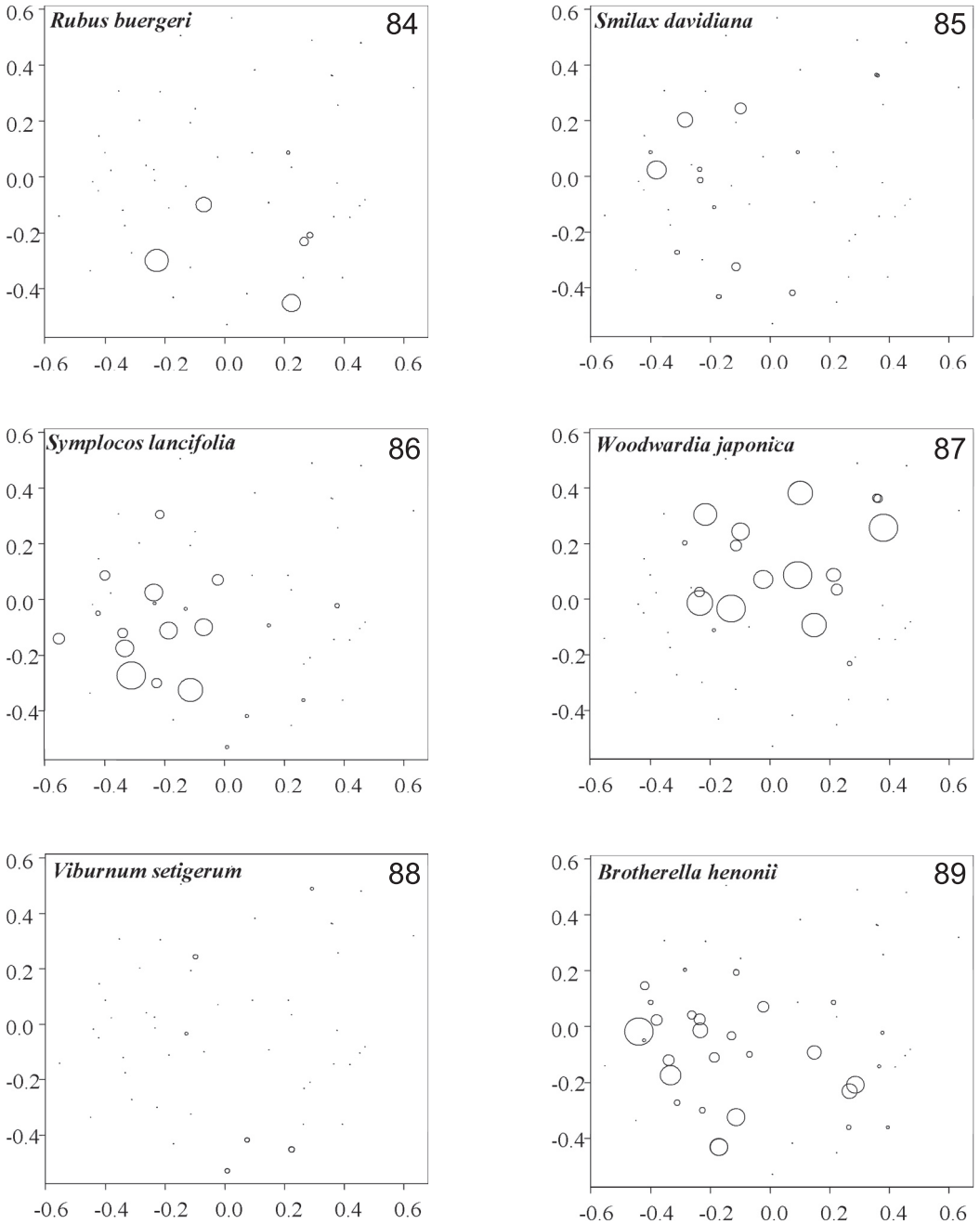

Figs 84–89. Liu Chong Guan: Distribution of species abundances in the GNMDS ordination of 50 plots, axes 1 (horizontal) and 2 (vertical). Frequency in subplots for each species in each plot proportional to circle size. Fig. 84. *Rubus buergeri*. Fig. 85. *Smilax davidiana*. Fig. 86. *Symplocos lancifolia*. Fig. 87. *Woodwardia japonica*. Fig. 88. *Viburnum setigerum*. Fig. 89. *Brotherella henonii*. Small dots indicate absence; circles indicate presence, diameter proportional with subplot frequency.

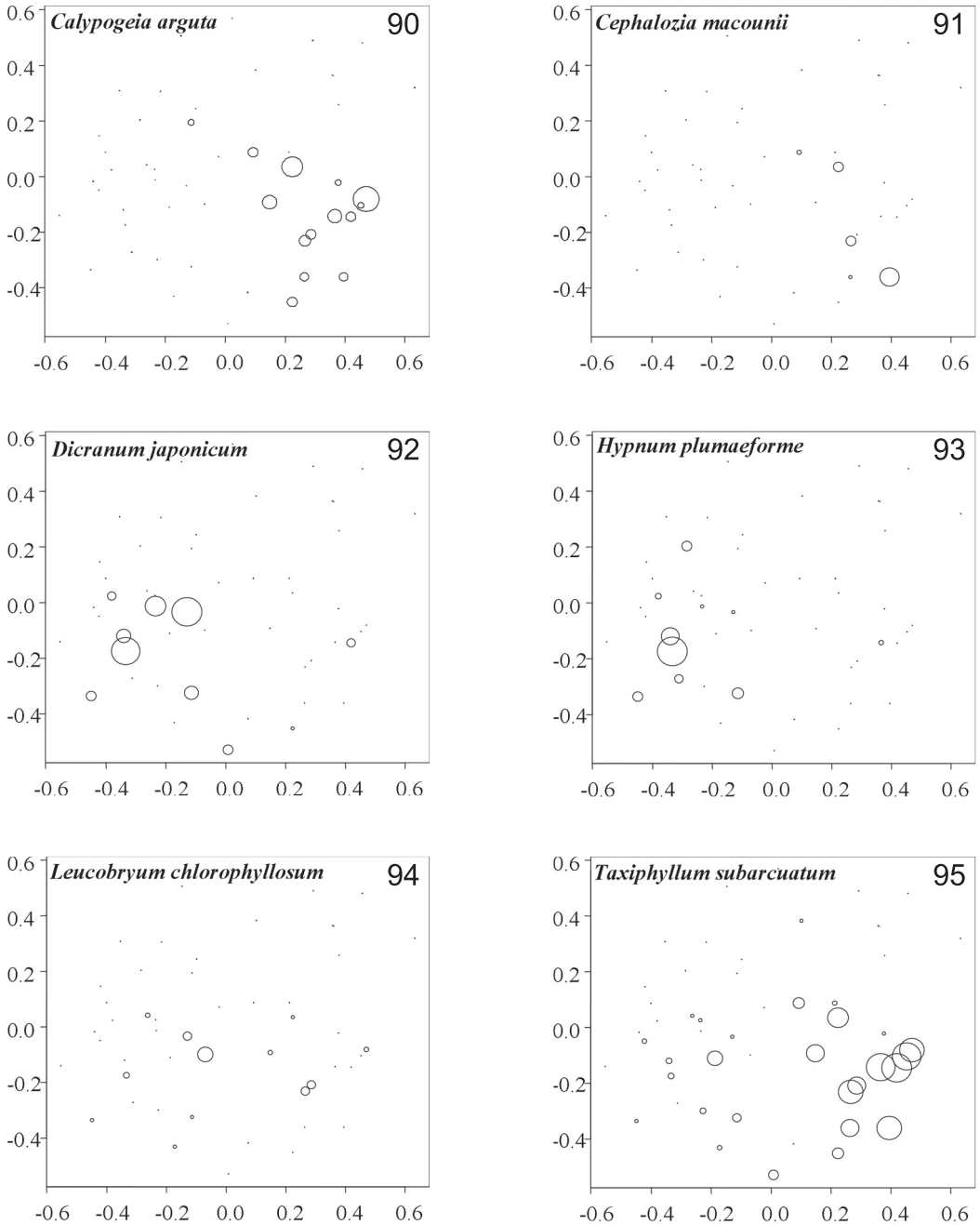

Figs 90–95. Liu Chong Guan: Distribution of species abundances in the GNMDS ordination of 50 plots, axes 1 (horizontal) and 2 (vertical). Frequency in subplots for each species in each plot proportional to circle size. Fig. 90. *Calypogeia arguta*. Fig. 91. *Cephalozia macounii*. Fig. 92. *Dicranum japonicum*. Fig. 93. *Hypnum plumaeforme*. Fig. 94. *Leucobryum chlorophyllosum*. Fig. 95. *Taxiphyllum subarcuatum*. Small dots indicate absence; circles indicate presence, diameter proportional with subplot frequency.

Correlations between environmental variables

A group of correlated variables consisted of pH_{H_2O}, pH_{CaCl_2}, concentrations of Ca and Mg, and the base saturation, which were pairwise positively correlated and negatively correlated with the aluminium saturation, concentrations of Al, Fe and H ($|\tau| > 0.35$ for all pairs; see Tab. 28, Fig. 96). Several variables were associated with this group: the concentration of K by positive correlation with the concentration of Ca and the soil base saturation, and by negative correlation with the soil aluminium saturation; the crown cover index by positive correlation with the concentration of Fe; the number of broadleaved trees by negative correlation with the concentration of Al; litter-layer depth by positive correlation with concentrations of Fe and H, and by negative correlation with soil pH_{CaCl_2}; organic-layer depth by negative correlation with soil pH_{CaCl_2}; and terrain roughness by negative correlations with soil pH_{H_2O} and soil pH_{CaCl_2}.

Another group of pairwise more or less strongly correlated variables included the litter index, the crown cover index and the number of broadleaved trees. Litter index was positively correlated with the crown cover index and negatively correlated with the number of broadleaved trees. The soil depth and the organic matter content were negatively associated with the number of broadleaved trees. Soil depth was also positively correlated with the number of coniferous trees. The two groups of variables were connected by the concentration of Fe and the litter-layer depth with both.

A third group of correlated variables, consisting mainly of topographic variables, included the terrain roughness, the heat index and the aspect favourability, the last mentioned positively correlated with the others. The concentration of Na and soil pH were associated with this group by negative correlations and the concentration of Fe and litter-layer depth were associated with this group by positive correlations.

A fourth group of pairwise more or less strongly positively correlated variables included the organic matter content and contents of total C and N. The number of broadleaved trees was associated with this group by negative correlation.

PCA ordination of environmental variables

Eigenvalues of the first two PCA axes were 0.320 and 0.130, thus 45.0 % of the variation in measured environmental variables was explained by the first two PCA axes.

Soil pH, soil base saturation and the concentration of Ca in soil obtained high loadings on PCA 1, while soil aluminium saturation and the concentrations of Al, Fe and H in soil, which were strongly negatively correlated to above mentioned variables group, obtained low loadings on this axis. Aspect favourability and soil dry matter content obtained high loadings on PCA 2, while low loadings were obtained by soil organic matter and total C and N in soil, which were more or less negatively correlated with aspect favourability and soil dry matter content.

PCA ordination results thus summarised major features of correlations between environmental variables in fewer dimensions (Tab. 28, Figs 96–97). Apparently, the variables of aluminium saturation, concentrations of Al, Fe and H were more or less negatively correlated with the soil nutrients components consisted of concentrations of Ca and Mg, and the base saturation, positively correlated with the tree influence variables included crown cover index and litter index; the soil nutrients components consisted of organic mater content, contents of total C and N were negatively correlated with the number of broadleaved trees.; and the topographic variables included the heat index and

Tab. 28. Lei Gong Shan: Kendall's rank correlation coefficients τ between 33 environmental variable in the 50 plots (lower triangle), with significant probabilities (upper triangle). Very strong correlations ($|\tau| \geq 4.0$, $P < 0.0001$) are indicated by bold face. n.s means significance probability $P > 0.1$. Numbers and abbreviation for names of environmental variables are in accordance with Tab. 2.

	1	2	3	4	5	6	7	8	9	10	11	12	13	14	15	16	17
01 Inclin	*	n.s	.0046	.0001	.0205	n.s	n.s	.0900	.0424	.0015	.0016	.0018	n.s	.0470	.0820	n.s	n.s
02 AspecF	–.1289	*	**.0000**	n.s	.0606	n.s	n.s	n.s	n.s	n.s	n.s	.0017	n.s	n.s	n.s	n.s	.0511
03 HeatIn	.2801	**.5994**	*	n.s	n.s	n.s	n.s	n.s	n.s	.0250	n.s	n.s	n.s	n.s	n.s	n.s	.0464
04 TerraM	.3896	–.0771	.0971	*	.0286	.0035	n.s	n.s	.0014	n.s	n.s	.0138	n.s	n.s	n.s	.0768	n.s
05 ConvS1	–.2361	.1895	.0703	–.2266	*	.0286	.0014	n.s	.0376	n.s	n.s	n.s	n.s	n.s	.0599	.0097	n.s
06 ConvV1	.1457	–.0389	–.0314	.2960	–.2224	*	n.s	n.s	n.s	n.s	n.s	n.s	n.s	n.s	n.s	.0291	n.s
07 ConvS9	–.1187	.0400	–.0136	–.0500	.3314	–.0866	*	n.s	n.s	.0720	n.s	n.s	n.s	n.s	n.s	n.s	n.s
08 ConvV9	.1702	.0217	.1504	.1468	–.0869	.1376	–.0897	*	n.s	.0156	.0249	n.s	n.s	n.s	n.s	n.s	n.s
09 SoilDM	–.2024	–.0373	–.0412	–.3239	.2111	–.1400	.0308	–.0444	*	n.s	n.s	.0112	n.s	n.s	.0006	**.0000**	n.s
10 LitLDM	.3373	.1534	.2355	.1394	–.0438	.0427	–.1951	.2577	.1579	*	.0002	n.s	.0223	.0076	.0047	.0092	.0004
11 OrgaLD	.3345	.0855	.1093	.1288	.0706	–.0380	–.0503	.2379	–.0290	.4260	*	n.s	n.s	n.s	n.s	.0290	.0054
12 SoilMLM	–.3090	.3074	.1335	–.2480	.0509	–.0604	.0136	.0092	.2505	.0225	–.0252	*	n.s	n.s	n.s	.0500	n.s
13 LitteI	.1113	.0017	.0689	.0132	.0405	–.1066	.0221	–.0009	.0515	.2471	.1176	.1339	*	**.0000**	.0390	.0013	.0012
14 CrowCI	.2036	–.0198	.0515	.0479	.0827	–.1292	.0330	.0122	.0736	.2907	.1675	.0499	**.7271**	*	.0092	.0009	.0014
15 RelaCN	.1789	.0301	.0343	–.0920	–.1970	–.0372	–.1343	–.1376	.3536	.3091	.0282	.1339	.2158	.2743	*	.0152	.0050
16 RelaDN	–.0200	–.0356	–.0158	.2065	–.3023	.2496	–.1010	.1336	**–.4657**	–.3181	–.2653	–.2227	–.3763	–.3892	–.2865	*	.0056
17 pH_{H_2O}	–.0283	–.1916	–.1950	–.0025	–.0883	.1283	.0825	–.0333	–.0968	–.3741	–.2912	–.1511	–.3259	–.3244	–.2860	.3150	*
18 pH_{CaCl_2}	–.1571	–.1168	–.1320	–.1499	–.0951	.0745	.0604	–.0825	–.1026	–.4086	–.3894	–.0994	–.2552	–.3322	–.2895	.3046	**.6897**
19 Al	.1467	.1328	.0645	.0887	.0466	–.0578	–.0492	.0224	.0643	.3074	.3424	.1237	.2501	.2737	.2989	–.3719	**–.4810**
20 Fe	.2056	.0435	.0768	.0895	.0449	–.0289	–.0772	.0947	.1023	.4218	.3488	.0598	.3370	.3785	.3247	–.3379	**–.6066**
21 H	.1317	.1755	.1560	.0498	.0516	–.0050	–.1137	.0839	.0775	.3614	.3029	.1613	.3165	.3234	.2749	–.3272	**–.6333**
22 Mn	–.0754	.1624	.1577	–.1444	.0466	–.0809	.1137	–.1603	.1006	.0036	–.0036	.1925	.1242	.0369	.0146	–.2957	–.0025
23 Ca	.0423	–.2821	–.0940	.0464	–.1211	.1469	.0594	–.0324	–.1204	–.2355	–.2133	–.2400	–.1225	–.1587	–.2732	.2484	**.4334**
24 Mg	–.0290	–.3411	–.2933	–.0616	–.0923	.1189	.0000	–.0872	.0198	–.1546	–.1918	–.1974	–.1752	–.2136	–.0711	.0854	.3712
25 Na	.0174	–.3805	–.3734	–.0245	–.0144	–.0660	.0747	–.0989	–.0594	–.1996	–.1864	–.1319	–.0544	–.0661	–.1088	.0223	.2270
26 K	–.0290	–.1148	.0727	.0296	–.0466	.0033	.0509	–.0258	–.0940	–.1169	–.0932	–.1826	.0255	–.0918	–.1841	.1065	.1352
27 C	.2743	–.1492	–.1201	.1241	–.0296	.1106	.1867	–.0407	.0049	.1007	.1757	–.1761	.1191	.0746	.1670	–.2642	–.0107
28 N	.1610	–.2141	–.2497	.0778	.0608	.0869	.2421	–.0723	.0392	–.0064	.0835	–.2056	.0456	.0078	.0719	–.2235	.0746
29 BS	–.0091	–.2575	–.1185	.0144	–.1024	.1222	.0424	–.0839	–.1072	–.2877	–.2707	–.2334	–.1803	–.2188	–.3023	.2721	**.5137**
30 AlS	.0224	.2411	.0842	–.0025	.1075	–.1205	–.0390	.0623	.1254	.2823	.2653	.2154	.1633	.2136	.3074	–.2852	**–.4662**
31 SO_4	.0887	.1296	.1054	–.0059	.0838	–.0974	–.0696	.1288	.2161	.2949	.3262	.1106	.1395	.1347	.1841	–.2484	–.2220
32 WDM	–.1541	.0549	.0016	–.1080	.0271	–.1873	–.0941	.0498	–.0008	–.1680	–.1819	.0671	–.1131	–.0875	–.0342	.2141	.1171
33 LOI	.1831	–.1492	–.1789	.0853	.0364	.1073	.1951	.0341	.0990	.1744	.1685	–.0549	.1803	.1381	.1276	–.3956	–.0860

Tab. 28 (continued). Lei Gong Shan: Kendall's rank correlation coefficients τ between 33 environmental variable in the 50 plots (lower triangle), with significant probabilities (upper triangle). Very strong correlations ($|\tau| \geq 4.0$, $P < 0.0001$) are indicated by bold face. n.s means significance probability $P > 0.1$. Numbers and abbreviation for names of environmental variables are in accordance with Tab. 2.

	18	19	20	21	22	23	24	25	26	27	28	29	30	31	32	33
01 Inclin	n.s	n.s	.0377	n.s	n.s	n.s	n.s	n.s	n.s	.0056	n.s	n.s	n.s	n.s	n.s	.0641
02 AspecF	n.s	n.s	n.s	.0733	.0975	.0040	.0005	.0001	n.s	n.s	.0306	.0086	.0139	n.s	n.s	n.s
03 HeatIn	n.s	n.s	n.s	n.s	n.s	n.s	.0027	.0001	n.s	n.s	.0114	n.s	n.s	n.s	n.s	.0669
04 TerraM	n.s	n.s	n.s	n.s	n.s	n.s	n.s	n.s	n.s	n.s	n.s	n.s	n.s	n.s	n.s	n.s
05 ConvS1	n.s	n.s	n.s	n.s	n.s	n.s	n.s	n.s	n.s	n.s	n.s	n.s	n.s	n.s	n.s	n.s
06 ConvV1	n.s	n.s	n.s	n.s	n.s	n.s	n.s	n.s	n.s	n.s	n.s	n.s	n.s	n.s	n.s	n.s
07 ConvS9	n.s	n.s	n.s	n.s	n.s	n.s	n.s	n.s	n.s	.0640	.0174	n.s	n.s	n.s	n.s	.0529
08 ConvV9	n.s	n.s	n.s	n.s	n.s	n.s	n.s	n.s	n.s	n.s	n.s	n.s	n.s	n.s	n.s	n.s
09 SoilDM	n.s	n.s	n.s	n.s	n.s	n.s	n.s	n.s	n.s	n.s	n.s	n.s	n.s	n.s	n.s	n.s
10 LitLDM	.0001	.0034	.0001	.0006	n.s	.0250	n.s	.0575	n.s	n.s	n.s	.0062	.0072	.0050	n.s	.0969
11 OrgaLD	.0002	.0011	.0008	.0037	n.s	.0412	.0664	.0744	n.s	n.s	n.s	.0096	.0111	.0018	.0816	n.s
12 SoilMLM	n.s	n.s	n.s	.0993	.0493	.0142	.0437	n.s	.0621	.0720	.0377	.0171	.0278	n.s	n.s	n.s
13 LitteI	.0113	.0128	.0008	.0016	n.s	n.s	.0812	n.s	n.s	n.s	n.s	.0727	n.s	n.s	n.s	.0727
14 CrowCI	.0011	.0069	.0002	.0014	n.s	n.s	.0348	n.s	n.s	n.s	n.s	.0307	.0348	n.s	n.s	n.s
15 RelaCN	.0045	.0033	.0014	.0068	n.s	.0072	n.s	n.s	.0699	n.s	n.s	.0029	.0025	.0699	n.s	n.s
16 RelaDN	.0074	.0010	.0029	.0039	.0091	.0284	n.s	n.s	n.s	.0198	.0511	.0164	.0119	.0284	.0588	.0005
17 pH_{H_2O}	**.0000**	**.0000**	**.0000**	**.0000**	n.s	**.0000**	.0002	.0205	n.s	n.s	n.s	**.0000**	**.0000**	.0234	n.s	n.s
18 pH_{CaCl_2}	*	**.0000**	**.0000**	**.0000**	n.s	**.0000**	.0007	n.s	.0121	n.s	n.s	**.0000**	**.0000**	.0004	n.s	n.s
19 Al	**–.5738**	*	**.0000**	**.0000**	n.s	**.0000**	.0010	n.s	.0045	.0523	n.s	**.0000**	**.0000**	.0160	n.s	.0049
20 Fe	**–.6617**	**.6138**	*	**.0000**	.0136	**.0000**	.0069	n.s	.0080	n.s	n.s	**.0000**	**.0000**	.0023	n.s	.0062
21 H	**–.6180**	**.6618**	**.6857**	*	n.s	**.0000**	.0045	n.s	n.s	n.s	n.s	**.0000**	**.0000**	.0167	n.s	.0105
22 Mn	.0803	–.0768	–.2411	–.0229	*	n.s	n.s	.0734	.0047	n.s	n.s	n.s	n.s	n.s	.0023	n.s
23 Ca	**.4246**	**–.5948**	**–.4847**	**–.4755**	.1552	*	**.0000**	n.s	**.0000**	n.s	n.s	**.0000**	**.0000**	.0045	.0034	n.s
24 Mg	.3328	–.3219	–.2640	–.2778	.0719	**.5180**	*	.0064	.0200	.0976	.0162	**.0000**	**.0000**	n.s	n.s	.0848
25 Na	.1475	–.0752	–.0629	–.1552	–.1748	.1111	.2663	*	n.s	n.s	.0385	n.s	n.s	n.s	n.s	.0004
26 K	.2459	–.2778	–.2591	–.1258	.2761	**.4150**	.2271	–.1471	*	n.s	n.s	.0001	**.0000**	.0350	.0365	n.s
27 C	–.0689	.1895	.1332	.0441	.0572	.0163	.1618	.0882	–.0359	*	**.0000**	n.s	n.s	n.s	.0047	**.0000**
28 N	.0597	.0422	.0364	–.0405	.0372	.0786	.2373	.2042	–.0107	**.7648**	*	n.s	n.s	n.s	.0418	**.0000**
29 BS	**.5148**	**–.7141**	**–.5729**	**–.5752**	.1438	**.8676**	**.5098**	.1487	.3775	–.0212	.0587	*	**.0000**	.0031	.0523	n.s
30 AlS	**–.4951**	**.7026**	**.5386**	**.5245**	–.1552	**–.8693**	**–.4918**	–.1046	**–.4150**	.0523	–.0190	**–.9232**	*	.0055	.0219	n.s
31 SO_4	–.3443	.2353	.2983	.2337	–.0670	–.2778	–.1422	–.0719	–.2059	.0719	.0786	–.2892	.2712	*	n.s	n.s
32 WDM	.1606	–.0016	–.0041	–.0653	–.2973	–.2858	–.1307	.0964	–.2042	–.2760	–.2008	–.1895	.2238	–.0343	*	.0086
33 LOI	–.1475	.2745	.2673	.2500	.0670	–.0621	.1683	.3431	.0033	.4379	.4771	–.1127	.1111	.1209	–.2564	*

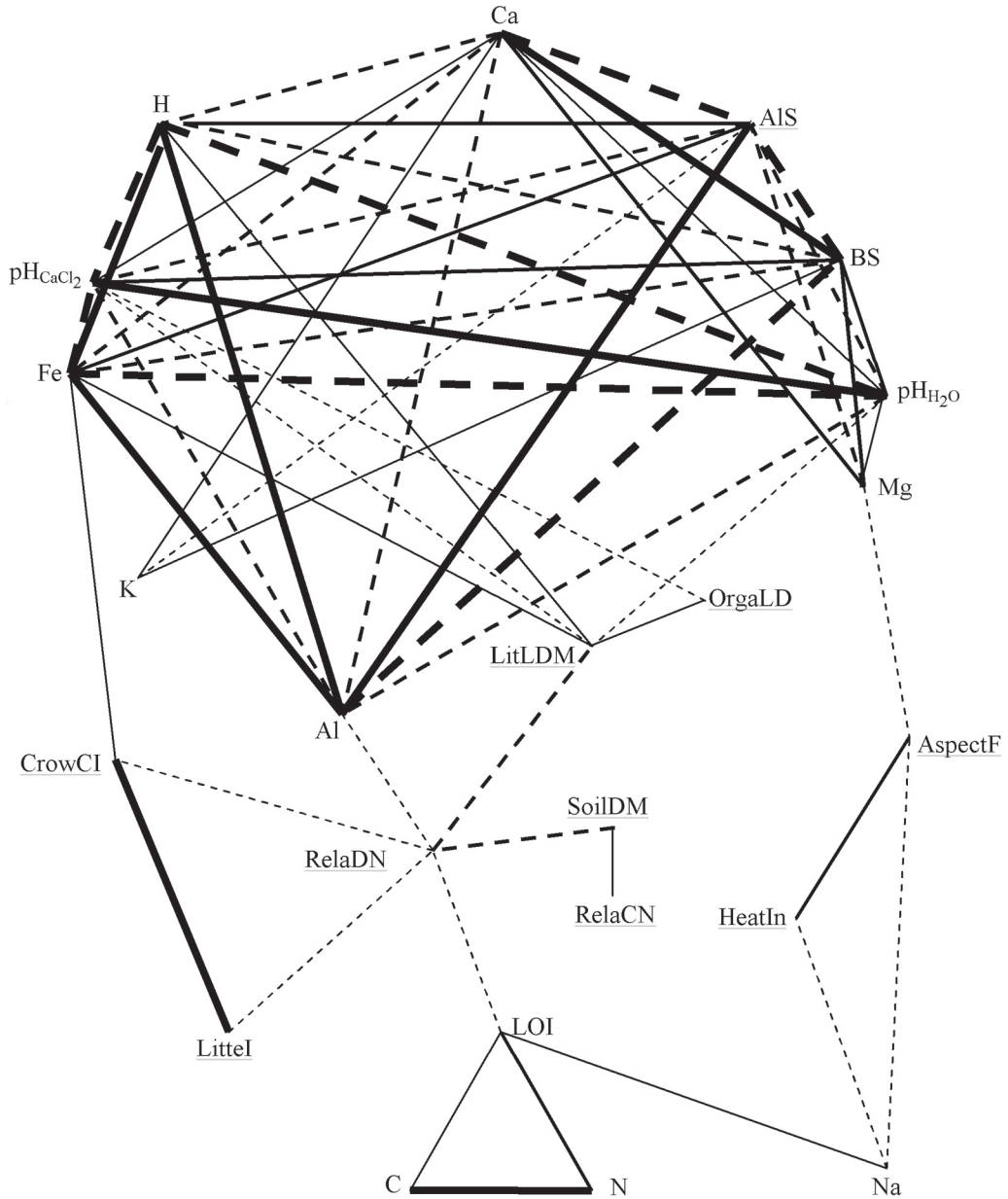

Fig. 96. Lei Gong Shan: Plexus diagram visualizing Kendall's τ between pairs of environmental variables. Significance probabilities for τ are indicated by lines with different thickness (in order of decreasing thickness): $|\tau| \geq 0.60$, $0.45 \leq |\tau| < 0.60$, and $0.35 \leq |\tau| < 0.45$. Continuous lines refer to positive correlations, broken lines to negative.

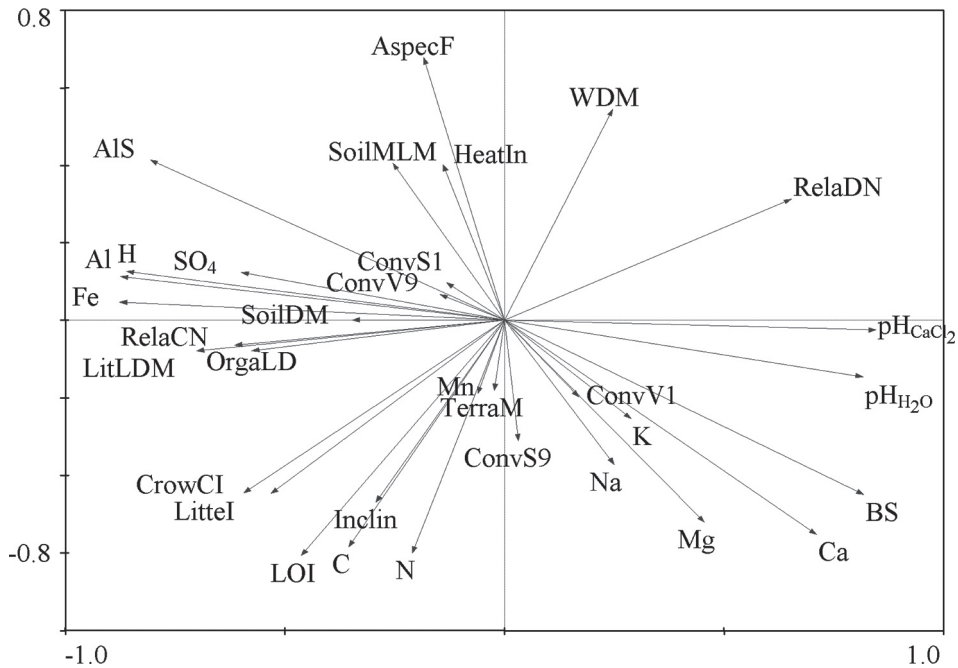

Fig. 97. Lei Gong Shan: PCA ordination of 33 environmental variables (names abbreviated in accordance with Tab.2), axes 1 (horizontal) and 2 (vertical). Loadings of variables on the ordination axes are shown by heads of variable vectors.

the aspect favourability were negatively correlated with soil pH, and positively correlated with the concentration of Fe and litter-layer depth.

GNMDS ordination

Good correspondence with respect to gradient length, core length and eigenvalues was found between corresponding axes of GNMDS 1 and DCA 1, and GNMDS 2 and DCA 2, respectively. There was no marked difference in eigenvalues between GNMDS 1 (DCA 1) and GNMDS 2 (DCA 2), indicating that the first two axes were the major compositional gradients.

The first two axes of the GNMDS ordination of the 50 1-m^2 plots had high eigenvalues (2.4984 and 2.2643, respectively) and gradient length of 3.7230 and 2.4371 S.D. units, respectively. Plots number 9, 16, 17, 20 and 49 made up a somewhat isolated group in space spanned by the first two GNMDS ordination axes, while the remaining plots were relatively evenly distributed in the GNMDS ordination (Fig. 98). No plot acted as outliers, as judged by core length (Tab. 29).

Tab. 29. Ordination of vegetation in the 50 plots in LGS: summary of properties for GNMDS and DCA axes 1–2 properties. Core length means length of the shortest interval containing 90 % of the plots relative to gradient length.

Corresponding axis		Unit	A	B
Axis No			GNMDS 1, DCA 1	GNMDS 2, DCA 2
GNMDS	Gradient length	HC	1.414	1.307
		S. D	3.723	2.437
	Core length	%	0.594	0.592
	Eigenvalue		2.498	2.264
DCA	Gradient length	S.D	4.140	3.166
	Core length	%	0.664	0.700
	Eigenvalue		0.538	0.346

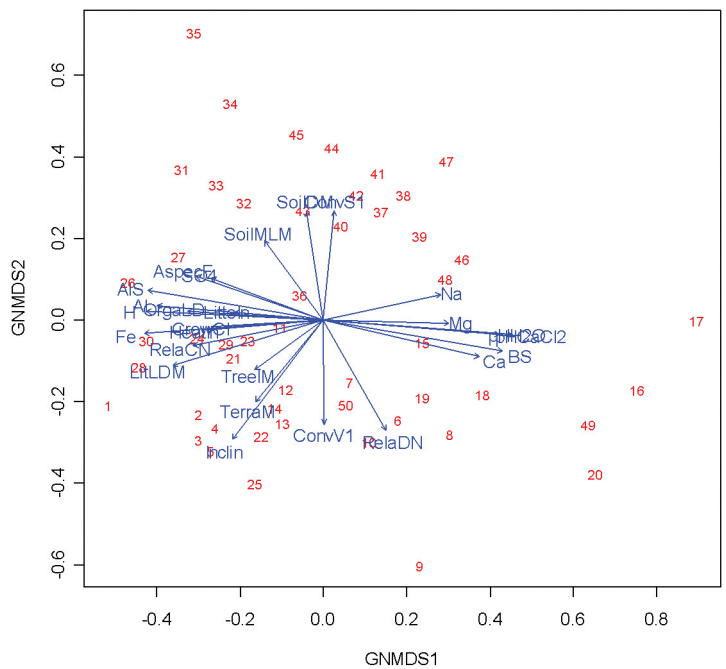

Fig. 98. Lei Gong Shan: GNMDS ordination biplots of 50 plots (indicated by their number) and significant environmental variables (i.e. with $P < 0.1$ according to goodness-of-fit test; see Tab. 34). Names of variables are abbreviated in accordance with Tab. 2. For each environmental variable the direction of maximum increase and the relative magnitude of increase in this direction is indicated by the direction and length of the vector arrows, axes 1 (horizontal) and 2 (vertical).

Relationship between ordination axes and environmental variables

GNMDS ordination biplots of plots and significant environmental variables

Positions of plot scores in the GNMDS ordination space were related to variation in environmental variables, as indicated by a several environmental variable vectors with significantly directed variation patterns in the ordination space (Fig. 98). Along the first two axes the following patterns appeared: (1) vectors for concentrations of Al, Fe and H in soil, soil aluminium saturation, aspect favourability and heat index, crown cover index and the number of coniferous trees, litter-layer depth, organic-layer depth pointed to the left (representing a gradient of increasing concentrations of Al, Fe and H in soil, soil aluminium saturation, light conditions, coniferous tree density, etc.); (2) vectors for soil pH_{CaCl_2}, soil pH_{H_2O}, concentrations of Ca, Mg and Na in soil, and soil base saturation pointed rightwards, almost directly in the opposite direction of vectors for (1); (3) vectors for soil moisture, soil depth and concavity/convexity sum index at 1-m^2 scale pointed upwards: and (4) vectors for inclination and the variance of concavity/convexity at 1-m^2 scale, and the number of broadleaved trees pointed to the lower. Thus, plots with relatively moist and deep soil occurred to the upper in the biplots, while plots with relatively dry soil and high broadleaved trees density to the lower. Plots with a relatively higher soil pH, higher concentrations of Ca and Mg in soil were situated in the right part of the biplots, while plots with relatively higher concentrations of Al, Fe and H in soil, higher soil aluminium saturation, thicker litter layer, higher coniferous trees density and more favourable light conditions were situated in the converse direction.

Split-plot GLM analysis of relationships between ordination axes and environmental variables

Variation (in plot scores) along GNMDS axis 1 was partitioned with 83.67 % at the macro-plot scale (i.e. between macro plots) and 16.33 % at the plot scale (i.e. between plots). Variation along GNMDS axis 2 was partitioned with 61.48 % at the macro-plot scale and 38.52 % at the plot scale (Tabs 30–31).

At the macro-plot scale, a total of 13 environmental variables were significantly ($P < 0.05$) and four were indicatively significantly ($P < 0.1$) related to GNMDS axis 1, two and one variables (at the $P < 0.05$ and $P < 0.1$ levels, respectively) were related to GNMDS axis 2. At the plot scale, a total of five were significantly and three were indicatively significantly related to GNMDS axis 1, two and one variables (at the $P < 0.05$ and $P < 0.1$ levels, respectively) were related to GNMDS axis 2 (Tabs 30–31).

At the macro-plot scale, the variables significantly negatively related to GNMDS axis 1 were aspect favourability, litter-layer depth, concentrations of Al, Fe and H in soil, soil aluminium saturation and SO_4 adsorption in soil. The variables of soil pH_{H_2O}, soil pH_{CaCl_2}, concentrations of Ca, Mg and Na in soil, and soil base saturation were significantly positively related to this axis ($P < 0.05$). The variables of organic-layer depth, soil moisture, crown cover index and the number of coniferous trees were indicatively significantly related to GNMDS axis 1 (negatively) ($0.05 < P < 0.1$). At the plot scale, terrain conditions, concentration of Al in soil, total C in soil and soil aluminium saturation decreased significantly along GNMDS axis 1 while significantly increasing soil base saturation ($P < 0.05$). The variance of concavity/convexity at 9-m^2 scale, soil pH_{H_2O} and soil pH_{CaCl_2} increased indicatively significantly along GNMDS axis 1 ($0.05 < P < 0.01$) (Tab. 30).

At the macro-plot scale, the variables significantly negatively related to GNMDS axis 2 were concavity/convexity sum index at both 1-m^2 and 9-m^2 scales ($P < 0.05$). Inclination was indicatively significantly related to this axis (positively) ($P = 0.0935$). At the plot scale, SO_4 adsorption ($P = 0.0441$) in soil decreased significantly along GNMDS axis 2 while indicatively significantly decreasing soil pH_{H_2O} ($P = 0.0943$) (Tab. 31).

Kendall's rank correlation between ordination axes and environmental variables

The variables most strongly negatively correlated with GNMDS axis 1 were Aspect favourability, heat index, litter-layer depth, organic-layer depth, concentrations of Al, Fe and H in soil, and soil aluminium saturation, and the variables most strongly positively correlated with this axis were soil pH_{H_2O}, soil pH_{CaCl_2}, concentrations of Ca, Mg and Na in soil, and soil base saturation ($0.30 \leq |\tau| \leq 0.52$). The variables more or less negatively strongly correlated with GNMDS axis 1 were litter index, crown cover index and the number of coniferous trees, soil moisture, and SO_4 adsorption in soil, and positively correlated with this axis was the concentration of K in soil ($0.2 \leq |\tau| \leq 0.3$) (Tab. 30).

The variables most strongly negatively correlated with GNMDS axis 2 were inclination and the number of broadleaved trees, and the variables most strongly positively correlated with this axis were concavity/convexity sum index at 1-m^2 scale and soil depth ($0.30 \leq |\tau| \leq 0.35$). The variable more or less strongly negatively correlated with GNMDS axis 2 was terrain conditions and the variance of concavity/convexity at 1-m^2 scale, and the variables positively correlated with this axis were concavity/convexity sum index at 9-m^2 scale and soil moisture ($0.2 \leq |\tau| \leq 0.3$) (Tab. 31).

Relationships between ordination axes and species number variables

Split-plot GLM analysis of relationships between ordination axes and species number variables

No any variable of species number was related with to GNMDS axis 1 (Tab. 32).

Along GNMDS axis 2, the fraction of variation explained by these three species number variables is 61.48 % at the macro-plot scale, and 38.52 % at the plot scale. The total number of species was significantly positively related to GNMDS axis 2 at the plot scale, while the number of vascular plants was indicatively significantly related to this axis (positively) at the plot scale (Tab. 33).

Kendall's rank correlation between ordination axes and species number variables

The number of vascular plants was somewhat strongly positively correlated with GNMDS axis 1 ($\tau = 0.2060$) (Tab. 32). No variable of species number was correlated with GNMDS axis 2 (Tab. 33).

Isoline diagrams for significant environmental and species number variables

A total of 21 environmental variables satisfied the criteria for making two-dimensional isoline diagrams (Tab. 34, Figs 99–119).

The distribution of species abundance in the GNMDS ordination

Out of a total of 137 species, 38 were found in at least 5 of the 50 plots (Tab.35, Figs 120–157).

Rubus irenaeus (Fig. 141), a typical example of vascular plants with wide ecological amplitude, was abundant in most plots. Other examples were *Aster ageratoides* (Fig. 122), *Oplismenus compositus* (Fig. 135) and *Paraprenanthes sororia* (Fig. 137).

Chiloscyphus latifolius (Fig. 155), a typical example of a bryophyte species with wide ecological amplitude, was abundant in most plots.

Vascular plant *Clastobryella cuculligera* (Fig. 145) was restricted to plots in lower left part of the GNMDS ordination diagram (related to a more favourable light conditions, a lower soil pH

Tab. 30. Lei Gong Shan: Split-plot GLM analysis and Kendall's nonparametric correlation coefficient τ between GNMDS axis 1 and 33 environmental variables (predictor) in the 50 plots. df_{resid}: degrees of freedom for the residuals; *SS*: total variation; *FVE*: fraction of total variation attributable to a given scale (macro plot or plot); SS_{expl}/SS: fraction of the variation attributable to the scale in question, explained by a variable; *r*: model coefficient (only given when significant at the α = 0.1 level, otherwise blank); *F*: *F* statistic for test of the hypothesis that *r* = 0 against the two-tailed alternative. Split-plot GLM relationships significant at level α = 0.05, *P*, *F*, *r* and SS_{expl}/SS, and Kendall's nonparametric correlation coefficient $|\tau| \geq 0.30$ are given in bold face. Numbers and abbreviations for names of environmental variables are in accordance with Tab. 2.

Predictor	Dependent variable = GNMDS 1 (*SS* = 39.0641)								Correlation between predictor and GNMDS 1
	Error level								
	Macro plot df_{resid} = 8 $SS_{macro\ plot}$ = 32.6857 *FVE* = 0.8367 of *SS*				Plot within macro plot df_{resid} = 39 SS_{plot} = 6.3784 *FVE* = 0.1633 of *SS*				Total
	$SS_{expl}/SS_{macro\ plot}$	*r*	*F*	*P*	SS_{expl}/SS_{plot}	*r*	*F*	*P*	τ
Inclin	0.0436		0.3646	0.5627	0.0013		0.0523	0.8203	–0.197
AspecF	**0.4020**	**–1.9570**	**5.3779**	**0.0490**	0.0390		1.5836	0.2157	**–0.409**
HeatIn	0.2932		3.3180	0.1060	0.0011		0.0430	0.8369	–0.413
TerraM	0.0003		0.0021	0.9647	**0.1221**	**–0.8422**	**5.4231**	**0.0252**	–0.157
ConvS1	0.0616		0.5255	0.4892	0.0184		0.7315	0.3976	–0.031
ConvV1	0.0845		0.7382	0.4152	0.0014		0.0541	0.8173	0.011
ConvS9	0.0452		0.3788	0.5553	0.0304		1.2224	0.2757	0.098
ConvV9	0.1239		1.1317	0.3185	0.0716	0.6069	3.0058	0.0909	–0.191
SoilDM	0.1049		.9378	0.3612	0.0047		0.1838	0.6705	–0.034
LitLDM	**0.4820**	**–2.2276**	**7.4447**	**0.0259**	0.0001		0.0036	0.9526	**–0.405**
OrgaLD	0.3954	–2.6556	5.2314	0.0515	0.0207		0.8259	0.3690	**–0.338**
SoilMLM	0.3626	–3.4960	4.5516	0.0654	0.0004		0.0143	0.9054	–0.216
LitteI	0.2335		2.4372	0.1571	0.0338		1.3665	0.2495	–0.217
CrowCI	0.3737	–2.8277	4.7728	0.0604	0.0076		0.2975	0.5885	–0.283
RelaCN	0.3436	–2.6572	4.1882	0.0749	0.0191		0.7608	0.3884	–0.296
RelaDN	0.2261		2.3367	0.1649	0.0079		0.3100	0.5808	0.193
pH_{H_2O}	**0.7519**	**4.9949**	**24.2470**	**0.0012**	0.0880	0.8848	3.7627	0.0597	**0.482**
pH_{CaCl_2}	**0.7031**	**5.1730**	**18.9440**	**0.0024**	0.0741	1.0023	3.1209	0.0851	**0.498**
Al	**0.6330**	**–3.2741**	**13.7980**	**0.0059**	0.1347	–0.7577	6.0689	0.0183	**–0.448**
Fe	**0.6552**	**–2.9785**	**15.2050**	**0.0045**	0.0567		2.3430	0.1339	**–0.457**
H	**0.7623**	**–3.7582**	**25.6590**	**0.0010**	0.0394		1.5983	0.2136	**–0.475**
Mn	0.0058		0.0463	0.8350	0.0011		0.0415	0.8396	0.083
Ca	**0.6592**	**3.2703**	**15.4710**	**0.0043**	0.0639		2.6609	0.1109	**0.448**
Mg	**0.5217**	**4.3427**	**8.7251**	**0.0183**	0.0159		0.6296	0.4323	**0.400**
Na	**0.4378**	**2.8553**	**6.2306**	**0.0372**	0.0003		0.0131	0.9093	**0.323**
K	0.2995		3.4209	0.1015	0.0066		0.2609	0.6124	0.248
C	0.0069		0.0558	0.8192	**0.1143**	**–0.8216**	**5.0312**	**0.0307**	–0.033
N	0.0100		0.0806	0.7838	0.0519		2.1330	0.1522	0.108
BS	**0.7451**	**3.1836**	**23.3870**	**0.0013**	**0.1166**	**0.7763**	**5.1464**	**0.0289**	**0.514**
AlS	**0.7214**	**–3.2331**	**2.7180**	**0.0019**	**0.1273**	**–0.7898**	**5.6896**	**0.0220**	**–0.487**
SO_4	**0.5581**	**–4.4060**	**1.1040**	**0.0130**	0.0300		1.2070	0.2787	–0.268
WDM	0.0023		0.0186	0.8948	0.0413		1.6787	0.2027	0.016
LOI	0.0221		0.1805	0.6821	0.0037		0.1453	0.7052	0.013

Tab. 31. Lei Gong Shan: Split-plot GLM analysis and Kendall's nonparametric correlation coefficient τ between GNMDS axis 2 and 33 environmental variables (predictor) in the 50 plots. df_{resid}: degrees of freedom for the residuals; *SS*: total variation; *FVE*: fraction of total variation attributable to a given scale (macro plot or plot); SS_{expl}/SS: fraction of the variation attributable to the scale in question, explained by a variable; *r*: model coefficient (only given when significant at the α = 0.1 level, otherwise blank); *F*: *F* statistic for test of the hypothesis that *r* = 0 against the two-tailed alternative. Split-plot GLM relationships significant at level α = 0.05, *P*, *F*, *r* and SS_{expl}/SS, and Kendall's nonparametric correlation coefficient $|\tau| \geq 0.30$ are given in bold face. Numbers and abbreviations for names of environmental variables are in accordance with Tab. 2.

Predictor	Dependent variable = GNMDS 2 (*SS* = 18.6450)								Correlation between predictor and GNMDS 2
	Error level								
	Macro plot df_{resid} = 8 $SS_{macro\ plot}$ = 11.4626 *FVE* = 0.6148 of *SS*				Plot within macro plot df_{resid} = 39 SS_{plot} = 7.1824 *FVE* = 0.3852 of *SS*				Total
	$SS_{expl}/SS_{macro\ plot}$	*r*	*F*	*P*	SS_{expl}/SS_{plot}	*r*	*F*	*P*	τ
Inclin	0.3117	–1.1175	3.6235	0.0935	0.0003		0.0101	0.9206	**–0.336**
AspecF	0.0004		0.0031	0.9567	0.0099		0.3886	0.5367	0.148
HeatIn	0.0176		0.1432	0.7150	0.0012		0.0474	0.8288	0.011
TerraM	0.2214		2.2743	0.1700	0.0002		0.0093	0.9238	–0.230
ConvS1	**0.4067**	**2.1100**	**5.4849**	**0.0473**	0.0000		0.0003	0.9872	**0.306**
ConvV1	0.2438		2.5787	0.1470	0.0000		0.0009	0.9757	–0.295
ConvS9	**0.6221**	**3.6781**	**13.1680**	**0.0067**	0.0102		0.4039	0.5288	0.245
ConvV9	0.0106		0.0857	0.7771	0.0158		0.6275	0.4331	–0.101
SoilDM	0.1829		1.7901	0.2177	0.0058		0.2275	0.6360	0.299
LitLDM	0.1112		1.0009	0.3464	0.0343		1.3852	0.2464	–0.096
OrgaLD	0.0067		0.0537	0.8225	0.0308		1.2403	0.2722	–0.019
SoilMLM	0.1822		1.7828	0.2185	0.0047		0.1831	0.6710	0.234
LitteI	0.0162		0.1319	0.7259	0.0148		0.5847	0.4491	0.022
CrowCI	0.0331		0.2738	0.6150	0.0001		0.0021	0.9640	–0.008
RelaCN	0.0601		0.5118	0.4947	0.0051		0.1984	0.6585	–0.034
RelaDN	0.1926		1.9080	0.2045	0.0001		0.0049	0.9445	**–0.330**
pH_{H_2O}	0.0280		0.2306	0.6440	0.0701	0.8382	2.9415	0.0943	–0.060
pH_{CaCl_2}	0.0119		0.0966	0.7639	0.0347		1.4035	0.2433	–0.046
Al	0.0334		0.2766	0.6132	0.0007		0.0288	0.8660	0.074
Fe	0.0965		0.8545	0.3823	0.0130		0.5138	0.4777	0.009
H	0.0523		0.4414	0.5251	0.0006		0.0245	0.8765	0.059
Mn	0.1731		1.6748	0.2317	0.0202		0.8039	0.3754	0.078
Ca	0.0072		0.0582	0.8154	0.0001		0.0032	0.9553	–0.158
Mg	0.0360		0.2989	0.5995	0.0044		0.1722	0.6805	–0.075
Na	0.0882		0.7741	0.4046	0.0020		0.0776	0.7821	0.034
K	0.0496		0.4179	0.5361	0.0255		1.0192	0.3189	–0.015
C	0.0036		0.0288	0.8695	0.0053		0.2099	0.6494	–0.021
N	0.0081		0.0654	0.8046	0.0271		1.0882	0.3033	0.032
BS	0.0134		0.1090	0.7497	0.0000		0.0015	0.9696	–0.141
AlS	0.0128		0.1038	0.7556	0.0000		0.0018	0.9662	0.132
SO_4	0.0001		0.0007	0.9795	**0.0999**	**0.8177**	**4.3264**	**0.0441**	0.149
WDM	0.0237		0.1944	0.6710	0.0214		0.8535	0.3612	0.071
LOI	0.0143		0.1164	0.7417	0.0611		2.5364	0.1193	0.106

Tab. 32. Lei Gong Shan: Split-plot GLM analysis and Kendall's nonparametric correlation coefficient τ between GNMDS axis 1 and two species number variables (predictor) in the 50 plots. df_{resid}: degrees of freedom for the residuals; *SS*: total variation; *FVE*: fraction of total variation attributable to a given scale (macro plot or plot); SS_{expl}/SS: fraction of the variation attributable to the scale in question, explained by a variable; *r*: model coefficient (only given when significant at the α = 0.1 level, otherwise blank); *F*: *F* statistic for test of the hypothesis that *r* = 0 against the two-tailed alternative. Split-plot GLM relationships significant at level α = 0.05, *P*, *F*, *r* and SS_{expl}/SS, and Kendall's nonparametric correlation coefficient $|\tau| \geq 0.30$ are given in bold face.

Predictor (number of species)	Dependent variable = GNMDS 1 (*SS* = 39.0641)								Correlation between predictor and GNMDS 1
	Error level								
	Macro plot df_{resid} = 8 $SS_{macro\ plot}$ = 32.6857 *FVE* = 0.8367 of *SS*				Plot within macro plot df_{resid} = 39 SS_{plot} = 6.3784 *FVE* = 0.1633 of *SS*				Total
	$SS_{expl}/SS_{macro\ plot}$	*r*	*F*	*P*	SS_{expl}/SS_{plot}	*r*	*F*	*P*	τ
Vascular plants	0.1689		1.6263	0.2380	0.0590		2.4456	0.1259	0.206
Bryophyte species	0.0007		0.0056	0.9423	0.0099		0.3901	0.5359	0.049

Tab. 33. Lei Gong Shan: Split-plot GLM analysis and Kendall's nonparametric correlation coefficient τ between GNMDS axis 2 and two species number variables (predictor) in the 50 plots. df_{resid}: degrees of freedom for the residuals; *SS*: total variation; *FVE*: fraction of total variation attributable to a given scale (macro plot or plot); SS_{expl}/SS: fraction of the variation attributable to the scale in question, explained by a variable; *r*: model coefficient (only given when significant at the α = 0.1 level, otherwise blank); *F*: *F* statistic for test of the hypothesis that r = 0 against the two-tailed alternative. Split-plot GLM relationships significant at level α = 0.05, *P*, *F*, *r* and SS_{expl}/SS, and Kendall's nonparametric correlation coefficient $|\tau| \geq 0.30$ are given in bold face.

Predictor (number of species)	Dependent variable = GNMDS 2 (*SS* = 18.6450)								Correlation between predictor and GNMDS 2
	Error level								
	Macro plot df_{resid} = 8 $SS_{macro\ plot}$ = 11.4626 *FVE* = 0.6148 of *SS*				Plot within macro plot df_{resid} = 39 SS_{plot} = 7.1824 *FVE* = 0.3852 of *SS*				Total
	$SS_{expl}/SS_{macro\ plot}$	*r*	*F*	*P*	SS_{expl}/SS_{plot}	*r*	*F*	*P*	τ
Vascular plants	0.2895		3.2601	0.1086	0.0743		3.1285	0.0848	–0.084
Bryophyte species	0.1191		1.0819	0.3287	0.0326		1.3156	0.2584	0.160

Tab. 34. Lei Gong Shan: Environmental and species number variables for which two-dimensional isoline diagrams were made: P value for relationship with GNMDS axis assessed by split-plot GLM (two scales = error levels), Kendall's correlation coefficient τ with axis, and R^2 between the original and predicted values (according to the isoline diagrams for the variable), used as a measure of goodness-of-fit of the isolines. Isoline diagrams were made for variables with split-plot GLM $P < 0.05$ at the macro plot or the plot scale and/or Kendall's correlation coefficient $|\tau| \geq 0.3$ with one GNMDS axis. P values < 0.05 and/or $|\tau| \geq 0.30$ in bold face. Numbers and abbreviations for names of environmental variables in accordance with Tab. 2 (NVP = number of vascular plants species; and NBS = number of bryophyte species).

Ordination axis	Variable names	The split plot GLM Error level		Kendall's ccorrelation between variable and ordination axis	Goodness-of-fit of the isolines
		$P_{\text{macro plot}}$	P_{plot}	τ_{total}	R^2
GNMDS 1	AspecF	**0.0490**	0.2157	**–0.409**	0.4386
	HeatIn	0.1060	0.8369	**–0.413**	0.2799
	TerraM	0.9647	**0.0252**	–0.157	0.4050
	LitLDM	**0.0259**	0.9526	**–0.405**	0.3792
	OrgaLD	0.0515	0.3690	**–0.338**	0.3289
	pH_{H_2O}	**0.0012**	0.0597	**0.482**	0.6266
	pH_{CaCl_2}	**0.0024**	0.0851	**0.498**	0.6693
	Al	**0.0059**	**0.0183**	**–0.448**	0.5878
	Fe	**0.0045**	0.1339	**–0.457**	0.3397
	H	**0.0010**	0.2136	**–0.475**	0.5076
	Ca	**0.0043**	0.1109	**0.448**	0.3793
	Mg	**0.0183**	0.4323	**0.400**	0.2350
	Na	**0.0372**	0.9093	**0.323**	0.3268
	C	0.8192	**0.0307**	–0.033	0.0907
	BS	**0.0013**	**0.0289**	**0.514**	0.6079
	AlS	**0.0019**	**0.0220**	**–0.487**	0.5903
	SO_4	**0.0130**	0.2787	–0.268	0.1949
GNMDS 2	Inclin	0.0935	0.9206	**–0.336**	0.5259
	ConvS1	**0.0473**	0.9872	**0.306**	0.1873
	ConvS9	**0.0067**	0.5288	0.245	0.1084
	RelaDN	0.2045	0.9445	**–0.330**	0.5125
	SO4	0.9795	**0.0441**	0.149	0.1949

and soil nutrients, a more varied topography, a thicker organic layer and litter layer, and a higher broadleaved trees density).

Bryophyte species *Rhyncostegium pallidifolium* (Fig. 152) was restricted to plots in the lower left part of the GNMDS ordination diagram (related to a more favourable light conditions, a higher inclination, a more varied topography, a thicker litter, a drier soil and a higher trees density).

The other two species group were clearly separated along the GNMDS ordination axes from the complex gradients; Vascular plants *Nothosmyrnium japonicum* (Fig. 134), *Pelea japonica* (Fig. 139), *Rubia cordifolia* (Fig. 140) and bryophyte species *Brachythecium pulchellum* (Fig. 143) were restricted to plots in the right hand of the GNMDS ordination diagram (related to a higher soil pH, a higher concentrations of Ca, Mg and Na in soil, a more unfavourable aspect), while vascular plant *Rubus malifolius* (Fig. 142) was restricted to plots in the left hand of the GNMDS ordination diagram (related to a opposite complex-gradient).

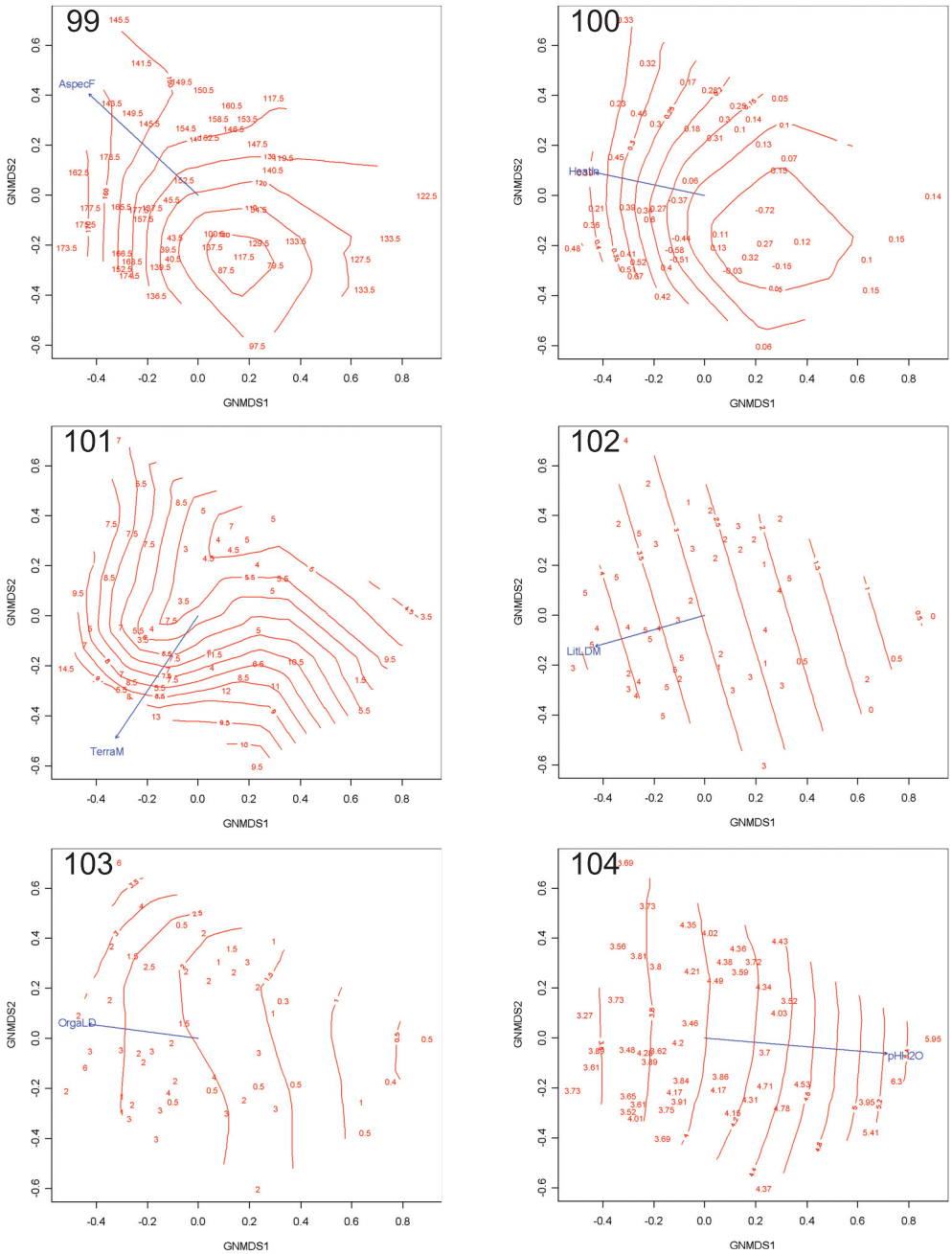

Figs 99–104. Lei Gong Shan: Isolines for environmental variables in the GNMDS ordination of 50 plots, axes 1 (horizontal) and 2 (vertical). Values for the environmental variables are plotted onto plots' position. Fig. 99. AspecF (R^2 = 0.4386). Fig. 100. HeatIn (R^2 = 0.2799). Fig. 101. TerraM (R^2 = 0.4050). Fig. 102. LitLDM (R^2 = 0.3792). Fig. 103. OrgaLD (R^2 = 0.3289). Fig. 104. pH_{H_2O} (R^2 = 0.6266). R^2 refers to the coefficient of determination between original and smoothened values as interpolated from the isolines. Numbers and abbreviations for names of environmental variables are in accordance with Tab.2.

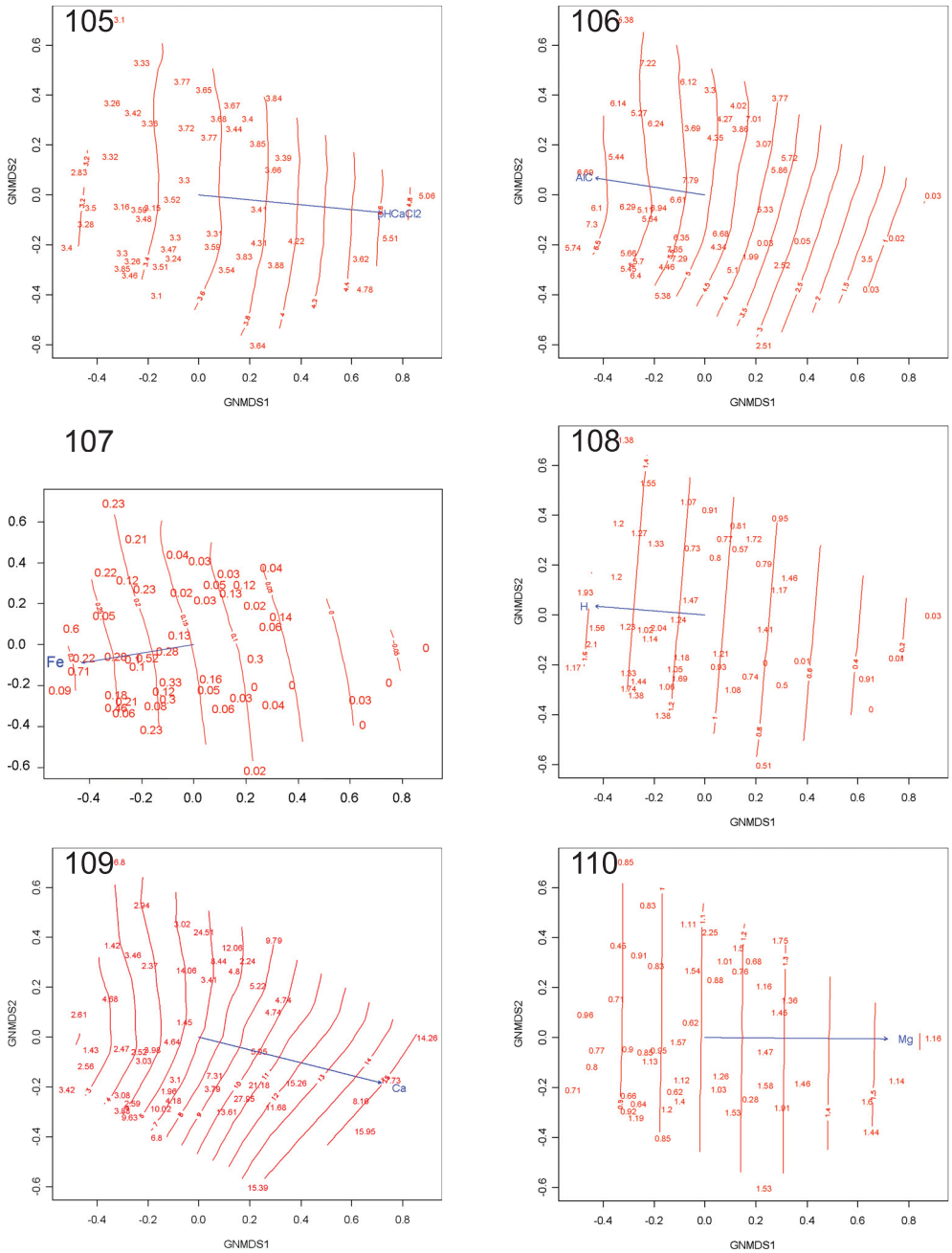

Figs 105–110. Lei Gong Shan: Isolines for environmental variables in the GNMDS ordination of 50 plots, axes 1 (horizontal) and 2 (vertical). Values for the environmental variables are plotted onto plots' position. Fig. 105. pH_{CaCl_2} ($R^2 = 0.6693$). Fig. 106. Al ($R^2 = 0.5878$). Fig. 107. Fe ($R^2 = 0.3397$). Fig. 108. H ($R^2 = 0.5076$). Fig. 109. Ca ($R^2 = 0.3793$). Fig. 110. Mg ($R^2 = 0.2350$). R^2 refers to the coefficient of determination between original and smoothened values as interpolated from the isolines. Numbers and abbreviations for names of environmental variables are in accordance with Tab.2.

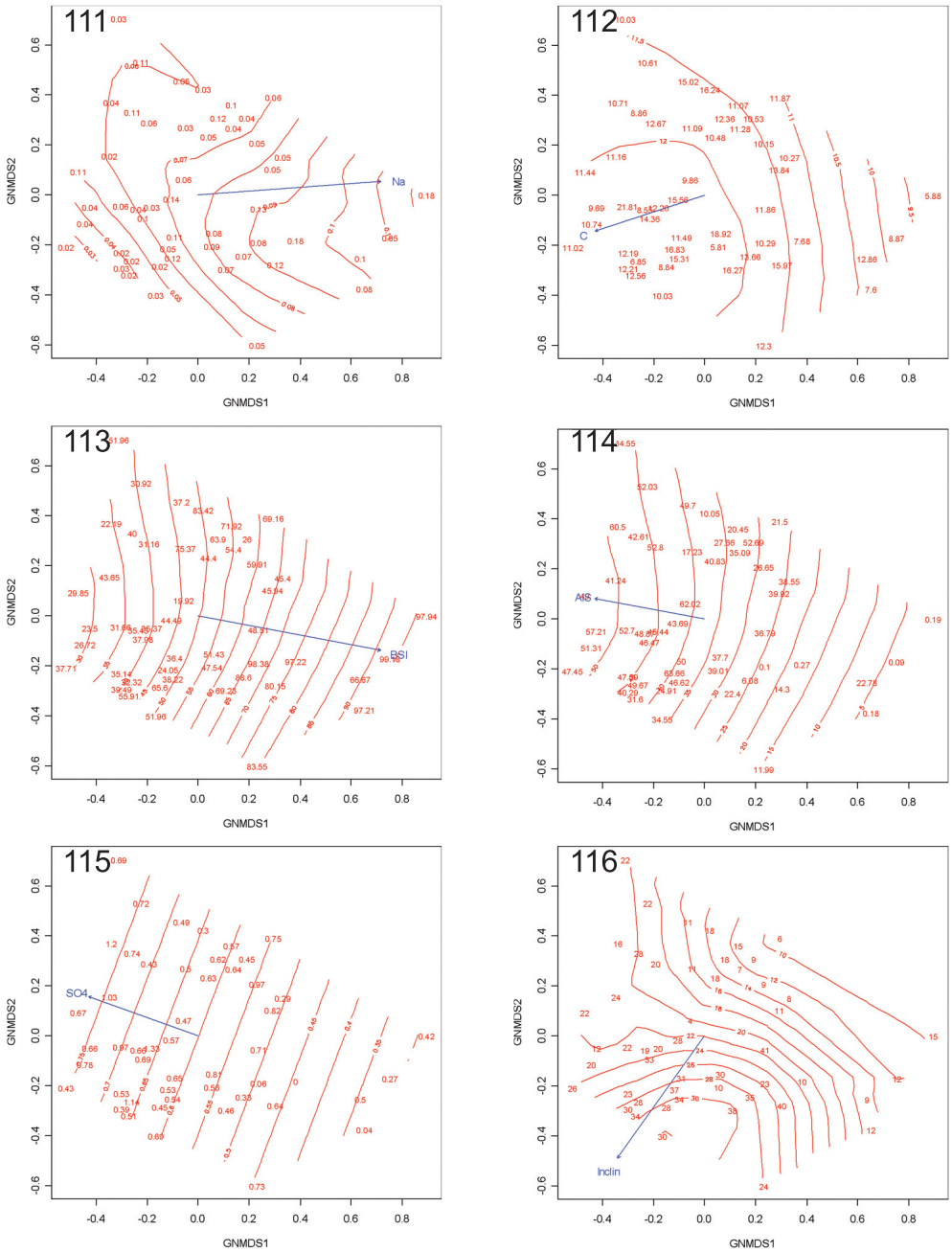

Figs 111–116. Lei Gong Shan: Isolines for environmental variables in the GNMDS ordination of 50 plots, axes 1 (horizontal) and 2 (vertical). Values for the environmental variables are plotted onto plots' position. Fig. 111. Na ($R^2 = 0.3268$). Fig. 112. C ($R^2 = 0.0907$). Fig. 113. BS ($R^2 = 0.6079$). Fig. 114. AlS ($R^2 = 0.5903$). Fig. 115. SO_4 ($R^2 = 0.1949$). Fig. 116. Inclin ($R^2 = 0.5259$). R^2 refers to the coefficient of determination between original and smoothened values as interpolated from the isolines. Numbers and abbreviations for names of environmental variables are in accordance with Tab.2.

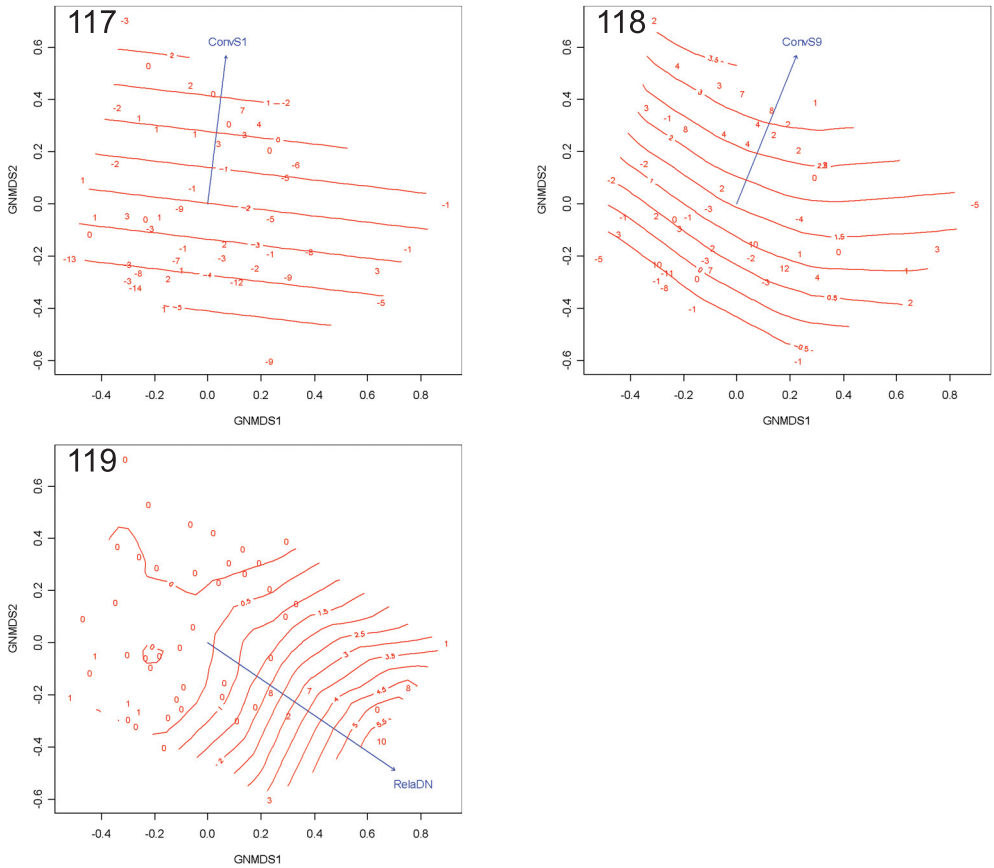

Figs 117–119. Lei Gong Shan: Isolines for environmental variables in the GNMDS ordination of 50 plots, axes 1 (horizontal) and 2 (vertical). Values for the environmental variables are plotted onto plots' position. Fig. 117. ConvS1 (R^2 = 0.1873). Fig. 118. ConvS9 (R^2 = 0.1084). Fig. 119. RelaDN (R^2 = 0.5125). R^2 refers to the coefficient of determination between original and smoothened values as interpolated from the isolines. Numbers and abbreviations for names of environmental variables are in accordance with Tab.2.

Bryophyte species *Rhyncostegium contractum* (Fig. 152) and *Chiloscyphus heterophyllus* (Fig. 154) were restricted to plots in the upper left hand of the GNMDS ordination diagram (related to a lower inclination, a more plane surface, a thicker litter, a higher coniferous trees density, and a more favourable light conditions, while bryophyte species *Plagiominum acutum* (Fig. 149) was restricted to plots in the lower right hand of the GNMDS ordination diagram (related to a opposite complex-gradient).

Tab. 35. Lei Gong Shan: Occurrence (number of plots in which the species was present) and local abundance (abundant = subplot frequency ≥ 8) of species recorded in five or more of the 50 plots.

Species	The total number of plots	
	Present	Abundant
Achyranthes longifolia	11	0
Antenoron filiforme	5	0
Aster ageratoides	31	3
Carex cruciata	7	1
Celastrus vaniotii	6	1
Deyeuxia arundinacea	12	2
Glechoma longituba	13	7
Gynostemma pentaphyllum	5	0
Hedera nepalensis	6	2
Hydrangea paniculata	10	0
Impatiens cyanantha	7	0
Impatiens dolichoceras	5	1
Ligularia intermedia	12	0
Lonicera acuminata	7	1
Nothosmyrnium japonicum	24	14
Oplismenus compositus	22	5
Oxalis griffithii	5	2
Paraprenanthes sororia	31	7
Parathelypteris beddomei	8	0
Pilea japonica	27	4
Rubia cordifolia	26	13
Rubus irenaeus	48	41
Rubus malifolius	15	10
Brachythecium pulchellum	28	4
Brachythecium plumosum	6	1
Clastobryella cuculligera	6	1
Herzogiella perrobusta	5	0
Hypnum plumaeforme	7	0
Leucobryum juniperoideum	9	0
Plagiominum acutum	14	2
Plagiothecium cavifolium	14	1
Rhyncostegium pallidifolium	28	23
Rhyncostegium contractum	16	14
Thuidium kanedae	15	1
Chiloscyphus heterophyllus	20	4
Chiloscyphus latifolius	28	6
Lejeuna flava	8	0
Metzgeria darjeelingensis	15	0

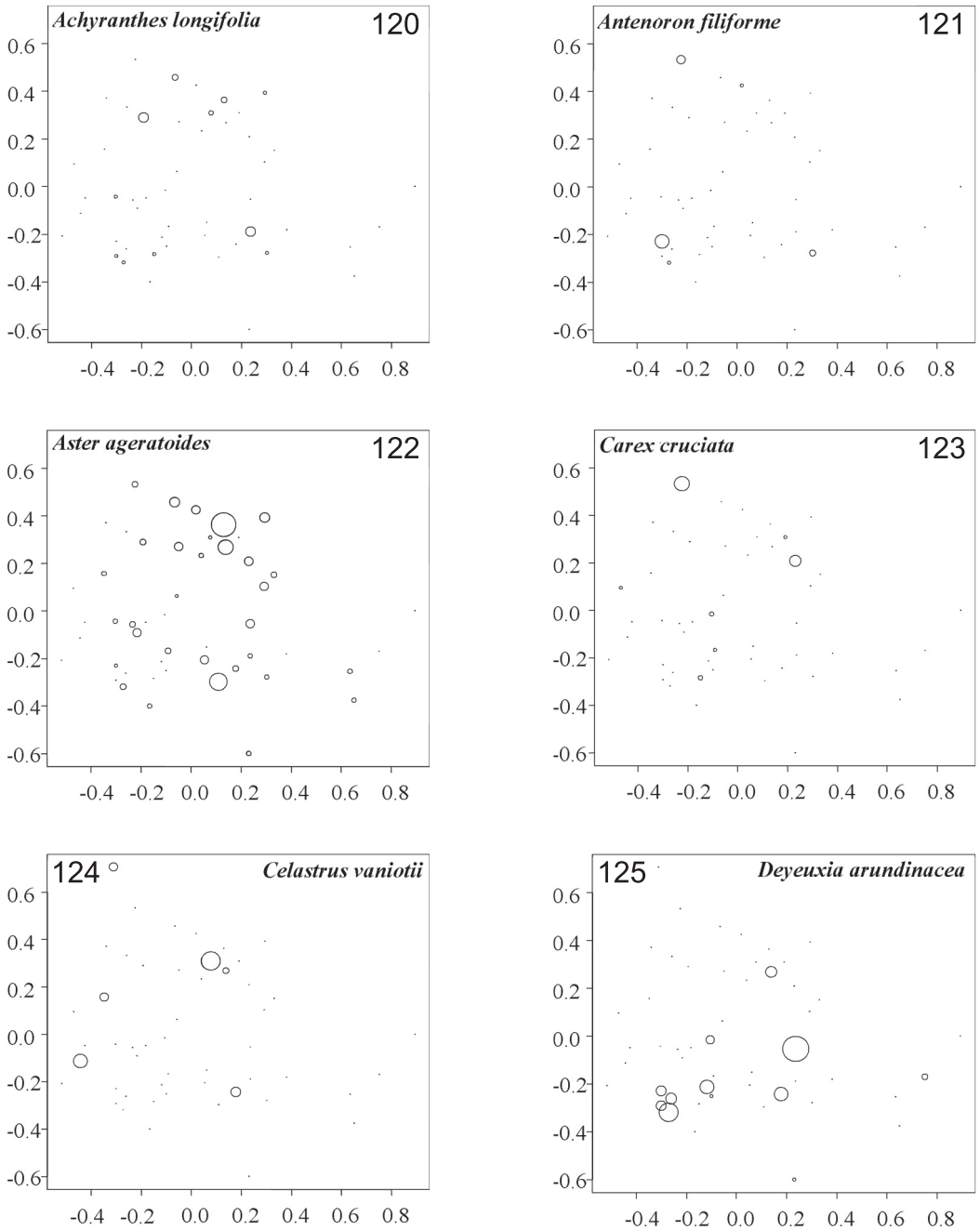

Figs 120–125. Lei Gong Shan: Distribution of species abundances in the GNMDS ordination of 50 plots, axes 1 (horizontal) and 2 (vertical). Frequency in subplots for each species in each plot proportional to circle size. Fig. 120. *Achyranthes longifolia*. Fig. 121. *Antenoron filiforme*. Fig. 122. *Aster ageratoides*. Fig. 123. *Carex cruciata*. Fig. 124. *Celastrus vaniotii*. Fig. 125. *Deyeuxia arundinacea*. Small dots indicate absence; circles indicate presence, diameter proportional with subplot frequency.

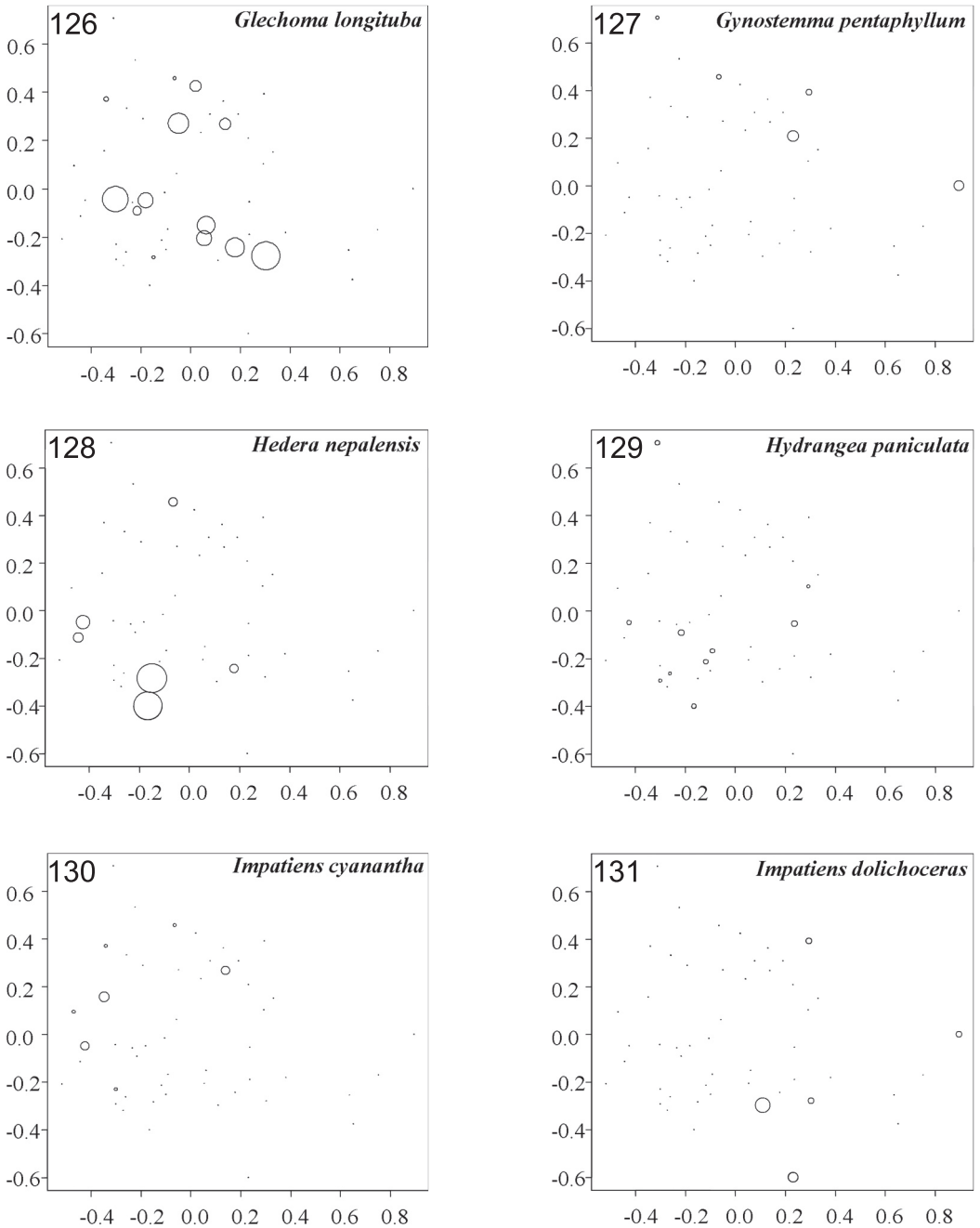

Figs 126–131. Lei Gong Shan: Distribution of species abundances in the GNMDS ordination of 50 plots, axes 1 (horizontal) and 2 (vertical). Frequency in subplots for each species in each plot proportional to circle size. Fig. 126. *Glechoma longituba*. Fig. 127. *Gynostemma pentaphyllum*. Fig. 128. *Hedera nepalensis*. Fig. 129. *Hydrangea paniculata*. Fig. 130. *Impatiens cyanantha*. Fig. 131. *Impatiens dolichoceras*. Small dots indicate absence; circles indicate presence, diameter proportional with subplot frequency.

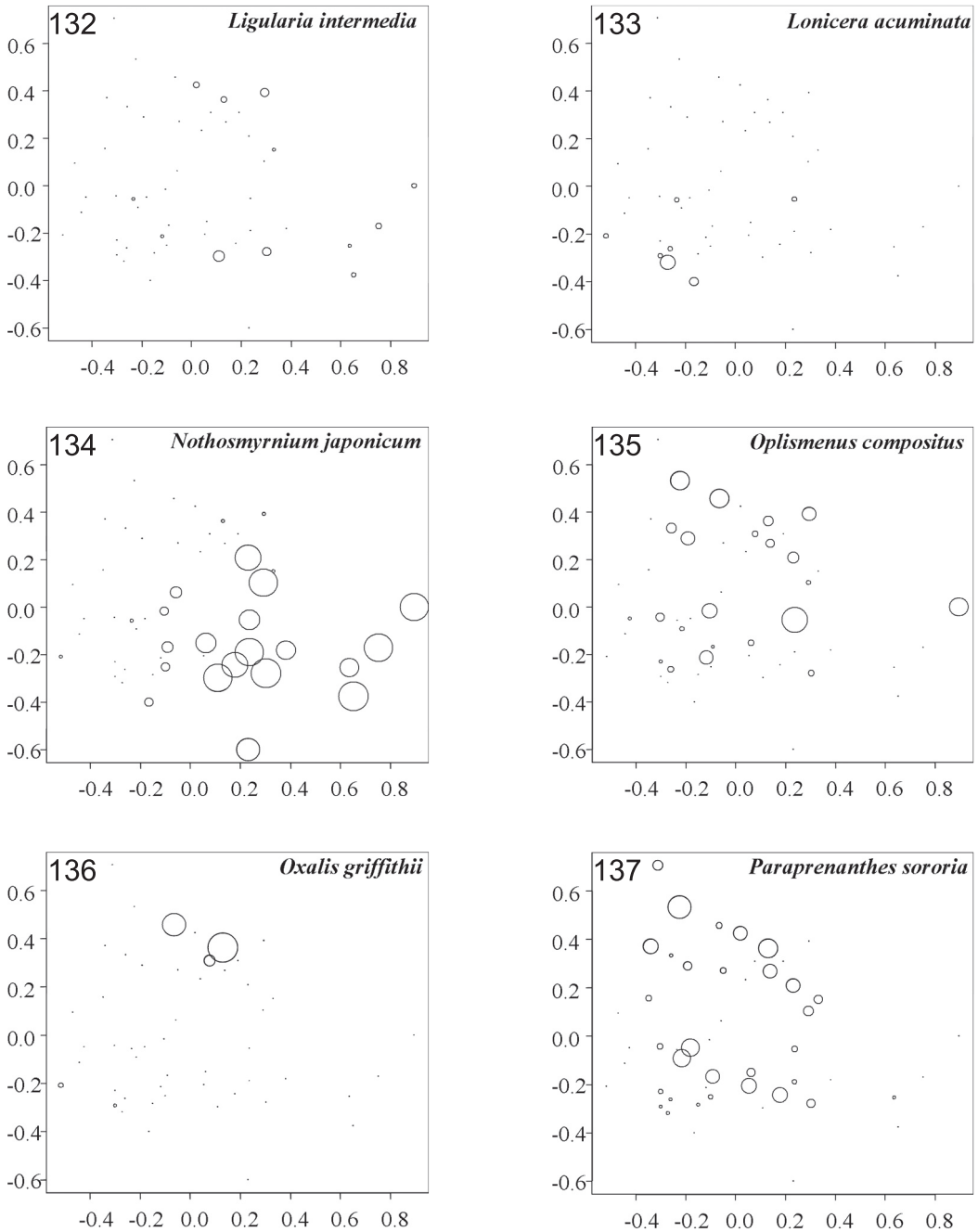

Figs 132–137. Lei Gong Shan: Distribution of species abundances in the GNMDS ordination of 50 plots, axes 1 (horizontal) and 2 (vertical). Frequency in subplots for each species in each plot proportional to circle size. Fig. 132. *Ligularia intermedia*. Fig. 133. *Lonicera acuminata*. Fig. 134. *Nothosmyrnium japonicum*. Fig. 135. *Oplismenus compositus*. Fig. 136. *Oxalis griffithii*. Fig. 137. *Paraprenanthes sororia*. Small dots indicate absence; circles indicate presence, diameter proportional with subplot frequency.

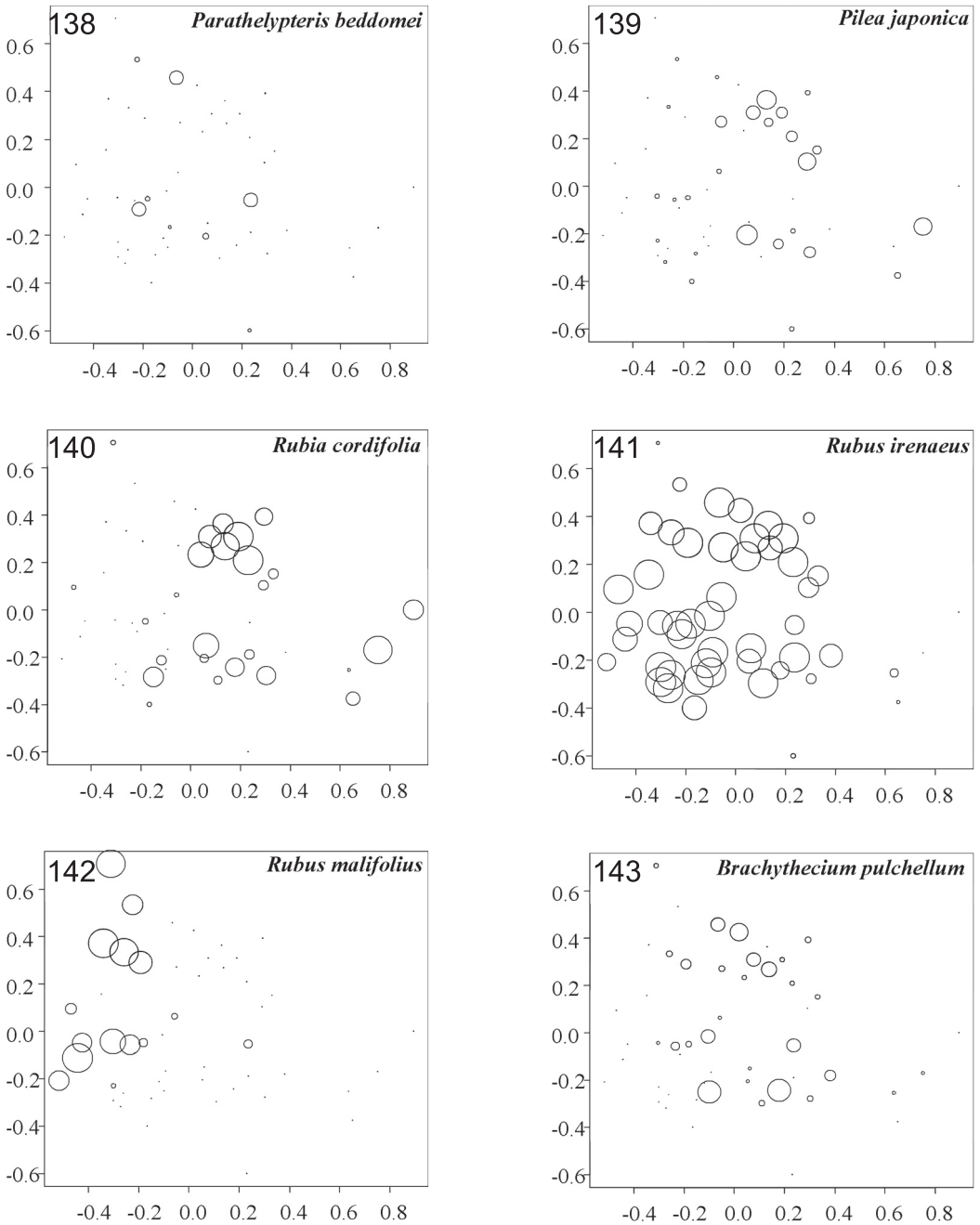

Figs 138–143. Lei Gong Shan: Distribution of species abundances in the GNMDS ordination of 50 plots, axes 1 (horizontal) and 2 (vertical). Frequency in subplots for each species in each plot proportional to circle size. Fig. 138. *Parathelypteris beddomei*. Fig. 139. *Pilea japonica*. Fig. 140. *Rubia cordifolia*. Fig. 141. *Rubus irenaeus*. Fig. 142. *Rubus malifolius*. Fig. 143. *Brachythecium pulchellum*. Small dots indicate absence; circles indicate presence, diameter proportional with subplot frequency.

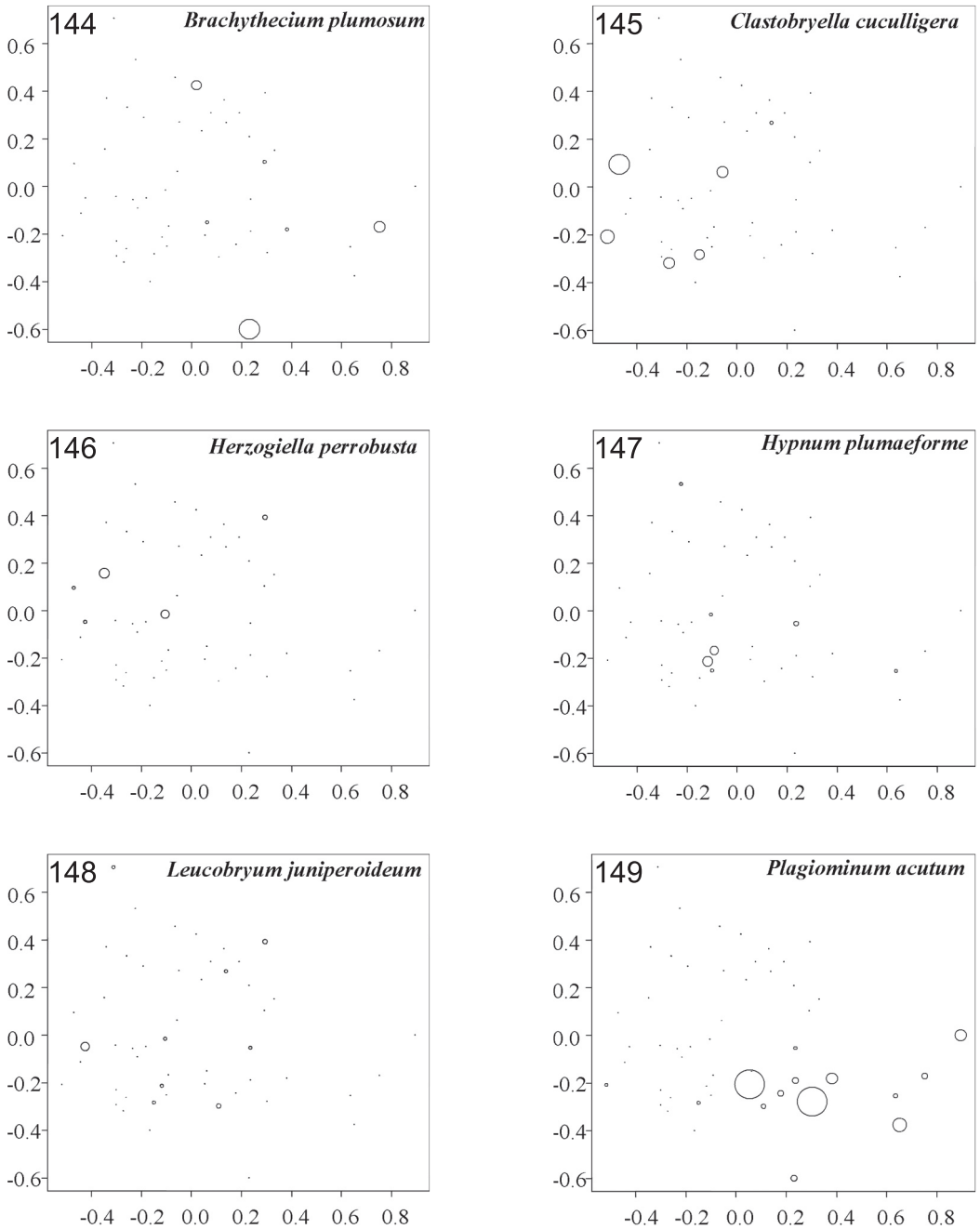

Figs 144–149. Lei Gong Shan: Distribution of species abundances in the GNMDS ordination of 50 plots, axes 1 (horizontal) and 2 (vertical). Frequency in subplots for each species in each plot proportional to circle size. Fig. 144. *Brachythecium plumosum*. Fig. 145. *Clastobryella cuculligera*. Fig. 146. *Herzogiella perrobusta*. Fig. 147. *Hypnum plumaeforme*. Fig. 148. *Leucobryum juniperoideum*. Fig. 149. *Plagiominum acutum*. Small dots indicate absence; circles indicate presence, diameter proportional with subplot frequency.

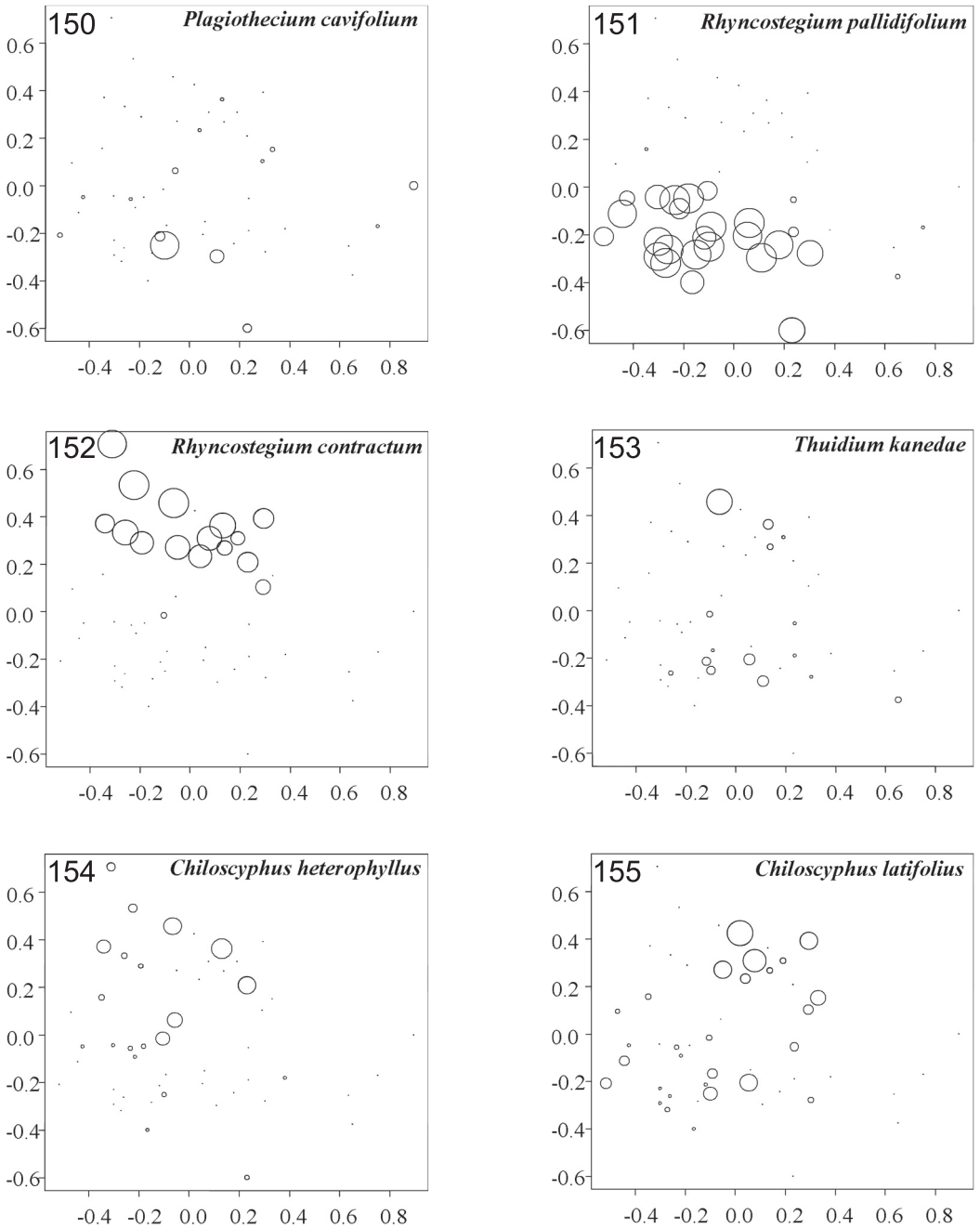

Figs 150–155. Lei Gong Shan: Distribution of species abundances in the GNMDS ordination of 50 plots, axes 1 (horizontal) and 2 (vertical). Frequency in subplots for each species in each plot proportional to circle size. Fig. 150. *Plagiothecium cavifolium*. Fig. 151. *Rhyncostegium pallidifolium*. Fig. 152. *Rhyncostegium contractum*. Fig. 153. *Thuidium kanedae*. Fig. 154. *Chiloscyphus heterophyllus*. Fig. 155. *Chiloscyphus latifolius*. Small dots indicate absence; circles indicate presence, diameter proportional with subplot frequency.

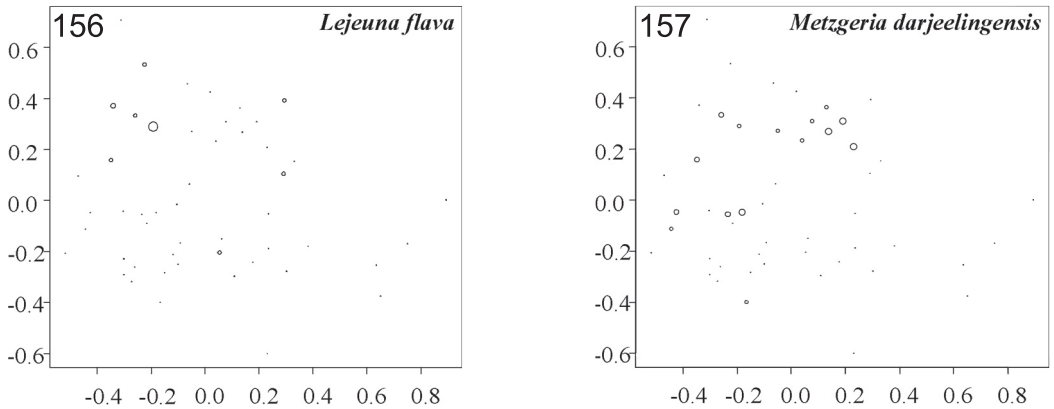

Figs 156–157. Lei Gong Shan: Distribution of species abundances in the GNMDS ordination of 50 plots, axes 1 (horizontal) and 2 (vertical). Frequency in subplots for each species in each plot proportional to circle size. Fig. 156. *Lejeuna flava*. Fig. 157. *Metzgeria darjeelingensis*. Small dots indicate absence; circles indicate presence, diameter proportional with subplot frequency.

CAI JIA TANG

Correlations between environmental variables

One group of strongly correlated variables was made up by concentrations of Al, Fe, H and K, the organic matter content, contents of total C and N with pairwise positive correlations, and the content of dry matter with negative correlations with all the first mentioned variables (Tab. 36, Fig. 158). The content of dry matter was also negatively correlated with the soil moisture.

Another group of strongly correlate variables consisted of the base saturation, concentrations of Ca and Mg with pairwise positive correlations, and the aluminium saturation with negative correlations with all the others. This group was associated with the first group via the base saturation by negative correlations with concentrations of Fe and Al, and the aluminium saturation by positive correlations with concentrations of Fe and Al.

The concentration of Mn was associated with both first and second group, i.e. by negative correlation with the concentration of Fe in the first group; by negative correlation with the aluminium saturation and by positive correlation with the concentration of Ca in the second group. The concentration of Mn was also negatively correlated with the number of coniferous trees

A third group of strongly correlated variables was made up by the topographic variables, which included the heat index, inclination and aspect favourability, the first mentioned was positively correlated with the others. This group had one connection with the second group, i.e. the positive correlation between the heat index and the aluminium saturation.

A fourth group of strongly correlated variables contained the litter index, crown cover index and organic-layer depth, the first mentioned was positively correlated with the others. This group was connected with second and third group via the soil depth, which was positively correlated with the litter index in this group, negatively correlated with the base saturation in second group and positively

Tab. 36. Cai Jia Tang: Kendall's rank correlation coefficients τ between 33 environmental variable in the 50 plots (lower triangle), with significant probabilities (upper triangle). Very strong correlations ($|\tau| \geq 4.0$, $P < 0.0001$) are indicated by bold face. n.s means significance probability $P > 0.1$. Numbers and abbreviation for names of environmental variables are in accordance with Tab. 2.

	1	2	3	4	5	6	7	8	9	10	11	12	13	14	15	16	17
001 Inclin	*	.0055	**.0000**	n.s	n.s	n.s	n.s	n.s	n.s	.0264	.0024	n.s	.0986	n.s	n.s	n.s	n.s
02 AspecF	.2754	*	**.0000**	n.s	n.s	n.s	n.s	n.s	**.0000**	n.s	.0101	.0511	.0726	n.s	n.s	n.s	.0760
03 HeatIn	**.5036**	**.7643**	*	n.s	n.s	n.s	n.s	n.s	.0001	n.s	.0023	n.s	.0420	n.s	.0743	n.s	.0438
04 TerraM	−.1320	−.0413	−.1133	*	.0340	.0040	.0397	.0997	n.s	n.s	n.s	n.s	n.s	n.s	n.s	n.s	n.s
05 ConvS1	.0803	.0555	.0919	−.2195	*	n.s	n.s	n.s	n.s	n.s	n.s	n.s	n.s	n.s	n.s	n.s	n.s
06 ConvV1	−.1116	−.0939	−.1389	.2907	−.1594	*	n.s	n.s	n.s	n.s	.0168	n.s	n.s	n.s	n.s	n.s	n.s
07 ConvS9	−.1633	−.0770	−.1303	.2128	.1518	.1061	*	n.s	n.s	n.s	.0015	n.s	n.s	n.s	.0203	n.s	n.s
08 ConvV9	−.1118	−.0685	−.0766	.1687	−.0132	.1594	.1054	*	n.s	.0945	.0525	n.s	n.s	n.s	n.s	n.s	n.s
09 SoilDM	.0629	**.4437**	.3747	.1531	.0940	−.0243	.1010	.1066	*	n.s	n.s	.0784	.0004	.0300	n.s	n.s	n.s
10 LitLDM	.2383	.1419	.1688	−.1584	.1444	−.1626	−.0536	−.1816	−.0139	*	.0314	n.s	n.s	n.s	n.s	n.s	n.s
11 OrgaLD	.3489	.2931	.3462	−.1666	.0193	−.2744	−.3721	−.2255	.0997	.2654	*	.0863	.0028	.0708	n.s	n.s	.0550
12 SoilMLM	−.0125	.1918	.1000	.1381	−.0811	.0755	.0282	.0667	.1744	−.0829	−.1952	*	n.s	n.s	.0163	n.s	n.s
13 LitteI	.1701	.1832	.2067	.0286	−.0136	−.0625	−.1477	−.0600	.3626	.1757	.3536	−.0654	*	**.0000**	n.s	n.s	n.s
14 CrowCI	.1200	.0513	.0561	.0175	.0142	−.0112	−.1074	−.1061	.2207	.0803	.2111	−.1631	**.7097**	*	.0296	n.s	n.s
15 RelaCN	.1018	.1219	.1911	−.1768	−.0309	−.0213	−.2573	−.1202	.0223	.0827	.1694	−.2580	.1698	.2400	*	.0139	n.s
16 RelaDN	−.0009	−.0336	−.0429	−.0511	−.0098	−.1564	.0770	.0610	−.0078	.1446	.0012	−.0129	.0931	.0795	−.2741	*	n.s
17 pH_{H_2O}	−.0996	−.1741	−.1971	.1076	.0443	.0928	.1220	.0396	−.1036	−.1139	−.2180	−.0345	−.1314	−.0639	−.1531	.1288	*
18 pH_{CaCl_2}	−.1384	−.0974	−.1652	.1808	.0985	−.0350	.0926	.0263	.0491	−.0536	−.1165	.0792	.0612	.0377	−.1164	.1269	.3770
19 Al	.1706	.2329	.3322	−.0159	−.0544	−.1323	−.1593	.0042	.2655	−.0789	.1632	.1852	.0851	−.0544	.1032	−.2281	−.2101
20 Fe	.1922	.1197	.2310	−.0159	−.1582	−.1025	−.1678	−.1388	.1034	.0092	.2258	.0475	.1112	.0119	.3077	−.2779	−.1251
21 H	.0961	.0820	.1690	−.0730	−.0953	−.1505	−.1048	−.1355	.1150	−.0165	.2003	.0672	.0434	−.0476	.2504	−.3173	−.1709
22 Mn	−.2236	−.1214	−.2163	.0781	.1140	.0678	.2240	.1860	−.0240	−.0495	−.2999	.1622	−.0886	−.0732	−.4033	.1355	.0548
23 Ca	−.0282	−.1312	−.1608	.0025	.0306	.0513	.1014	−.0261	−.2755	.0183	−.1494	.0229	−.2380	−.1429	.0210	−.0772	.1349
24 Mg	−.0166	−.1263	−.1461	.0025	−.0493	.0116	.0929	−.0210	−.2159	−.0128	−.0984	.1147	−.1199	−.1089	−.0191	−.1029	.1333
25 Na	.0613	−.0459	−.0024	.0562	−.0698	.0017	−.0860	.0766	−.0157	−.2734	−.1748	.3490	−.1042	−.1276	−.0592	−.2298	−.0237
26 K	.1027	.0951	.1380	.0243	−.0425	−.1075	.0145	−.0480	.1464	−.1560	−.0359	.2819	−.0261	−.1378	−.0936	−.1269	−.0384
27 C	−.0099	.0197	.0221	.0109	−.0596	−.0943	−.0810	−.0682	.0588	−.0064	.0394	.1328	.0774	.0043	−.0631	−.1244	−.0008
28 N	.0050	.0066	.0173	−.0466	−.0481	−.1453	−.0336	−.0085	−.0526	−.0324	−.0479	.2234	−.1053	−.1847	−.1853	−.0234	.0273
29 BS	−.1375	−.2722	−.3110	−.0546	.0289	.1174	.1031	−.0631	**−.4111**	.0624	−.1841	−.1557	−.2467	−.1055	−.0153	.1098	.1856
30 AlS	.2352	.2854	.3682	.0109	−.0715	−.0661	−.2019	.0143	.3350	−.0110	.2235	.0852	.1963	.0800	.1070	−.1201	−.1954
31 SO_4	.1226	.1050	.1690	.1603	.1174	.0661	.0724	.1473	.2903	−.1945	.0452	.0967	.0052	−.0868	.0573	−.2916	−.0237
32 WDM	−.0066	−.0787	−.0400	−.0747	.0204	.0248	−.0622	−.0766	−.1547	.1504	.1355	−.3802	.0486	.1378	.2102	.2504	.0025
33 LOI	.0696	.1378	.1461	.0646	−.0561	−.1058	−.0349	−.0143	.1944	−.1174	.0544	.2507	.0556	−.0681	.0172	−.3036	−.0450

Tab. 36 (continued). Cai Jia Tang: Kendall's rank correlation coefficients τ between 33 environmental variable in the 50 plots (lower triangle), with significant probabilities (upper triangle). Very strong correlations ($|\tau| \geq 4.0$, $P < 0.0001$) are indicated by bold face. n.s means significance probability $P > 0.1$. Numbers and abbreviation for names of environmental variables are in accordance with Tab. 2.

	18	19	20	21	22	23	24	25	26	27	28	29	30	31	32	33
01 Inclin	n.s	.0844	.0519	n.s	.0237	n.s	n.s	n.s	n.s	n.s	n.s	n.s	.0173	n.s	n.s	n.s
02 AspecF	n.s	.0175	n.s	n.s	n.s	n.s	n.s	n.s	n.s	n.s	n.s	.0055	.0036	n.s	n.s	n.s
03 HeatIn	.0924	.0007	.0179	.0834	.0266	.0994	n.s	n.s	n.s	n.s	n.s	.0014	.0002	.0834	n.s	n.s
04 TerraM	.0721	n.s	n.s	n.s	n.s	n.s	n.s	n.s	n.s	n.s	n.s	n.s	n.s	n.s	n.s	n.s
05 ConvS1	n.s	n.s	n.s	n.s	n.s	n.s	n.s	n.s	n.s	n.s	n.s	n.s	n.s	n.s	n.s	n.s
06 ConvV1	n.s	n.s	n.s	n.s	n.s	n.s	n.s	n.s	n.s	n.s	n.s	n.s	n.s	n.s	n.s	n.s
07 ConvS9	n.s	n.s	.0967	n.s	.0266	n.s	n.s	n.s	n.s	n.s	n.s	n.s	.0457	n.s	n.s	n.s
08 ConvV9	n.s	n.s	n.s	n.s	.0630	n.s	n.s	n.s	n.s	n.s	n.s	n.s	n.s	n.s	n.s	n.s
09 SoilDM	n.s	.0072	n.s	n.s	n.s	.0053	.0288	n.s	n.s	n.s	n.s	**.0000**	.0007	.0033	n.s	.0490
10 LitLDM	n.s	n.s	n.s	n.s	n.s	n.s	n.s	.0098	n.s	n.s	n.s	n.s	n.s	.0663	n.s	n.s
11 OrgaLD	n.s	n.s	.0466	.0774	.0082	n.s	n.s	n.s	n.s	n.s	n.s	n.s	.0489	n.s	n.s	n.s
12 SoilMLM	n.s	.0586	n.s	n.s	.0976	n.s	n.s	.0004	.0040	.1752	.0237	.1119	n.s	n.s	.0001	.0105
13 LitteI	n.s	n.s	n.s	n.s	n.s	.0192	n.s	n.s	n.s	n.s	n.s	.0152	.0534	n.s	n.s	n.s
14 CrowCI	n.s	n.s	n.s	n.s	n.s	n.s	n.s	n.s	n.s	n.s	.0684	n.s	n.s	n.s	n.s	n.s
15 RelaCN	n.s	n.s	.0041	.0194	.0002	n.s	n.s	n.s	n.s	n.s	.0863	n.s	n.s	n.s	.0496	n.s
16 RelaDN	n.s	.0246	.0062	.0018	n.s	n.s	n.s	.0235	n.s	n.s	n.s	n.s	n.s	.0041	.0136	.0028
17 pH_{H_2O}	.0001	.0315	n.s	.0804	n.s	n.s	n.s	n.s	n.s	n.s	n.s	.0576	.0456	n.s	n.s	n.s
18 pH_{CaCl_2}	*	.0511	.0107	.0277	.0265	.0552	n.s	n.s	n.s	n.s	n.s	.0403	.0123	n.s	n.s	n.s
19 Al	−.1915	*	**.0000**	**.0000**	.0576	.0113	n.s	.0001	**.0000**	.0014	.0112	**.0000**	**.0000**	.0016	**.0000**	**.0000**
20 Fe	−.2506	**.6343**	*	**.0000**	**.0000**	.0533	n.s	.0234	.0002	.0278	n.s	**.0000**	**.0000**	.0187	.0234	**.0000**
21 H	−.2161	**.5494**	**.7159**	*	.0011	n.s	n.s	.0149	.0001	.0088	.0531	.0006	.0008	.0748	.0084	**.0000**
22 Mn	.2178	−.1853	**−.4563**	−.3192	*	.0002	.0005	n.s	n.s	n.s	n.s	.0020	.0001	n.s	.0493	n.s
23 Ca	.1882	−.2473	−.1886	−.0547	.3633	*	**.0000**	n.s	n.s	n.s	n.s	**.0000**	**.0000**	n.s	n.s	n.s
24 Mg	.1487	−.1086	−.0237	.1069	.3388	**.6980**	*	.1891	.0080	.0205	.0454	.0001	**.0000**	n.s	.0290	.0196
25 Na	.0600	.3845	.2212	.2376	.0155	.1135	.1282	*	**.0000**	.0076	.0020	n.s	.0960	.0329	**.0000**	**.0000**
26 K	.0337	**.4759**	.3649	.3943	.0449	.1265	.2588	**.5331**	*	.0002	.0002	.0316	.0456	.0136	**.0000**	**.0000**
27 C	.0337	.3129	.2149	.2557	.0972	.1332	.2263	.2606	.3636	*	**.0000**	n.s	n.s	n.s	.0002	**.0000**
28 N	.0730	.2498	.1393	.1904	.1525	.1443	.1970	.3042	.3669	**.7698**	*	n.s	n.s	n.s	**.0000**	.0001
29 BS	.2013	**−.6294**	**−.4727**	−.3355	.3012	**.5820**	.3812	−.1314	−.2098	−.1152	−.0618	*	**.0000**	.0051	.0142	.0017
30 AlS	−.2457	**.6604**	**.4808**	.3273	−.3812	**−.5673**	**−.4318**	.1624	.1951	.1136	.0651	**−.8090**	*	.0048	.0776	.0048
31 SO_4	−.0189	.3078	.2294	.1739	−.1200	−.1037	−.0824	.2082	.2408	.1087	.0519	−.2735	.2751	*	.0069	.0023
32 WDM	−.0419	**−.4171**	−.2212	−.2571	−.1918	−.0873	−.2131	**−.4971**	**−.5722**	−.3668	**−.4015**	.2392	−.1722	−.2637	*	**.0000**
33 LOI	−.0008	**.5624**	**.4155**	**.4678**	.0269	.0596	.2278	**.4335**	**.6294**	**.4632**	.3982	−.3061	.2751	.2980	**−.6588**	*

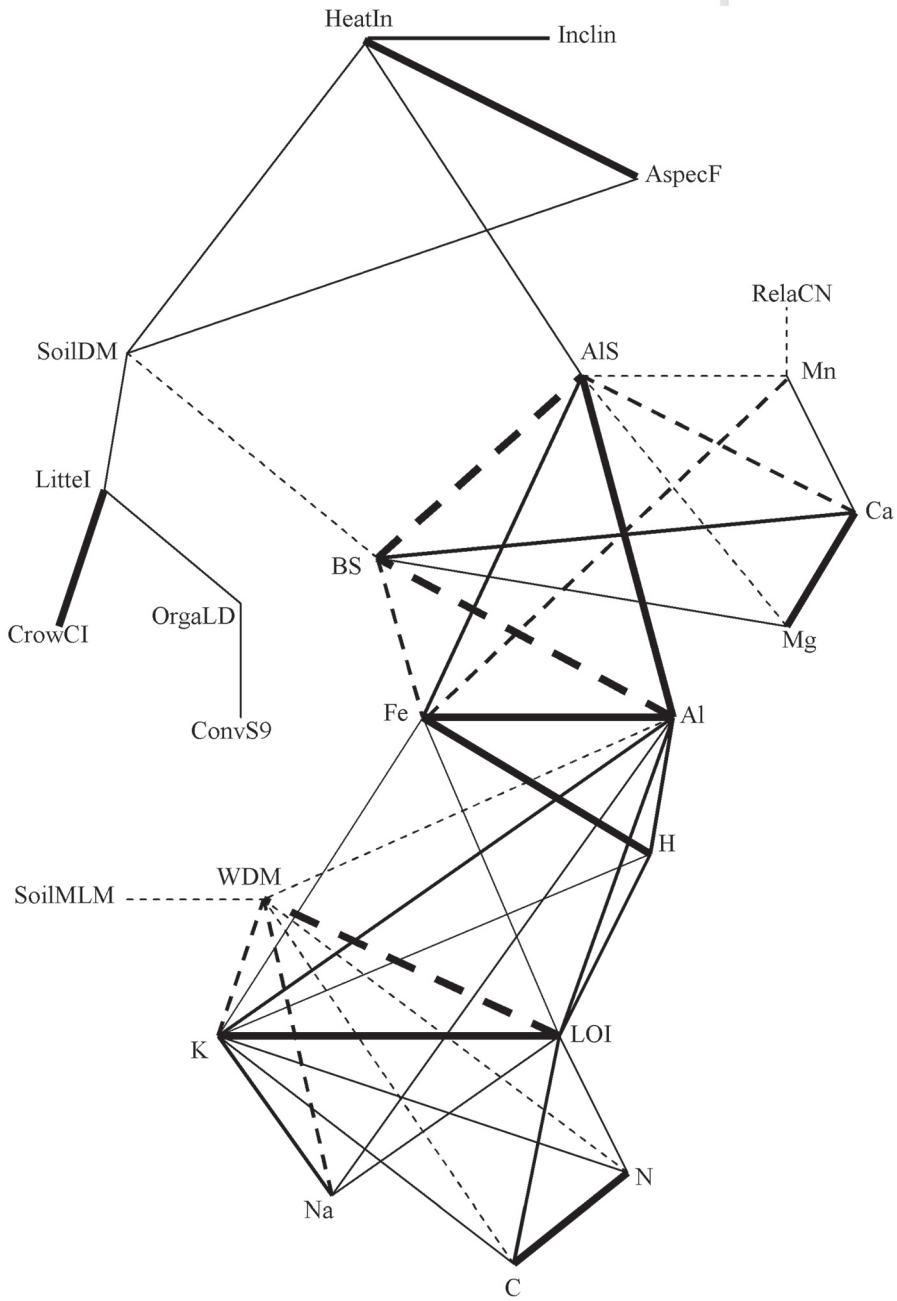

Fig. 158. Cai Jia Tang: Plexus diagram visualizing Kendall's τ between pairs of environmental variables. Significance probabilities for τ are indicated by lines with different thickness (in order of decreasing thickness): $|\tau| \geq 0.60$, $0.45 \leq |\tau| < 0.60$, and $0.35 \leq |\tau| < 0.45$. Continuous lines refer to positive correlations, broken lines to negative.

correlated with the heat index in third group. Organic-layer depth was positively correlated with the concavity/convexity at sum index at 9-m^2 scale (Tab. 36, Fig. 158).

PCA ordination of environmental variables

Eigenvalues of the first two PCA axes were 0.228 and 0.178, thus 40.6 % of the variation in measured environmental variables was explained by the first two PCA axes.

The concentration of Mn in soil and soil base saturation obtained high loadings on PCA 1, while heat index, aspect favourability, litter index, crown cover index and the number of coniferous trees, obtained low loadings on this axis. Concentration of Na and K in soil and soil organic matter content obtained high loadings on PCA 2, while low loading was obtained by soil dry matter content.

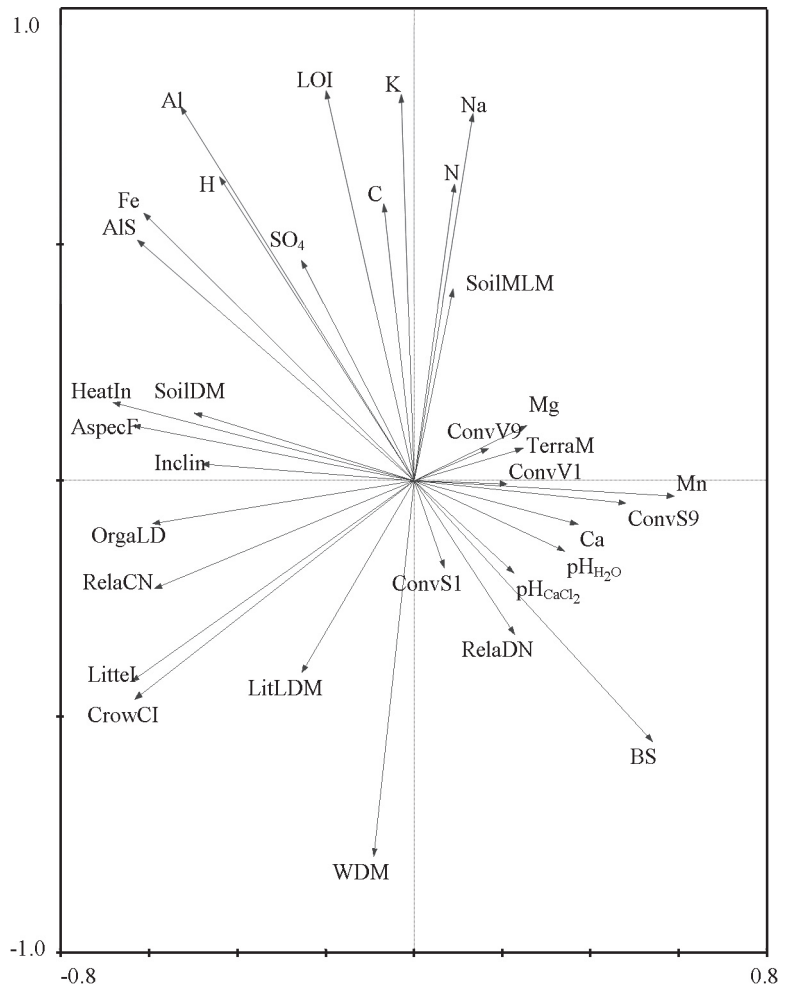

Fig. 159. Cai Jia Tang: PCA ordination of 33 environmental variables (names abbreviated in accordance with Tab.2), axes 1 (horizontal) and 2 (vertical). Loadings of variables on the ordination axes are shown by heads of variable vectors.

PCA ordination results thus summarised major features of correlations between environmental variables in fewer dimensions (Tab. 36, Figs 158−159). Visibly, the variables consisted of cconcentrations of Al, Fe, H, K and Na, aluminium saturation, the organic matter content, contents of total C and N with pairwise positive correlations were negatively correlated with the content of dry matter and base saturation, and positively correlated with the topographic variables of the heat index, inclination and aspect favourability. The tree influence variables contained the litter index, crown cover index and the numbers of coniferous trees were positively correlated with the topographic variables like the heat index, inclination and aspect favourability, and negatively correlated with the base saturation (Tab. 36, Fig. 158).

GNMDS ordination

Good correspondence with respect to gradient length, core length and eigenvalues was found between GNMDS 1 and DCA 1, and GNMDS 2 and DCA 2, respectively. There was a marked drop in eigenvalues occurred from GNMDS1 (DCA 1) to GNMDS2 (DCA 2), indicating that the first axis was the major compositional gradients.

The first axis of the GNMDS ordination of the 49 1-m^2 plots (plot number 5 omitted) had high eigenvalue 3.2696 and gradient length of 3.8510 S.D. units, respectively. Plots number 20, 30 and 40 made up a somewhat isolated group in the space spanned by the first two GNMDS ordination axes, while the remaining plots were relatively evenly distributed in the GNMDS ordination (Fig. 160). No plot acted as outliers, as judged by core length (Tab. 37).

Relationship between ordination axes and environmental variables

GNMDS ordination biplots of 49 plots and significant environmental variables

Positions of plot scores in the GNMDS ordination space were related to variation in environmental variables, as indicated by a several environmental variable vectors with significantly directed variation patterns in the ordination space (Fig. 160). Along the first two axes the following patterns appeared:

Tab. 37. Ordination of vegetation in the 49 plots (plots number 5 omitted) in CJT: summary of properties for GNMDS and DCA axes 1–2 properties. Core length means length of the shortest interval containing 90 % of the plots relative to gradient length.

Corresponding axis		Unit	A	B
Axis No			GNMDS 1, DCA 1	GNMDS 2, DCA 2
GNMDS	Gradient length	HC	1.210	1.153
		S. D	3.851	2.805
	Core length	%	0.765	0.780
	Eigenvalue		3.270	1.958
DCA	Gradient length	S.D	5.140	3.373
	Core length	%	0.509	0.508
	Eigenvalue		0.550	0.339

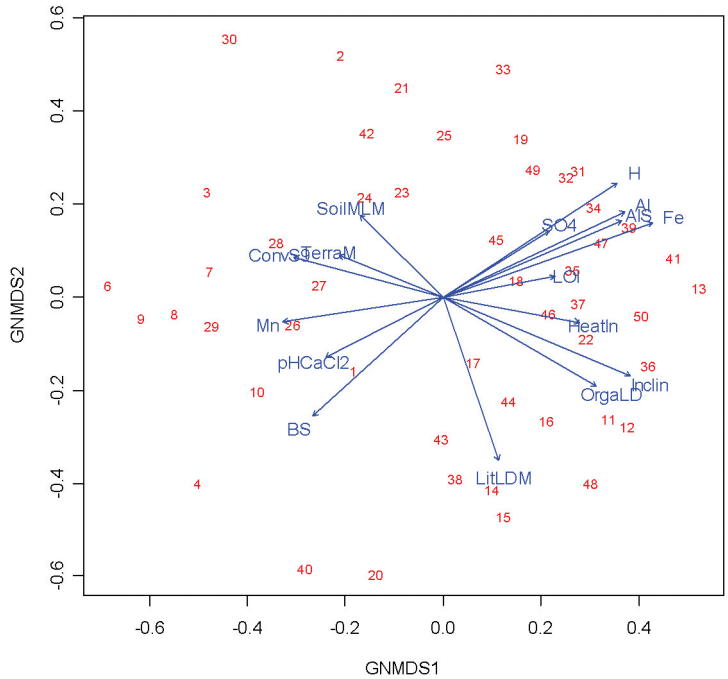

Fig. 160. Cai Jia Tang: GNMDS ordination biplots of 49 plots (indicated by their number, plot number 5 omitted) and significant environmental variables (i.e. with $P < 0.1$ according to goodness-of-fit test; see page 120). Names of variables are abbreviated in accordance with Tab. 2. For each environmental variable the direction of maximum increase and the relative magnitude of increase in this direction is indicated by the direction and length of the vector arrows, axes 1 (horizontal) and 2 (vertical).

(1) vectors for concentrations of Al, Fe and H in soil, and soil aluminium saturation pointed to the upper-right (representing a gradient of increasing concentrations of Al, Fe and H and soil aluminium saturation); (2) vectors for soil pH_{CaCl_2}, the concentration of Mn in soil and soil base saturation pointed lower-leftwards, almost directly in the opposite direction of vectors for concentrations of Al, Fe and H in soil, and soil aluminium saturation; (3) vector for soil moisture, terrain conditions and concavity/convexity sum index at 9-m^2 scale pointed upper-leftwards; and (4) vectors for organic-layer depth, litter-layer depth and inclination pointed lower-rightwards in the biplots. Thus, plots with relatively moist soil and rough topography occurred to the upper-left of the biplots, while plots with relatively dry soil, thick organic layer, and thick litter layer to the lower right of the biplots. Plots with a relatively higher soil pH and higher concentration of Mn in soil were situated in the lower-left of the biplots, while plots with relatively lower concentrations of Al, Fe and H in soil, and lower soil aluminium saturation were situated in the converse direction.

Split-plot GLM analysis of relationships between ordination axes and environmental variables

Variation (in plot scores) along GNMDS axis 1 was partitioned with 78.01 % at the macro-plot scale (i.e. between macro plots) and 21.99 % at the plot scale (i.e. between plots). Variation along GNMDS axis 2 was partitioned with 34.18 % at the macro-plot scale and 65.82 % at the plot scale (Tabs 38−39).

At the macro-plot scale, a total of seven environmental variables were significantly and two were indicatively significantly related to GNMDS axis 1, and two and three variables (at the $P < 0.05$ and $P < 0.1$ levels, respectively) were related to GNMDS axis 2. At the plot scale, concentration of Na in soil was indicatively significantly related to GNMDS axis 1 (negatively) ($P = 0.0680$), and the concentration of H in soil was significantly positively related to GNMDS axis 2 ($P = 0.0083$).

At the macro-plot scale, the variables significantly positively related to GNMDS axis 1 were inclination, organic-layer depth, concentrations of Al, Fe and H in soil, and soil aluminium saturation ($P \leq 0.05$), while soil SO_4 adsorption was indicatively significantly related to this axis (positively) ($P = 0.0843$). The variable significantly negatively related to this axis was soil pH_{CaCl_2} ($P \leq 0.05$), while concavity/convexity sum index at 9-m^2 scale was indicatively significantly related to this axis (negatively) ($P = 0.0897$). The variables significantly negatively related to GNMDS axis 2 were litter-layer depth and the concentration of Ca in soil ($P \leq 0.05$), while soil base saturation was indicatively significantly related to this axis (negatively) ($P = 0.0922$). Terrain conditions and the variance of concavity/convexity at 9-m^2 scale were indicatively significantly related to this axis (positively) ($P \leq 0.1$) (Tabs 38−39).

Kendall's rank correlation between ordination axes and environmental variables

The variables most strongly negatively correlated with GNMDS axis 1 were concavity/convexity sum index at 9-m^2 scale and the concentration of Mn in soil and soil base saturation, and the variables most strongly positively correlated with this axis were inclination and heat index, organic-layer depth, concentrations of Al, Fe and H in soil, and soil SO_4 adsorption ($0.30 \leq |\tau| \leq 0.45$). The variables more or less positively strongly correlated with GNMDS axis 1 were the number of coniferous trees and the concentration of K in soil, and the variables negatively correlated this axis were terrain conditions, variance of concavity/convexity at 1-m^2 scale and soil pH_{CaCl_2} ($0.20 \leq |\tau| < 0.30$) (Tab. 38) .

Litter-layer depth was most strongly negatively correlated with GNMDS axis 2 ($\tau = -0.3380$). The variables more or less strongly negatively correlated with GNMDS axis 2 were soil base saturation and organic-layer depth, and the variable positively correlated with this axis was the concentration of H in soil($0.20 \leq |\tau| < 0.30$) (Tab. 39).

Relationships between ordination axes and species number variables

Split-plot GLM analysis of relationships between ordination axes and species number variables

The number of bryophyte species was significantly related to GNMDS axis 1 at the macro-plot scale. The number of vascular plants was significantly positively related to GNMDS axis 2 at the macro-plot scale. The number of bryophyte species was significantly positively related to GNMDS axis at the plot scale (Tabs 40−41).

Kendall's rank correlation between ordination axes and species number variables

The number of bryophyte species was most strongly positively correlated with GNMDS axis 1 ($\tau = 0.3140$), and strongly positively correlated with GNMDS axis 2 ($\tau = 0.2360$). The total number of species was most strongly positively correlated with GNMDS axis 2 ($\tau = 0.3530$). The number of vascular plants was strongly correlated with GNMDS axis 1 (negatively, $\tau = -0.2610$) and 2 (positively, $\tau = 0.2850$), respectively ($0.33 < \tau < 0.36$) (Tabs 40−41).

Tab. 38. Cai Jia Tang: Split-plot GLM analysis and Kendall's nonparametric correlation coefficient τ between GNMDS axis 1 and 33 environmental variables (predictor) in the 49 plots (plot number 5 omitted). df_{resid}: degrees of freedom for the residuals; *SS*: total variation; *FVE*: fraction of total variation attributable to a given scale (macro plot or plot); SS_{expl}/SS: fraction of the variation attributable to the scale in question, explained by a variable; *r*: model coefficient (only given when significant at the α = 0.1 level, otherwise blank); *F*: *F* statistic for test of the hypothesis that *r* = 0 against the two-tailed alternative. Split-plot GLM relationships significant at level α = 0.05, *P*, *F*, *r* and SS_{expl}/SS, and Kendall's nonparametric correlation coefficient $|\tau| \geq 0.30$ are given in bold face. Numbers and abbreviations for names of environmental variables are in accordance with Tab. 2.

Predictor	Dependent variable = GNMDS 1 (*SS* = 51.5617)								Correlation between predictor and GNMDS 1
	Error level								
	Macro plot df_{resid} = 8 $SS_{macro\ plot}$ = 40.2222 *FVE* = 0.7801 of *SS*				Plot within macro plot df_{resid} = 39 SS_{plot} = 11.3395 *FVE* = 0.2199 of *SS*				Total
	$SS_{expl}/SS_{macro\ plot}$	*r*	*F*	*P*	SS_{expl}/SS_{plot}	*r*	*F*	*P*	τ
Inclin	**0.5152**	**3.2168**	**8.5013**	**0.0194**	0.0186		0.7182	0.4020	**0.390**
AspecF	0.0379		0.3149	0.5901	0.0003		0.0113	0.9160	0.173
HeatIn	0.1792		1.7459	0.2229	0.0337		1.3268	0.2566	**0.323**
TerraM	0.2590		2.7962	0.1330	0.0324		1.2728	0.2663	−0.288
ConvS1	0.0485		0.4075	0.5411	0.0245		0.9528	0.3352	0.133
ConvV1	0.1515		1.4288	0.2662	0.0235		0.9130	0.3454	−0.247
ConvS9	0.3178	−3.2738	3.7266	0.0897	0.0537		2.1575	0.1501	**−0.340**
ConvV9	0.1724		1.6662	0.2328	0.0483		1.9270	0.1732	−0.186
SoilDM	0.0235		0.1929	0.6722	0.0046		0.1763	0.6770	0.077
LitLDM	0.0882		0.7741	0.4046	0.0004		0.0158	0.9007	0.133
OrgaLD	**0.4462**	**3.5874**	**6.4465**	**0.0348**	0.0001		0.0048	0.9451	**0.353**
SoilMLM	0.1112		1.0008	0.3464	0.0029		0.1124	0.7393	−0.157
LitteI	0.0511		0.4309	0.5300	0.0082		0.3141	0.5785	0.150
CrowCI	0.0398		0.3316	0.5806	0.0037		0.1417	0.7087	0.049
RelaCN	0.0911		0.8023	0.3966	0.0505		2.0213	0.1633	0.238
RelaDN	0.2205		2.2624	0.1710	0.0078		0.2977	0.5885	−0.084
pH_{H_2O}	0.0503		0.4240	0.5332	0.0000		0.0000	0.9991	−0.147
pH_{CaCl_2}	**0.6493**	**−8.2041**	**14.8150**	**0.0049**	0.0399		1.5777	0.2168	−0.250
Al	**0.4209**	**2.9083**	**5.8142**	**0.0424**	0.0008		0.0321	0.8587	**0.403**
Fe	**0.4543**	**2.2633**	**6.6605**	**0.0326**	0.0680		2.7705	0.1042	**0.425**
H	**0.4440**	**3.1514**	**6.3875**	**0.0354**	0.0025		0.0946	0.7601	**0.350**
Mn	0.2681		2.9299	0.1253	0.0414		1.6400	0.2081	**−0.315**
Ca	0.0527		0.4452	0.5234	0.0192		0.7452	0.3934	−0.191
Mg	0.0045		0.0364	0.8534	0.0144		0.5544	0.4611	−0.124
Na	0.0669		0.5739	0.4704	0.0734	−0.8221	3.0085	0.0909	0.068
K	0.2253		2.3266	0.1657	0.0035		0.1348	0.7156	0.202
C	0.2467		2.6202	0.1442	0.0090		0.3432	0.5615	0.124
N	0.0603		0.5129	0.4942	0.0179		0.6941	0.4100	0.052
BS	0.2240		2.3099	0.1670	0.0191		0.7414	0.3946	**−0.330**
AlS	**0.4579**	**3.2013**	**6.7567**	**0.0317**	0.0090		0.3461	0.5598	**0.417**
SO_4	0.3268	3.9892	3.8837	0.0843	0.0001		0.0032	0.9550	0.194
WDM	0.0506		0.4260	0.5323	0.0201		0.7802	0.3826	−0.061
LOI	0.2584		2.7874	0.1336	0.0409		1.6203	0.2108	0.199

Tab. 39. Cai Jia Tang: Split-plot GLM analysis and Kendall's nonparametric correlation coefficient τ between GNMDS axis 2 and 33 environmental variables (predictor) in the 49 plots (plot number 5 omitted). df_{resid}: degrees of freedom for the residuals; *SS*: total variation; *FVE*: fraction of total variation attributable to a given scale (macro plot or plot); SS_{expl}/SS: fraction of the variation attributable to the scale in question, explained by a variable; *r*: model coefficient (only given when significant at the α = 0.1 level, otherwise blank); *F*: *F* statistic for test of the hypothesis that *r* = 0 against the two-tailed alternative. Split-plot GLM relationships significant at level α = 0.05, *P*, *F*, *r* and SS_{expl}/SS, and Kendall's nonparametric correlation coefficient $|\tau| \geq 0.30$ are given in bold face. Numbers and abbreviations for names of environmental variables are in accordance with Tab. 2.

Predictor	Dependent variable = GNMDS 2 (*SS* = 23.2173)								Correlation between predictor and GNMDS 2
	Error level								
	Macro plot df_{resid} = 8 $SS_{macro\ plot}$ = 7.9357 *FVE* = 0.3418 of *SS*				Plot within macro plot df_{resid} = 39 SS_{plot} = 15.2816 *FVE* = 0.6582 of *SS*				Total
	$SS_{expl}/SS_{macro\ plot}$	*r*	*F*	*P*	SS_{expl}/SS_{plot}	*r*	*F*	*P*	τ
Inclin	0.2129		2.1643	0.1795	0.0004		0.0153	0.9023	−0.126
AspecF	0.0191		0.1557	0.7034	0.0001		0.0033	0.9542	−0.008
HeatIn	0.0501		0.4215	0.5344	0.0298		1.1690	0.2864	−0.005
TerraM	0.3655	2.3023	4.6091	0.0641	0.0066		0.2516	0.6189	0.070
ConvS1	0.0353		0.2928	0.6031	0.0109		0.4178	0.5219	−0.014
ConvV1	0.2533		2.7140	0.1381	0.0006		0.0216	0.8838	0.128
ConvS9	0.1820		1.7803	0.2188	0.0086		0.3306	0.5687	0.106
ConvV9	0.3224	2.1172	3.8072	0.0868	0.0002		0.0074	0.9317	0.184
SoilDM	0.2043		2.0545	0.1897	0.0013		0.0492	0.8256	0.178
LitLDM	**0.6361**	**−2.0137**	**13.9840**	**0.0057**	0.0556		2.2383	0.1429	**−0.338**
OrgaLD	0.1571		1.4913	0.2568	0.0184		0.7107	0.4045	−0.219
SoilMLM	0.0704		0.6054	0.4589	0.0452		1.8002	0.1877	0.179
LitteI	0.0111		0.0897	0.7722	0.0485		1.9354	0.1723	−0.048
CrowCI	0.0024		0.0190	0.8938	0.0122		0.4681	0.4980	−0.038
RelaCN	0.0579		0.4919	0.5030	0.0138		0.5301	0.4710	−0.012
RelaDN	0.1273		1.1675	0.3114	0.0002		0.0060	0.9388	−0.068
pH_{H_2O}	0.0151		0.1228	0.7351	0.0021		0.0788	0.7804	0.003
pH_{CaCl_2}	0.0454		0.3808	0.5543	0.0199		0.7714	0.3853	−0.144
Al	0.0924		0.8142	0.3933	0.0209		0.8114	0.3734	0.174
Fe	0.0342		0.2836	0.6088	0.0572		2.3064	0.1371	0.175
H	0.0484		0.4066	0.5415	**0.1697**	**1.7859**	**7.7666**	**0.0083**	0.209
Mn	0.0008		0.0067	0.9367	0.0081		0.3085	0.5819	−0.078
Ca	0.0072		0.0582	0.8154	0.0001		0.0032	0.9553	−0.158
Mg	0.1649		1.5796	0.2443	0.0003		0.0119	0.9138	−0.119
Na	0.0931		0.8214	0.3912	0.0252		0.9814	0.3281	0.148
K	0.0195		0.1587	0.7008	0.0086		0.5687	0.3305	0.082
C	0.0001		0.0010	0.9761	0.0128		0.4942	0.4864	0.020
N	0.0013		0.0105	0.9210	0.0135		0.5214	0.4747	0.011
BS	0.3138	−1.2805	3.6579	0.0922	0.0102		0.3901	0.5360	−0.260
AlS	0.1491		1.4013	0.2705	0.0001		0.0048	0.9450	0.184
SO_4	0.1684		1.6195	0.2389	0.0019		0.0704	0.7922	0.155
WDM	0.1064		0.9527	0.3576	0.0161		0.6201	0.4359	−0.070
LOI	0.0679		0.5830	0.4671	0.0301		10.1794	0.2843	0.058

Tab. 40. Cai Jia Tang: Split-plot GLM analysis and Kendall's nonparametric correlation coefficient τ between GNMDS axis 1 and two species number variables (predictor) in the 49 plots (plot number 5 omitted). df_{resid}: degrees of freedom for the residuals; *SS*: total variation; *FVE*: fraction of total variation attributable to a given scale (macro plot or plot); SS_{expl}/SS: fraction of the variation attributable to the scale in question, explained by a variable; *r*: model coefficient (only given when significant at the α = 0.1 level, otherwise blank); *F*: *F* statistic for test of the hypothesis that *r* = 0 against the two-tailed alternative. Split-plot GLM relationships significant at level α = 0.05, *P*, *F*, *r* and SS_{expl}/SS, and Kendall's nonparametric correlation coefficient $|\tau| \geq 0.30$ are given in bold face.

Predictor (number of species)	Dependent variable = GNMDS 1 (*SS* = 5.0933) Error level								Correlation between predictor and GNMDS 1
	Macro plot df_{resid} = 8 $SS_{macro\ plot}$ = 3.9731 *FVE* = 0.7801 of *SS*				Plot within macro plot df_{resid} = 38 SS_{plot} = 1.1202 *FVE* = 0.2199 of *SS*				Total
	$SS_{expl}/SS_{macro\ plot}$	*r*	*F*	*P*	SS_{expl}/SS_{plot}	*r*	*F*	*P*	τ
Vascular plants	0.2934		3.3221	0.1058	0.0000		0.0000	0.9950	−0.261
Bryophyte species	**0.5062**	**0.1742**	**8.2014**	**0.0210**	0.0273		0.0683	0.3079	**0.314**

Tab. 41. Cai Jia Tang: Split-plot GLM analysis and Kendall's nonparametric correlation coefficient τ between GNMDS axis 2 and two species number variables (predictor) in the 49 plots (plot number 5 omitted). df_{resid}: degrees of freedom for the residuals; *SS*: total variation; *FVE*: fraction of total variation attributable to a given scale (macro plot or plot); SS_{expl}/SS: fraction of the variation attributable to the scale in question, explained by a variable; *r*: model coefficient (only given when significant at the α = 0.1 level, otherwise blank); *F*: *F* statistic for test of the hypothesis that r = 0 against the two-tailed alternative. Split-plot GLM relationships significant at level α = 0.05, *P*, *F*, *r* and SS_{expl}/SS, and Kendall's nonparametric correlation coefficient $|\tau| \geq 0.30$ are given in bold face.

Predictor (number of species)	Dependent variable = GNMDS 2 (*SS* = 3.9235) Error level								Correlation between predictor and GNMDS 2
	Macro plot df_{resid} = 8 $SS_{macro\ plot}$ = 1.3410 *FVE* = 0.3418 of *SS*				Plot within macro plot df_{resid} = 38 SS_{plot} = 2.5825 *FVE* = 0.6582 of *SS*				Total
	$SS_{expl}/SS_{macro\ plot}$	*r*	*F*	*P*	SS_{expl}/SS_{plot}	*r*	*F*	*P*	τ
Vascular plants	**0.6291**	**0.0864**	**13.5690**	**0.0062**	0.0075		0.2854	0.5963	0.285
Bryophyte species	0.0488		0.3589	0.5395	0.1442	**0.0712**	**1.7845**	**0.0157**	0.236

Tab. 42. Lei Gong Shan: Environmental and species number variables for which two-dimensional isoline diagrams were made: P value for relationship with GNMDS axis assessed by split-plot GLM (two scales = error levels), Kendall's correlation coefficient τ with axis, and R^2 between the original and predicted values (according to the isoline diagrams for the variable), used as a measure of goodness-of-fit of the isolines. Isoline diagrams were made for variables with split-plot GLM $P < 0.05$ at the macro plot or the plot scale and/or Kendall's correlation coefficient $|\tau| \geq 0.3$ with one GNMDS axis. P values < 0.05 and/or $|\tau| \geq 0.30$ in bold face. Numbers and abbreviations for names of environmental variables in accordance with Tab. 2 (NVP = number of vascular plants species; and NBS = number of bryophyte species).

Ordination axis	Variable names	The split plot GLM Error level		Kendall's ccorrelation between variable and ordination axis	Goodness-of-fit of the isolines
		$P_{\text{macro plot}}$	P_{plot}	τ_{total}	R^2
GNMDS 1	Inclin	0.0194	0.4020	0.390	0.5029
	HeatIn	0.2229	0.2566	0.323	0.1256
	ConvS9	0.0897	0.1501	−0.340	0.1923
	OrgaLD	0.0348	0.9451	0.353	0.2872
	pH_{CaCl_2}	0.0049	0.2168	−0.250	0.6739
	Al	0.0424	0.8587	0.403	0.2741
	Fe	0.0326	0.1042	0.425	0.4010
	H	0.0354	0.7601	0.350	0.2730
	Mn	0.1253	0.2081	−0.315	0.3908
	BS	0.1670	0.3946	−0.330	0.3401
	AlS	0.0317	0.5598	0.417	0.3979
	NBS	0.5062	0.0273	0.314	0.0485
GNMDS 2	LitLDM	0.0057	0.1429	−0.338	0.4229
	H	0.5415	0.0083	0.209	0.2730
	Ca	0.0467	0.9398	−0.165	0.1284
	NVP	0.0035	.0943	0.335	0.5741

Isoline diagrams for significant environmental and species number variables

A total of 14 environmental variables and two species number variables satisfied the criteria for making two-dimensional isoline diagrams (Tab. 42, Figs 161−175).

The distribution of species abundance in the GNMDS ordination

Out of a total of 76 species, 22 were found in at least 5 of the 49 plots (plot number 5 omitted, Tab. 43, Figs 176−197).

Dryopteris fuscipes (Fig. 180) and *Lophatherum gracile* (Fig. 184), typical examples of vascular plants with wide ecological amplitude, were abundant in most plots, but *Dryopteris fuscipes* was absent from plots with high GNMDS 2 scores (i.e. on sites with thin litter), and *Lophatherum gracile* was absent from plots with low GNMDS 2 scores (i.e. on sites with thick litter layer).

Pseudotaxiphyllum pohliaecarpum (Fig. 195), a typical example of bryophyte species with wide ecological amplitude, was abundant in most plots.

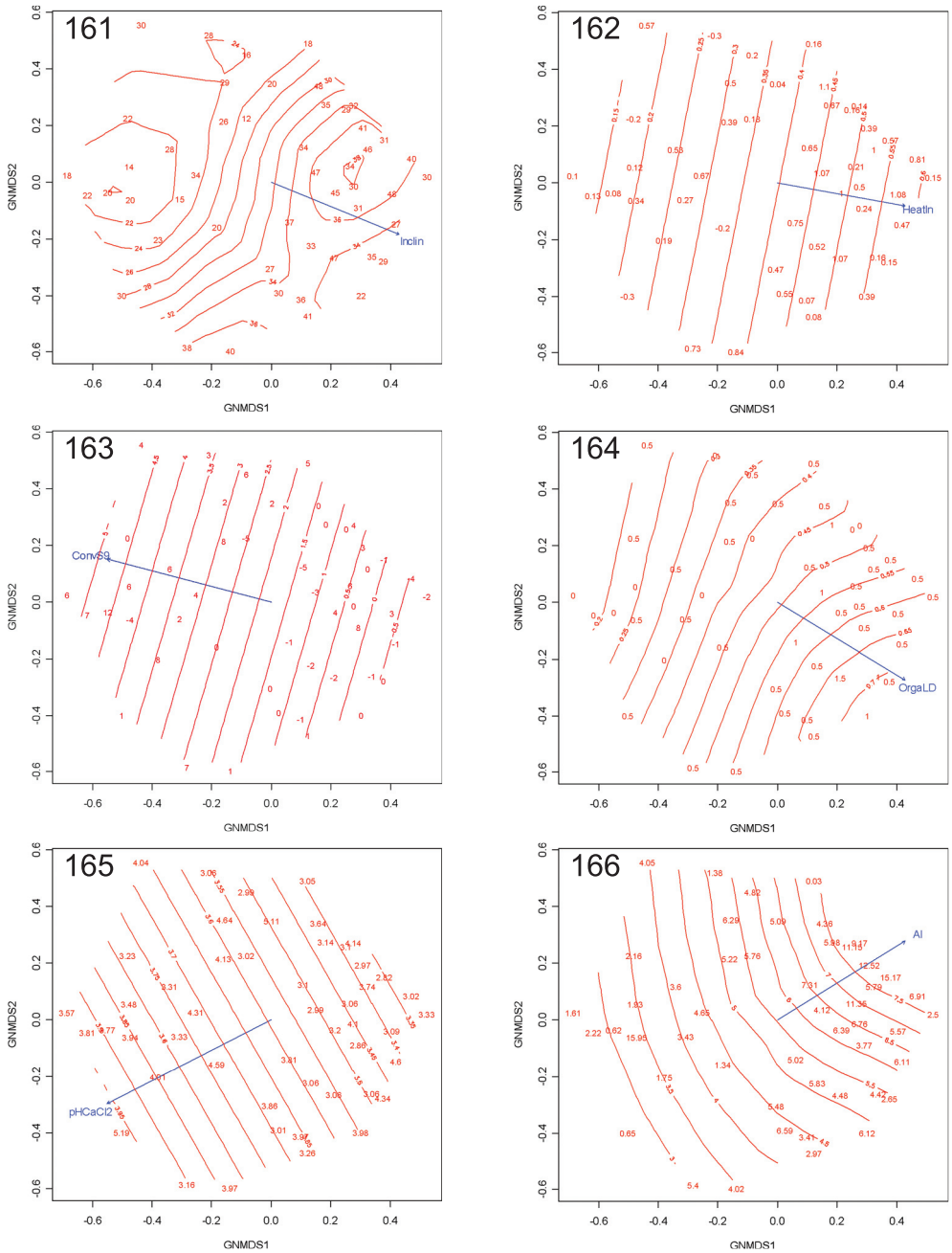

Figs 161−166. Cai Jia Tang: Isolines for environmental variables in the GNMDS ordination of 49 plots (plot number 5 omitted), axe 1 (horizontal) and 2 (vertical). Values for the environmental variables are plotted onto plots' position. Fig. 161. Inclin ($R^2 = 0.5029$). Fig. 162. HeatIn ($R^2 = 0.1256$). Fig. 163. ConvS9 ($R^2 = 0.1923$). Fig. 164. OrgaLD ($R^2 = 0.2827$). Fig. 165. pH_{CaCl_2} ($R^2 = 0.0739$). Fig. 166. Al ($R^2 = 0.2741$). R^2 refers to the coefficient of determination between original and smoothened values as interpolated from the isolines. Numbers and abbreviations for names of environmental variables are in accordance with Tab.2.

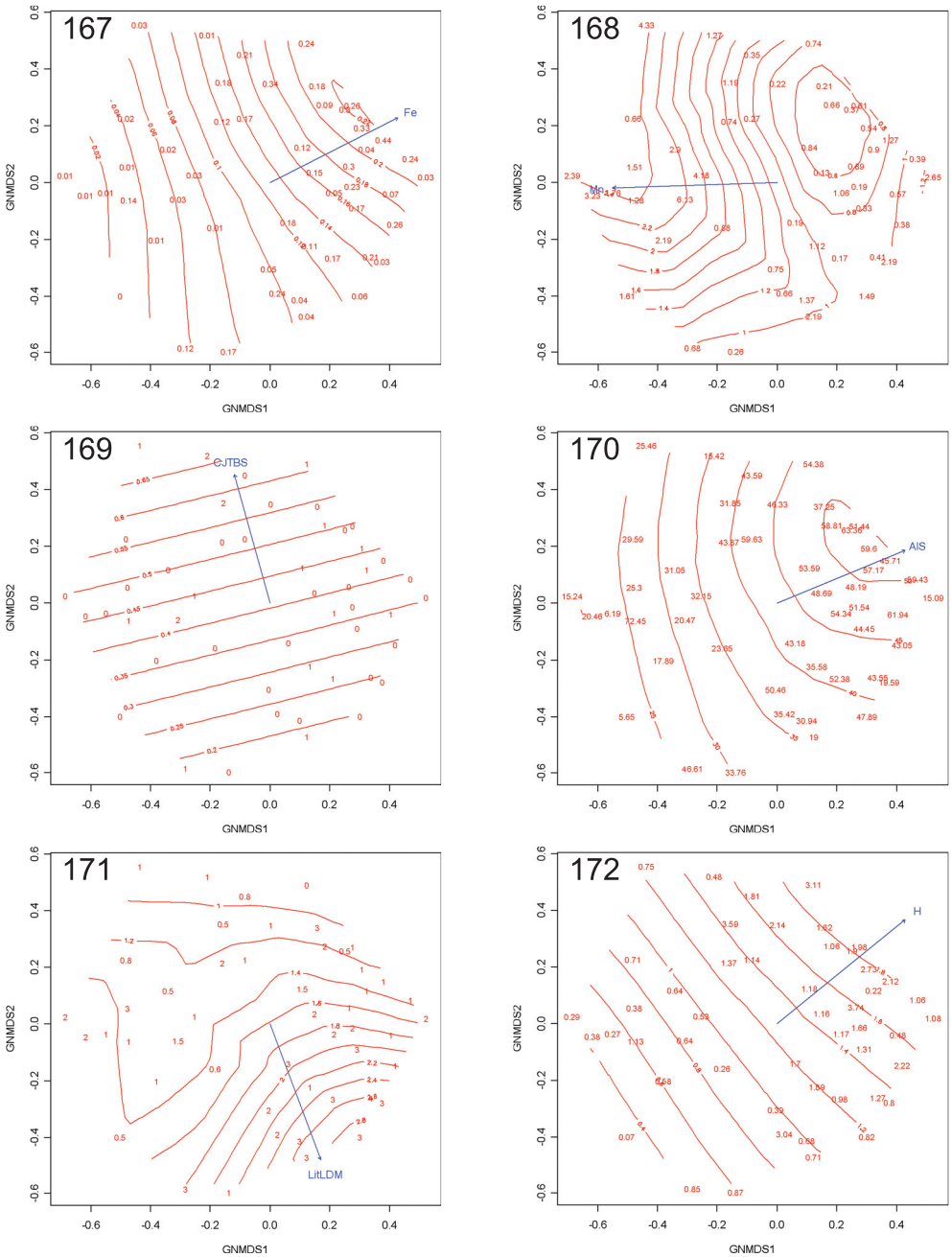

Figs 167−172. Cai Jia Tang: Isolines for environmental variables in the GNMDS ordination of 49 plots (plot number 5 omitted), axe 1 (horizontal) and 2 (vertical). Values for the environmental variables are plotted onto plots' position. Fig. 167. Fe (R^2 = 0.4010). Fig. 168. Mn (R^2 = 0.3908). Fig. 169. BS (R^2 = 0.3401). Fig. 170. AlS (R^2 = 0.3979). Fig. 171. LitLDM (R^2 = 0.4229). Fig. 172. H (R^2 = 0.2730). R^2 refers to the coefficient of determination between original and smoothened values as interpolated from the isolines. Numbers and abbreviations for names of environmental variables are in accordance with Tab.2.

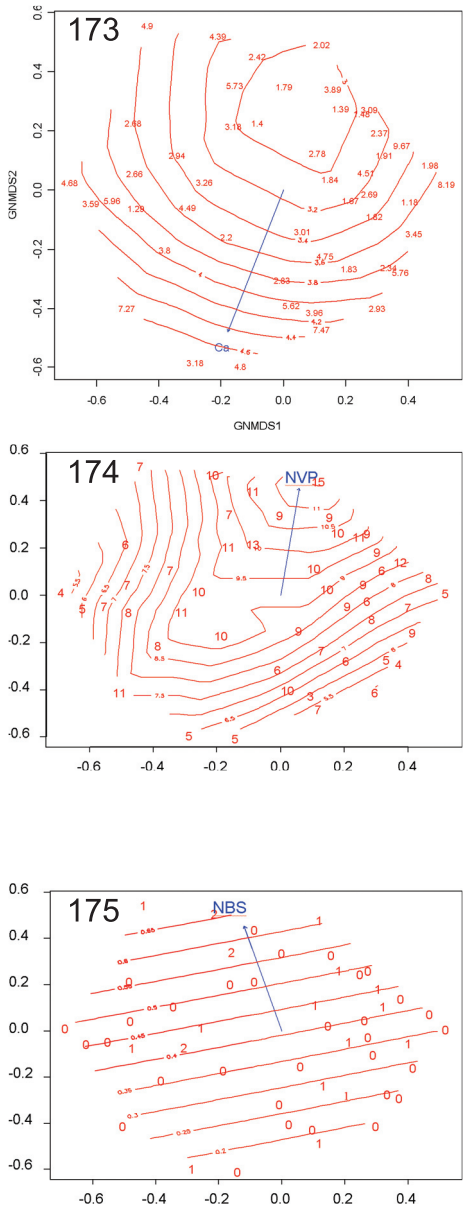

Figs 173−175. Cai Jia Tang: Isolines for variables of species number in the GNMDS ordination of 49 plots (plot number 5 omitted), axe 1 (horizontal) and 2 (vertical). Values for the variables of species number are plotted onto plots' position. Fig. 173. Ca (R^2 = 0.1284). Fig. 174. NVP (number of vascular plants) (R^2 = 0.5741). Fig. 175. NBS (number of bryophyte species) (R^2 = 0.0485). R^2 refers to the coefficient of determination between original and smoothened values as interpolated from the isolines.

Tab. 43. Cai Jia Tang: Occurrence (number of plots in which the species was present) and local abundance (abundant = subplot frequency ≥ 8) of species recorded in five or more of the 49 plots (plot number 5 omitted).

Species	The total number of plots	
	Present	Abundant
Aster ageratoides	6	0
Camellia sinensis	14	1
Carex brunnea	8	1
Deyeuxia arundinacea	10	2
Dryopteris fuscipes	30	4
Gardneria multiflora	5	3
Lindera glauca	7	2
Liriope spicata	13	1
Lophatherum gracile	24	4
Loropetalum chinense	18	6
Rhododendron simsii	20	6
Rubus lambertianus	16	10
Smilax china	15	0
Woodwardia japonica	9	3
Diphyscium foliosum	11	0
Hypnum plumaeforme	16	0
Isopterygium albescens	22	11
Isopterygium fauriei	7	1
Leucobryum juniperoideum	27	4
Pseudotaxiphyllum pohliaecarpum	21	6
Trachycystis microphylla	14	2
Calypogeia muellerana	7	1

Rubus lambertianus (Fig. 187) was restricted to plots in left part of the GNMDS ordination diagram (related to a lower inclination, a more varied topography, a thinner organic layer, and a lower concentrations of Al, Fe and H in soil, and a lower soil aluminium saturation), while *Isopterygium albescens* (Fig. 192) was restricted to plots in the opposite direction and gradients of *Rubus lambertianus*.

Deyeuxia arundinacea (Fig. 179), *Rhododendron simsii* (Fig. 186), *Hypnum plumaeforme* (Fig. 191), *Isopteriygium fauriei* (Fig. 193), *Leucobryum juniperoideum* (Fig. 194) and *Trachycystis microphylla* (Fig. 196) were restricted to plots in the upper right part of the GNMDS ordination diagram (related to a higher concentrations of Al, Fe and H in soil, a lower soil base saturation and a lower soil pH).

Loropetalum chinense (Fig. 185) and *Woodwardia japonica* (Fig. 189) were restricted to plots in the upper part of the GNMDS ordination diagram (related to a convex surface), while *Liriope spicata* (Fig. 182) was restricted to plots in lower part of the GNMDS ordination diagram (related to concave surface).

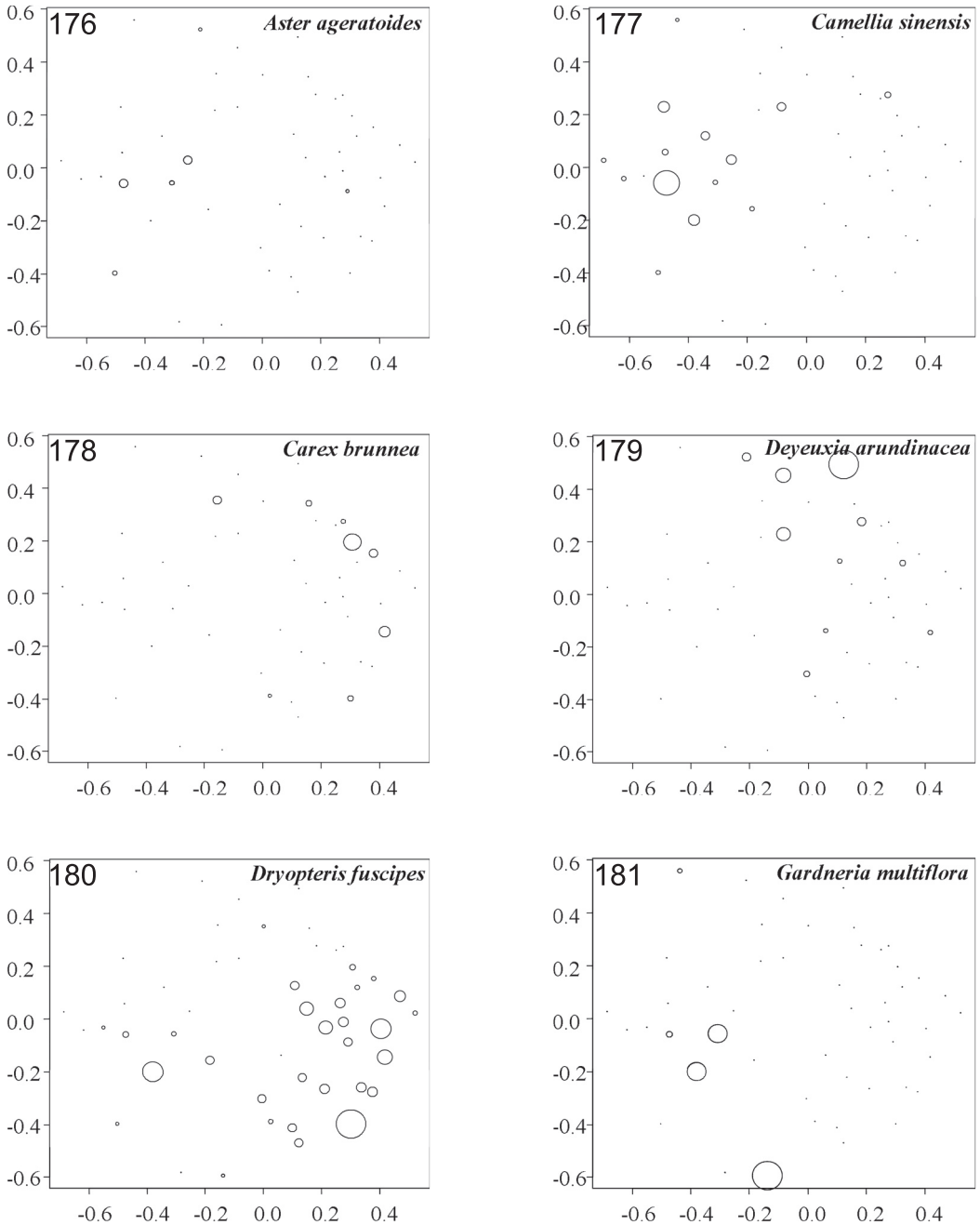

Figs 176–181. Cai Jia Tang: Distribution of species abundances in the GNMDS ordination of 49 plots (plot number 5 omitted), axes 1 (horizontal) and 2 (vertical). Frequency in subplots for each species in each plot proportional to circle size. Fig. 176. *Aster ageratoides*. Fig. 177. *Camellia sinensis*. Fig. 178. *Carex brunnea*. Fig. 179. *Deyeuxia arundinacea*. Fig. 180. *Dryopteris fuscipes*. Fig. 181. *Gardneria multiflora*. Small dots indicate absence; circles indicate presence, diameter proportional with subplot frequency.

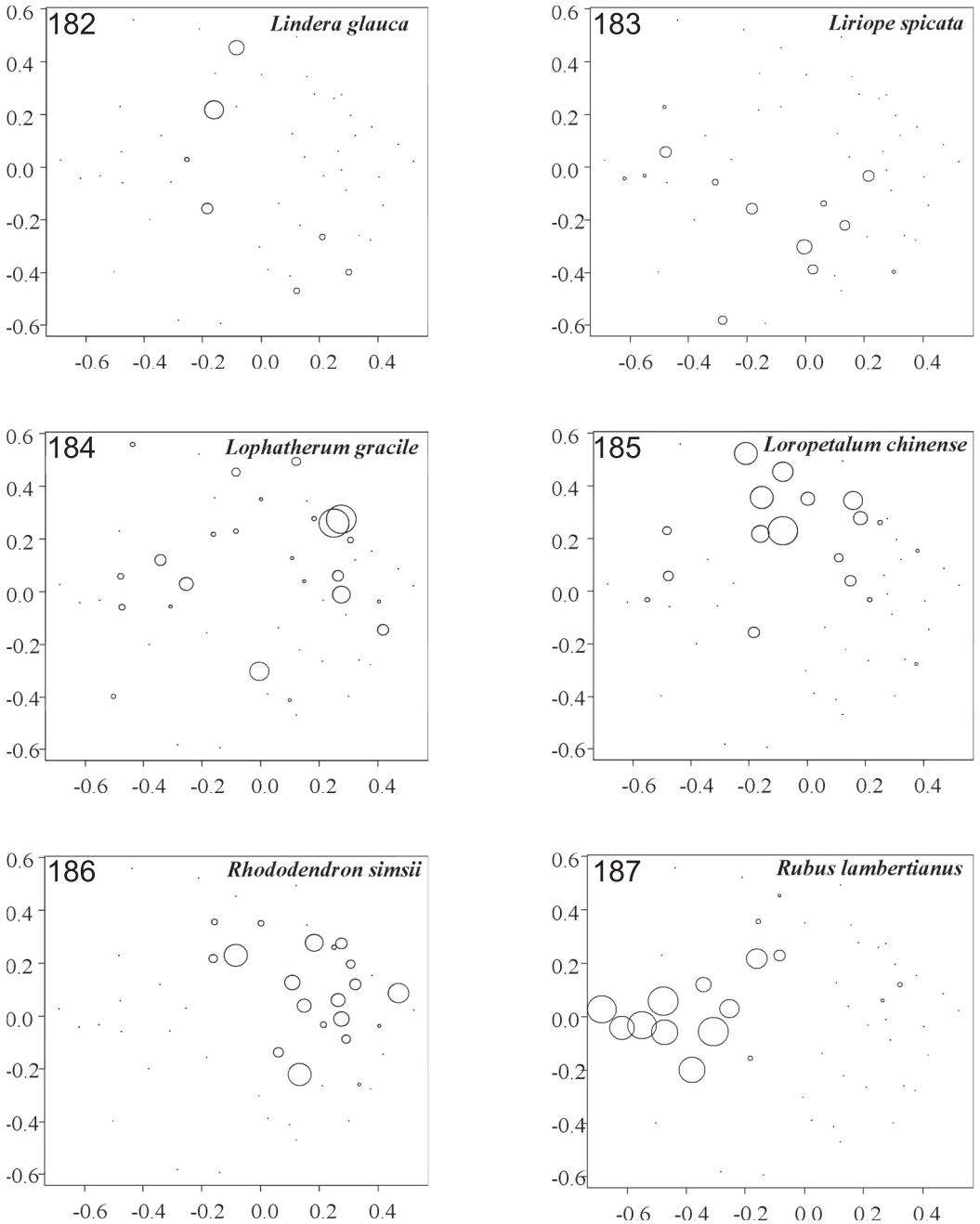

Figs 182–187. Cai Jia Tang: Distribution of species abundances in the GNMDS ordination of 49 plots (plot number 5 omitted), axes 1 (horizontal) and 2 (vertical). Frequency in subplots for each species in each plot proportional to circle size. Fig. 182. *Lindera glauca*. Fig. 183. *Liriope spicata*. Fig. 184. *Lophatherum gracile*. Fig. 185. *Loropetalum chinense*. Fig. 186. *Rhododendron simsii*. Fig. 187. *Rubus lambertianus*. Small dots indicate absence; circles indicate presence, diameter proportional with subplot frequency.

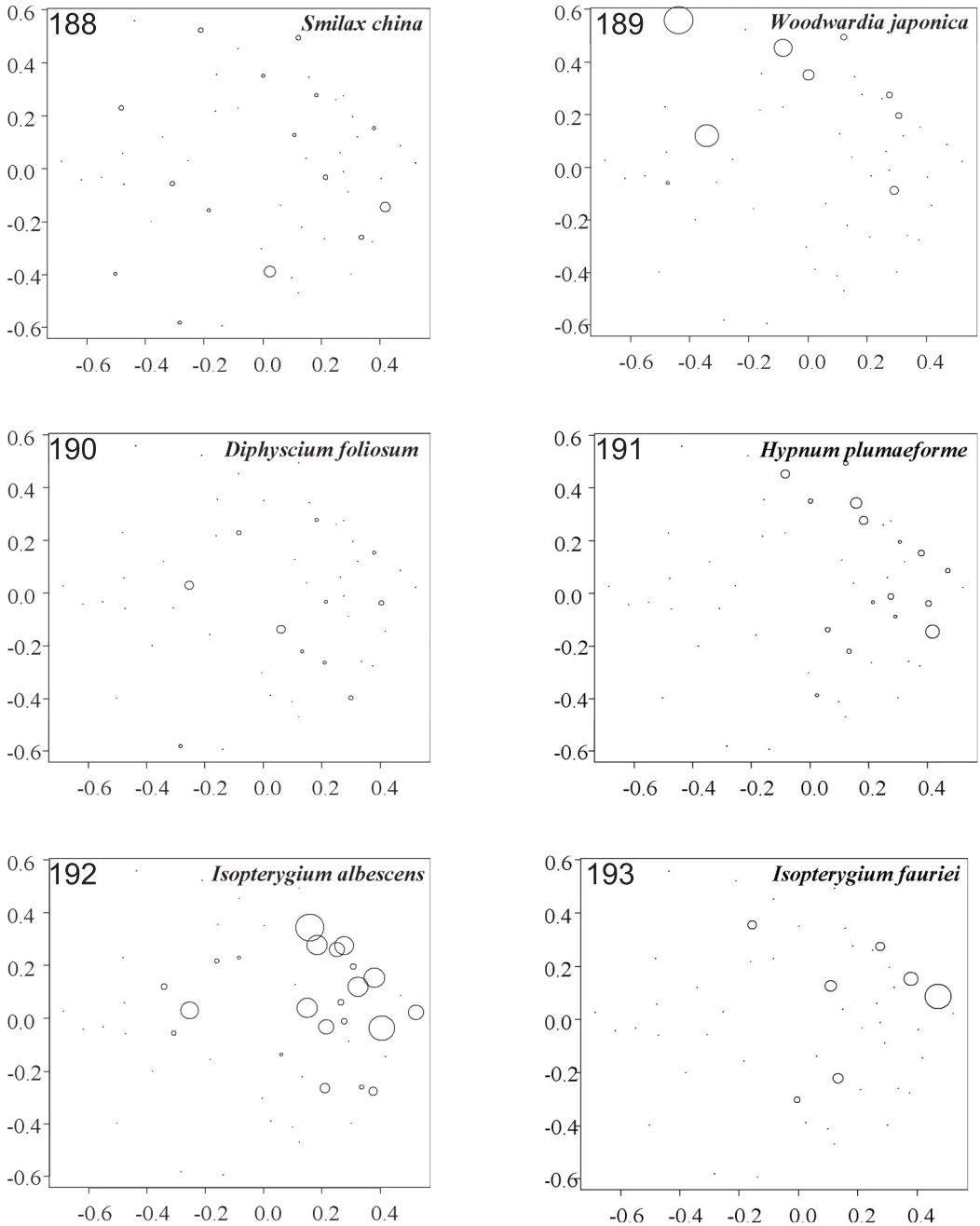

Figs 188–193. Cai Jia Tang: Distribution of species abundances in the GNMDS ordination of 49 plots (plot number 5 omitted), axes 1 (horizontal) and 2 (vertical). Frequency in subplots for each species in each plot proportional to circle size. Fig. 188. *Smilax china*. Fig. 189. *Woodwardia japonica*. Fig. 190. *Diphyscium foliosum*. Fig. 191. *Hypnum plumaeforme*. Fig. 192. *Isopterygium albescens*. Fig. 193. *Isopterygium fauriei*. Small dots indicate absence; circles indicate presence, diameter proportional with subplot frequency.

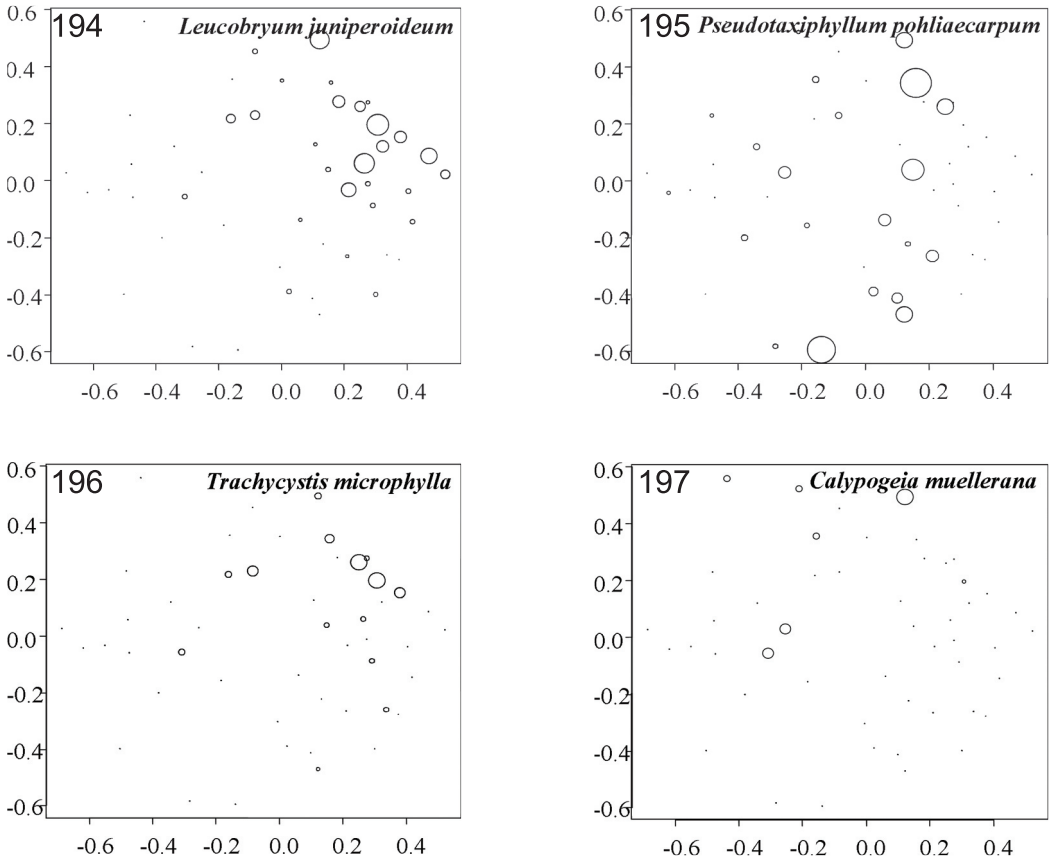

Figs 194–197. Cai Jia Tang: Distribution of species abundances in the GNMDS ordination of 49 plots (plot number 5 omitted), axes 1 (horizontal) and 2 (vertical). Frequency in subplots for each species in each plot proportional to circle size. Fig. 194. *Leucobryum juniperoideum*. Fig. 195. *Pseudotaxiphyllum pohliaecarpum*. Fig. 196. *Trachycystis microphylla*. Fig. 197. *Calypogeia muellerana*. Small dots indicate absence; circles indicate presence, diameter proportional with subplot frequency.

LIU XI HE

Correlations between environmental variables

A group of pairwise strongly correlated variables was made up by contents of total C and N, the organic matter content and the content of dry matter. The three first mentioned were pairwise positively correlated, while the content of dry matter was negatively correlated with each of the first three variables (Tab. 44 and Fig. 198).

The organic matter content together with the SO_4 adsorption and soil depth made up another group, with pairwise positive correlations. The organic matter content was also positively correlation with the inclination.

Tab. Tab. 44. Liu Xi He: Kendall's rank correlation coefficients τ between 33 environmental variable in the 50 plots (lower triangle), with significant probabilities (upper triangle). Very strong correlations ($|\tau| \geq 4.0$, $P < 0.0001$) are indicated by bold face. n.s means significance probability $P > 0.1$. Numbers and abbreviation for names of environmental variables are in accordance with Tab. 2.

	1	2	3	4	5	6	7	8	9	10	11	12	13	14	15	16	17
001 Inclin	.	n.s	.0808	n.s	n.s	n.s	n.s	n.s	.0022	n.s	n.s	n.s	.0588	.0061	n.s	n.s	n.s
02 AspecF	−.0977	.	.0000	.0011	.0081	n.s	n.s	n.s	.0465	n.s	n.s	n.s	.0145	.0094	.0228	n.s	n.s
03 HeatIn	−.1809	.7890	.	.0096	.0016	n.s	n.s	n.s	.0436	n.s	n.s	n.s	.0633	.0229	.0108	n.s	n.s
04 TerraM	.1223	−.3450	−.2730	.	n.s	.0002	n.s	.0028	n.s	n.s	n.s	n.s	.0024	.0045	.0081	. n.s	.0388
05 ConvS1	−.1525	.2790	.3310	−.1253	*	n.s	.0024	n.s	n.s	n.s	n.s	n.s	n.s	.0465	**.0002**	n.s	n.s
06 ConvV1	.0050	−.1383	−.0833	.4060	.0185	*	n.s	.0005	n.s	n.s	n.s	n.s	n.s	n.s	n.s	.0559	n.s
07 ConvS9	−.0681	.1224	.1050	.0445	.3290	.1599	*	n.s	n.s	n.s	.0106	n.s	.0719	.0278	.0039	n.s	n.s
08 ConvV9	−.0828	−.1458	−.0540	.3180	.0193	.3650	.0274	*	.0064	n.s	n.s	n.s	n.s	n.s	n.s	n.s	n.s
09 SoilDM	.3200	.2050	.2070	−.0868	.1127	−.1079	.0403	−.2840	*	n.s	n.s	n.s	n.s	.0989	n.s	n.s	n.s
10 LitLDM	−.1107	−.0116	.0058	.0336	.0192	−.1817	−.0335	−.0776	.0245	*	.0370	n.s	n.s	n.s	n.s	n.s	n.s
11 OrgaLD	−.0677	.0238	.0575	−.0713	.0210	−.0208	−.2960	.0126	.0466	.2630	*	.0372	.0778	n.s	n.s	n.s	n.s
12 SoilMLM	−.0522	.1070	.0107	−.1446	−.0090	−.0954	.1222	.0089	−.1141	−.0917	−.2350	*	.0042	.0632	n.s	n.s	n.s
13 LitteI	.0999	−.2520	−.1906	.1713	−.1105	.0489	−.1899	−.0928	.1429	.1502	.1996	−.2940	*	**.0000**	n.s	n.s	n.s
14 CrowCI	.1912	−.2680	−.2340	.1373	−.2100	−.0679	−.2330	−.1404	.1707	.0887	.0432	−.1913	**.6460**	*	n.s	n.s	n.s
15 RelaCN	−.0844	.2740	.3050	−.3270	**.4570**	−.0122	.3550	−.1490	.1657	−.0142	−.0761	.0312	.0134	−.1225	*	n.s	n.s
16 RelaDN	−.1577	.1762	.1633	−.1234	.0478	−.2096	−.0478	−.1188	−.0258	.0812	.0635	−.0041	.0516	−.1055	.0362	*	n.s
17 pH_{H_2O}	−.0315	.0905	.1202	−.2180	.1242	−.1243	−.0311	−.0630	−.0722	−.0813	.1594	.0311	−.0458	−.0713	.1293	.0679	*
18 pH_{CaCl_2}	.0030	.1151	.0845	−.1037	.0080	−.1076	−.0562	−.1469	.0587	.1362	.1474	−.0107	−.1387	−.1743	−.1222	.1527	.2450
19 Al	.0256	−.1717	−.2030	.1813	−.1798	.1358	−.1319	.1373	−.0175	−.0428	.1804	−.0755	.1467	.1431	−.2163	−.2620	−.0010
20 Fe	.1730	−.0844	−.0793	.0270	−.0040	−.0387	.1159	−.0039	.0448	−.0405	−.1894	.2340	.0165	.0321	.1482	.1488	.0087
21 H	.0039	**−.4280**	−.3650	.3580	−.1778	.2810	.0340	.2630	−.2120	−.1980	−.1962	.0291	.1001	.0360	−.0859	−.1098	−.1250
22 Mn	−.1376	−.0572	−.0406	.2230	−.0999	.2210	−.1279	.2610	−.2650	−.0868	.2187	−.2870	.0437	−.0302	−.3260	−.1981	.0552
23 Ca	−.1848	.0048	.0773	.0831	.0040	.2570	−.0040	.1746	−.2280	−.1540	.1669	−.1608	−.0321	−.1470	−.1511	−.1037	.1870
24 Mg	−.1356	−.1329	−.0309	.1452	−.0559	.1656	−.0460	.2080	−.2260	−.1100	.1781	−.1046	.0826	.0575	−.2282	−.2290	.1909
25 Na	−.1573	−.0068	.0464	−.0731	.1758	.0466	.0080	.0863	−.0428	−.1285	.1466	−.0232	−.0262	−.1665	−.0356	−.0852	.0630
26 K	.0236	.0029	.0522	.1793	−.0839	.0704	−.0899	.0922	−.1518	−.0405	.0879	−.0484	.0709	.1022	−.2045	−.0893	.1056
27 C	.1449	.1994	.1590	−.0251	−.0180	.0467	.0431	−.0679	.2230	−.2480	−.0373	−.1535	.1608	.1602	.0862	−.2320	.0049
28 N	.1107	.1073	.0839	.0217	−.0991	.1230	.0031	.0061	.1167	−.3000	−.0571	−.1541	.1818	.1660	.0429	−.2850	−.0391
29 BS	−.1435	.1251	.1972	−.0611	.0460	.0387	.0520	−.0177	−.1869	−.1123	−.0045	−.0446	−.0962	−.1159	−.0148	.0544	.1831
30 AlS	.1927	−.0029	−.0696	−.0331	.0120	−.1160	−.0959	−.0863	.2630	.1169	.1150	−.0097	.1234	.1743	.0178	−.0359	−.0707
31 SO_4	.2710	.3190	.3340	−.1272	.1638	−.1557	−.0619	−.1982	**.4750**	.0521	.1353	−.1724	.1254	.1607	.0948	.0195	.0630
32 WDM	−.2540	−.1988	−.1701	.0932	−.0859	−.0406	−.0619	.0314	−.1908	.1679	−.0902	.0775	−.0204	.0497	−.0978	.1940	−.1521
33 LOI	.3580	.2610	.2340	−.0932	.1059	−.0744	−.0500	−.0981	**.4070**	−.1192	.2165	−.2110	.1312	.1022	.0919	−.0811	.0785

Tab. 44 (continued). Liu Xi He: Kendall's rank correlation coefficients τ between 33 environmental variable in the 50 plots (lower triangle), with significant probabilities (upper triangle). Very strong correlations ($|\tau| \geq 4.0, P < 0.0001$) are indicated by bold face. n.s means significance probability $P > 0.1$. Numbers and abbreviation for names of environmental variables are in accordance with Tab. 2.

	18	19	20	21	22	23	24	25	26	27	28	29	30	31	32	33
01 Inclin	n.s	n.s	.0949	n.s	n.s	.0745	n.s	n.s	n.s	n.s	n.s	n.s	.0629	.0088	.0144	.0006
02 AspecF	n.s	.0936	n.s	**.0000**	n.s	n.s	n.s	n.s	n.s	.0521	n.s	n.s	n.s	.0018	.0522	.0108
03 HeatIn	n.s	.0468	n.s	.0003	n.s	n.s	n.s	n.s	n.s	n.s	n.s	.0534	n.s	.0011	.0956	.0219
04 TerraM	n.s	.0848	n.s	.0007	.0337	n.s	n.s	n.s	.0883	n.s	n.s	n.s	n.s	n.s	n.s	n.s
05 ConvS1	n.s	.0867	n.s	.0903	n.s	n.s	n.s	.0939	n.s	n.s	n.s	n.s	n.s	n.s	n.s	n.s
06 ConvV1	n.s	n.s	n.s	.0072	.0341	.0139	n.s	n.s	n.s	n.s	n.s	n.s	n.s	n.s	n.s	n.s
07 ConvS9	n.s	n.s	n.s	n.s	n.s	n.s	n.s	n.s	n.s	n.s	n.s	n.s	n.s	n.s	n.s	n.s
08 ConvV9	n.s	n.s	n.s	.0110	.0116	.0914	.0444	n.s	n.s	n.s	n.s	n.s	n.s	.0554	n.s	n.s
09 SoilDM	n.s	n.s	n.s	.0389	.0100	.0266	.0279	n.s	n.s	.0307	n.s	.0689	.0105	**.0000**	.0633	**.0001**
10 LitLDM	n.s	n.s	n.s	.0831	n.s	n.s	n.s	n.s	n.s	.0301	.0106	n.s	n.s	n.s	n.s	n.s
11 OrgaLD	n.s	n.s	.0925	.0814	.0521	n.s	n.s	n.s	n.s	n.s	n.s	n.s	n.s	n.s	n.s	.0545
12 SoilMLM	n.s	n.s	.0219	n.s	.0051	n.s	n.s	n.s	n.s	n.s	n.s	n.s	n.s	.0919	n.s	.0390
13 LitteI	n.s	n.s	n.s	n.s	n.s	n.s	n.s	n.s	n.s	n.s	.0848	n.s	n.s	n.s	n.s	n.s
14 CrowCI	n.s	n.s	n.s	n.s	n.s	n.s	n.s	n.s	n.s	n.s	n.s	n.s	.0898	n.s	n.s	n.s
15 RelaCN	n.s	.0708	n.s	n.s	.0065	n.s	.0567	n.s	.0877	n.s	n.s	n.s	n.s	n.s	n.s	n.s
16 RelaDN	n.s	.0146	n.s	n.s	.0646	n.s	.0327	n.s	n.s	.0311	.0096	n.s	n.s	n.s	.0703	n.s
17 pH_{H_2O}	.0169	n.s	n.s	n.s	n.s	.0676	.0621	n.s	n.s	n.s	n.s	.0735	n.s	n.s	n.s	n.s
18 pH_{CaCl_2}	*	n.s	n.s	.0280	.3732	n.s	.0633	n.s	n.s	n.s	n.s	n.s	n.s	.0407	n.s	n.s
19 Al	−.0330	*	n.s	.0478	.0052	n.s	.0078	.0109	.0705	.0022	.0013	.0020	.0002	n.s	.0938	.0457
20 Fe	.0058	−.0493	*	.0004	**.0000**	.0052	n.s	n.s	n.s	n.s	n.s	n.s	n.s	n.s	n.s	n.s
21 H	−.2250	.2020	.3580	*	n.s	n.s	.0595	n.s	n.s	n.s	n.s	n.s	n.s	.0001	n.s	.0261
22 Mn	−.0913	.2850	**−.4550**	−.0068	*	**.0000**	**.0000**	n.s	.0261	.0974	.0208	.0301	n.s	n.s	.0735	n.s
23 Ca	−.1088	.1382	−.2850	.0783	**.5360**	*	**.0000**	.0039	.0052	n.s	n.s	**.0000**	**.0001**	.0595	n.s	n.s
24 Mg	−.1904	.2710	−.0705	.1923	**.4300**	**.5030**	*	.0020	**.0000**	n.s	.0885	.0020	.0109	.0621	n.s	n.s
25 Na	−.0369	.2600	−.0821	.0184	.1671	.2950	.3160	*	.2219	.0260	.0389	n.s	n.s	n.s	n.s	n.s
26 K	−.0738	.1845	.0937	.1130	.2270	.2850	**.4800**	.1246	*	n.s	n.s	.0097	.0500	n.s	n.s	n.s
27 C	.0234	.3130	−.1076	−.0533	.1696	.1134	.1463	.2280	.1192	*	**.0000**	n.s	n.s	.0134	.0001	**.0000**
28 N	−.0281	.3370	−.0909	.0469	.2430	.1348	.1787	.2170	.0789	**.8110**	*	n.s	n.s	.0997	.0004	**.0001**
29 BS	−.0971	−.3160	−.1517	−.0937	.2210	.5030	.3160	.1150	.2640	−.0475	−.0749	*	**.0000**	n.s	n.s	n.s
30 AlS	.1263	.3800	.0184	−.1130	−.1575	−.4050	−.2600	−.0010	−.2000	.1483	.1408	**−.7350**	*	.0083	n.s	.0274
31 SO_4	.2100	.0010	−.0435	−.3870	−.0686	−.1923	−.1903	−.0937	−.0531	.2530	.1727	−.1246	.2700	*	.0083	**.0000**
32 WDM	−.1088	−.1710	.1556	.1285	−.1826	−.1517	−.0879	−.1188	.0184	−.3890	−.3700	.0010	−.1266	−.2700	*	**.0000**
33 LOI	.1399	.2040	−.0493	−.2270	.0725	.0029	−.0106	.1362	.1072	**.4930**	**.4020**	−.0802	.2250	**.5340**	**−.5570**	*

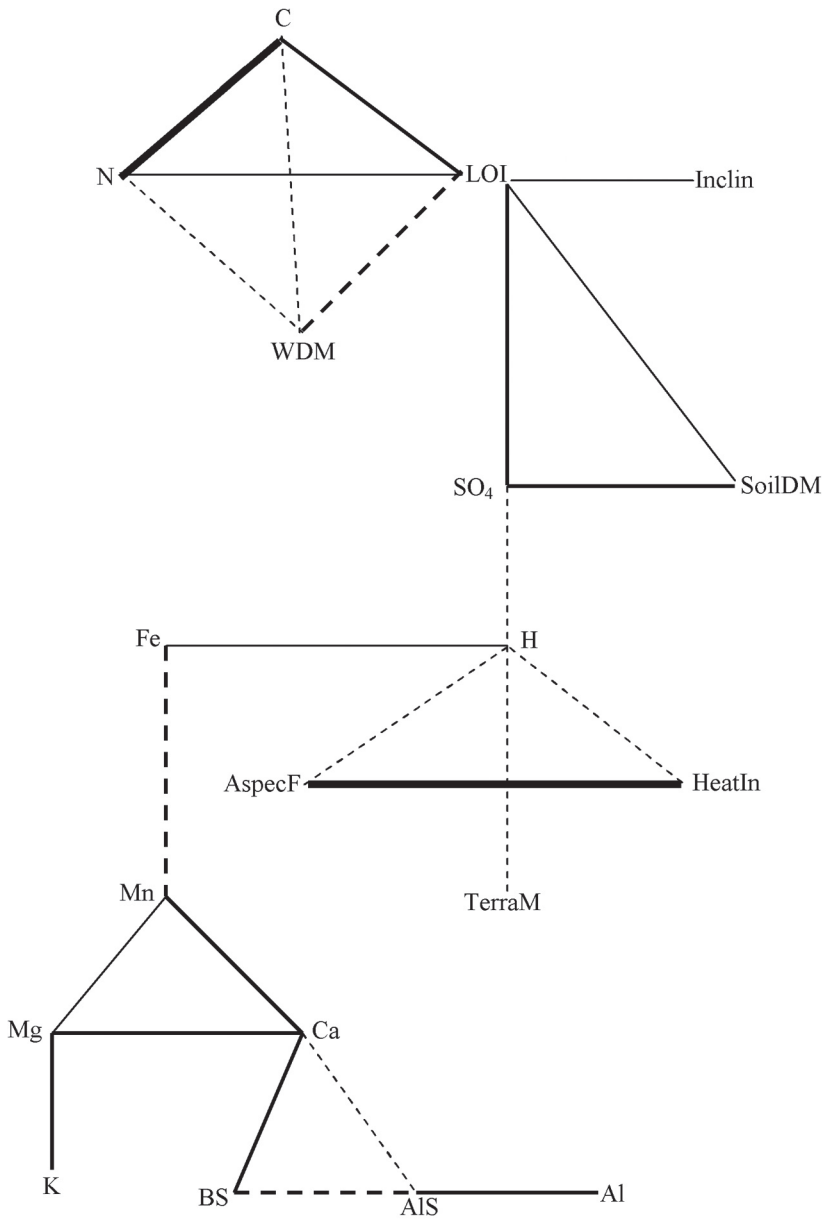

Fig. 198. Liu Xi He: Plexus diagram visualizing Kendall's τ between pairs of environmental variables. Significance probabilities for τ are indicated by lines with different thickness (in order of decreasing thickness): $|\tau| \geq 0.60$, $0.45 \leq |\tau| < 0.60$, and $0.35 \leq |\tau| < 0.45$. Continuous lines refer to positive correlations, broken lines to negative.

A third group of strongly correlated variables consisted of the concentration of H, aspect favorability and the heat index. Aspect favorability and heat index was positively correlated with each other, but negatively correlated with the concentration of H. Two variables were connected with this group, i.e. the concentration of H by positive correlation with the concentration of Fe, and by negative correlation with the terrain roughness.

A fourth group of pairwise strongly positively correlated variables were made up by the concentrations of Mn, Mg and Ca. Two variables were associated with this group, i.e. the concentration of K by positive correlation with the concentration of Mg, the concentration of Fe by negative correlation with the concentration of Mn.

The concentration of Ca was also included in a fifth group of correlated variables. This group consisted of the concentration of Ca, the base saturation and the aluminum saturation. The concentration of Ca and the base saturation were positively correlated with each other, but negatively correlated with the aluminum saturation.

PCA ordination of environmental variables

Eigenvalues of the first two PCA axes were 0.205 and 0.152, thus 35.6% of the variation in measured environmental variables was explained by the first two PCA axes.

Heat index, aspect favourability and the number of coniferous trees obtained high loadings on PCA 1, while terrain conditions and crown cover index obtained low loadings on this axis. Soil dry matter content obtained high loadings on PCA 2, while low loadings were obtained by concentrations of Mn, Mg and Ca in soil, total C and N in soil, and soil organic matter content.

PCA ordination results thus summarised major features of correlations between environmental variables in fewer dimensions (Tab. 44, Figs 198–199). Visibly, the soil nutrients variables consisted of contents of total C and N, the organic matter content, and the concentrations of Mn, Mg, Ca, Na and K were more or less strongly negatively correlated with the content of dry matter. The topographic variables contained aspect favorability and heat index were negatively correlated with the concentration of H, tree influence variables like crown cover index and litter index, and topographic variables consisted of terrain roughness and inclination.

GNMDS ordination

Good correspondence with respect to gradient length, core length and eigenvalues was found between GNMDS 1 and DCA 1, GNMDS 3 and DCA 2, and GNMDS 2 and DCA 3, respectively. There was a marked drop in eigenvalue occurred from GNMDS 1 (DCA 1) to GNMDS 2 (DCA 3), indicating that the first axis was the major compositional gradients.

The first axis of the GNMDS ordination of the 46 1-m^2 plots (plots number 38, 47, 48 and 49 omitted) had high eigenvalue 2.2946 and gradient length of 3.1890 S.D. units, respectively. The plots were relatively evenly distributed in the GNMDS ordination (Figs 200–201). No plots acted as outliers, as judged by core length (Tab. 45).

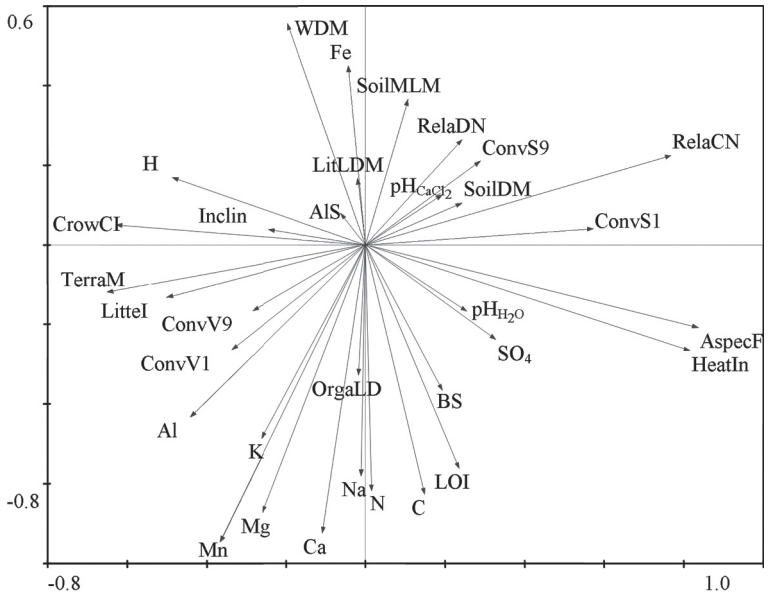

Fig. 199. Liu Xi He: PCA ordination of 33 environmental variables (names abbreviated in accordance with Tab.2), axes 1 (horizontal) and 2 (vertical). Loadings of variables on the ordination axes are shown by heads of variable vectors.

Tab. 45. Ordination of vegetation in the 46 plots (plots number 38, 47, 48 and 49 omitted) in LXH: summary of properties for GNMDS and DCA axes 1–3 properties. Core length means length of the shortest interval containing 90% of the plots relative to gradient length.

Corresponding axis		Unit	A	B	C
Axis No			GNMDS 1, DCA 1	GNMDS 2, DCA 3	GNMDS 3, DCA 2
GNMDS	Gradient length	HC	0.840	0.688	0.637
		S. D	3.189	2.828	2.557
	Core length	%	0.807	0.789	0.857
	Eigenvalue		2.295	1.740	1.465
DCA	Gradient length	S.D	3.829	3.093	3.233
	Core length	%	0.689	0.611	0.711
	Eigenvalue		0.527	0.288	0.400

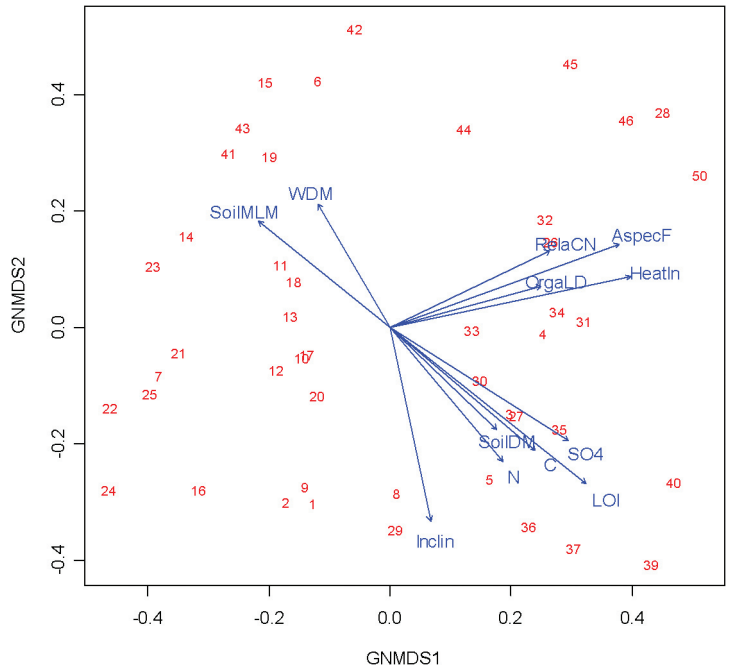

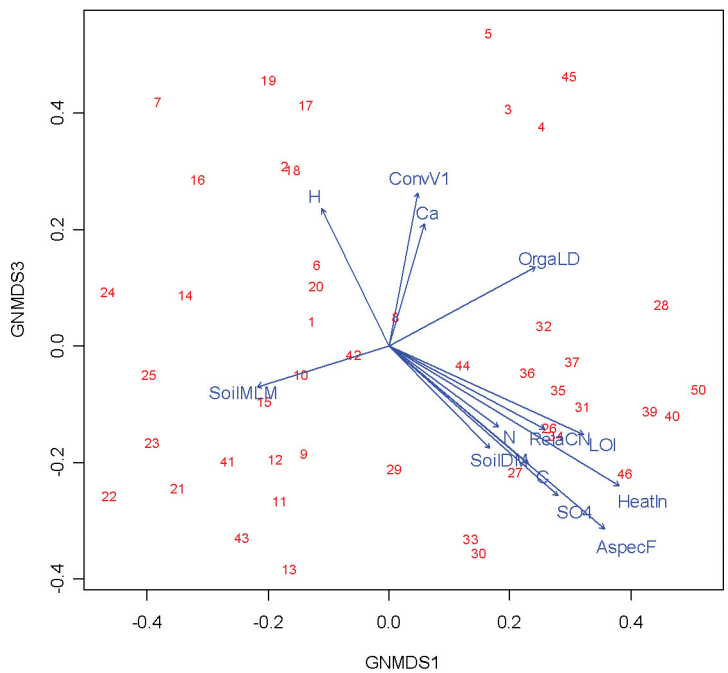

Figs 200–201. Liu Xi He: GNMDS ordination biplots of 46 plots (indicated by their number, plots number 38, 47, 48 and 49 omitted) and significant environmental variables (i.e. with $P < 0.1$ according to goodness-of-fit test; see Tab. 52). Names of variables are abbreviated in accordance with Tab. 2. For each environmental variable the direction of maximum increase and the relative magnitude of increase in this direction are indicated by the direction and length of the vector arrows. Fig. 200. Axes 1 (horizontal) and 2 (vertical). Fig. 201. Axes 1 (horizontal) and 3 (vertical).

Relationships between ordination axes and environmental variables

GNMDS ordination biplots of 46 plots and significant environmental variables

Positions of plot scores in the GNMDS ordination space were related to variation in environmental variables, as indicated by a several environmental variable vectors with significantly directed variation patterns in the ordination space (Figs 200–201). Along the first two axes the following patterns appeared: (1) vector for heat index, aspect favourability, the number of coniferous trees and organic-layer depth vectors pointed to the upper right of the biplots (representing a gradient of increasing light conditions, number of coniferous trees and organic-layer depth); (2) vectors for soil moisture and soil dry matter content pointed to the upper left; (3) vectors for soil organic matter content, total C and N in soil, soil SO_4 adsorption and soil depth pointed lower rightwards, almost directly in the opposite direction of vectors for soil moisture and soil dry matter content. Thus, plots with a relatively moist soil occurred to the left in the biplots, while a relatively dry soil occurred to the right.

Along the third axis, vectors for aspect favourability, heat index, the variance of concavity/convexity at 1-m^2 scale and concentrations of H and Ca in soil pointed towards higher GNMDS 3 scores, while vectors for SO_4 adsorption, crown cover index, litter index and soil depth pointed towards lower GNMDS 3 scores.

Split-plot GLM analysis of relationships between ordination axes and environmental variables

Variation (in plot scores) along GNMDS 1 was partitioned with 79.24 % at the macro-plot scale (i.e. between macro plots) and 20.76 % at the plot scale (i.e. between plots). For the GNMDS 2 variation was partitioned with 64.72 % at the macro-plot scale and 35.28 % at the plot scale. For the GNMDS 3 variation was partitioned with 55.59 % at the macro-plot scale and 44.41 % at the plot scale (Tabs 46–48).

At the macro-plot scale, two environmental variables were significantly and two were indicatively significantly related to GNMDS axis 1, three and two variables (at the $P < 0.05$ and $P < 0.1$ levels, respectively) were related to GNMDS axis 2, and four and two variables (at the $P < 0.05$ and $P < 0.1$ levels, respectively) were related to GNMDS axis 3, respectively. At the plot scale, five environmental variables were significantly and three were indicatively significantly related to GNMDS axis 1, four and two variables (at the $P < 0.05$ and $P < 0.1$ levels, respectively) were related to GNMDS axis 2, and three and four variables (at the $P < 0.05$ and $P < 0.1$ levels, respectively) were related to GNMDS axis 3, respectively.

At the macro-plot scale, the variables significantly positively related to GNMDS axis 1 were aspect favourability and heat index ($P < 0.05$), and organic-layer depth and soil organic matter content were indicatively significantly related to this axis (positively) ($P < 0.1$). At the plot scale, the variance of concavity/convexity at 1-m^2 scale, organic-layer depth, and concentrations of Mn and Ca in soil were significantly positively related to GNMDS axis 1. The concentration of Al in soil and soil organic matter content were indicatively significantly related to this axis (positively), and the concentration of Fe in soil was indicatively significantly related to this axis (negatively) ($P < 0.1$) (Tab. 46).

At the macro-plot scale, the variables significantly negatively related to GNMDS axis 2 were terrain conditions and litter index, and variable significantly positively related to this axis was soil moisture ($P < 0.05$). Inclination and the variance of concavity/convexity at 1-m^2 scale were indicatively significantly related to GNMDS axis 2 (negatively) ($P < 0.1$). At the plot scale, inclination was significantly negatively related to GNMDS axis 2, and concentrations of Al, Mg, Na and K in soil were significantly positively related to this axis ($P < 0.05$), while the concentration of H in soil was indicatively significantly related to this axis (positively) ($P < 0.1$) (Tab. 47).

At the macro-plot scale, the variables significantly negatively related to GNMDS axis 3 were aspect favourability and soil SO_4 adsorption ($P < 0.05$), while soil depth and heat index were indicatively significantly related to this axis (negatively) ($P < 0.1$). The variance of concavity/convexity at 9-m^2 scale and the concentration of H in soil were significantly positively related to this axis ($P < 0.05$). At the plot scale, the variables strongly positively related to GNMDS axis 3 were concentrations of Ca and Na in soil, heat index and concavity/convexity sum index at 1-m^2 scale ($P < 0.05$); organic-layer depth and the number of broadleaved trees were indicatively significantly related to this axis (positively) ($P < 0.05$). Inclination was significantly negatively related to this axis ($P < 0.05$) (Tab. 48).

Kendall's rank correlation between ordination axes and environmental variables

The variables most strongly positively correlated with GNMDS axis 1 were organic-layer depth, the number of coniferous trees, and soil organic matter content ($0.30 \leq \tau \leq 0.35$). The variables more or less strongly negatively correlated with GNMDS axis 1 was soil moisture, and the variables positively correlated with this axis were aspect favourability and heat index, total C in soil and soil SO_4 adsorption ($0.20 < |\tau| < 0.30$).

The variable most strongly negatively correlated with GNMDS axis 2 was inclination ($\tau = -0.3260$). The variables more or less strongly positively correlated with GNMDS axis 2 were soil moisture and soil dry matter content, and the variable negatively correlated with this axis was total C in soil and soil organic matter content ($0.20 < |\tau| < 0.30$).

The variable most strongly negatively correlated with GNMDS axis 3 was aspect favourability ($\tau = -0.3540$). The variables more or less strongly negatively correlated with GNMDS axis 3 were heat index, total C in soil and soil SO_4 adsorption, and the variables positively correlated with this axis were terrain conditions and the variance of concavity/convexity at 9-m^2 scale ($0.20 < |\tau| < 0.30$).

Relationships between ordination axes and species number variables

Split-plot GLM analysis of relationships between ordination axes and species number variables

The number of bryophyte species was significantly negatively related to GNMDS axis 2 at the macro-plot scale. The fraction of variation explained by the number of bryophyte species at the macro-plot scale was 52.67 % (Tab. 50).

The number of bryophyte species was indicatively significantly related to GNMDS axis 3 (positively) at the macro-plot scale. The fractions of variation explained by the number of bryophyte species at the macro-plot scale was 30.69 % (Tab. 51).

Kendall's rank correlation between ordination axes and species number variables

The total number of species was most strongly negatively correlated with the GNMDS 1 ($\tau = -0.3120$). The number of vascular plants ($\tau = -0.2740$) and the number of bryophyte species ($\tau = -0.2450$) were both more or less strongly negatively correlated with GNMDS 1 (Tab. 49). The number of bryophyte species was most strongly negatively correlated with the GNMDS 2 ($\tau = -3690$) (Tab. 50). No variable of species number was strongly correlated with the GNMDS 3 (Tab. 51).

Tab. 46. Liu Xi He: Split-plot GLM analysis and Kendall's nonparametric correlation coefficient τ between GNMDS 1 and 33 environmental variables (predictor) in the 46 plots (plots number 38, 47, 48 and 49 omitted). df_{resid}: degrees of freedom for the residuals; *SS*: total variation; *FVE*: fraction of total variation attributable to a given scale (macro plot or plot); SS_{expl}/SS: fraction of the variation attributable to the scale in question, explained by a variable; *r*: model coefficient (only given when significant at the α = 0.1 level, otherwise blank); *F*: *F* statistic for test of the hypothesis that *r* = 0 against the two-tailed alternative. Split-plot GLM relationships significant at level α = 0.05, *P*, *F*, *r* and SS_{expl}/SS, and Kendall's nonparametric correlation coefficient $|\tau| \geq 0.30$ are given in bold face. Numbers and abbreviations for names of environmental variables are in accordance with Tab. 2.

Predictor	Dependent variable = GNMDS 1 (*SS* = 35.2270)								Correlation between predictor and GNMDS 1
	Error level								
	Macro plot df_{resid} = 8 $SS_{macro\ plot}$ = 27.9137 *FVE* = 0.7924 of *SS*				Plot within macro plot df_{resid} = 35 SS_{plot} = 7.3133 *FVE* = 0.2076 of *SS*				Total
	$SS_{expl}/SS_{macro\ plot}$	*r*	*F*	*P*	SS_{expl}/SS_{plot}	*r*	*F*	*P*	τ
Inclin	0.0076		0.0610	0.8110	0.0059		0.2060	0.6527	0.087
AspecF	**0.4119**	**1.5290**	**5.6020**	**0.0455**	0.0167		0.5937	0.4462	0.257
HeatIn	**0.5039**	**2.0014**	**8.1259**	**0.0215**	0.0457		1.6756	0.2040	0.296
TerraM	0.0384		0.3198	0.5872	0.0713		2.6877	0.1101	–0.085
ConvS1	0.1875		1.8467	0.2112	0.0119		0.4201	0.5211	0.152
ConvV1	0.0101		0.0814	0.7827	**0.2067**	**1.6294**	**9.1187**	**0.0047**	0.057
ConvS9	0.0006		0.0045	0.9484	0.0435		1.5920	0.2154	–0.030
ConvV9	0.0121		0.0983	0.7620	0.0120		0.4256	0.5184	0.016
SoilDM	0.1529		1.4440	0.2639	0.0189		0.6742	0.4171	0.179
LitLDM	0.0031		0.0245	0.8795	0.0016		0.0569	0.8129	0.043
OrgaLD	0.3540	3.8887	4.3837	0.0696	**0.1318**	**0.6953**	**5.3143**	**0.0272**	**0.318**
SoilMLM	0.2311		2.4050	0.1595	0.0376		1.3688	0.2499	–0.219
LitteI	0.0189		0.1543	0.7047	0.0629		2.3509	0.1342	0.172
CrowCI	0.0825		0.7189	0.4211	0.0000		0.0002	0.9875	–0.028
RelaCN	0.2224		2.2875	0.1689	0.0138		0.4912	0.4880	**0.338**
RelaDN	0.0702		0.6045	0.4593	0.0579		2.1502	0.1515	0.112
pH_{H_2O}	0.0169		0.1375	0.7204	0.0001		0.0024	0.9610	0.053
pH_{CaCl_2}	0.0034		0.0275	0.8725	0.0058		0.2038	0.6545	0.082
Al	0.0123		0.0992	0.7608	0.1049	1.2193	4.1004	0.0506	–0.038
Fe	0.0257		0.2111	0.6581	0.0936	–0.8187	3.6148	0.0655	0.007
H	0.0696		0.5981	0.4615	0.0030		0.1057	0.7470	–0.167
Mn	0.0026		0.0205	0.8896	**0.3006**	**1.8509**	**15.0460**	**0.0004**	0.013
Ca	0.0006		0.0050	0.9455	**0.2178**	**1.5387**	**9.7432**	**0.0036**	0.067
Mg	0.0017		0.0135	0.9104	0.0513		1.8934	0.1776	–0.094
Na	0.0003		0.0026	0.9606	0.0450		1.6491	0.2075	0.049
K	0.0107		0.0869	0.7757	0.0066		0.2327	0.6325	0.086
C	0.2614		2.8317	0.1309	0.0008		0.0278	0.8686	0.230
N	0.1779		1.7313	0.2247	0.0008		0.0292	0.8653	0.167
BS	0.0090		0.0730	0.7939	0.0020		0.0706	0.7921	0.026
AlS	0.0008		0.0066	0.9374	0.0091		0.3199	0.5753	0.073
SO_4	0.2768		3.0613	0.1183	0.0008		0.0282	0.8676	0.281
WDM	0.0296		0.2442	0.6345	0.0409		1.4910	0.2302	–0.115
LOI	0.3063	2.0293	3.5320	0.0970	0.0807	1.4491	3.0727	0.0884	**0.341**

Tab. 47. Liu Xi He: Split-plot GLM analysis and Kendall's nonparametric correlation coefficient τ between GNMDS 2 and 33 environmental variables (predictor) in the 46 plots (plots number 38, 47, 48 and 49 omitted). df_{resid}: degrees of freedom for the residuals; *SS*: total variation; *FVE*: fraction of total variation attributable to a given scale (macro plot or plot); SS_{expl}/SS: fraction of the variation attributable to the scale in question, explained by a variable; *r*: model coefficient (only given when significant at the α = 0.1 level, otherwise blank); *F*: *F* statistic for test of the hypothesis that *r* = 0 against the two-tailed alternative. Split-plot GLM relationships significant at level α = 0.05, *P*, *F*, *r* and SS_{expl}/SS, and Kendall's nonparametric correlation coefficient $|\tau| \geq 0.30$ are given in bold face. Numbers and abbreviations for names of environmental variables are in accordance with Tab. 2.

Predictor	Dependent variable = GNMDS 2 (*SS* = 28.4755)								Correlation between predictor and GNMDS 2
	Error level								
	Macro plot df_{resid} = 8 $SS_{macro\ plot}$ = 18.4295 *FVE* = 0.6472 of *SS*				Plot within macro plot df_{resid} = 35 SS_{plot} = 10.0460 *FVE* = 0.3528 of *SS*				Total
	$SS_{expl}/SS_{macro\ plot}$	*r*	*F*	*P*	SS_{expl}/SS_{plot}	*r*	*F*	*P*	τ
Inclin	0.3101	–1.7715	3.5955	0.0945	**0.1139**	**–1.0250**	**4.4998**	**0.0411**	**-0.326**
AspecF	0.1459		1.3662	0.2761	0.0038		0.1335	0.7170	0.121
HeatIn	0.0600		0.5104	0.4953	0.0053		0.1848	0.6700	0.079
TerraM	**0.4758**	**–3.1132**	**7.2602**	**0.0273**	0.0702		2.6413	0.1131	-0.077
ConvS1	0.0014		0.0109	0.9194	0.0212		0.7566	0.3903	0.052
ConvV1	0.3873	–4.4532	5.0564	0.0547	0.0059		0.2069	0.6520	-0.193
ConvS9	0.0024		0.0189	0.8940	0.0070		0.2485	0.6213	-0.026
ConvV9	0.1378		1.2786	0.2909	0.0028		0.0994	0.7544	-0.106
SoilDM	0.0593		0.5041	0.4979	0.0323		1.1669	0.2874	-0.127
LitLDM	0.2100		2.1264	0.1829	0.0303		1.0923	0.3031	0.196
OrgaLD	0.0000		0.0000	0.9962	0.0393		1.4321	0.2395	0.047
SoilMLM	**0.4158**	**2.9581**	**5.6934**	**0.0441**	0.0561		2.0805	0.1581	0.238
LitteI	**0.5158**	**–2.6307**	**8.5224**	**0.0193**	0.0403		1.4684	0.2337	-0.135
CrowCI	0.2950		3.3472	0.1047	0.0018		0.0632	0.8030	-0.122
RelaCN	0.0995		0.8843	0.3746	0.0029		0.1003	0.7534	0.071
RelaDN	0.1470		1.3790	0.2740	0.0022		0.0771	0.7829	0.163
pH_{H_2O}	0.0140		0.1138	0.7445	0.0099		0.3484	0.5588	0.046
pH_{CaCl_2}	0.0408		0.3400	0.5759	0.0000		0.0000	0.9992	0.027
Al	0.0192		0.1566	0.7027	**0.1199**	**1.5281**	**4.7692**	**0.0358**	0.073
Fe	0.0389		0.3241	0.5848	0.0441		1.6146	0.2122	0.090
H	0.1397		1.2996	0.2873	0.0794	0.7955	3.0166	0.0912	-0.065
Mn	0.1754		1.7013	0.2284	0.0114		0.4032	0.5296	-0.144
Ca	0.2015		2.0186	0.1932	0.0508		1.8737	0.1798	-0.129
Mg	0.1891		1.8659	0.2091	**0.1724**	**1.4923**	**7.2915**	**0.0106**	0.009
Na	0.1104		0.9926	0.3483	**0.2263**	**0.8006**	**1.2380**	**0.0029**	0.086
K	0.0032		0.0258	0.8764	0.0919	0.7577	3.5417	0.0682	0.115
C	0.1334		1.2319	0.2993	0.0024		0.0855	0.7717	-0.179
N	0.1686		1.6224	0.2385	0.0163		0.5782	0.4521	-0.261
BS	0.0280		0.2303	0.6442	0.0125		0.4421	0.5105	-0.015
AlS	0.0420		0.3508	0.5700	0.0166		0.5891	0.4479	0.020
SO_4	0.0429		0.3587	0.5658	0.0543		2.0102	0.1651	-0.123
WDM	0.1791		1.7457	0.2230	0.0016		0.0574	0.8121	0.219
LOI	0.1999		1.9987	0.1951	0.0003		0.0110	0.9170	-0.225

Tab. 48. Liu Xi He: Split-plot GLM analysis and Kendall's nonparametric correlation coefficient τ between GNMDS 3 and 33 environmental variables (predictor) in the 46 plots (plots number 38, 47, 48 and 49 omitted). df_{resid}: degrees of freedom for the residuals; *SS*: total variation; *FVE*: fraction of total variation attributable to a given scale (macro plot or plot); SS_{expl}/SS: fraction of the variation attributable to the scale in question, explained by a variable; *r*: model coefficient (only given when significant at the α = 0.1 level, otherwise blank); *F*: *F* statistic for test of the hypothesis that *r* = 0 against the two-tailed alternative. Split-plot GLM relationships significant at level α = 0.05, *P*, *F*, *r* and SS_{expl}/SS, and Kendall's nonparametric correlation coefficient $|\tau| \geq 0.30$ are given in bold face. Numbers and abbreviations for names of environmental variables are in accordance with Tab. 2.

Predictor	Dependent variable = GNMDS 3 (*SS* = 21.7418)								Correlation between predictor and GNMDS 3
	Error level								
	Macro plot df_{resid} = 8 $SS_{macro\ plot}$ = 12.0860 *FVE* = 0.5559 of *SS*				Plot within macro plot df_{resid} = 35 SS_{plot} = 9.6558 *FVE* = 0.4441 of *SS*				Total
	$SS_{expl}/SS_{macro\ plot}$	*r*	*F*	*P*	SS_{expl}/SS_{plot}	*r*	*F*	*P*	τ
Inclin	0.0306		0.2526	0.6288	**0.1763**	**–1.2502**	**7.4926**	**0.0097**	-0.126
AspecF	**0.4441**	**–1.0447**	**6.3902**	**0.0354**	0.0001		0.0040	0.9497	**-0.319**
HeatIn	0.3958	–1.1671	5.2405	0.0513	0.1002	2.1022	3.8979	0.0563	-0.230
TerraM	0.2476		2.6326	0.1433	0.0033		0.1155	0.7360	0.233
ConvS1	0.2649		2.8832	0.1279	0.1040	1.1941	4.0623	0.0516	0.000
ConvV1	0.2764		3.0561	0.1186	0.0444		1.6246	0.2109	0.168
ConvS9	0.0022		0.0179	0.8968	0.0014		0.0482	0.8275	0.000
ConvV9	**0.4484**	**2.9086**	**6.5023**	**0.0342**	**0.0036**		0.1264	0.7243	0.206
SoilDM	0.3510	–2.3415	4.3261	0.0711	0.0002		0.0085	0.9272	-0.169
LitLDM	0.0491		0.4132	0.5383	0.0013		0.0471	0.8295	-0.008
OrgaLD	0.0101		0.0816	0.7824	0.0930	0.6709	3.5871	0.0665	0.169
SoilMLM	0.0113		0.0916	0.7699	0.0173		0.6158	0.4379	-0.136
LitteI	0.0525		0.4436	0.5241	0.0217		0.7759	0.3844	-0.007
CrowCI	0.0066		0.0530	0.8236	0.0009		0.0330	0.8569	-0.114
RelaCN	0.0636		0.5429	0.4823	0.0357		1.2966	0.2626	-0.136
RelaDN	0.0010		0.0081	0.9304	0.0795	0.8885	3.0213	0.0910	0.124
pH_{H_2O}	0.2351		2.4583	0.1555	0.0133		0.4724	0.4964	-0.044
pH_{CaCl_2}	0.0630		0.5375	0.4844	0.0417		1.5217	0.2256	0.012
Al	0.0061		0.0495	0.8296	0.0113		0.4012	0.5306	-0.055
Fe	0.1082		0.9710	0.3533	0.0078		0.2737	0.6042	0.005
H	**0.8612**	**3.3657**	**49.6170**	**0.0001**	**0.0125**		0.4425	0.5103	0.171
Mn	0.0574		0.4874	0.5049	0.0383		1.3933	0.2458	0.115
Ca	0.0564		0.4778	0.5090	**0.1302**	**1.3674**	**5.2410**	**0.0282**	0.169
Mg	0.0001		0.0005	0.9830	0.0472		1.7343	0.1964	0.094
Na	0.0041		0.0326	0.8612	**0.1294**	**0.5935**	**5.2029**	**0.0288**	0.098
K	0.0119		0.0965	0.7640	0.0213		0.7602	0.3892	0.007
C	0.1882		1.8548	0.2103	0.0272		0.9780	0.3295	-0.222
N	0.0482		0.4048	0.5424	0.0662		2.4805	0.1243	-0.171
BS	0.0017		0.0136	0.9100	0.0459		1.6847	0.2028	0.063
AlS	0.1474		1.3826	0.2735	0.0082		0.2911	0.5930	-0.158
SO_4	**0.4898**	**–1.5998**	**7.6789**	**0.0243**	**0.0038**		0.1351	0.7154	-0.277
WDM	0.2376		2.4932	0.1530	0.0150		0.5324	0.4704	0.107
LOI	0.2643		20.8746	0.1284	0.0457		1.6756	0.2040	-0.113

Tab. 49. Liu Xi He: Split-plot GLM analysis and Kendall's nonparametric correlation coefficient τ between GNMDS 1 and two species number variables (predictor) in the 46 plots (plots number 38, 47, 48 and 49 omitted). df_{resid}: degrees of freedom for the residuals; *SS*: total variation; *FVE*: fraction of total variation attributable to a given scale (macro plot or plot); SS_{expl}/SS: fraction of the variation attributable to the scale in question, explained by a variable; *r*: model coefficient (only given when significant at the α = 0.1 level, otherwise blank); *F*: *F* statistic for test of the hypothesis that *r* = 0 against the two-tailed alternative. Split-plot GLM relationships significant at level α = 0.05, *P*, *F*, *r* and SS_{expl}/SS, and Kendall's nonparametric correlation coefficient $|\tau| \geq 0.30$ are given in bold face.

Predictor (number of species)	Dependent variable = GNMDS 1 (*SS* = 35.2270)								Correlation between predictor and GNMDS 1
	Error level								
	Macro plot df_{resid} = 8 $SS_{macro\ plot}$ = 27.9137 *FVE* = 0.7924 of *SS*				Plot within macro plot df_{resid} = 35 SS_{plot} = 7.3133 *FVE* = 0.2076 of *SS*				Total
	$SS_{expl}/SS_{macro\ plot}$	*r*	*F*	*P*	SS_{expl}/SS_{plot}	*r*	*F*	*P*	τ
Vascular plants	0.1215		1.1066	0.3236	0.0714		2.6930	0.1098	–0.274
Bryophyte species	0.1464		1.3717	0.2752	0.0402		1.4648	0.2343	–0.245

Tab. 50. Liu Xi He: Split-plot GLM analysis and Kendall's nonparametric correlation coefficient τ between GNMDS 2 and two species number variables (predictor) in the 46 plots (plots number 38, 47, 48 and 49 omitted). df_{resid}: degrees of freedom for the residuals; *SS*: total variation; *FVE*: fraction of total variation attributable to a given scale (macro plot or plot); SS_{expl}/SS: fraction of the variation attributable to the scale in question, explained by a variable; *r*: model coefficient (only given when significant at the α = 0.1 level, otherwise blank); *F*: *F* statistic for test of the hypothesis that *r* = 0 against the two-tailed alternative. Split-plot GLM relationships significant at level α = 0.05, *P*, *F*, *r* and SS_{expl}/SS, and Kendall's nonparametric correlation coefficient $|\tau| \geq 0.30$ are given in bold face.

Predictor (number of species)	Dependent variable = GNMDS 2 (*SS* = 28.4755)								Correlation between predictor and GNMDS 2
	Error level								
	Macro plot df_{resid} = 8 $SS_{macro\ plot}$ = 18.4295 *FVE* = 0.6472 of *SS*				Plot within macro plot df_{resid} = 35 SS_{plot} = 10.0460 *FVE* = 0.3528 of *SS*				Total
	$SS_{expl}/SS_{macro\ plot}$	*r*	*F*	*P*	SS_{expl}/SS_{plot}	*r*	*F*	*P*	τ
Vascular plants	0.0180		0.1465	0.7119	0.0025		0.0894	0.7668	–0.005
Bryophyte species	**0.5267**	**–0.3041**	**8.9041**	**0.0175**	0.0550		2.0360	0.1625	**–0.369**

Tab. 51. Liu Xi He: Split-plot GLM analysis and Kendall's nonparametric correlation coefficient τ between GNMDS 3 and two species number variables (predictor) in the 46 plots (plots number 38, 47, 48 and 49 omitted). df_{resid}: degrees of freedom for the residuals; *SS*: total variation; *FVE*: fraction of total variation attributable to a given scale (macro plot or plot); SS_{expl}/SS: fraction of the variation attributable to the scale in question, explained by a variable; *r*: model coefficient (only given when significant at the α = 0.1 level, otherwise blank); *F*: *F* statistic for test of the hypothesis that *r* = 0 against the two-tailed alternative. Split-plot GLM relationships significant at level α = 0.05, *P*, *F*, *r* and SS_{expl}/SS, and Kendall's nonparametric correlation coefficient $|\tau| \geq 0.30$ are given in bold face.

Predictor (number of species)	Dependent variable = GNMDS 3 (*SS* = 21.7418) Error level								Correlation between predictor and GNMDS 3
	Macro plot df_{resid} = 8 $SS_{macro\ plot}$ = 12.0860 *FVE* = 0.5559 of *SS*				Plot within macro plot df_{resid} = 35 SS_{plot} = 9.6558 *FVE* = 0.4441 of *SS*				Total
	$SS_{expl}/SS_{macro\ plot}$	*r*	*F*	*P*	SS_{expl}/SS_{plot}	*r*	*F*	*P*	τ
Vascular plants	0.2990		3.4124	0.1019	0.0015		0.0539	0.8177	0.143
Bryophyte species	0.3069	0.1880	3.5429	0.0966	0.0433		1.5834	0.2166	0.153

Isoline diagrams for significant environmental species number variables

A total of 22 environmental variables and one species number variables satisfied the criteria for making two-dimensional isoline diagrams (Tab. 52, Figs 202–224).

The distribution of species abundance in the GNMDS ordination

Out of a total of 147 species, 41 were found in at least 5 of the 46 plots (Figs 225–265).

Isopterygium pohliaecarpum (Fig. 261), a typical examples of bryophyte species with wide ecological amplitude, was abundant in most plots, but was absent from plots with high GNMDS 2 scores (i.e. on sites with low inclination and thick litter layer).

Castanopsis fissa (Fig. 231), a typical example of vascular plant species with wide ecological amplitude, was abundant in most plots, but was absent from plots with low GNMDS 2 scores (i.e. on sites with high inclination).

Selaginella doederleinii (Fig. 251) was restricted to plots in left part of the GNMDS ordination diagram (related to a thinner organic layer, a lower coniferous trees density and a lower soil organic matter content), while *Adiantum flabellulatum* (Fig. 225), *Millettia reticulata* (Fig. 246) and *Woodwardia japonica* (Fig. 257) were restricted to plots in right part of GNMDS ordination diagram (related to a almost opposite complex-gradient of *Selaginella doederleinii* (Fig. 251).

Tab. 52. Liu Xi He: Environmental and species number variables for which two-dimensional isoline diagrams were made: P value for relationship with GNMDS axis assessed by split-plot GLM (two scales = error levels), Kendall's correlation coefficient τ with axis, and R^2 between the original and predicted values (according to the isoline diagrams for the variable), used as a measure of goodness-of-fit of the isolines. Isoline diagrams were made for variables with split-plot GLM $P < 0.05$ at the macro plot or the plot scale and/or Kendall's correlation coefficient $|\tau| \geq 0.3$ with one GNMDS axis. P values < 0.05 and/or $|\tau| \geq 0.30$ in bold face. Numbers and abbreviations for names of environmental variables in accordance with Tab. 2 (NVP = number of vascular plants species; and NBS = number of bryophyte species).

Ordination axis	Variable names	The split plot GLM Error level		Kendall's ccorrelation between variable and ordination axis	Goodness-of-fit of the isolines
		$P_{\text{macro plot}}$	P_{plot}	τ_{total}	R^2
GNMDS 1	AspecF	**0.0455**	0.4462	0.257	0.4659
	HeatIn	**0.0215**	0.2040	0.296	0.5896
	ConvV1	0.7827	**0.0047**	0.057	0.0652
	OrgaLD	0.0696	**0.0272**	**0.318**	0.1616
	RelaCN	0.1689	0.4880	**0.338**	0.6778
	Mn	0.8896	**0.0004**	0.013	0.3557
	Ca	0.9455	**0.0036**	0.067	0.2555
	LOI	0.0970	0.0884	**0.341**	0.5287
GNMDS 2	Inclin	0.0945	**0.0411**	**–0.326**	0.5856
	TerraM	**0.0273**	0.1131	–0.077	0.0193
	SoilMLM	**0.0441**	0.1581	0.238	0.0013
	LitteI	**0.0193**	0.2337	–0.135	0.0746
	Al	0.7027	**0.0358**	0.073	0.0430
	Mg	0.2091	**0.0106**	0.009	0.0036
	Na	0.3483	**0.0029**	0.086	0.0058
	NBS	**0.0175**	0.1625	**–0.369**	0.3883
GNMDS 3	Inclin	0.6288	**0.0097**	–0.126	0.5948
	AspecF	**0.0354**	0.9497	**–0.319**	0.3989
	ConvV9	**0.0342**	0.7243	0.206	0.0345
	H	**0.0001**	0.5103	0.171	0.0499
	Ca	0.5090	0.0282	0.169	0.2721
	Na	0.8612	0.0288	0.098	0.0278
	SO_4	**0.0243**	0.7154	–0.277	0.4122

Allantodia metteniana (Fig. 226), *Pteris insignis* (Fig. 248), *Scleria hebecarpa* (Fig. 250), and *Calypogeia tosana* (Fig. 259) were restricted to plots in lower left part of GNMDS ordination diagram (related to a lower coniferous trees density and a thinner organic layer).

Fissidens taxifolius (Fig. 260) was restricted to plots in lower right part of GNMDS ordination diagram (related to higher soil organic matter content and deeper soil).

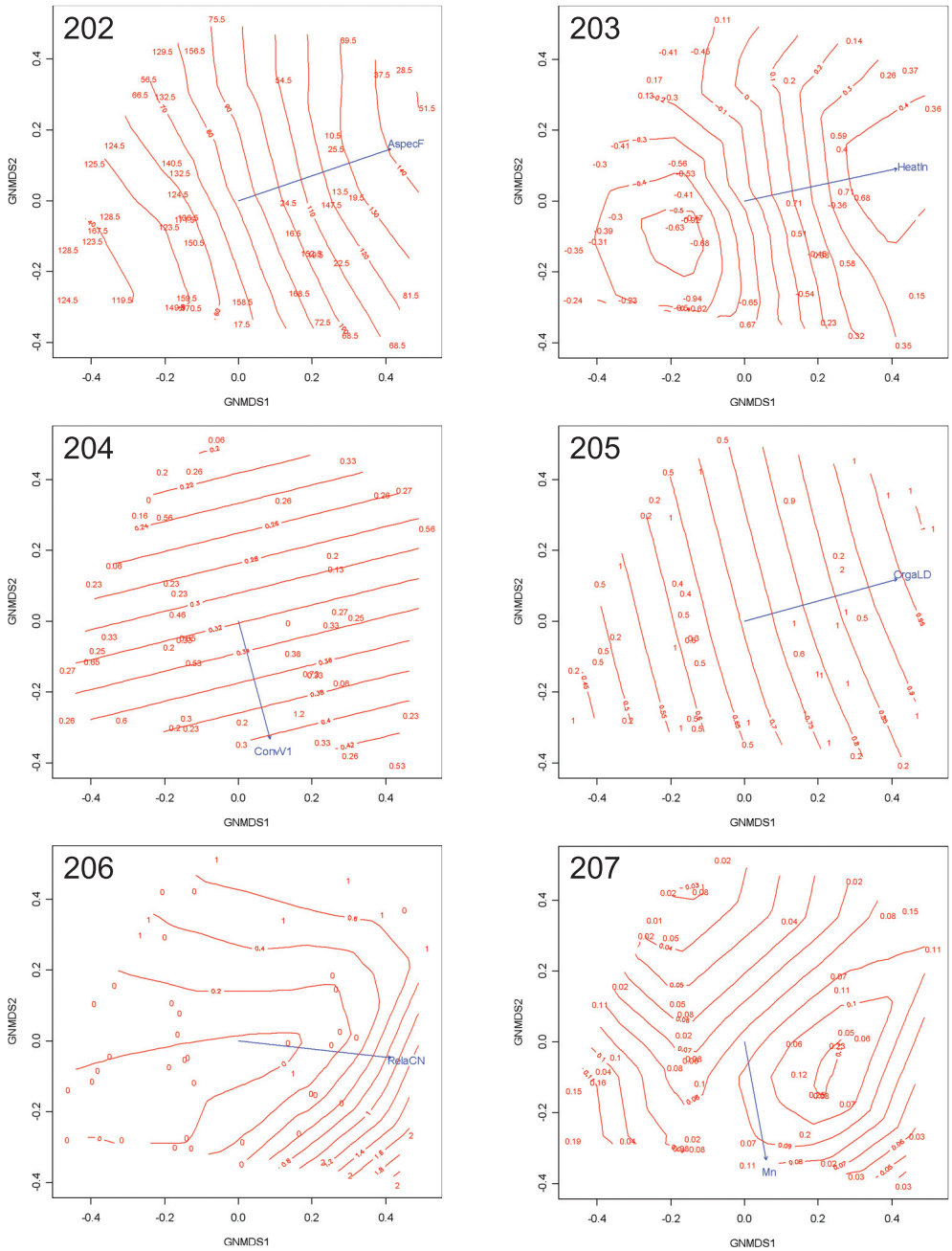

Figs 202–207. Liu Xi He: Isolines for environmental variables in the GNMDS ordination of 46 plots (plots number 38, 47, 48 and 49 omitted), axe 1 (horizontal) and 2 (vertical). Values for the environmental variables are plotted onto plots' position. Fig. 202. AspecF ($R^2 = 0.4659$). Fig. 203. HeatIn ($R^2 = 0.5896$). Fig. 204. ConvV1 ($R^2 = 0.0652$). Fig. 205. OrgaLD ($R^2 = 0.1616$). Fig. 206. RelaCN ($R^2 = 0.6778$). Fig. 207. Mn ($R^2 = 0.3557$). R^2 refers to the coefficient of determination between original and smoothened values as interpolated from the isolines. Numbers and abbreviations for names of environmental variables are in accordance with Tab.2.

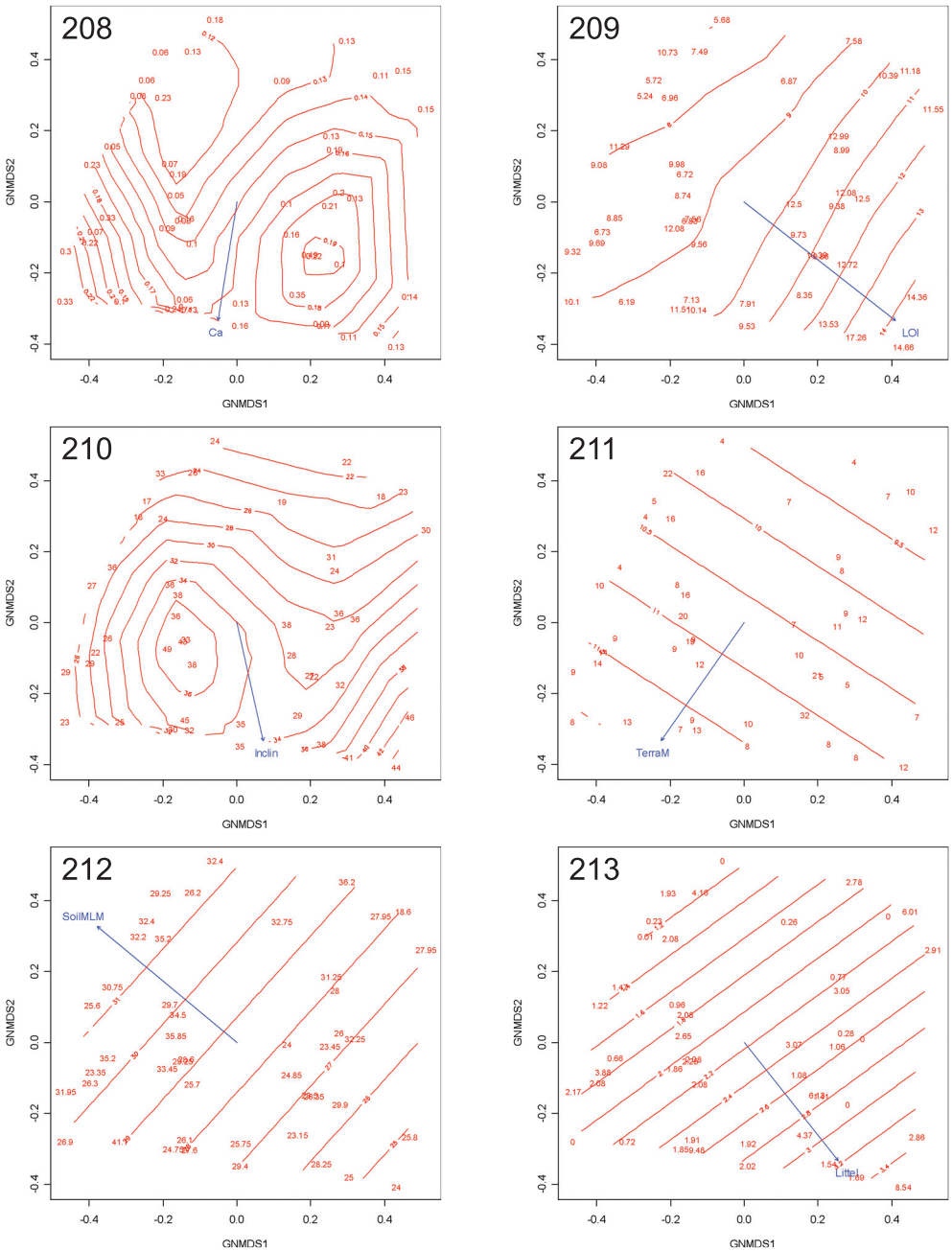

Figs 208–213. Liu Xi He: Isolines for environmental variables in the GNMDS ordination of 46 plots (plots number 38, 47, 48 and 49 omitted), axe 1 (horizontal) and 2 (vertical). Values for the environmental variables are plotted onto plots' position. Fig. 208. Ca (R^2 = 0.2555). Fig. 209. LOI (R^2 = 0.5287). Fig. 210. Inclin (R^2 = 0.5856). Fig. 211. TerraM (R^2 = 0.0193). Fig. 212. SoilMLM (R^2 = 0.0013). Fig. 213. LitteI (R^2 = 0.0746). R^2 refers to the coefficient of determination between original and smoothened values as interpolated from the isolines. Numbers and abbreviations for names of environmental variables are in accordance with Tab.2.

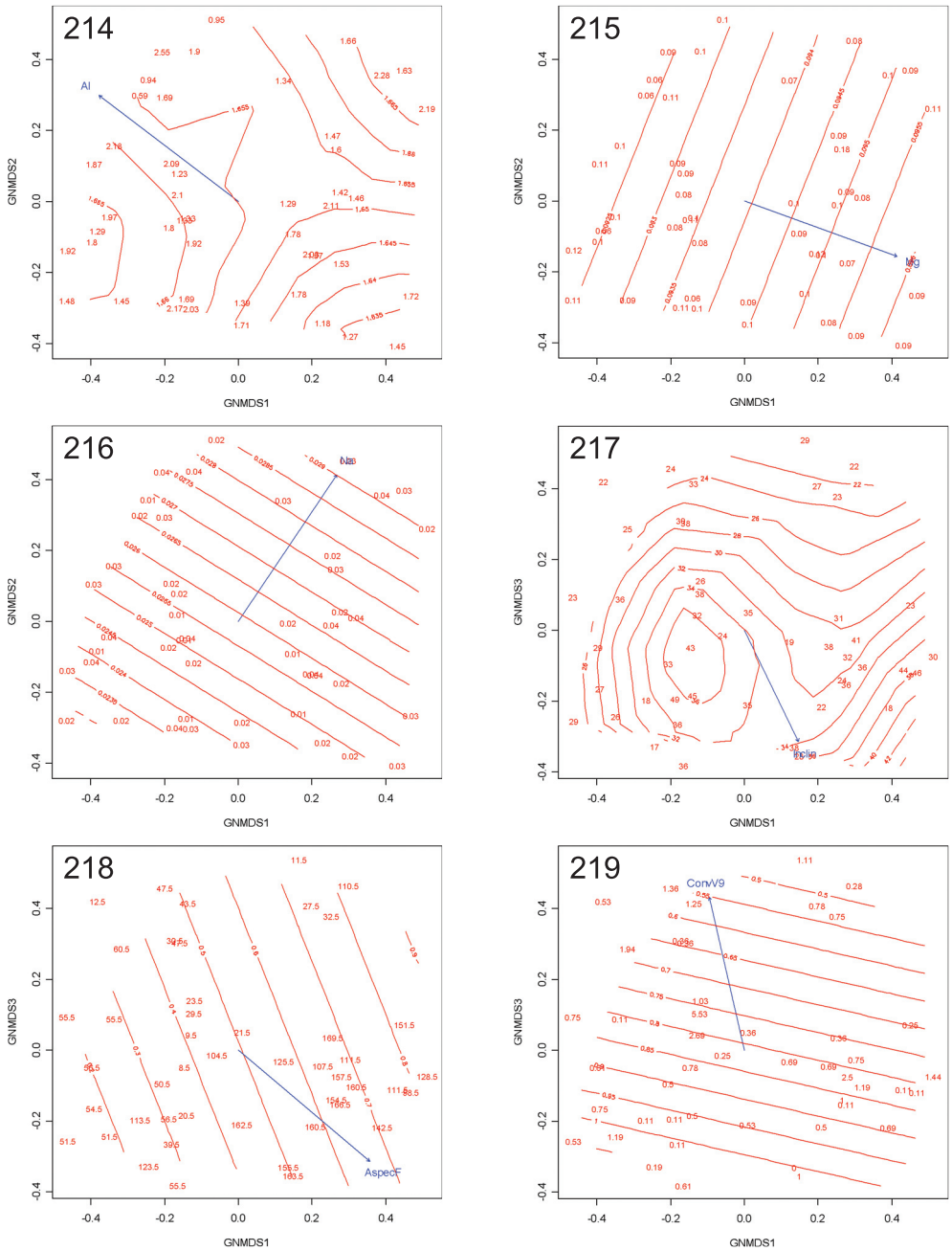

Figs 214–219. Liu Xi He: Isolines for environmental variables in the GNMDS ordination of 46 plots (plots number 38, 47, 48 and 49 omitted), axe 1 (horizontal) and 2 (vertical). Values for the environmental variables are plotted onto plots' position. Fig. 214. Al (R^2 = 0.0430). Fig. 215. Mg (R^2 = 0.0036). Fig. 216. Na (R^2 = 0.0058). Fig. 217. Inclin (R^2 = 0.5948). Fig. 218. AspecF (R^2 = 0.3989). Fig. 219. ConvV9 (R^2 = 0.0345). R^2 refers to the coefficient of determination between original and smoothened values as interpolated from the isolines. Numbers and abbreviations for names of environmental variables are in accordance with Tab.2.

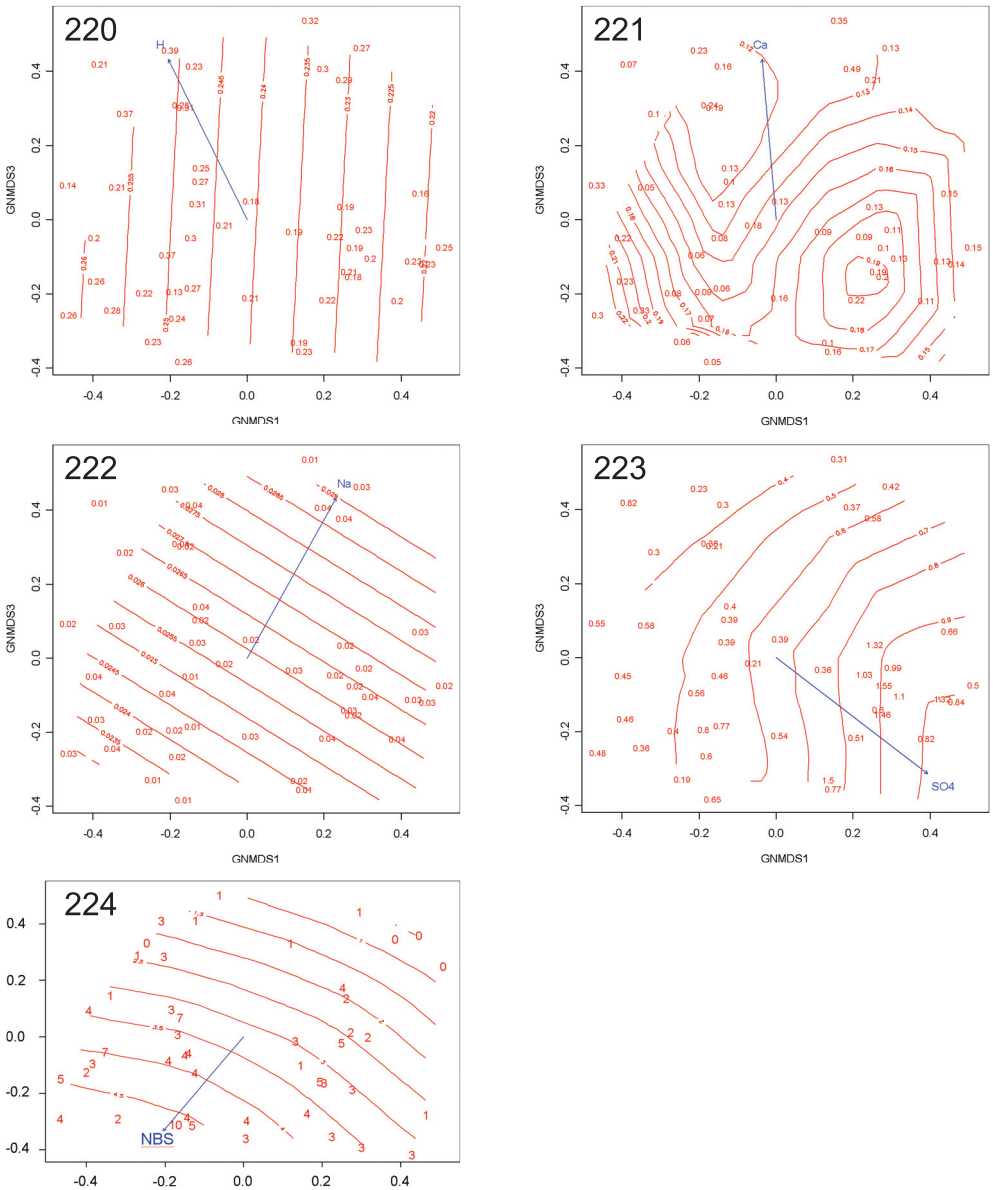

Figs 220–224. Liu Xi He: Isolines for environmental variables in the GNMDS ordination of 46 plots (plots number 38, 47, 48 and 49 omitted), axe 1 (horizontal) and 3 (vertical) Values for the environmental variables are plotted onto plots' position. Fig. 220. H (R^2 = 0.0499). Fig. 221. Ca (R^2 = 0.2721). Fig. 222. Na (R^2 = 0.0278). Fig. 223. SO_4 (R^2 = 0.4122). Fig. 224. NBS (the number of bryophyte species) (R^2 = 0.3883). R^2 refers to the coefficient of determination between original and smoothened values as interpolated from the isolines. Numbers and abbreviations for names of environmental variables are in accordance with Tab.2.

Tab. 53. Liu Xi He: Occurrence (number of plots in which the species was present) and local abundance (abundant = subplot frequency ≥ 8) of species recorded in five or more of the 46 plots (plots number 38, 47, 48 and 49 omitted).

Species	The total number of plots	
	Present	Abundant
Adiantum flabellulatum	17	2
Allantodia metteniana	10	3
Alyxia vulgaris	12	0
Anoectochilus roxburghii	7	0
Ardisia crenata var. bicolor	6	0
Blastus cochinchinensis	6	0
Castanopsis fissa	26	8
Cinnamomum parthenoxylon	8	0
Croton lachnocarpus	16	0
Dendronpanax proteus	8	0
Dryopteris podophylla	8	1
Embelia rudis	11	1
Eriobotrya fragrans	5	0
Gahnia tristis	10	1
Gnetum montanum	9	0
Hypolytrum nemorum	5	1
Itea chinensis	12	0
Litsea rotundifolia	9	0
Lophatherum gracile	8	1
Maesa perlarius	16	1
Millettia dielsiana	6	0
Millettia reticulata	10	0
Pericampylus glaucus	5	0
Pteris insignis	7	1
Rapanea neriifolia	8	0
Scleria hebecarpa	15	5
Selaginella doederleinii	25	10
Selaginella heterostachys	9	1
Smilax lanceifolia	10	0
Symplocos adenopus	5	1
Syzygium buxifolium	6	0
Wikstroemia nutans	6	0
Woodwardia japonica	15	5
Calypogeia arguta	25	7
Calypogeia tosana	10	2
Fissidens taxifolius	6	1
Isopterygium pohliaecarpum	37	13
Kurzia gonyotricha	6	0
Pallavicinia subciliata	5	0
Thuidium pristocalyx	11	3
Leucobryum bowringii	6	0

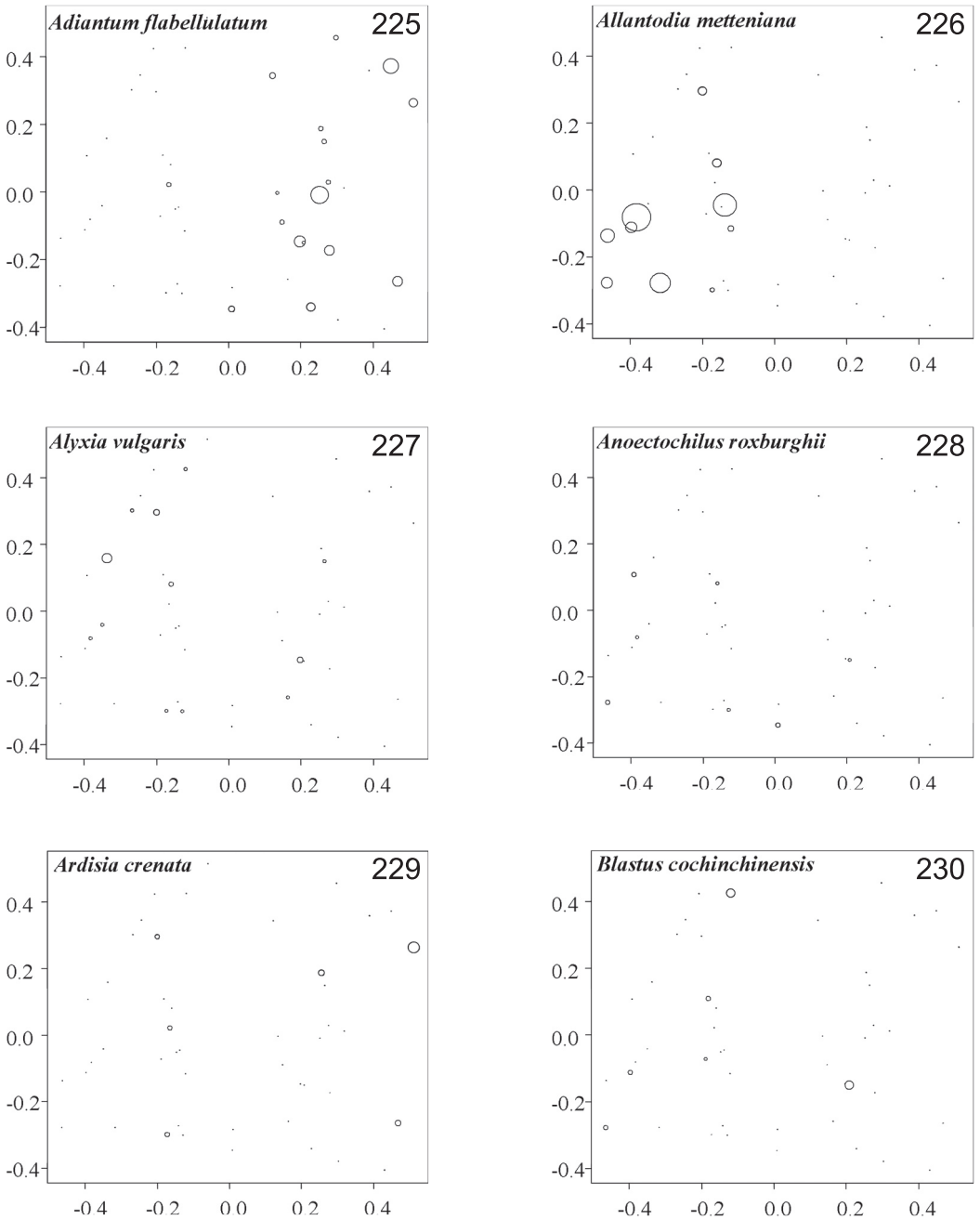

Figs 225–230. Liu Xi He: Distribution of species abundances in the GNMDS ordination of 46 plots (plots number 38, 47, 48 and 49 omitted), axes 1 (horizontal) and 2 (vertical). Frequency in subplots for each species in each plot proportional to circle size. Fig. 225. *Adiantum flabellulatum*. Fig. 226. *Allantodia metteniana*. Fig. 227. *Alyxia vulgaris*. Fig. 228. *Anoectochilus roxburghii*. Fig. 229. *Ardisia crenata*. Fig. 230. *Blastus cochinchinensis*. Small dots indicate absence; circles indicate presence, diameter proportional with subplot frequency.

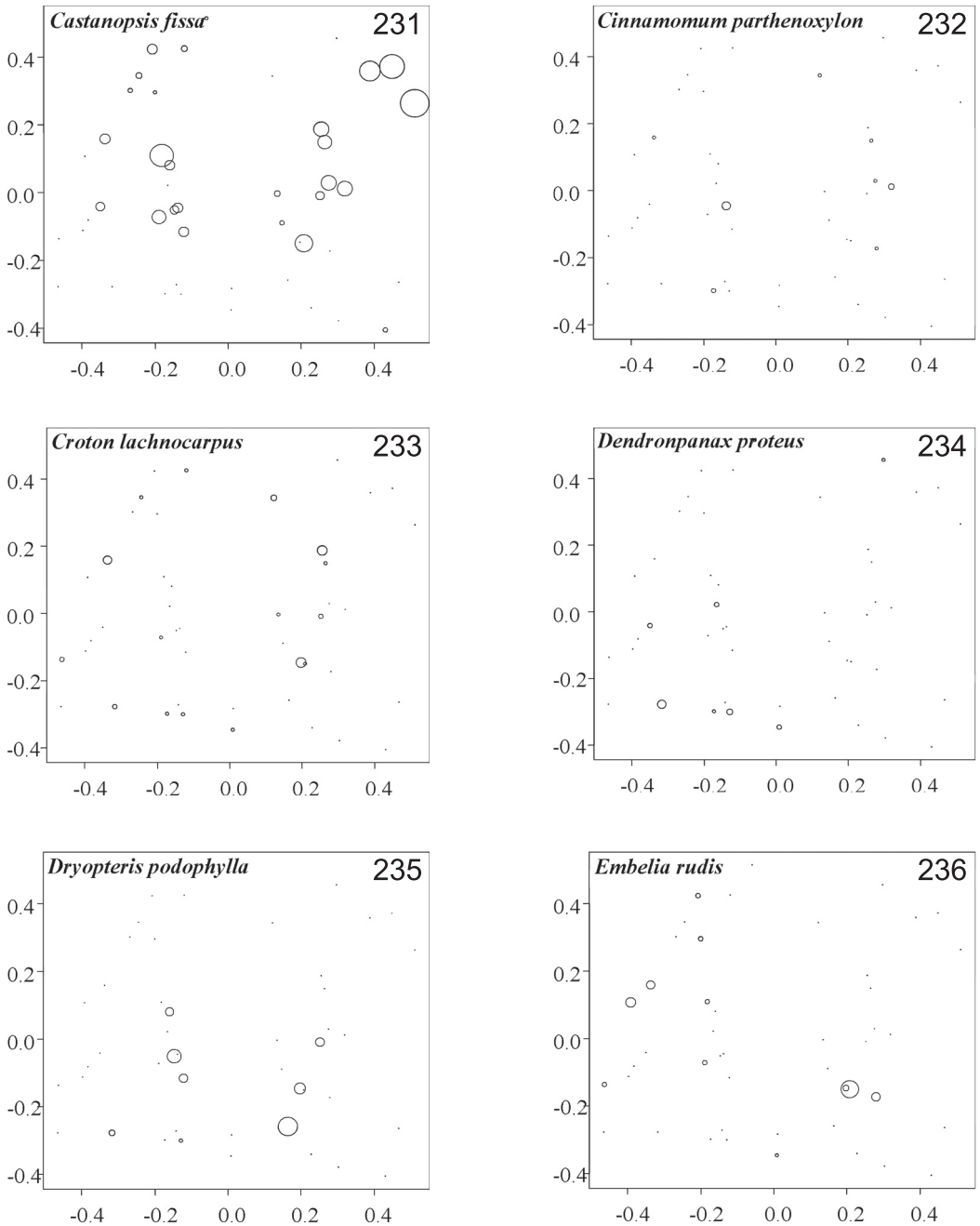

Figs 231–236. Liu Xi He: Distribution of species abundances in the GNMDS ordination of 46 plots (plots number 38, 47, 48 and 49 omitted), axes 1 (horizontal) and 2 (vertical). Frequency in subplots for each species in each plot proportional to circle size. Fig. 231. *Castanopsis fissa*. Fig. 232. *Cinnamomum parthenoxylon*. Fig. 233. *Croton lachnocarpus*. Fig. 234. *Dendronpanax proteus*. Fig. 235. *Dryopteris podophylla*. Fig. 236. *Embelia rudis*. Small dots indicate absence; circles indicate presence, diameter proportional with subplot frequency.

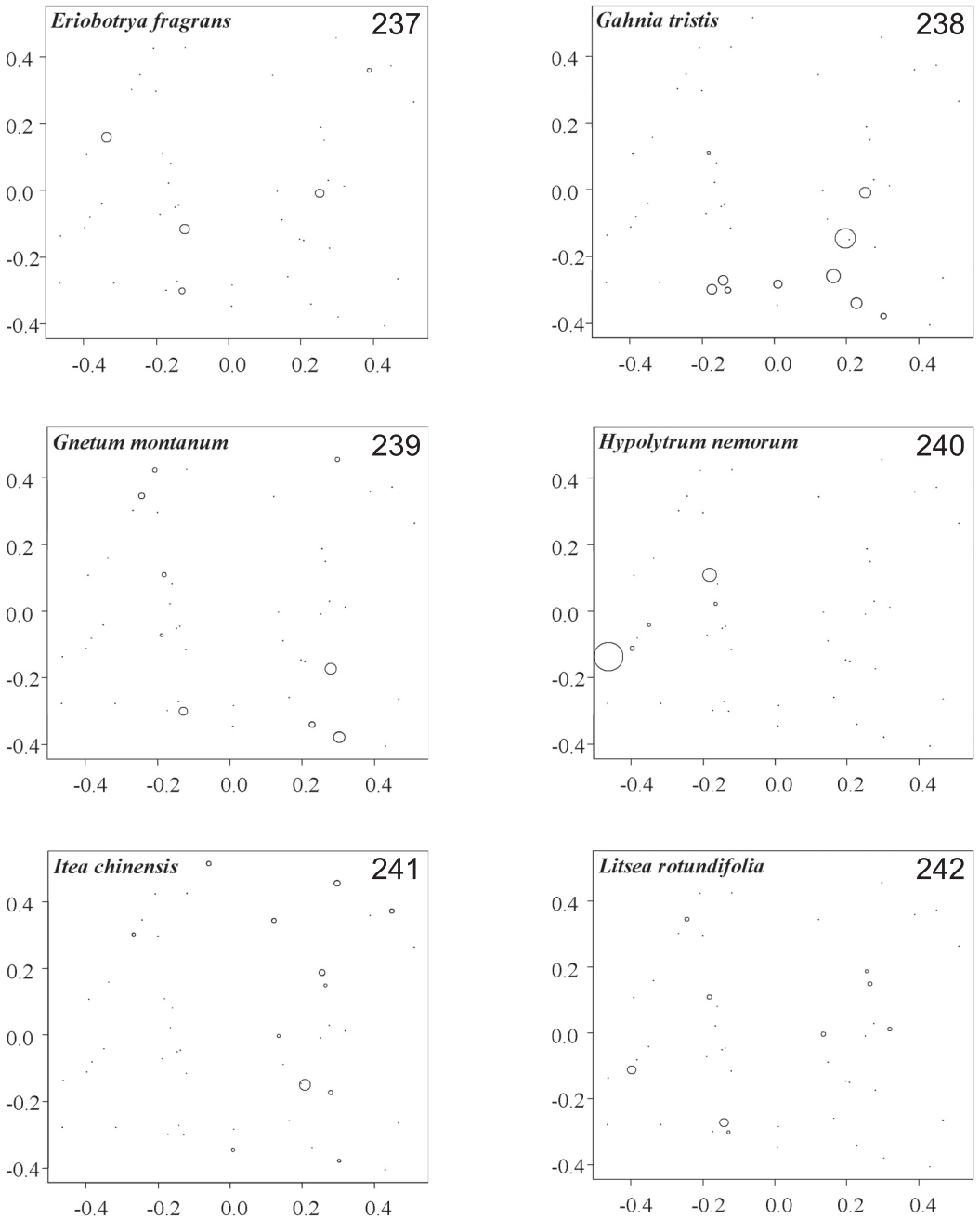

Figs 237–242.Liu Xi He: Distribution of species abundances in the GNMDS ordination of 46 plots (plots number 38, 47, 48 and 49 omitted), axes 1 (horizontal) and 2 (vertical). Frequency in subplots for each species in each plot proportional to circle size. Fig. 237. *Eriobotrya fragrans*. Fig. 238. *Gahnia tristis*. Fig. 239. *Gnetum montanum*. Fig. 240. *Hypolytrum nemorum*. Fig. 241. *Itea chinensis*. Fig. 242. *Litsea rotundifolia*. Small dots indicate absence; circles indicate presence, diameter proportional with subplot frequency.

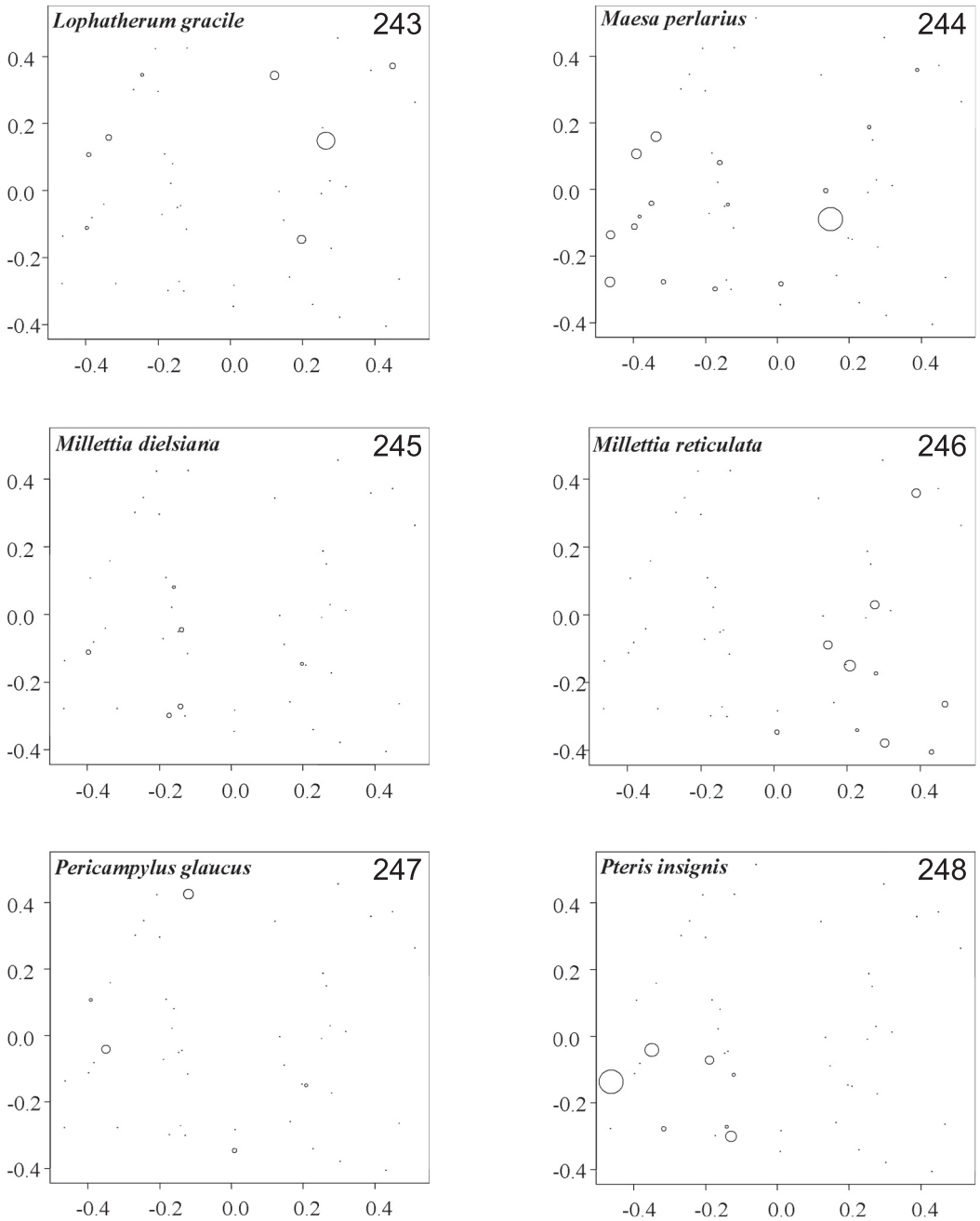

Figs 243–248. Liu Xi He: Distribution of species abundances in the GNMDS ordination of 46 plots (plots number 38, 47, 48 and 49 omitted), axes 1 (horizontal) and 2 (vertical). Frequency in subplots for each species in each plot proportional to circle size. Fig. 243. *Lophatherum gracile*. Fig. 244. *Maesa perlarius*. Fig. 245. *Millettia dielsiana*. Fig. 246. *Millettia reticulata*. Fig. 247. *Pericampylus glaucus*. Fig. 248. *Pteris insignis*. Small dots indicate absence; circles indicate presence, diameter proportional with subplot frequency.

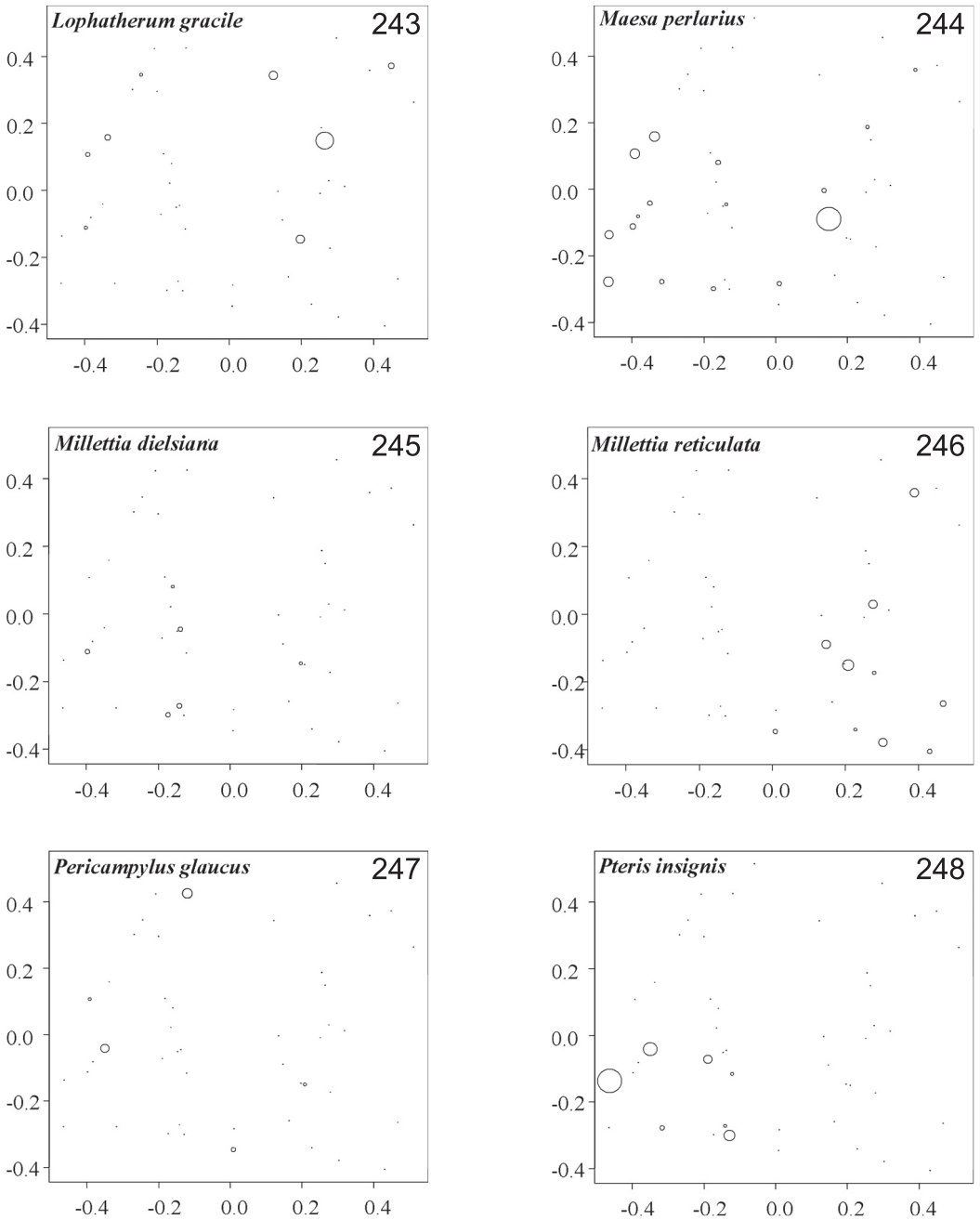

Figs 243–248. Liu Xi He: Distribution of species abundances in the GNMDS ordination of 46 plots (plots number 38, 47, 48 and 49 omitted), axes 1 (horizontal) and 2 (vertical). Frequency in subplots for each species in each plot proportional to circle size. Fig. 243. *Lophatherum gracile*. Fig. 244. *Maesa perlarius*. Fig. 245. *Millettia dielsiana*. Fig. 246. *Millettia reticulata*. Fig. 247. *Pericampylus glaucus*. Fig. 248. *Pteris insignis*. Small dots indicate absence; circles indicate presence, diameter proportional with subplot frequency.

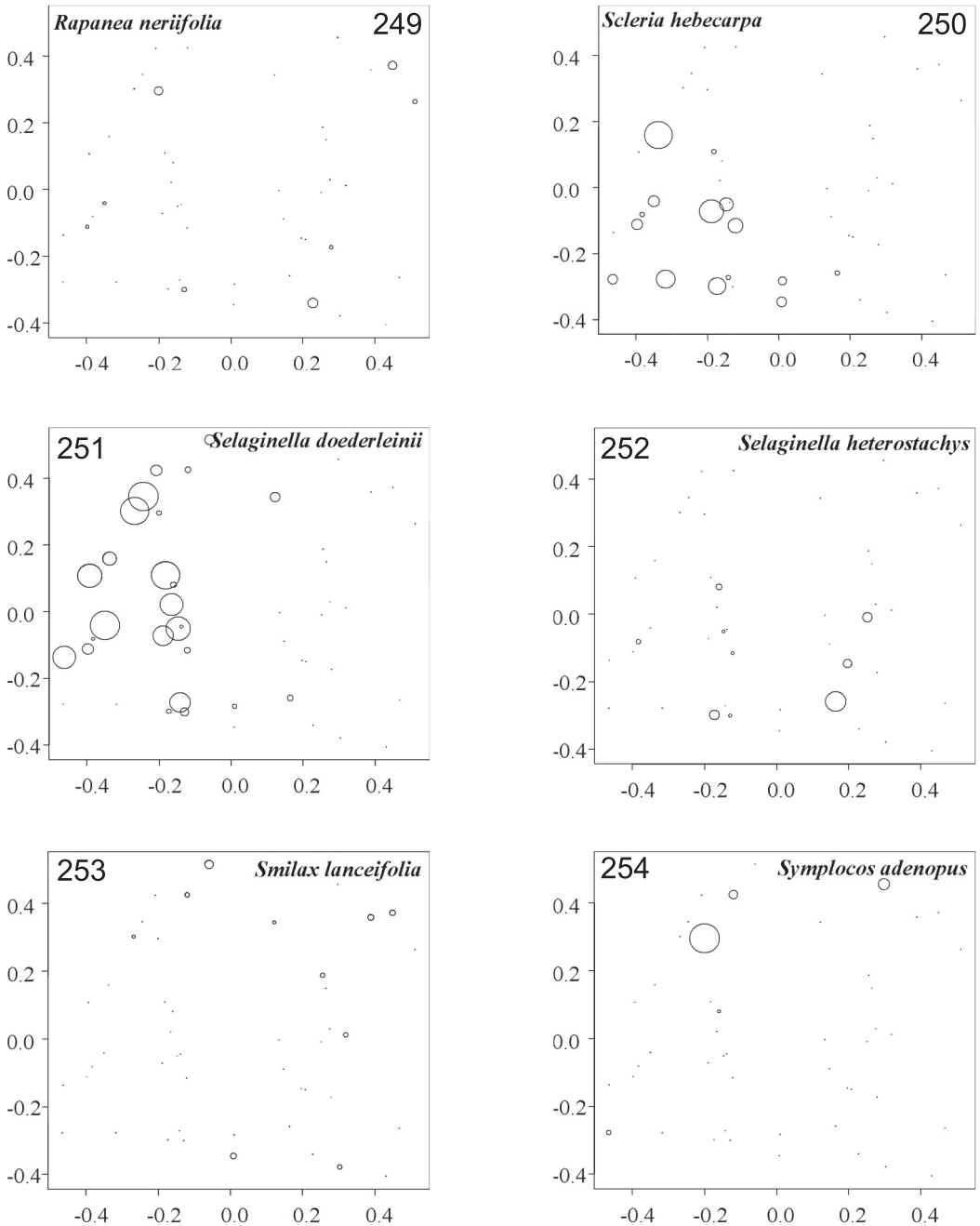

Figs 249–254. Liu Xi He: Distribution of species abundances in the GNMDS ordination of 46 plots (plots number 38, 47, 48 and 49 omitted), axes 1 (horizontal) and 2 (vertical). Frequency in subplots for each species in each plot proportional to circle size. Fig. 249. *Rapanea neriifolia*. Fig. 250. *Scleria hebecarpa*. Fig. 251. *Selaginella doederleinii*. Fig. 252. *Selaginella heterostachys*. Fig. 253. *Smilax lanceifolia*. Fig. 254. *Symplocos adenopus*. Small dots indicate absence; circles indicate presence, diameter proportional with subplot frequency.

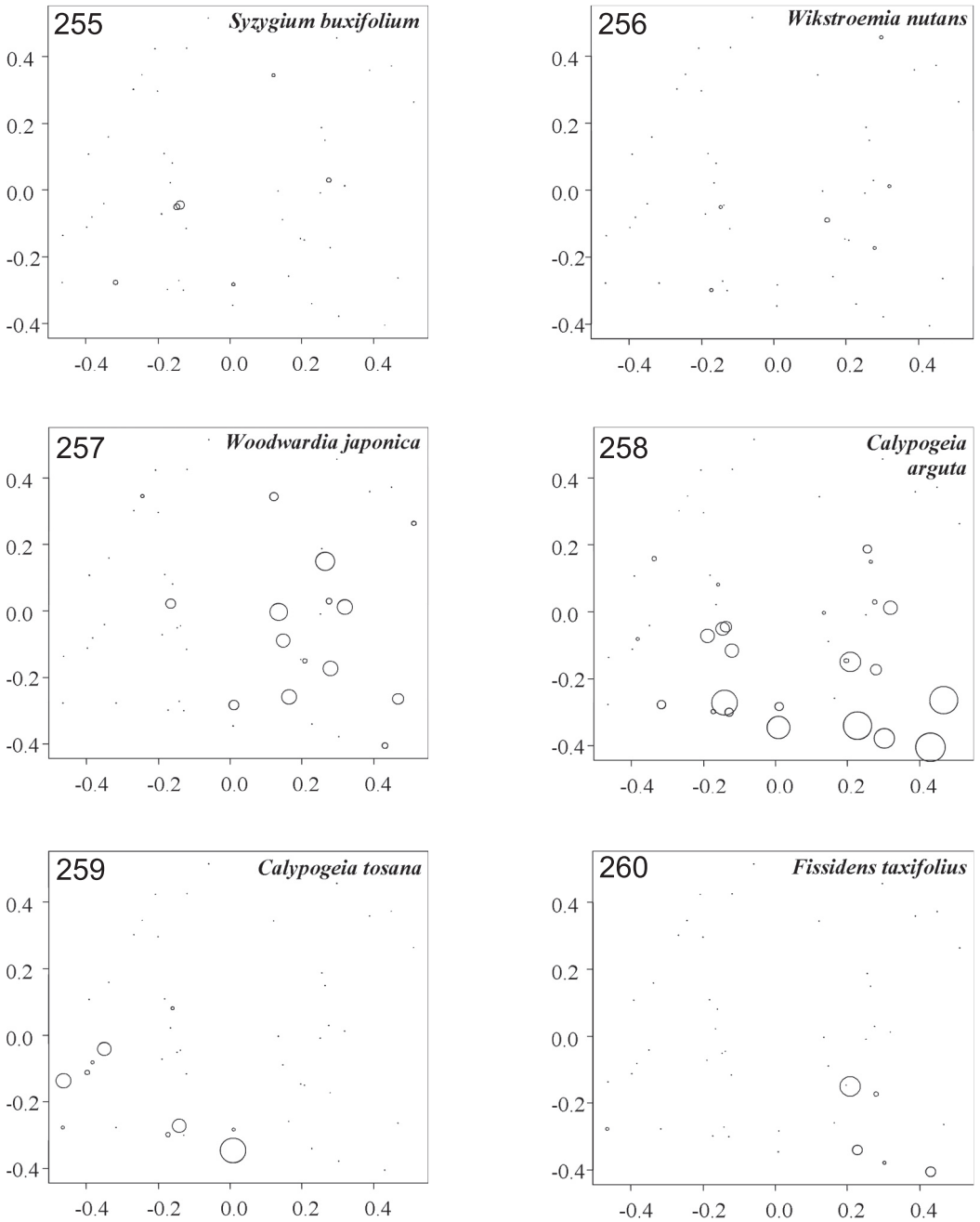

Figs 255–260.Liu Xi He: Distribution of species abundances in the GNMDS ordination of 46 plots (plots number 38, 47, 48 and 49 omitted), axes 1 (horizontal) and 2 (vertical). Frequency in subplots for each species in each plot proportional to circle size. Fig. 255. *Syzygium buxifolium*. Fig. 256. *Wikstroemia nutans*. Fig. 257. *Woodwardia japonica*. Fig. 258. *Calypogeia arguta*. Fig. 259. *Calypogeia tosana*. Fig. 260. *Fissidens taxifolius*. Small dots indicate absence; circles indicate presence, diameter proportional with subplot frequency.

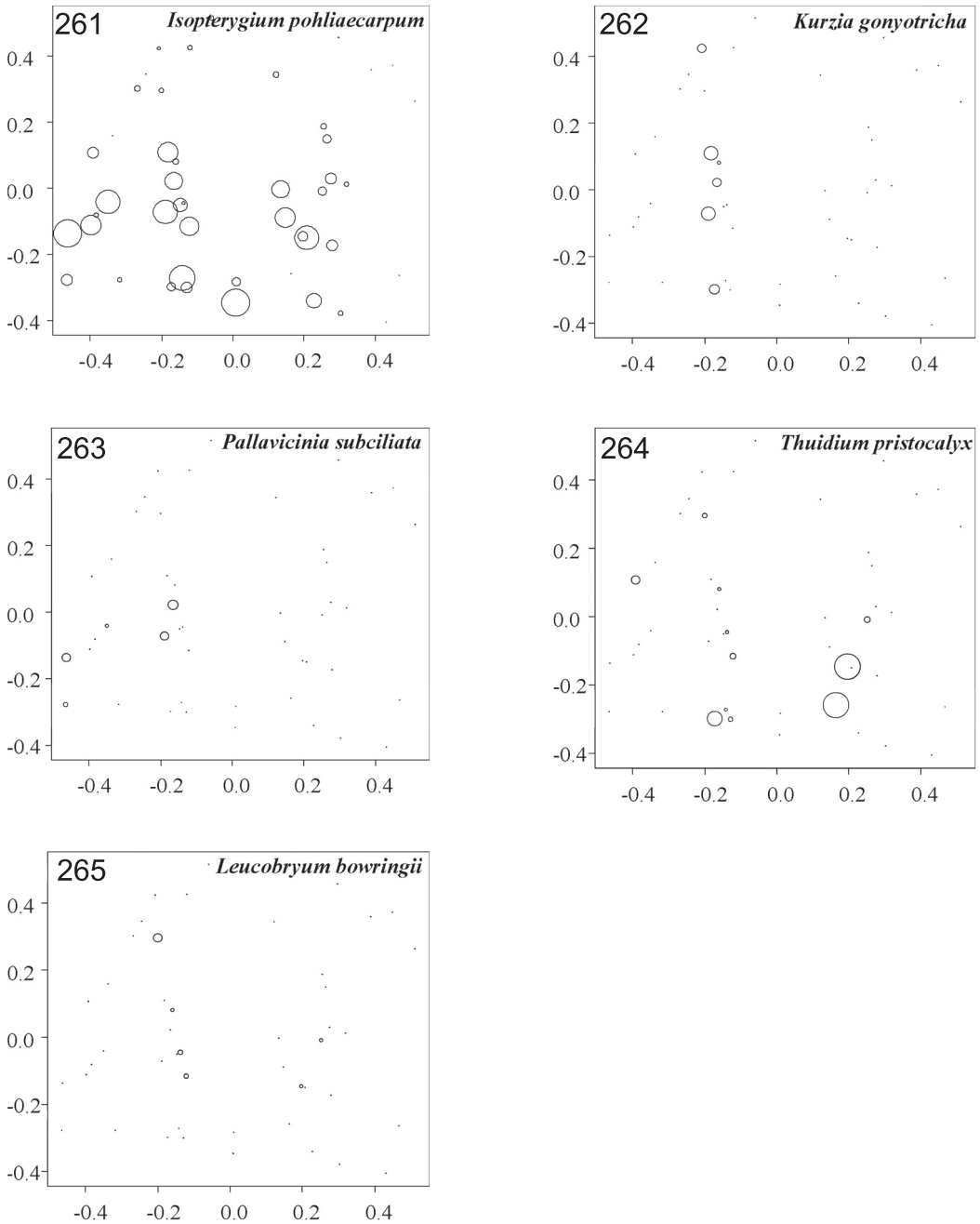

Figs 261–265.Liu Xi He: Distribution of species abundances in the GNMDS ordination of 46 plots (plots number 38, 47, 48 and 49 omitted), axes 1 (horizontal) and 2 (vertical). Frequency in subplots for each species in each plot proportional to circle size. Fig. 261. *Isopterygium pohliaecarpum*. Fig. 262. *Kurzia gonyotrichas*. Fig. 263. *Pallavicinia subciliata*. Fig. 264. *Trichosteleum mammosum*. Fig. 265. *Leucobryum bowringii*. Small dots indicate absence; circles indicate presence, diameter proportional with subplot frequency.

INTERPRETATION OF THE MAIN GRADIENTS IN EACH OF FIVE STUDY AREAS

The five study areas differed considerably with respect to which environmental complex gradient that was most strongly related to the main coenoclines (gradients in species composition as revealed by ordination). This difference between the areas is likely to be due to differences (1) in local environmental conditions; (2) with respect to regional, climatic, conditions (Tab. 1), and (3) in land-use history, tree-stand age, etc. (e.g. in LGS the forest may be older than in the other areas). The ecoclines (gradients in species composition and environment) identified by interpretation of the coenoclines obtained as *corresponding ordination axes* (p. 28–29) for the five study areas will be discussed in the discussion chapter.

TIE SHAN PING

GNMDS 1

The first coenocline (GNMDS 1) runs from sites with higher soil pH_{CaCl_2} and lower concentrations of Fe and H in soil, more varied soil surface topography, thicker litter to *vice versa* (Tab. 54). The first three variables all explain a considerable but non-significant fraction of the variation in plot scores at macro-plot scale (SSmacro > 27 %), and they are moderately correlated with GNMDS axis 1 ($0.23 < |\tau| < 0.30$). Furthermore, soil pH_{CaCl_2} and concentrations of Fe and H are negatively correlated (Tab. 10 and Figs 7–8). The isoline diagram (Fig. 20) shows considerable variation in H concentrations among plots similarly placed along this axis and soil pH_{H_2O} is unrelated to the axis as is also the concentrations of Ca, Al and other elements often related to pH. Significant split-plot GLM relationships with two environmental variables are observed (Tab. 54). Surface ruggedness at the 1-m^2 scale (variation in microtopography) explains a significant fraction of the variation in plot scores at macro-plot scale (SSmacro = 41 %), but is nevertheless likely to be ecologically non-significant as surface ruggedness at 1-m^2 in general reflects variation on a finer scale than between macro plots. Litter-layer depth explains a significant fraction of the variation in plot scores at plot scale (SSplot = 11 %), but the isoline diagram (Fig. 15) shows that litter-layer depth varies considerably between plots with similar positions along GNMDS 1 and that this variable is more strongly related to GNMDS axis 2. This suggests that the litter-layer depth is not the primary cause of this coenocline. We therefore consider this coenocline not clearly related to recorded environmental factors.

There is no strong change in species number along this coenocline (Tab. 15, 54), but two dominating vascular plants species, *Dryopteris erythrosora* (Fig. 30) and *Woodwardia japonica* (Fig. 49), were restricted to plots with low score for this axis and more or less absent from plots with high scores. A comparison of Figs 2, 9 and 50 reveals that macro plots in the eastern part of the study area (Nos 4, 6 and 7) have lower abundance of *Woodwardia japonica* and have higher scores along this axis than the remainder of plots. This accords with the result that most of the variation in plot scores is expressed at the macro-plot scale (c. 72 %). This coenocline therefore mainly expresses variation at scales in the range 25–250 m (Fig. 2).

The broad-scale pattern observed along this axis may suggest that historical factors, e.g. related

to land-use (macro plots with high scores are situated closer to the road and likely to be more impacted by land- use), are important. Until further information is available, *no ecocline interpretation* is presently possible for GNMDS 1.

GNMDS 2

The second coenocline (GNMDS 2) runs from concave sites with higher inclination, a thinner litter layer and more shallow soil, with prevalence of coniferous over deciduous trees, to *vice versa*. Relatively strong correlations and significant split-plot GLM relationships with seven environmental variables are observed (Tab. 54). The observed relationship between the axis and aspect favourability at the plot scale (also τ is very low) is likely to be ecologically non-significant as aspect favourability in general merely reflects variation on a broader scale. The isoline diagram Fig. 17 shows that the occurrence of deciduous trees is related to the axis in a complex way and Fig. 16 shows considerable variation in coniferous tree density between plots in similar positions along the axis. This suggests that the occurrence of trees is not the primary cause of this coenocline. Furthermore, correlations between soil depth, litter-layer depth and topographic variables are strong (Tab. 10 and Figs 7–8).

The strong decrease in bryophyte species number observed along this coenocline (Tabs 16 and 54), from 3–5(–7) at the low-score end of the axis to 0(–1) at the high-score end (Fig. 24) reflects the occurrence of eight plots highly unfavourable for bryophytes. Isoline diagrams (Figs 11 and 15) show that these eight bryophyte-devoid plots have an inclination of less than 10º and a litter-layer depth of 2–4 cm, while plots with bryophytes lack or have a very shallow litter layer and relatively high inclination. This indicates that occurrence of high bryophyte abundance and species number is conditioned on presence of steeper sites in which litter does not accumulate.

Almost equal variation in plot scores is expressed at the macro-plot and plot scales (c. 53 vs. 47 %). Strong relationships between plot scores and variables at both scales (note that the four litter-layer depth-topography variables all explain a considerable fraction of the variation in plot scores at both scales, although the variation is not in all cases significant; see Tabs 12 and 54) shows that this coenocline expresses variation over a wide range of scales from between plot within macro plots (1–10 m) to between macro plots (25–250 m, Fig. 2).

Available evidence unanimously identifies GNMDS 2 as a *litter-topography-related ecocline* with bryophyte exclusion by heavy litter accumulation on flat terrain as a prominent element.

GNMDS 3

The third coenocline (GNMDS 3) runs from sites with higher inclination, higher soil moisture and higher total N (and C) content at the macro-plot scale (c. 50 % of the variation along the axis is expressed at each scale) to *vice versa*, and from sites with higher surface ruggedness (ConvV1), lower soil depth, higher concentration of H in soil, higher soil aluminium saturation and lower soil dry matter content to *vice versa* at the plot scale (Tab. 54). Relatively strong correlations and significant split-plot GLM relationships with five environmental variables are observed (Tab. 54). Isoline diagrams (Figs 14 and 18–19) show considerable variability with respect to soil depth and variance of concavity/convexity at the 1-m^2 scale along GNMDS axis 3, and both of these variables are also related to GNMDS axis 2, but then mostly at the macro-plot scale. Furthermore, isoline diagrams (Figs 20 and 22) also show considerable variability with respect to the concentrations of H and aluminium saturation in soil along GNMDS axes 1 and 3, at the plot and macro-plot scales, respectively. This suggests that soil depths, the variance of concavity/convexity at 1-m^2, the concentration of H and aluminium saturation in soil are not primary causes of this coenocline.

Tab. 54. The basis for interpretation of the vegetation gradients in TSP (GNMDS axes): Kendall's correlation coefficient τ with strongly related environmental and species number variables, and split-plot GLM of plot scores: VEmacro = fraction of variation in plot scores attributed to the macro-plot scale; SSmacro = fraction of VEmacro explained by variation in the variable in question, at the macro-plot scale; SSplot = fraction of (1 – VEmacro) explained by variation in the variable in question, at the plot scale; relationships significant at $\alpha = 0.05$ level or $|\tau| \geq 0.30$ in bold-faced. Interpretation = judgment of the ecological importance of the observed relationship. Affiliation of environmental variables to group and abbreviation of names of environmental variables are shown in Table 2.

Axis	Strongly related variables in each group		τ	VEmacro	SSmacro	SSplot	Interpretation
1	Topography	ConvV1	–0.165	0.716	**0.410**	0.044	The coenocline is relatively strongly related to surface ruggedness (ConvV1) at macro-plot scale; relatively strongly related to litter-layer depth at plot scale; and moderately related to three variables related to soil acidity at the macro-plot scale; but no ecocline interpretation is possible for this axis
	Litter-layer depth	LitLDM	–0.094		0.048	**0.110**	
	Soil chemistry	pH_{CaCl_2}	–0.291		0.280	0.053	
		Fe	0.285		0.286	0.079	
		H	0.238		0.331	0.036	
2	Topography	Inclin	**–0.303**	0.531	0.257	**0.148**	The coenocline is strongly related to a complex gradient expressed at several scales, from convex sites with a higher inclination and a thinner litter layer to *vice versa*
		AspecF	0.135		0.150	**0.097**	
		ConvV1	–0.201		0.242	0.025	
		ConvS9	–0.294		**0.492**	0.089	
	Soil depth	SoilDM	**0.355**		**0.466**	0.072	
	Litter-layer depth	LitLDM	**0.408**		**0.537**	0.153	
	Tree influence	RelaCN	**–0.315**		0.326	0.065	
		RelaDN	0.077		0.016	**0.144**	
	Soil chemistry	Ca	–0.239		0.381	0.014	
		K	–0.216		0.288	0.036	
		BS	–0.205		0.343	0.001	
	Bryophyte species number	NBS	**–0.498**		**0.550**	**0.265**	Shows that the coenocline is followed by strong variation in bryophyte species number, on both scales
3	Topography	Inclin	–0.264	0.496	0.179	0.034	The coenocline is moderately related to inclination, soil moisture, total N and C content at macro-plot scale; moderately related to soil dry matter content at plot scale; and relatively strongly related to surface ruggedness (ConvV1), soil depth, concentrations of H and aluminium saturation in soil at plot scale. No ecocline interpretation is possible for this axis.
		ConvV1	–0.196		0.002	**0.191**	
	Soil depth	SoilDM	0.207		0.031	**0.113**	
	Soil moisture	SoilMLM	–0.259		0.249	0.045	
		H	–0.118		0.004	**0.100**	
	Soil chemistry	C	**–0.301**		0.248	0.041	
		N	–0.260		0.205	0.037	
		AlS	–0.004		0.160	**0.150**	
		WDM	0.223		0.097	0.088	

The organic matter (total C) content is relatively strongly correlated to GNMDS axis 3, while several variables often related to organic matter content, among others soil moisture and total N content (as well as several other variables, e.g. the crown cover index, and concentrations of Al and Mg in soil; see Tab. 14) explain about 25 % of the variation in plots scores expressed at the macro-plot scale and are moderately correlated with the axis ($0.25 < |\tau| < 0.30$). As for GNMDS axis 1, the variables related to this axis do not add up to logically coherent complex gradients and *no ecocline interpretation* is therefore at present possible for GNMDS 3.

GNMDS 1

The first coenocline (GNMDS 1) runs from sites with more convex micro topography with higher litter fall, lower number of broadleaved trees, higher crown cover index, a thicker organic layer, and a lower concentration of Mn in soil to *vice versa*, as shown by the relatively strong correlations and significant split-plot GLM relationships at the macro-plot scale (Tab. 55), at which most of the variation (c. 70 %) is expressed. Macro plots 1, 3, 4 and 6 occupy the high-score end of the axis. These macro plots are not geographically separated from macro plots with lower scores along the axis, indicating that variation along the axis is expressed at scales in the range 50–250 m (Fig. 3). The convexity at the 1-m^2 scale which explains a significant fraction of the variation in plot scores at macro-plot scale (SSmacro = 75 %), is however likely to be ecologically non-significant as convexity at the 1-m^2 scale in general reflects variation on a finer scale. The concentration of Mn in soil shows highest correlation with ordination axis but explains a insignificant fraction of the variation in macro-plot scale (c. 26 %). This suggests that the concentration of Mn in soil is not the primary cause of this coenocline. Isoline diagrams (Fig. 59–61) show relatively strong trends with respect to organic-layer depth, litter index and crown cover index along the axis, indicating that tree influence including organic-layer depth are important parts of the complex-gradient on which the coenocline depends. Sites with a well developed organic layer are mainly associated with relatively high tree density, higher crown cover, and dominance of coniferous rather than deciduous trees. No clear pattern of variation in species number, neither for vascular plants nor bryophytes, is observed along the axis (Tabs 24, 55).

GNMDS 2

The second coenocline (GNMDS 2) runs from sites with a thinner litter layer, a higher soil pH and lower concentrations of Fe and H in soil to vice versa (Tab. 55). The almost equal amounts of variation in plot scores expressed at the macro-plot and plot scales (Tab. 55) and the considerable variation in convexity at the 9-m^2 scale among plots that occupy similar positions along the axis, suggest that convexity at the 9-m^2 scale is not a primary cause of this coenocline even though it explains most of the variation in plot scores at the macro-plot scale.

A strong decrease in bryophyte species number, from 2–6 at the low-score end of the axis to 0–1 at the high-score end (Fig. 71) reveals a group of 11 plots highly unfavourable for bryophytes, and, to a minor degree for vascular plants as well (Tab. 25 and Fig. 70) at the high-score end of the axis. Figs 65 and 71 show that the 11 plots that make up this group of bryophyte-devoid plots are distinguished by a litter-layer depth of 4–7 cm, while the other plots which have bryophytes lack or have a very shallow litter layer. This indicates, like for GNMDS 2 in TSP, that the presence of a more or less thick litter layer, which is unfavourable to bryophytes, is decisive for this coenocline. Further similarities with the topography-litter ecocline in TSP is the relatively high fraction of variation in plot scores taking place at the plot scale, and that both litter-layer depth and bryophyte species number are the variables most strongly related to the axis at the plot scale. This indicates that variation in litter-layer depth is an important factor controlling bryophyte species occurrence at fine scales, and that factors controlling litter-layer depth also varies on scales broader than the macro plots.

The strong decrease in bryophyte species number along this coenocline is followed by a decrease also in vascular plant species number from 6–8 at the low-score end of the axis to 1–3(–5) at the high score end (Fig. 70). Isolines for soil pH_{CaCl_2} (Fig. 68) and the number of vascular plant

species (Fig. 70) in the GNMDS ordination shows that sites with higher soil pH also tend to have higher vascular plant species number (most plots with vascular plant species number ≥ 6 have soil pHCaCl2 higher than 3.1). This may indicate that GNMDS 2 consists of a gradient in soil acidity and element concentrations that determines favourability for vascular plants, running parallel with a gradient in litter-layer depth that determines favourability for bryophytes.

Common ecocline interpretation for GNMDS 1 AND GNMDS 2

The relationship of variables related to tree influence to both of GNMDS 1 and GNMDS 2 (Figs 57 and 62) opens for the possibility that the two coenoclines are related to one and the same complex of environmental gradients. Fig. 57 shows that this is indeed the case: most environmental variable vectors point towards the lower right or the upper left in the GNMDS ordination diagram, indicating that they are related to both of GNMDS axes 1 and 2. This complex gradient runs from open, low-grown deciduous forest or rather thickets in depressions with less acid soil to denser, conifer-dominated forests associated with high litter-layer depth. Examples of species restricted to plots in the lower right part of the GNMDS ordination diagram are *Dryopteris erythrosora* (Fig. 76) and *Calypogeia arguta* (Fig. 90). GNMDS 1 and GNMDS 2 express two different aspects of variation along this complex gradient; GNMDS 1 more related to forest density and tree-layer dominance at between macro-plot scales; GNMDS 2 more related to litter-layer depth and soil acidity at within macro-plot scales.

Thus, a joint interpretation of GNMDS axes 1 and 2 identifies one composite *tree influence-litter-soil acidity ecocline* in the LCG area, that has three components: (1) variation in total species composition and species number related to tree influence (and conifer dominance) at a broader scale (both macro-plot and plot scales); (2) variation in bryophyte species composition and species number related to litter mostly on within-macro-plot scales; and (3) variation in vascular plant species composition and species number most likely related to soil acidity and soil element concentrations as well as soil moisture on macro-plot scale.

LEI GONG SHAN

GNMDS 1

The first coenocline (GNMDS 1) runs from sites with favourable aspect, lower soil pH and mineral nutrient concentrations and a thicker litter/organic layer,, to *vice versa* (Tab. 56). Strong correlations and significant split-plot GLM relationships with 16 environmental variables are observed (Tab. 56), of which pH, Ca and Mg concentrations and base saturation are positively related to the axis and H, Al and Fe concentrations are negatively related to the axis as typical for strong soil acidity-mineral nutrient gradients. The isoline diagram (Fig. 103) shows considerable variation in organic-layer depth between plots in similar positions along the axis, suggesting that variation in soil organic matter is not the primary cause of this coenocline. Figs 98 and 102 show that plots from macro plot 4 which are almost devoid of litter and mostly with distinctly higher soil pH than other plots (Figs 104–105) and prominence of deciduous trees (Fig. 119) occupy the high-score end of this axis. Unlike coenoclines related to litter depth in TSP and LCG, bryophyte species number is not related to the coenocline, and plots in macro plot 4 are not richer in bryophytes than other plots showing that this coenocline does not parallel the litter-related ecoclines of those areas. This is probably mainly due to macro plots 4

Tab. 55. The basis for interpretation of the vegetation gradients in LCG (GNMDS axes): Kendall's correlation coefficient τ with strongly related environmental and species number variables, and split-plot GLM of plot scores: VEmacro = fraction of variation in plot scores attributed to the macro-plot scale; SSmacro = fraction of VEmacro explained by variation in the variable in question, at the macro-plot scale; SSplot = fraction of (1 – VEmacro) explained by variation in the variable in question, at the plot scale; relationships significant at $\alpha = 0.05$ level or $|\tau| \geq 0.3$ in bold-faced. Interpretation = judgment of the ecological importance of the observed relationship. Affiliation of environmental variables to group and abbreviation of names of environmental variables are shown in Table 2.

Axis	Strongly related variables in each group		τ	VEmacro	SSmacro	SSplot	Interpretation
1	Topography	ConvS1	**–0.300**	0.698	**0.748**	0.001	The coenocline is mainly expressed at macro-plot scale, running from sites with a higher amounts of litter fall, a lower number of broadleaved trees, and a higher crown cover index to *vice versa*
	Litter-layer depth	LitLDM	–0.221		0.147	0.064	
	Organic-layer depth	OrgaLD	–0.272		**0.621**	0.007	
	Tree influence	LitteI	–0.218		**0.630**	0.046	
		RelaCN	–0.208		0.080	0.074	
		RelaDN	**0.331**		0.289	0.056	
		CrowCI	–0.184		**0.669**	0.070	
	Soil chemistry	Mn	**0.350**		0.260	0.003	
2	Topography	ConvS9	0.210	0.495	**0.811**	0.001	The coenocline expresses variation at both scales, running from sites with a thinner litter layer, and a higher soil pH to *vice versa*
	Litter-layer depth	LitLDM	**0.349**		0.252	**0.126**	
	Tree influence	TreeIM	–0.053		0.101	**0.112**	
	Soil moisture	SoilMLM	0.048		0.072	**0.124**	
	Soil chemistry	pH_{H_2O}	–0.284		0.330	0.053	
		pH_{CaCl_2}	**–0.326**		0.351	0.086	
		Al	0.221		0.364	0.001	
		Fe	**0.344**		**0.407**	0.024	
		H	**0.319**		0.375	0.062	
		SO_4	0.243		0.164	0.035	
	Vascular plants species number	NVP	–0.267		**0.708**	0.003	Bryophyte and to a lesser degree also vascular plant species number decrease along the axis
	Bryophyte species number	NBS	**–0.533**		**0.411**	0.326	

has been over flooded during rain season.

The first coenocline (GNMDS 1) mainly separates NE and SE-facing macro plots 2–4 and 10 from macro plots 1 and 5–9 situated at the opposite, SW-facing slope (compare Figs 4 and 98). A strong, negative, relationship between aspect favourability, decreasing along this axis (Tab. 47) and vascular plant species number, increasing along this axis, is observed (Tabs 32 and 56). This suggests that aspect favourability is important for the observed variation in species composition represented by this coenocline, and that 'unfavourable' aspects are richer in vascular plant species.

Almost all the variation in plot scores (84 %; the highest fraction observed for any ordination axis in the five study areas) is expressed at the macro plot scale. This accords with the strong clustering of plots from the same macro plot in Fig. 101. High fraction of variation attributable to the macro-plot scale also accords with the result that the soil acidity-mineral nutrient variables strongly related to the coenocline all mostly explain variation in plot scores at the macro-plot scale (Tabs 30 and 56), while aspect favourability and litter variables explain relatively less variation at this scale.

A slight increase in vascular plant species number is observed along this coenocline (Tabs 32 and 56). Several vascular plant species like *Nothosmyrnium japonicum* (Fig. 134), *Pelea japonica*

Tab. 56. The basis for interpretation of the vegetation gradients in LGS (GNMDS axes): Kendall's correlation coefficient τ with strongly related environmental and species number variables, and split-plot GLM of plot scores: VEmacro = fraction of variation in plot scores attributed to the macro-plot scale; SSmacro = fraction of VEmacro explained by variation in the variable in question, at the macro-plot scale; SSplot = fraction of (1–VEmacro) explained by variation in the variable in question, at the plot scale; relationships significant at $\alpha = 0.05$ level or $|\tau| \geq 0.3$ in bold-faced. Interpretation = judgment of the ecological importance of the observed relationship. Affiliation of environmental variables to group and abbreviation of names of environmental variables are shown in Table 2.

Axis	Strongly related variables in each group		τ	VEmacro	SSmacro	SSplot	Interpretation
1	Topography	AspecF	**–0.409**	0.837	**0.402**	0.039	The coenocline is related to a complex gradient mainly expressed at the macro-plot scale, running from sites with favourable aspect, lower soil pH and mineral nutrients concentrations and a thick litter layer to *vice versa*
		HeatIn	**–0.413**		0.293	0.001	
		TerraM	–0.157		0.000	**0.122**	
	Litter-layer depth	LitLDM	**–0.405**		**0.482**	0.000	
	Organic-layer depth	OrgaLD	**–0.338**		0.395	0.021	
	Soil moisture	SoilMLM	–0.216		0.363	0.000	
	Tree influence	LitteI	–0.217		0.234	0.034	
		CrowCI	–0.283		0.374	0.008	
		RelaCN	–0.296		0.344	0.019	
	Soil chemistry	pH_{CaCl_2}	**0.498**		**0.752**	0.088	
		pH_{H_2O}	**0.482**		**0.703**	0.074	
		Al	**–0.448**		**0.633**	**0.135**	
		Fe	**–0.457**		**0.655**	0.057	
		H	**–0.475**		**0.762**	0.039	
		Ca	**0.448**		**0.659**	0.064	
		Mg	**0.400**		**0.522**	0.016	
		Na	**0.323**		**0.438**	0.000	
		K	0.248		0.300	0.007	
		C	–0.033		0.007	**0.114**	
		BS	**0.514**		**0.745**	**0.117**	
		AlS	**–0.487**		**0.721**	**0.127**	
		SO_4	–0.268		**0.558**	0.030	
	Vascular plants species number	NVP	0.206		0.028	0.181	Shows a slight increase in vascular plants species number along the gradient from low to high soil pH
2	Topography	Inclin	**–0.336**	0.615	0.312	0.000	The coenocline is relatively moderately related several environmental variables and mainly expressed at macro scale, running from more concave sites with a higher inclination and a higher number of broadleaved trees to *vice versa*
		ConvS1	**0.306**		**0.407**	0.000	
		ConvV1	–0.295		0.244	0.000	
		ConvS9	0.245		**0.622**	0.010	
		TerraM	–0.230		0.221	0.000	
	Soil depth	SoilDM	0.299		0.183	0.006	
	Soil moisture	SoilMLM	0.234		0.182	0.005	
	Tree influence	RelaDN	**–0.330**		0.193	0.000	
		TreeIM	–0.097		0.061	**0.145**	

(Fig. 139), *Rubia cordifolia* (Fig. 140) are restricted to plots with high GNMDS 1 scores, suggesting that the *ecocline reflects mainly the response of vascular plants partly to soil acidity and soil mineral nutrient concentrations and partly to topography and litter* which vary on the macro-plot scale (25–100 m; see Fig. 4).

GNMDS 2

The second coenocline (GNMDS 2) runs from concave, steeper sites to *vice versa* (Tab. 56). The isoline diagram (Fig. 119) shows that the inverse relationship of deciduous tree number to this axis is mainly due to occurrence of high number of deciduous trees in three plots from macro plot 4 (16, 18 and 19). Figs 116–118 show that the variation in inclination and terrain shape (convexity) among plots at similar positions along GNMDS 2 is strong. Even though inclination in general decreases along the axis and the terrain shifts from more concave to more convex, the plots that make up the extremes along the axis do not differ considerably with respect to inclination (Fig. 116) and fine-scale convexity (Fig. 117).

No strong change in species number takes place along this coenocline (Tabs 33 and 56) for which c. 61 % of the variation in plot scores is expressed at the macro-plot scale. The few variables related to GNMDS 2 and the inconsistent relationships observed between the axis and environmental variables make *no clear ecocline interpretation* possible for GNMDS 2. The axis may therefore probably represent minor variation in species composition related to macro plot or study-area specific causes.

CAI JIA TANG

GNMDS 1

The first coenocline (GNMDS 1) runs from less acid sites with higher base saturation on more convex surfaces with low inclination, to *vice versa* (Tab. 57). Relatively strong correlations ($|\tau| > 0.3$) and significant split-plot GLM relationships are observed with 11 environmental variables (Tab. 57), among others the heat index and organic-layer depth (positively related to the axis) and convexity at the 9-m^2 scale (negatively related to the axis). The variation in plot scores is mostly expressed at the macro-plot scale (c. 78 % of the variation; Tab. 57). The isoline diagrams (Figs 161–163 and 165–168) show relatively strong trends with respect to inclination, heat index, convexity and soil pH along the axis, while heat index and convexity deviate from inclination, soil acidity and related variables (Al, Fe and H concentrations) in explaining less variation at the macro-plot scale (Tab. 57). Fig. 168 shows that organic-layer depth varies but very slightly among plots. This indicates that GNMDS 1 is not primarily determined by organic-layer depth, heat index or convexity but expresses variation at the macro-plot scale (c. 50–400 m) related to soil acidity and topography. This also accords with the result that pH expresses the largest fraction of variation at the macro-plot scale and that the other soil acidity-related variables also express variation primarily at the macro-plot scale. GNMDS 1 separates macro plots to a large extent according to geographic position in the study area. The low-lying macro plots 1 and 2 (mainly included bamboos, no other trees and shrubs) and macro plots 5 and 6 in the middle part of the area (Figs 5 and 160) have low scores while the steep macro plots 7–10, situated at high elevations (Figs 5 and 164) and mostly having low soil pH (Figs 160 and 165) have high scores.

Vascular plants species number decreases slightly along this coenocline (Tabs 40 and 57). Several vascular plant species like *Rubus lambertianus* (Fig. 187) was restricted to plots in left part of the GNMDS ordination diagram, and *Deyeuxia arundinacea* (Fig. 179) and *Rhododendron simsii* (Fig. 186) were restricted to plots in the upper right part of the GNMDS ordination diagram. Bryophyte species number showed the opposite trend along this coenocline (Tabs 40 and 57, Fig. 175); several

Tab. 57. The basis for interpretation of the vegetation gradients in CJT (GNMDS axes): Kendall's correlation coefficient τ with strongly related environmental and species number variables, and split-plot GLM of plot scores: VEmacro = fraction of variation in plot scores attributed to the macro-plot scale; SSmacro = fraction of VEmacro explained by variation in the variable in question, at the macro-plot scale; SSplot = fraction of (1 – VEmacro) explained by variation in the variable in question, at the plot scale; relationships significant at $\alpha = 0.05$ level or $|\tau| \geq 0.3$ in bold-faced. Interpretation = judgment of the ecological importance of the observed relationship. Affiliation of environmental variables to group and abbreviation of names of environmental variables are shown in Table 2.

Axis	Strongly related variables in each group		τ	VEmacro	SSmacro	SSplot	Interpretation
1	Topography	Inclin	**0.390**	0.780	**0.515**	0.019	The coenocline is related to a complex gradient mainly expressed at the macro-plot scale, running from less acid sites with higher base saturation on more convex surfaces with low inclination to *vice versa*
		HeatIn	**0.323**		0.179	0.034	
		ConvS9	**−0.340**		0.318	0.054	
		TerraM	−0.288		0.259	0.032	
		ConvV1	−0.247		0.152	0.024	
	Organic-layer depth	OrgaLD	**0.353**		**0.446**	0.000	
	Tree influence	RelaCN	0.238		0.091	0.051	
	Soil chemistry	pH_{CaCl_2}	−0.250		**0.649**	0.040	
		Al	**0.403**		**0.421**	0.001	
		Fe	**0.425**		**0.454**	0.068	
		H	**0.350**		**0.444**	0.003	
		AlS	**0.417**		**0.458**	0.009	
		BS	**−0.330**		0.224	0.019	
		K	0.202		0.225	0.004	
		Mn	**−0.315**		0.268	0.041	
	Vascular plants species number	NVP	−0.261		0.293	0.000	Vascular plants species number slightly decreases along the gradient
	Bryophyte species number	NBS	**0.314**		**0.506**	0.027	Bryophyte species number increases along the gradient
2	Litter-layer depth	LitLDM	**−0.338**	0.342	**0.636**	0.056	The coenocline is related to a gradient mainly expressed at plot scale, running, from sites with a thicker litter layer to *vice versa*
	Organic-layer depth	OrgaLD	−0.219		0.157	0.018	
	Soil chemistry	H	0.209		0.048	**0.170**	
		Ca	−0.165		**0.408**	0.000	
		BS	−0.260		0.314	0.010	
	Vascular plants species number	NVP	0.285		**0.629**	0.008	Both bryophyte and vascular plant species number increase along the gradient
	Bryophyte species number	NBS	0.236		0.049	**0.144**	

bryophyte species like *Hypnum plumaeforme* (Fig. 191), *Isopteriygium fauriei* (Fig. 193), *Leucobryum juniperoideum* (Fig. 194) and *Trachycystis microphylla* (Fig. 196) were restricted to plots with high scores along GNMDS axis 1. Most likely, favourability for vascular plant species increases with increasing pH while favourability for bryophytes increases with increasing inclination (Fig. 161).

GNMDS 2

The second coenocline (GNMDS 2) runs from sites with a thicker litter layer and higher H and Ca concentrations to *vice versa*. The isoline diagram (Fig. 172) shows that the concentration of H in soil is mainly related to GNMDS axis 1 and that H varies strongly among plots with similar scores along

this axis, and Fig. 173 shows considerably variation in concentration of Ca in soil between plots in similar positions along the axis. This indicates that the concentrations of H and Ca in soil are not the primary causes of this coenocline.

Variation in plot scores is mostly expressed at the plot scale (c. 66 % of the variation in plot scores; Tab. 57) at which considerable increase in bryophyte species number along the coenocline is also observed (Tabs 41 and 57). Four bryophyte species, *Hypnum plumaeforme* (Fig. 191), *Isopteriygium fauriei* (Fig. 193), *Leucobryum juniperoideum* (Fig. 194) and *Trachycystis microphylla* (Fig. 196), were restricted to plots in the upper right part of the GNMDS ordination diagram. This indicates that this GNMDS 2 at least partly expresses increasing favourability for bryophytes towards sites with a shallower litter layer (Fig. 171), but Fig. 175 shows that bryophyte abundance is generally very low in this study area and a comparison of Figs 171 and 175 indicates that many plots with low litter-layer depth are also devoid of bryophytes. Furthermore, no clear relationship between bryophyte occurrence and litter-layer depth at the single-plot scale is observed, contrary to the TSP and LCG areas, and litter-layer depth deviates from bryophyte species number in explaining variation in species composition mainly at the macro-plot scale. Thus, although the axis expresses litter-related variation in bryophyte favourability, other factors are likely to be important for the response of bryophytes to GNMDS 2 in this area.

Vascular plant species number also increases considerably along GNMDS 2 (Tabs 41 and 57): several vascular plants species like *Dryopteris fuscipes* (Fig. 180) are absent from plots with high GNMDS 2 scores while others, e.g. *Lophatherum gracile* (Fig. 184), is absent from plots with low GNMDS 2 scores. The inverse relationship between vascular plant species number (Fig. 174) and litter-layer depth (Fig. 171), mainly expressed at the macro-plot scale, suggests that this litter-related ecocline is complex, with variation on several scales, affecting both bryophytes and vascular plants.

Common ecocline interpretation for GNMDS 1 and GNMDS 2

The relationship of soil pH-related variables to both of GNMDS 1 and GNMDS 2 (Figs 160, 165–168, 170 and 172) indicates that the two coenoclines are related to one complex of environmental gradients. Fig. 160 shows that this is indeed the case: most environmental variable vectors point towards the lower left or the upper right in the GNMDS ordination diagram, indicating that they are related to both of GNMDS axes 1 and 2. This complex gradient runs from less acid soil, thicker litter to more acid soil associated with high inclination. Typical examples of species restricted to plots in upper right part of the GNMDS ordination diagram are *Deyeuxia arundinacea* (Fig. 179), *Rhododendron simsii* (Fig. 186), *Hypnum plumaeforme* (Fig. 191), *Isopteriygium fauriei* (Fig. 193), *Leucobryum juniperoideum* (Fig. 194) and *Trachycystis microphylla* (196). GNMDS 1 and GNMDS 2 express two different aspects of variation along this complex gradient; GNMDS 1 more related to soil acidity and inclination at between macro-plot scales; GNMDS 2 more related to litter-layer depth at also between macro-plot scales.

Available evidence thus identifies one composite *soil acidity-litter-inclination ecocline* in the CJT area, that has three components: (1) variation in total species composition and species number related to litter, inclination and soil acidity on the macro-plot scale; (2) variation in vascular plant species composition and species number most likely related to soil acidity on a macro-plot scale; and (2) variation in bryophyte species composition and species number related to litter and inclination at both macro-plot and plot scales.

GNMDS 1

The first coenocline (GNMDS 1) mainly separates N- and E-facing macro plots 1–5, situated SW of the valley that runs from NW to SE through the study area, from macro plots 6–10 situated at the opposite, S- and W-facing slope (compare Figs 6 and 200). This is clear also from the c. 79 % of the variation in plot scores expressed at the macro-plot scale (Tab. 58). The two variables which most strongly reflect this macro-plot scale variation are aspect favourability and the related heat index (Tab. 58). Several variables related to this axis point to important ecological differences between the NE-facing low-score and SE-facing high-score macro plots: low soil moisture, higher importance of conifers, a thicker organic layer with higher organic matter content and higher concentrations of Mn and Ca in soil are typical of south- and westerly exposed slopes (Tab. 58). The isoline diagram (Fig. 209) does, however, show that organic matter content is related to the both GNMDS axes 1 and 2, and Figs 205 and 207–208 show that the organic-layer depth and concentrations of Mn and Ca in soil are related to the axis in a complex way. These suggest that organic matter content, organic-layer depth, and concentrations of Mn and Ca in soil are not the primary causes of this coenocline, which is interpreted as an ecocline mainly related to broad-scale *topography and coniferous tree density.*

Both of vascular plant and bryophyte species number decrease along this coenocline (Tabs 49 and 58). This indicates, like for GNMDS 1 in LGS, that the 'unfavourable' aspects are richer in species, especially for vascular plants. Typical examples of species concentrated to one of the slopes are *Allantodia metteniana* (Fig. 224) and *Selaginella doederleinii* (Fig. 250) restricted to plots in left part of the GNMDS ordination diagram, while *Adiantum flabellulatum* (Fig. 225), *Millettia reticulata* (Fig. 245) and *Woodwardia japonica* (Fig. 256) were restricted to plots in right part of GNMDS ordination diagram.

GNMDS 2

The second coenocline (GNMDS 2) runs from sites with higher inclination, drier soil and higher concentrations of Al, Mg and Na to *vice versa* (Tab. 58). The isoline diagram (Fig. 214) shows that the concentration of Al in soil is related to the axis in a complex way and Figs 215–216 show that concentrations of Mg and Na in soil varies but very slightly among plots. This suggests that none of these three element concentrations are primary causes of this coenocline. Fig. 212 shows that the soil moisture is mainly related to the both GNMDS axes 1 and 2, and that considerably variation exists in soil moisture between plots in similar positions along the axes. This suggests that soil moisture is not the primary causes of this coenocline either.

Bryophyte species number decreases strongly along this coenocline (Tabs 50 and 58, Fig. 224), from 3–4(–5) at the low-score end of the axis to 0–1(–3) at the high-score end (Fig. 224). All plots devoid of bryophytes (plots Nos 28, 41, 46 and 50) are situated in S- and W-facing slopes and Fig. 224 shows that bryophyte species number is related to both of axes 1 and 2 and independent of soil moisture since the vectors for the two variables are at right angles (Figs 212 and 224). Fig. 210 shows that the four plots devoid of bryophytes have low inclination [17–18(–23) degrees] compared to other plots. Furthermore, several bryophyte species like *Isopterygium pohliaecarpum* (Fig. 260) and *Calypogeia arguta* (Fig. 257) were abundant in most plots, but were absent from plots with high GNMDS 2 scores and that *Calypogeia tosana* (Fig. 258) was restricted to plots in lower left part of GNMDS ordination diagram. These patterns indicate that higher inclination, which is favourable to

Tab. 58. The basis for interpretation of the vegetation gradients in LXH (GNMDS axes): Kendall's correlation coefficient τ with strongly related environmental and species number variables, and split-plot GLM of plot scores: VEmacro = fraction of variation in plot scores attributed to the macro-plot scale; SSmacro = fraction of VEmacro explained by variation in the variable in question, at the macro-plot scale; SSplot = fraction of (1 – VEmacro) explained by variation in the variable in question, at the plot scale; relationships significant at $\alpha = 0.05$ level or $|\tau| \geq 0.3$ in bold-faced. Interpretation = judgment of the ecological importance of the observed relationship. Affiliation of environmental variables to group and abbreviation of names of environmental variables are shown in Table 2.

Axis	Strongly related variables in each group		τ	VEmacro	SSmacro	SSplot	Interpretation
1	Topography	AspecF	0.257	0.792	**0.412**	0.017	The coenocline is mainly due to variation at the macro-plot scale, separating macro plots sites with unfavourable aspect from macro plots with favourable aspect. Several variables, among others conifer dominance, soil moisture, organic-layer depth, and organic matter differs between plots from the two slopes
		HeatIn	0.296		**0.504**	0.046	
		ConvV1	0.057		0.010	**0.207**	
	Organic-layer depth	OrgaLD	**0.318**		0.354	**0.132**	
	Soil moisture	SoilMLM	–0.219		0.231	0.038	
		RelaCN	**0.338**		0.222	0.014	
	Soil chemistry	Mn	0.013		0.003	**0.301**	
		Ca	0.067		0.000	**0.218**	
		LOI	**0.341**		0.306	0.081	
		C	0.230		0.261	0.001	
		SO_4	0.281		0.277	0.001	
	Vascular plants species number	NVP	–0.274		0.123	0.071	Both bryophyte and vascular plant species number slightly decrease along the gradient
	Bryophyte species number	NBS	–0.245		0.146	0.040	
2	Topography	Inclin	**–0.326**	0.647	0.310	**0.114**	The coenocline is related to a complex gradient expressed at both scales, running from sites with a higher inclination to *vice versa*
		TerraM	–0.077		**0.476**	0.070	
	Tree influence	LitteI	–0.135		**0.516**	0.040	
	Litter-layer depth	LitLDM	0.196		0.210	0.030	
	Soil moisture	SoilMLM	0.238		**0.416**	0.056	
	Soil chemistry	Al	0.073		0.019	**0.120**	
		Mg	0.009		0.189	**0.172**	
		Na	0.086		0.110	**0.226**	
		N	–0.261		0.169	0.016	
		LOI	–0.225		0.200	0.000	
		WDM	0.219		0.179	0.002	
	Bryophyte species number	NBS	**–0.369**		**0.527**	0.055	Bryophyte species number strongly decrease along the axis
3	Topography	Inclin	–0.126	0.556	0.031	**0.176**	The coenocline is not consistently related to an interpretable complex gradient
		AspecF	**–0.354**		**0.444**	0.000	
		ConvV9	0.206		**0.448**	0.004	
		HeatIn	–0.288		0.396	0.100	
		TerraM	0.233		0.248	0.003	
	Soil chemistry	H	0.171		**0.861**	0.013	
		Ca	0.169		0.056	**0.130**	
		Na	0.098		0.004	**0.129**	
		SO_4	–0.277		**0.490**	0.004	
		C	–0.222		0.188	0.027	

bryophytes, is decisive for this coenocline. However, the variation in inclination (Fig. 210) along the axis is complex and inclination is not clearly related to variation in bryophyte species number along the axis (Fig. 224). Unlike other gradients with strong variation in bryophyte species number (cf. GNMDS 2 in the TSP, LCG and CJT areas), litter depth is less strongly related to variation along the axis in this case. A weak, positive, relationship between the litter-layer depth and this axis on one hand (Tab. 47) and bryophyte species number along this axis is, however, observed. This variation, like variation in bryophyte species number, is mostly but not exclusively expressed at the macro-plot scale (Tabs 47, 50 and 58) at which c. 52 % of variation in plot scores is expressed. We therefore interpret GNMDS 2 as *topography and litter related ecocline* mainly reflected in bryophyte species number and composition at several scales.

GNMDS 3

The third coenocline (GNMDS 3) runs from sites with a more smooth surface (low value for ConvV9), favourable aspect (but not separating N- and E-facing from S- and W-facing slopes the way GNMDS 1 does), lower concentrations of H in soil and higher SO_4 adsorption of the soil to *vice versa* (Tab. 58). The isoline diagram shows that the SO_4 adsorption and concentration of Na in soil are related both to GNMDS axes 1 and 3 (Figs 222–223); there is considerable variation in the surface ruggedness at 9-m^2 scale and concentration of H in soil between plots in similar positions along the axis (Figs 219–220) and the concentration of Ca in soil is also related to the axis in a complex way (Fig. 221). This suggests that neither of these factors are primary causes of this coenocline.

No strong change in variables of species number is observed along this coenocline (Tabs 51 and 58), for which c. 56 % of the variation is expressed at the macro-plot scale. Because the variables related to the axis do not add up to logically coherent complex gradients *no ecocline interpretation* is at present possible for GNMDS 3.

SUMMARY OF INTERPRETATION

In total, four more or less consistent ecoclines were found:

(1) A *litter-related ecocline* reflected in favourability for bryophytes, found as the second axis (GNMDS 2) in the four areas TSP, LCG, CJT and LXH and expressing variation on both the plot and macro-plot scales. In LGS, a coenocline was observed that was related to litter in a complex way, not paralleling the litter-related ecoclines of the other four areas.

(2) A *topography-related ecocline* reflected in variation for both vascular plants and bryophytes was found as the first axis (GNMDS 1) in the three areas LGS, CJT and LXH, and as the second axis (GNMDS 2) in two areas TSP and LXH. Variation along this ecocline is also expressed on both scales. Evidently, this ecocline contains an element of variation related to inclination reflected in favourability for bryophytes, and an element of variation related to aspect favourability reflected in favourability for both vascular plants and bryophytes (e.g. in LXH and LGS). Variation possibly related to topography but without a clear affinity to the ecocline found in the other areas was observed as GNMDS 2 in the LCG area where convexity at the 9-m^2 scale explains 81 % of ordination scores at the macro-plot scale.

(3) An *ecocline related to soil acidity and soil mineral nutrients*, expressed at the macro-plot scale. Relationships to soil acidity is observed in two areas along the first axis (LGS, CJT), and one

area along the second axis (LCG), in TSP as a slight relationship between the first GNMDS axis and pH. Relationships to soil mineral nutrients is observed in one area LGS, while in the other four areas only single or a few variables reflecting mineral nutrients or total C and N in soil show more or less strong or moderate relationships with main ordination axis although no clear soil mineral nutrient-related gradient occurred there.

(4) An *ecocline related to tree density*, with variation mainly at the macro-plot scale, is observed as the first axis (GNMDS 1) in two areas, LCG and LXH, as part of a main, complex, ecocline. This ecocline contains an element of variation related to both coniferous and broadleaved tree density in LCG, and an element of variation related to coniferous tree density in LXH.

Four out of 11 consensus ordination axes could not be interpreted ecologically by the environmental available variables. This may indicate that factors of importance differ from those that were thought of at the beginning of the study, which were mostly inherited from studies of boreal forest vegetation. This result also opens for the possibility that gradients in species composition may occur in Chinese subtropical forests which are not strongly related to environmental factors, but mainly shaped by historical factors or the effect of dominating or key species which strongly modify the habitat as experienced by other species.

Besides, soil moisture was measured in a different way than earlier studies. Sometimes we were unable to use the instrument, e.g. miss values in some of the more moist plots and in some of the stony plots. Soil moisture could be an important variable if we had correct measurements.

DISCUSSION

THE RELATIVE PERFORMANCES OF DCA, LNMDS AND GNMDS ORDINATION METHODS

Correlation coefficients calculated between corresponding axes of different ordinations and Procrustes analyses underpin each other, clearly demonstrating that LNMDS and GNMDS produce very similar ordinations. Furthermore, we find that GNMDS ordinations are generally more similar to DCA than are LNMDS although the agreement between all of DCA, LNMDS and GNMDS ordinations was generally good. In a situation when different methods produce similar results the choice between methods becomes less important but paralle use of the methods provides an opportunity to check that a consistent gradient structure is found (R. Økland 1996).

Our result that LNMDS and GNMDS ordinations based on the KYST algorithm (Kruskal 1964, Kruskal et al. 1973) produce closely similar results represents one of the very first thorough comparisons of these two widely used NMDS methods. This result also implies that a wide range of software applications are likely to produce ordinations that are more or less indistinguishable with respect to performance; the KYST algorithm is used in most or all of the popular NMDS software applications, including the vegan package (Oksanen 2007, Oksanen et al. 2007) of R freeware (Anonymous 2004a).

The comparison between GNMDS and DCA also show that although the two methods in most cases identify the same main coenoclines, flawed results are also occasionally produced. On the one hand, the fact that both GNMDS and DCA identify the same main gradients in most cases means that the choice among these two, which has been discussed with so strong emotions for twenty-five years, may be less decisive than often argued. On the other hand, the occasional failure (e.g. tongue-effect in DCA, polynomial distortion axes in GNMDS) of both of these two methods to extract the 'true' gradient structure suggests that the ultimate choice between them may matter.

Outlying plots occur both in DCA and LNMDS ordinations. Careful examination of the outlying plots reveals four points of interest: (1) DCA seems to be more sensitive than LNMDS and GNMDS to plots with deviating species composition. Our study demonstrates several instances of plots with somewhat deviating species composition that behave as outliers in DCA while not in LNMDS or GNMDS: e.g. in CJT plot number 5 with in total four species of which one with a idiosyncratic (species-specific) pattern (App. 5), in LXH plot number 38 with in total 11 species of which four with idiosyncratic patterns, plot number 47 with in total eight species of which three idiosyncratic, and plot number 49 with in total five species (App. 7). (2) LNMDS seems to be more vulnerable than GNMDS and DCA to plots with deviating number of species, as plots with strongly deviating number of species more regularly appear as outliers in LNMDS ordination: e.g. in LXH plot number 48 with in total three species of which two with idiosyncratic patterns (App. 7) and CJT plot number 5 with in total four species of which one idiosyncratic (App. 5). This sensitivity of LNMDS to plots which with low species number accords with findings of T. Økland (1996). (3) DCA seems to have a stronger tendency than LNMDS and GNMDS to identify as new outliers plots with a somewhat deviating species composition after outliers in the initial DCA ordination of the full data set (all plots) have been removed: e.g. in CJT plot number 4 with in total 11 species of which three with idiosyncratic patterns (App. 6). (4) GNMDS seems to be the method which is overall the least sensitive to plots with deviating species composition and species number among the three compared methods. Plots

with somewhat deviating species composition and species number that appear as outliers in DCA and LNMDS often do not appear as outliers in GNMDS (e.g. the CJT and LXH outliers referred to above). This may indicates, on the one hand, GNMDS ordination can avoid of influence from deviate plots, on the other hand, GNMDS ordination may ignore the true vegetation structure if deviate plots are the real with deviating species composition and species number.

The sensitivity of LNMDS to plots with strongly deviating species number may, at least partly, be an effect of the way rank-ordered floristic dissimilarities between plots are used in the ordination algorithm (Minchin 1987) while the sensitively of DCA to plots with deviating species composition may be due to the weighted averaging of plot scores with species abundances as weights in the DCA ordination algorithm (Hill & Gauch 1980, ter Braak & Prentice 1988), by which rare species are more heavily weighed. The difference between the methods can be exemplified by two ecologically similar plots, both having the same weighted average of species optima using species abundances as weights, but the first containing only half of the species occurring in the second (or the same species that all have low abundances in one plot and high abundances in the other). In DCA, these two plots will inevitably be placed at the same position along the ordination axis. LNMDS, however, will perceive these two plots as different (which they are, in terms of floristic dissimilarity, but not in terms of floristic composition as related to an underlying gradient) and try to separate them in the ordination by a distance that reflects the relative magnitude of the floristic dissimilarity from other plots.

The lower tendency of GNMDS than LNMDS to identify outlying plots is likely to result from the difference between GNMDS and LNMDS ordination algorithms. In GNMDS, overall goodness-of-fit (overall stress Φ) is calculated from one Shepard diagram based upon all dissimilarity and ordination-diagram distance values (except values disregarded a priori; none in our study). In LNMDS, the stress Φ_j is calculated in two steps; via Shepard diagrams (and stress values) obtained separately for each plot. Apparently, plots with a species composition that deviates somewhat from the rest influence overall stress more strongly in LNMDS than in GNMDS.

The term outlier refers to observations with a variable distribution that deviate so strongly much that of the other observations that its relationship with other observations appears to be poorly defined and one might suspect it to be generated by a different process. For those reasons, outlying observations are commonly discarded and new analyses carried out on the remainder of observations (R. Økland 1990, T. Økland 1996). However, our observation that plots may be identified as outliers by one method while not by another method indicates that the presence of outliers does not only reflect properties of the data as such but also properties of the ordination methods. We demonstrate that DCA is more sensitive to presence of rare species with idiosyncratic distribution on plots than GNMDS. This may mean that DCA better captures a real property of the data or that GNMDS better than DCA better manages to find structure in the data even if it weakened by occurrence of deviating single species. We cannot conclusively judge between these two viewpoints, although a contribution to sensitivity of DCA from the upweighing of rare species by implicit use of chi-square distances in the ordination algorithm (Minchin 1987) suggests that plots with outlying behaviour in DCA while not in GNMDS may not be 'real' outliers. Anyway, the different behaviour of DCA and GNMDS with respect to treatment of outliers is an additional reason why DCA and NMDS should always be applied in parallel. The fundamental differences between the two methods provide an opportunity for controlling if the gradient structure identified by the other method is appropriate (R. Økland 1996).

DCA suffers from two potential disadvantages (Minchin 1987). The first of these, the tongue-effect problem, implies that near one end of the first axis plot positions along the second axis (and axes of higher order) are concentrated around the mean plot score along this axis. The tongue effect is caused by the detrending algorithm of DCA (Minchin 1987, R. Økland 1990) which, instead of preventing the occurrence of spurious axes instead may distort relationships between axis-two positions and the true underlying complex gradient. The occurrence of tongues on the second axis in three

out of five DCA ordinations in our study [LGS (App. 4), CJT (App. 5) and LXH (App. 7)] is one of the main reasons why we did not choose DCA for ecological interpretation. The significance of the tongue effect is disputed, since there is no *a priori* way to distinguish a tongue arising because there is little variation in species composition along the second most important complex gradient near one end of the major complex gradient from a tongue arising because the underlying gradient structure has been distorted. The second potential disadvantage of DCA is that it assumes that the species response curves are unimodal and symmetrical (Minchin 1987) which is rarely the case with real data (R. Økland 1986a, b, Minchin 1989, Rydgren et al. 2003). Variation in response-curve shapes is an inevitable potential source of distortions in ordinations that are based upon a statistical model, which cannot be remedied by model improvement (R. Økland 1990).

Removal of outliers may to some extent reduce the tongue-effect problem as exemplified in CJT and LXH (Apps 5–8). On the other hand, non-linear rescaling as implemented in DCA provides robust estimates of compositional turnover (R. Økland 1990) and DCA may therefore produce ordinations that are good in the sense that the axes are scaled in units of compositional turnover, related to the major underlying complex gradients. Therefore, to use or not to use DCA for ordination of species-plot data is likely to remain an unsettled debate among ecologists.

Although not appearing in any NMDS ordinations in this study, a major general disadvantage of NMDS (both LNMDS and GNMDS) ordination methods is that polynomial distortion axes may appear although this does not seem to happen very often (R. Økland & Eilertsen 1993). R. Økland & Eilertsen (1993) and Rydgren (1993) attribute occurrence of polynomial distortion axes in NMDS to allowance of more dimensions for the ordination than there are real gradients in the data (also see Shepard 1974). Absence of curvilinear distortions in our NMDS ordinations also indicates that NMDS may be less sensitive to the variation in species response curves than DCA (Ruokolainen & Salo 2006). The apparent absence of curvilinear distortions in NMDS solutions in the present study suggests that correct (low) dimensionality is chosen for the NMDS by demanding that NMDS axes shall correspond to axes obtained by DCA. Thus, we demonstrate that the concept of corresponding ordination axes established in this study is also useful for determining correct dimensionality in NMDS.

We find for the plot scale that LNMDS axes are more strongly related to environmental variables than are DCA axes, while for the macro plot scale GNMDS axes were more strongly related to environmental variables than are DCA axes. This apparently supports the view of Faith et al. (1987), Minchin (1987, 1991) and Pitkänen (1997, 2000) that NMDS is somewhat superior to DCA in recovering main gradients in vegetation. However, many studies find the opposite result, that correlations with environmental variables are somewhat stronger for DCA than for NMDS. For instance, T. Økland (1996) show that DCA apparently recovers the variation in vegetation along the first ordination axis in ten boreal spruce forests in Norway, mostly corresponding to a complex-gradient in soil acidity and mineral nutrient availability, better than LNMDS 1. The Procrustes comparison of the performance of four ordination methods (CA, DCA, PCA, NMDS) on a complex vegetation data set by Ruokolainen & Salo (2006) exemplifies that metric scaling methods, particularly CA and DCA, may recover the main gradient much better than NMDS by quantitative comparison while non-metric scaling out-performed metric scaling by judgments by graphical criteria. The now quite numerous studies in which the performances of these ordination methods have been compared by parallel use on the same data do not give a clear answer to the general question which family of methods as globally best, NMDS or DCA. This may imply that with selected realistic models, the relative performance of DCA and NMDS is dependent on properties of the data set (R. Økland 1990).

Ordination serves a hypothesis generating purpose, to extract gradient structure in vegetation data sets with unknown structure (R. Økland 1990). A good ordination method therefore has to be flexible with respect to its handling of realistic variation in data properties (R. Økland 1990). No consensus so far exists with respect to the relative merits of the best variants in each family of ordination

methods. Our results show that the compared ordination techniques, DCA, LNMDS and GNMDS, are all mostly able to extract the (same) main gradient structure from multidimensional species spaces, but our results also reveal that the methods differ with respect to emphasis on different data-set properties. DCA is generally more similar to LNMDS than to GNMDS. DCA seems to be sensitive to plots with deviating species composition and often displays a clear tongue effect. LNMDS appears to be vulnerable to plots with deviating number of species. GNMDS seems to be overall less sensitive to plots with deviating species composition and species number than DCA or LNMDS. We conclude that none of the compared ordination methods may guarantee extraction of the major gradient of a data set. The tendency of DCA and NMDS methods normally to produce quite similar results does, however, suggest that the long controversy over which is best might now be replaced by recognition that methods of the two families should be used in parallel to supplement each other in a strategy for ensuring that a reliable consensus ordination is found (R. Økland 1996).

The ideal ordination method has so far not been developed, and it still remains open if there are opportunities for further methodological improvements (R. Økland 1990). As for the DCA concept, the potential for further developments are small because heuristic *a posteriori* corrections of symptoms that the model is wrong will always be at risk of producing new distortions (like in the case of detrending by segments in DCA). Over the last decade, use of NMDS has increased on the expense of DCA (Palmer 2000). With respect to GNMDS, options now implemented in vegan (Oksanen et al. 2007) for omission of unreliable dissimilarities and step-across by flexible shortest path (Williamson 1978) or extended dissimilarities (De'ath 1999) provide interesting developments that deserve thorough testing. Furthermore, NMDS methods like the Semi-strong Hybrid Scaling (SHS) (Belbin 1991, 1993a, 1993b) and Hybrid Multidimensional Scaling (HMDS) (Faith et al. 1987), which have previously been shown to perform well but have never been thoroughly tested, should be compared with GNMDS. Thus, considerable opportunities for improvement of NMDS ordinations may still exist.

THE MAIN ECOCLINES IN SUBTROPICAL FORESTS IN SOUTH AND SOUTH-WEST CHINA

Interpretation of GNMDS ordinations of understorey plant species composition in the five Chinese subtropical forests studied reveals that compositional gradients depend on four major underlying complex environmental gradients: litter-layer depth, topography, soil acidity/soil mineral nutrient concentrations and tree density. These four ecoclines have variation in vegetation at the between macro-plot scale (linear scale 25 m and broader), but some variation between plots within macro plots (linear scale below 10 m) is also evident. The four gradients will be considered one by one in order of decreasing overall importance to the studied forests.

The ecocline related to litter-layer depth

By modifying micro-environmental conditions, leaf litter may affect the distribution of individuals of different species. Litter distribution is considered a major structuring force in many ecosystems (Carson & Peterson 1990, Foster & Gross 1997). In our study, a litter-related ecocline reflected in favourability for bryophytes is found in the four areas TSP, LCG, CJT and LXH. It is mostly expressed both on the between and within macro-plot scales although the operating mechanism

(exclusion of bryophytes by heavy litter cover) operates on fine scales (T. Økland 1988, Barik et al. 1992, Marsh & Pearman, 1997, Magura et al. 2005). However, when litter layer properties are more or less homogeneous over areas larger than the macro plot [e.g. due to topography (low inclination), dense tree stands, etc.), variation related to this ecocline may express itself on broader scales. In LGS, a litter-related coenocline appears that is not clearly reflected in variation in bryophyte species composition and species number. This demonstrates that sets of variables related to this and related ecoclines may vary to some extent among areas.

Litter-layer depth is usually affected by terrain conditions and topographic positions. This is typically exemplified by the LCG study area, in which particularly sparse litter layers occur in the very steep macro-plot 6 and in the nearly flat macro plot 4 where litter is recurrently removed after heavy rain by flooding of the adjacent small river. Our results are thus consistent with earlier findings that the litter-layer depth is dependent on topography, such as inclination (Dwyer & Merriam 1981, Orndorff & Lang 1981, T. Økland 1988), aspect (Dwyer & Merriam 1981, Orndorff & Lang 1981), treefall pit and mound complexes (Beatty & Sholes 1988). In LGS and LCG we also observe a positive relationship between litter-layer depth and tree influence (e.g. tree density and dominance of coniferous trees) while litter-layer depth is negatively related to density of coniferous trees in TSP. In general, more litter tends to accumulate below trees than between trees in sites with more or less homogeneous topography (e.g. low inclination and smooth surface; Barik et al. 1992, Ostertag 1998) and strong relationships usually exist between tree influence variables and litter-layer depth (as we observe, notably in LGS). In general litter affects e.g. the occurrence of bryophytes and other species as seen in our study. The effect of trees on litter distribution is, however, modified by surface topography. In sites with a convex surface and high inclination (like TSP sites dominated by coniferous litter), litter is redistributed even from below dense coniferous tree stands.

The positive relationships between litter-layer depth and aspect favourability and heat index in the two areas TSP and LCG suggest that litter decomposition may decrease towards very dry sites. Reduced microbial activity in drier sites may, at least partly, explain the negative relationship between soil pH and litter-layer depth in LGS. Furthermore, this demonstrates why litter-layer depth in some areas contribute to a more comprehensive complex-gradient that also includes environmental variables like soil pH and soil mineral nutrients, e.g. in LGS.

Litter-layer depth clearly affects bryophyte species distributions. Our results consistently show that in the studied Chinese subtropical forests high abundance/high species number for bryophytes is mostly restricted to steep plots or at other sites were litter fails to accumulate (TSP, LCG, CJT and LXH). Typical examples of bryophyte species with wide ecological amplitude that are abundant in most plots except plots from sites with low inclination and a thick litter layer are *Taxiphyllum subarcuatum* (Fig. 54) and *Leucobryum bowringii* (Fig. 53) in TSP; *Brotherella henonii* (Fig. 89) and *Taxiphyllum subarcuatum* (Fig. 95) in LCG; *Hypnum plumaeforme* (Fig. 191), *Isopteriygium fauriei* (Fig. 193), *Leucobryum juniperoideum* (Fig. 194) and *Trachycystis microphylla* (Fig. 196) in CJT; and *Isopterygium pohliaecarpum* (Fig. 260) in LXH. The effect of litter is probably one of the most important factors regulating bryophyte species composition in forests (Sydes & Grime 1981, Xiong & Nilsson 1999). The possible mechanisms responsible for the negative relationship between presence of a litter layer (which is conditioned on terrain topography) and bryophyte performance are that: (1) a thick, persistent litter layer will inhibit the development of a vigorous bryophyte layer (Wheeler & Giller 1982; van Tooren et al. 1988), physically and by heavy shading (Sveinbjörnsson & Oechel 1992, Xiong & Nilsson 1999); (2) a thicker litter prevents light and moisture supply, therefore brings death of moss individuals and hinders establishment of recruitments; (3) Toxins, e.g. tannis and polyphenols, are important modifiers of leaf-litter decomposition (Swift et al. 1979) and are probably also toxic for some bryophytes in close contact with the litter (Weibull 2001); and (4) litter-decomposing fungi sometimes appear to have a detrimental effect on litter-covered bryophytes

(Weibull 2001).

This study confirms the results of T. Økland (1988) from beach forest, and of Pausas (1994), R. Økland (1995b, 2000) and Weibull (2001), who have found that the negative impact of the increasing amount of litter from coniferous trees on bryophytes. Herbaceous litter has been shown to have a positive effect on bryophyte growth (Rincon 1988, 1990), probably because of the increase in nutrient availability (Bates 1994). Tarkhova & Ipatov (1975) identified both positive and negative effects from coniferous-needle litter on five common boreal forest floor bryophytes, while Sydes & Grime (1981) showed the negative impact of the increasing amount of litter from deciduous trees on *Mnium hornum*. Except the litter cover ground which prevents bryophytes to establish, these may also indicate that the canopy tree species and the throughfall chemistry and chemical composition of leaf litter are the important factors explaining the variation in bryophyte species composition (Weibull 2001). In the present study litter-related ecoclines that mainly occurred in acidic coniferous dominating forests. In relatively pristine area LGS, one reason for no clear litter-related ecocline could be due to a relatively high soil pH, while in LXH, weak relationships between litter-layer depth and bryophytes are probably because of relatively high precipitation and broadleaved dominating forests. The litter decomposing is probably very fast in LXH. These results are also to some extent supported by Saetre (1999) who suggested that relatively low precipitation and the coniferous litter had a negative influence on the species.

The topography-related ecocline

Our results show that the most important coenocline in subtropical mixed broadleaf and coniferous forests is related to a complex-gradient in topography, at both macro plot and plot scales. This is demonstrated by a topography-related ecocline reflected in variation both in vascular plant and bryophyte species composition in four areas (TSP, LGS, CJT and LXH), related to inclination in three areas (TSP, CJT and LXH) and aspect favourability and heat index in two (LGS and CJT). Although the species that make up these coenoclines and the environmental variables that contribute to the underlying complex gradients differ strongly among areas, the relationships between topographic variables and ordination axes consistently tend to be the strongest observed in our study. Only in one area, LCG, no clear topography-related ecocline is found. In that area, however, convexity at the 9-m^2 scale explains 81% of the variation at the macro-plot scale (the highest value encountered for a single variable), indicating that topography is generally important for the variation in species composition in S and SW Chinese subtropical forests.

Topography variables (e.g. inclination, aspect favourability, terrain conditions etc.) are indirect gradients in the terminology of Austin (1980), but nevertheless play an important role in the variation of stand structure of mountain forests (e.g. Schimel et al. 1985, Zak et al. 1991, Brubaker 1993, Enoki et al. 1997). Topography may, however, influence species distribution patterns more or less directly, in a physical way (Foster 1988, Hunter & Parker 1993). Microhabitat heterogeneity affects the distribution of plant species by providing microhabitats suitable for bryophytes and thus enhancing diversity in forests (Masaki et al. 1992, Condit et al. 2000, Yamada et al. 2000, Takyu et al. 2002, Enoki 2003). The strong relationship between the topographic variable inclination (topographical position) and bryophyte species number along ordination axes observed in TSP, CJT and LXH reflects that higher inclination often brings about a thinner litter layer which is favourable to bryophytes (previous section on the ecocline related to litter depth). Thus, the previous ecocline related to litter depth can also make up one facet of a very complex ecocline related to topography.

Another, quite different facet of topography-related variation is due to variation in aspect, as observed in LGS and LXH. In the studied SE Chinese subtropical forests low-radiation slopes [‘un-

favourable' aspects in the terminology of R. Økland & Eilertsen (1993) and T. Økland (1996)] are richer in species and have higher soil moisture than sunny southern and western slopes, indicating that the latter may become too dry for many species too maintain stable populations. This is exemplified by the relatively pristine area LGS with low pollution loads in which a topographic gradient extends from sites with south-westerly aspect and high incoming radiation, dominated by 'sun plants' like *Rubus malifolius* (Fig. 142), and large bryophyte species like *Rhyncostegium pallidifolium* (Fig. 151) and *Rhyncostegium contractum* (Fig. 152), to northeast-facing sites dominated by 'shade plants' like *Nothosmyrnium japonicum* (Fig. 134), *Pelea japonica* (Fig. 139), *Rubia cordifolia* (Fig. 140), and small bryophytes species like *Brychythecium pulchellum* (Fig. 143) and *Plagiominum acutum* (Fig. 149). Similar trends are found also in LXH in which topography-related variation extends from south-westerly facing sites with high incoming radiation dominated by drought-tolerant vascular plants like *Adiantum flabellulatum* (Fig. 225), *Millettia reticulata* (Fig. 245) and *Woodwardia japonica* (Fig. 256) to sites with facing north and east dominated by vascular plant species like *Allantodia metteniana* (Fig. 224) and *Selaginella doederleinii* (Fig. 250). Furthermore, a slight increase in vascular plants species number along this coenocline is observed in both areas (Tabs 56 and 58). These observations are consistent with patterns observed for subtropical forests in southern Taiwan (Chen et al. 1997) and experiments in an old-growth subtropical evergreen broad-leaved forest in south-western Japan (Ito et al. 2004) also showed that the distributions of most species were influenced by topography. Furthermore, this accords with the result of Zhao et al (2005) that altitude is the main factor affecting the spatial pattern of plant species diversity on Mt. Shennongjia, central China because temperature decreases with altitude.

Our results suggest that vegetation pattern related to soil surface topography may actually arise by action of many alternative causal factors that operate on non-uniform soil surfaces: drainage, water availability, leaching, mineral nutrients supply, acidity (pH) and variation in litter cover. In fact, topographic variables are more or less strongly related to soil chemical and physical variables in all our five study areas. This supports the general view that some of the variation in soil properties within a defined climatic region may result from topographic heterogeneity (Huddleston & Riecken 1973, Daniels et al. 1987, Honeycutt et al. 1990, Feldman et al. 1991, Brubaker et al. 1993). Notably, vegetation gradients related to 'aspect favourability' tended also to be related to soil pH and soil mineral nutrients concentrations (cf. T. Økland 1996)). For instance in LGS the ecocline related to topography runs from a dry, acid site poor in mineral nutrients to a mesic, less acid richer site.

In CJT, the topography gradient extends from sites with low inclination dominated by vascular plant species like *Rubus lambertianus* (Fig. 187) to high-inclination sites dominated by vascular plant species like *Deyeuxia arundinacea* (Fig. 179) and *Rhododendron simsii* (Fig. 186), and bryophyte species like *Hypnum plumaeforme* (Fig. 191), *Isopteriygium fauriei* (Fig. 193), *Leucobryum juniperoideum* (Fig. 194) and *Trachycystis microphylla* (Fig. 196). Vascular plants species number also decreases slightly along this coenocline, while bryophyte species number shows the opposite trend and soil pH decrease strongly. In this case, inclination and soil pH may together explain the variation in both vascular plants and bryophytes on a macro plot scale; variation in vascular plant species composition and species number most likely related to soil acidity and variation in bryophyte species composition and species number related to inclination.

The more or less strong negative correlation between soil depth and inclination observed in three areas (TSP, LCG and LGS) indicates lower soil stability and occasional retardation of soil-forming processes in steep slopes due to erosion and minor 'earth-slides' (Tooren & During 1988, Fransson 2003). Furthermore, ridges and steep slopes with shallower soil are likely to experience more and longer periods with moisture deficit than the less steep slopes with deeper soil. Both of these mechanisms may explain why steep slopes favour drought resistant bryophyte species like *Leucobryum bowringii* (Fig. 53) and why vascular plants have problems with survival at such sites

(cf. T. Økland 1988, T. Økland et al. 2003).

Topographic heterogeneity is likely to occur on all scales down to within-plot scales and affect species distributions over the entire range of spatial scales. Those who know this part of China and its forests are also familiar with the diversity of 'micro' and 'macro niches' brought about by great topographical variation. Our results show that topography-dependent variation is omnipresent although there is considerable variation, between and within study areas, with respect to which single environmental factors are strongly related to variation in species composition and although the species that make up the corresponding coenocline also vary in number and identity among study areas. For instance, the number of species recorded in total in the plots varies from 65 in TSP to 147 in LXH and also the average number of species per 1-m^2 plot varies very much from 7.88 in LCG to 13.65 in LXH. Although the variation in species number and species composition between areas is very high, the number of species on one forest is often low comparing to e.g. boreal forests, especially for bryophytes (compared T. Økland 1996). This is due to preference of bryophytes for a cooler climate (Studlar 1982, Futamura & Wheelwright 2000). The high number of vascular plants in Chinese subtropical forests suggests that the habitat heterogeneity provided by a varied topography is an important factor for the high understorey species richness in these subtropical forests. Our results thus accord with the view that topography is a main determinant of gradients in species richness and composition on scales from the global to the local, along with properties such as the (regional) species pool, the fertility of the site and regional spatial heterogeneity (Taylor et al. 1990, Zobel 1997, Grace 2001a, 2001b). Most likely species richness and composition is related to gradients of global productivity and dynamics, which decline with increasing latitude (Grime 1979, 2001, Pianka 1966, Robinson 1966, Wright 1983), among others due to declining energy supplies (Whittaker et al. 2001, Willig et al. 2003).

The ecocline related to soil acidity and soil mineral nutrients

Variation in species composition related to soil acidity is observed in three areas, LCG, LGS and CJT, and variation also related to soil mineral nutrients concentrations is observed in one of these areas, LGS. In all cases this variation is mostly expressed at between macro-plot scales (> ca. 25 m). Furthermore, several variables related to soil acidity show a moderately strong relationship with the main ordination axis in TSP. The relative importances of this ecocline, and the contribution of different variables to the complex soil acidity and soil mineral nutrients gradient, vary between areas. Variables that contribute at least in one area are: concentrations of mineral nutrients Ca, Mg, Na and K in soil, base saturation, soil pH (both extractants) and concentrations of elements the chemistry of which is strongly dependent on or contributing to soil acidity (soil Al, Fe and H in soil, and aluminium saturation). These variables have been shown to be related to variation in ground vegetation composition in many types of forests such as boreal forests (R. Økland & Eilertsen 1993, T. Økland 1996), subtropical rain forests (Chen et al. 1997) and mixed mesophytic forest (McEwan et al. 2005).

The soil-vegetation relationship is well established but still not fully understood (Lindzen 1992, Scholes & van Breemen 1997), because of the complex and multivariate nature of mineral soils and humus forms (Baillie et al. 1987). Soil pH is the single variable which best reflects variation in vascular plant species composition in two areas LCG and CJT; soil pH and mineral nutrients together reflect variation in vascular plant species composition in LGS. In these areas, vascular plant species number in 1-m^2 plots increases with soil pH. Soil pH affects soil (decomposer) fauna and thus, indirectly, plants via availability of mineral nutrients for plant uptake (Eldor 2007). Bacteria and earthworms replace fungi as dominant decomposers along a gradient from acidic to basic conditions (Romell 1935, Nykvist 1961, Lindgren 1975). Soil pH is primarily determined by the parent material

[soils over calcareous rock have high pH; Partel (2002)] but with high rainfall or high concentrations of acidifying substances in the rain, leaching of base cations occur as revealed by numerous studies (Mclaughlin & Wimmer 1999). Our results that soil pH is positively related with concentrations of mineral nutrients Ca, Mg, Na and K (LGS) and Mn (TSP) and negatively correlated with acidity-related elements like Fe (TSP, LCG, LGS and CJT) concords with a general patterns (Bragazza & Gerdol 2002, T. Økland et al. 2004, Wu et al. 2006): availability of important nutrients is higher on high-pH soils while concentrations of potentially toxic elements like Al decrease (T. Økland, 1996). An important aspect of the soil acidity-mineral nutrient gradient is variation in humus-layer properties (Green et al. 1993); vascular plant species (Pausas 1994) as well as bryophytes (T. Økland et al. 1999) depend on properties of the humus layer.

The positive relationship between soil pH and coniferous tree density, and the negative relationship between soil pH and broadleaved tree density observed in LGS accord with the general preference of coniferous tree species for more acid and nutrient-poor soils (Vanhala et al. 1996, Ewald 2000, T. Økland et al. 2004). Also variation in the modes of gap formation and forest dynamics along soil acidity and mineral nutrient gradients (Jans et al. 1993) indirectly influence ground vegetation patterns.

Topography may influence soil acidity and mineral nutrient concentrations, as also pointed out in the previous discussion of the ecocline related to topography. This is exemplified by the CJT area in which concentrations of Al, Fe and H and soil aluminium saturation decrease while pH increase from the upper ridge down slope. Down slope transport processes bring about variation in soil chemical properties along elevation gradients (Chen et al. 1997) and strengthen the effect of increasing humidity with increasing elevation (e.g. Tamm 1959, Moen 1998) resulting from increasing rainfall and decreasing potential evapotranspiration. A humid climate favours leaching of soils from uniform parent material (Parker 1989).

The significantly positive relationships observed among concentrations of Mn, Ca, Mg, Na and K in soil suggest that the dynamics of these nutrients are closely related to each other. The contents of total C and N, and organic matter content in soil, is also more or less strongly related to the same coenoclines as the major mineral nutrients in LXH, and Mn and Ca concentrations vary along GNMDS axis 3 in TSP. Even though our results did not reveal a distinct coenocline related to organic matter (total C and organic matter content) or N concentrations, these variables may still be important for the differentiation of the vegetation in cases when they are part of an acidity-mineral nutrient complex gradient. The complex relationships among factors along this ecocline is further exemplified by the positive relationship between soil organic matter content and the water-holding capacity of soils (Hudson 1994); many waterlogged but mineral-rich soils have lower water mass percentage than seemingly drier samples with higher organic matter contents (Nekola 2004). This results in a strongly negative relationship between contents of dry matter and organic matter in soil in all five areas, and the negative correlation between the soil moisture and soil dry matter content in two areas (LCG and CJT).

According to Westman & Roggers (1977) and Matson et al. (1999) phosphorus is the most strongly limiting nutrient in subtropical rain forest ecosystems. This has so far been substantiated by fertilization experiments in several boreal ecosystems (e.g. van den Burg 1991, Nilsen 2001) and montane tropical forests (Nomura & Kikuzawa 2003, Benner et al. 2007). We did not include phosphorus in our soil measurement program, which opens for the possibility that phosphorus is one of the 'missing factors' in our study. This should be investigated further.

Vascular plants species number in 1-m^2 plots increase with increasing soil pH in three areas (LCG, LGS and CJT) and with increasing soil nutrient concentrations in one area, LGS. No clear relationships were, however, found between soil pH or mineral nutrient concentrations and bryophyte species number. This is consistent with the nutrition of most species in the two plant groups; forest

bryophytes obtain most of their nutrients from the throughfall precipitation and leachates from trees and other forest plants (Rieley et al. 1979, Solangaarachchi & Harper 1987, Rambo & Muir 1998, R. Økland 1995b, 2000) and are, thus, more independent of the mineral soil than vascular plants (but see T. Økland et al. 1999). Vascular plants, on the other hand, are directly dependent on the soil and its properties for uptake of water and mineral nutrients (Sjörs & Gunnarsson 2002).

Coenoclines related to soil acidity and nutrient concentrations (including pH and concentrations of exchangeable cations and total N and P in soil) have been reported from several boreal ecosystems (e.g. R. Økland & Eilertsen 1993, T. Økland 1996), subtropical rain forests (Chen et al. 1997) and mixed mesophytic forest (McEwan et al. 2005). Demonstration in the present study of similar ecoclines in Chinese subtropical forests (apparently in LGS), may suggest this is a strong candidate for a universally important ecocline in forests and other land ecosystems.

The ecocline related to tree density

We observe a strong compositional gradient related to tree density in two areas LCG (both coniferous trees and broadleaved trees) and LXH (coniferous trees), with variation at the macro-plot scale. In LCG which vascular plants like *Miscanthus sinensis* (Fig. 78), *Pteridium aquilinum* (Fig. 82) and *Smilax davidiana* (Fig. 85) are restricted to plots in sites with a higher coniferous trees density while bryophyte species like *Calypogeia arguta* (Fig. 90) and *Cephalozia macounii* (Fig. 91) are restricted to plots with relatively high broadleaf tree density. In the other three areas no relationship between coenoclines and tree influence or tree-layer density gradient occurs, or relatively weak relationships with one or two variables are observed. This result thus only partly confirms predictions by Zhao et al. (2005) for central Chinese forests and results of other studies in subtropical (e.g. Chen et al. 1997, Enoki & Abe 2004) and tropical forests (Tuomist et al. 1995, Svenning 1999), suggesting that one of the 2-3 most important vegetation gradients in (sub) tropical forest vegetation is related to the gap structure of the tree layer, running from below trees to openings between trees. An ecocline related to tree density or single-tree influence is also well established for boreal forests (R. Økland & Eilertsen 1993, 1996, T. Økland 1996, R. Økland et al. 1999).

A coenocline related to forest canopy structure and foliage height distribution partly results from variation in plant responses to a gradient of understorey light availability (Oberbauer et al. 1988, Nicotra et al. 1999, Tang et al. 1999), exemplified by immediate changes in the vegetation after gaps are created (Parker 1996), tree regeneration patterns (Clark et al. 1996, Nicotra et al. 1999) and, eventually, the distribution of understorey trees (Aber 1979, Brown & Parker 1994, van Pelt & Franklin 1999, Denslow & Guzman 2000). Canopy structure is in turn affected by topography through complex relationships between topography and other factors (Gale 2000). Tree canopies also influence the understorey vegetation in several other ways, e.g. through littershed and effects on soil moisture conditions (R. Økland & Eilertsen 1993, T. Økland 1996; also see discussion of the topography ecocline).

A strong negative relationship between the litter index and soil moisture in LXH accords with the view that in subtropical forests litter is more rapidly decomposed in moist than in drier sites if other environmental variables are similar (Wang et al. 2004). Furthermore, tree influence variables are more or less strongly related to soil mineral nutrient concentrations, i.e. with Mg in TSP, Mn in LCG, CJT and LXH, and with soil pH in LCG and LGS, and with concentrations of Fe and H in soil (in all areas except LXH). This is a result of the uneven distribution of litter and precipitation brought about by the trees (R. Økland & Eilertsen 1993, T. Økland 1988, 1996) and shows that ecoclines related to tree density (also in LCG) are complex gradients to which several factors contribute, including soil pH, litter-layer depth and topography.

The largest bryophyte species number at study-area scale is found in LGS (Tab. 4), probably due to more moist climatic conditions (Tab. 1). In this area, bryophytes were preferably found under trees, e.g. close to tree stems (personal observations). The most likely reason for this is that the climate is moist enough for bryophytes to gain positive net photosynthesis in locally drier sites (T. Økland 1996), ant that cover of litter is often sparse at small patches and "pocket" close to roots and stems due to macro-topography variation. In the other areas, bryophytes seemingly prefer more open forest although light intensity and air and soil temperatures are significantly higher in gaps than under trees (Arunachalam & Arunachalam 2000).

In the Chinese subtropical forests studied by us species composition is only relatively weakly related to tree-layer density and no observation is made suggesting that the spatial pattern of single trees affect the distribution of understorey species as observed in boreal forests (R. Økland et al. 1999). The reason for this difference may be that (sub)tropical forests generally have a more closed canopy layer (with less distinct and smaller canopy gaps), by which light, throughfall precipitation and canopy leachates are redistributed on ground level in ways that are more or less unrelated to the stems of individual trees. This hypothesis should, however, be investigated further.

SAMPLE-PLOT SIZE AND IDENTIFIED ECOCLINES

The size of sample plots (the grain of a study; Wiens 1989, Dungan et al. 2002) is known to affect compositional turnover, sample similarity, species relationships, and ordinations results (Gauch & Stone 1979, Noy-Meir & Van der Maarel 1987). Any reduction in sample plot size leads to weakening of structure and relationships in the data matrix (R. Økland et al. 1990). In our study of vegetation-gradient relationships in five Chinese subtropical forests the variation (in plot scores) along GNMDS ordination axes mainly occur at the between-macro plot scale (which generally were more than 25 m apart) for all five first axes (GMNDS 1), for three out of five second axes and one out of two third axes. This suggests that variation in these forests, in species composition and environment, is most prominent on broader scales. However, finer-scaled variation, mostly reflected in the distribution of bryophytes on the forest floor in relation to occurrence of soil without a stable litter layer, also occurs (see ecocline related to litter-depth, p. 161–165, 178).

Our results accord with those of other studies in temperate and (sub) tropical forests. Thus Ren et al. (2006) found variation in life-form composition of vascular plants along an elevation gradient in the Dongling Mts of China, concluding that variation along gradients occurred at broader scales while patterns were patchy at finer scales. The spatial scaling of variation in subtropical forests does, on the other hand, seem to differ from boreal forests in which fine-scaled variation (within stands) is of higher importance than variation between stands (R. Økland et al. 2001b, T. Økland et al. 2003, Heimstad 2007). This difference indicates that subtropical and tropical forests on one hand, and temperate and boreal forests on the other, differ fundamentally in the spatial scaling of important ecosystem processes and, hence, in the spatial scales of compositional patterns. Furthermore, this difference accords with the notion that ecological phenomena are hierarchically structured (Allen & Starr 1982), but shows that the levels of this hierarchy at which most of the variation occurs varies among forest ecosystems, perhaps along latitudinal gradients.

The use in the present study of a nested sampling design (Austin 1981) and split-plot GLM has proved useful for resolving scale-dependent relationships between vegetation and environment (also see Mathiassen & Økland 2007, R. Økland 2007, Austad et al. in press). Our results demonstrate the importance of selecting an appropriate plot size, because patterns that can be revealed depend on the

scale of observation (R. Økland 1990, Whittaker et al. 2001). However, patterns at a given scale are composed of structures at even finer scales, and are themselves a component of high-level structures visible at larger scale (O'Neill et al. 1996). The strength of patterns at each of these scales do, however, vary, often in complex ways, with a shift from dependence on local, edaphic complex gradients at finer scales to regional, climatic gradients at broader (between study area) scales.

CONCLUSION AND RECOMMENDATIONS FOR FURTHER STUDIES

We find generally good agreement between the results obtained by DCA, LNMDS and GNMDS ordination. LNMDS and GNMDS produce very similar ordinations, and DCA is more similar to GNMDS than to LNMDS. We demonstrate that all of the three methods may occasionally produce ordinations that are inappropriate from the point of view of finding the main gradient structure of compositional data. Thus, NMDS and DCA should be used together for corroboration. The procedure for determining corresponding axes in this study from parallel ordinations by different methods appears promising for future ordination studies.

Gradient analyses of forests ground vegetation and its relationships to environmental variables underscore the prominent role of litter, topography, soil pH and mineral nutrient concentrations, and tree density/crown cover conditions in controlling understorey vegetation patterns in Chinese subtropical forests. We were, however, unable to explain four of the corresponding axes identified by three ordination methods. This indicates that a search for new variables of potential importance for compositional variation in these forests, beyond those included in the present study, should start. Other important factors may include biotic variables such as dispersal limitation, interactions between species, predation (Wright 2002, Munzbergova & Herben 2005) and historical use and other impact (Matlack 1994, Guntenspergen1 & Levenson 1997, Graae et al. 2004, Ito et al. 2004).

The four interpreted coenoclines can be generalised as follows: (1) variation in total species composition and species number related to topography (e.g. aspect) and tree influence, on scales broader than ca. 25 m; (2) variation in vascular plant species composition and species number related to soil acidity and soil nutrient concentrations on the broad scale; and (3) variation in bryophyte species composition and species number related to litter and topography (e.g. inclination) on a variety of scales down to the 1-m plot scale. The importance of different environmental variables on the variation in vegetation is thus clearly scale dependent. We also demonstrate variation in species composition at even broader scales: the five studied areas differ strongly with respect to species composition. The areas do, however, share the property that many species (mainly different in different areas) are present in each set of 50 plots while the number of species in each plot is quite low. This accords with the dominance of broad-scaled compositional patterns and may also explain the differences between areas with respect to main ecoclines.

It is increasingly acknowledged that traditional statistical tests have severe limitations when ecological patterns are to be analysed, among others because they do not allow for proper analysis of scale dependence and nested sampling (Legendre 1993, R. Økland 2007). Split-plot GLM allows flexible handling of nested data over a two or more hierarchical levels and thus improves our understanding of relationships across scales.

It is outside the scope of the present paper to discuss the ecology and habitat preferences of single ground vegetation species in S and SW Chinese subtropical forests. We have, however, found distributions of individual species in ecologically interpreted ordinations important for a complementary understanding of vegetation-environment relationships, in particular when strong relationships

between ordination axes and measured environmental variables are not found. For example, our analyses of bryophyte species distribution [e.g. *Leucobryum bowringii* (Fig. 53), *Brotherella henonii* (Fig. 89), *Taxiphyllum subarcuatum* (Figs 54 and 95) and *Isopterygium pohliaecarpum* (Fig. 261)] reveal close a relationship to steep sites without a permanent litter layer; and a coenocline that we were unable to interpret ecologically differentiated between sites with dominant fern species like *Woodwardia japonica* (Figs 49, 88 and 189) and *Dryopteris erythrosora* (Figs 30 and 76) and sites from which these species were absent. This opens for the possibility that key species are important in shaping habitats on finer scales.

Our study shows that plot-based nested sampling of vegetation and data analysis by ordination techniques provides a strong basis for understanding vegetation-environment relationships also in subtropical forests. The study also provides a fundament for studies of vegetation change, e.g. in response to airborne pollutants and climate change, by repeated analysis of the permanently marked plots (cf. R. Økland & Eilertsen 1996, Lawesson et al. 2000, T. Økland et al. 2004). The results do, however, suggest that two sets of plots scale (1-m^2 plots and bigger plots around them) for vegetation pattern analyses in future studies of subtropical forests, and search for environmental factors that may explain patterns of variation so far left unexplained should be encouraged.

Five monitoring areas are obviously too few. In regions which like China, comprise a broad range of forest ecosystem types and extremely high number of vascular plants (almost 30,000) and display strong variation along regional climatic and deposition gradients. This is clearly shown by the tendency for individualistic behaviour of the study areas included in the present study.

In China, forest damage has occurred in many sites in the provinces of our study, especially in the forests close to urban areas. In Nanshan mountains in Chongqing municipality, especially on the most pollutes western side, total dieback of forest trees and ground vegetation have been observed, while on the eastern side facing away from the city, scattered signs of damage to Masson pine and some bryophytes were obvious (Zhao et al. 1988). Possible reasons for the forest damage have been discussed in several scientific papers (Ma 1996, Bian & Yu 1992, Wang et al. 2007). In our sites located relatively more far away from urban areas, we don't find similar severe effects on ground vegetation. Anyhow, our project will give policy makers important information over time if the monitoring activities continue. China increased use of coal combined with the Chinese environmental strategies aiming reduced particle emissions can be dangerous, as the removal of alkaline dust may result in increased acidity of the precipitation. Another tendency going in the same direction is building of higher and higher stacks, which will improve the condition at ground level near the source, but promote long-range transport of pollutants. Hence, there is an obvious potential for enhanced acidification in areas today receiving high loading of sulphur as well as significant deposition of base cations, which partly counteracts the effect of acid rain. The situation in our monitoring areas, in relatively more remote and partly more sensitive mountainous areas, which presently receive little acid deposition, could also worsen if the level and composition of the fallout change as a result of such emission-control strategies.

We suggest that reductions in emissions of air pollutants in China will have large benefits. However, it is essential that effects on the local, regional and global levels are considered in an integrated way, where effect studies on ground vegetation plays an important role equal to effect studies on other parts of the natural environment as well as effect studies of humans, and materials. The continuation of IMPACTS and similar ground vegetation projects will hopefully give policy makers valuable information to prevent unwanted negative side effects of environmental change.

ACKNOWLEDGEMENT

This study was financially supported by the Norwegian government through NORAD (Norwegian Agency for Development Co-operation) and Chinese government through SEPA (State Environmental Protection Administration). The field work and analysis mainly charged by the Institute of Ecology, Chinese Research Academy of Environmental Sciences (CRAES), Beijing Normal University (BNU) and the Norwegian Forest and Landscape Institute (Skogoglandscap). J.H. Zhang from Guangzhou Research Institute of Environmental Protection, R.J. Xiang from Hunan Research Institute of Environmental Protection Science, D.W. Zhao from Chongqing Institute of Environmental Science and Monitoring, J.S. Xiao from Guizhou Research Institute of Environmental Protection Science, and related colleagues from the Chinese Meteorological Administration are thanked for kindly making the study area's climate data available to us. We are grateful to H. Shang and Y.H. Wang from the Chinese Academy of Forest (CAF), who provided canopy tree data. Rolf Vogt from Department of Chemistry, University of Oslo (Uio) is thanked for providing soil chemistry data. We gratefully acknowledge Y. He and D. G. Tang from Chinese Research Academy of Environmental Sciences (CRAES), Lei Duan from Tsinghua University, Min Shao from Peking University, Xiaoshan Zhang from Research Center for Eco-Environmental Sciences, Chinese Academy of Sciences (CAS), Svein Solberg from Norwegian Forest and Landscape Institute (Skogoglandscap), Wenche Aas from Norwegian Institute for Air Research (NILU), Thorjørn Larssen and Espen Lydersen from Norwegian Institute for Water Research (NIVA), Jan Mulder from Norwegian University of Life Sciences for help and support during the project. Two reviewers Klaus Høiland and Vegar Bakkestuen are highly appreciated. Special thanks to Valter Angell at Norwegian Institute of International Affairs (NUPI) for helping us with the language, to Jan Wesenberg at Department of Botany, Natural History Museum, University of Oslo for editing this monograph, and to the University of Oslo for the Quota scholarship.

REFERENCES

Aber, J. D. 1979. Foliage-height profiles and succession in Northern hardwood forest. – Ecology 60: 18–23.

Alban, D. H. 1982. Effects of nutrients accumulation by aspen, spruce, and pine on soil properties. – Soil Sci Soc Am J. 46: 853–861.

Allen, T. F. H. & Starr, T. B. 1982. Hierarchy: Perspectives for ecological complexity. – University of Chicago Press, Chicago, IL, US, pp. 310.

Andersson, M. 1988. Toxicity and Tolerance of Aluminum in Vascular Plants – a Literature-Review. – Water Air Soil Pollut. 39: 439–462.

Anonymous. 2004a. R Version 2.3.1 for Windows. URL: http://cran.r-project.org [The R foundation for statistical computing].

Anonymous. 2004b. R: a language and environment for statistical computing. URL: http://cran.r-project.org. [The R development core team, The R foundation for statistical computing].

Antoine, G. & Niklaus, E. 2000. Predictive habitat distribution models in ecology. – Ecol Model. 135: 147–186.

Arunachalam, A. & Arunachalam, K. 2000. Influence of gap size and soil properties on microbial biomass in a subtropical humid forest of north-east India. – Plant. Soil. 223: 185–193.

Auestad, I., Rydgren, K. & Økland, R. H. Scale-dependence of vegetation – environment relationships in semi-natural grasslands. – J. Veg. Sci. (in press)

Austin, M. P. 1980. Searching for a model for use in vegetation analysis. – Vegetatio. 42: 11–21.

Austin, M. P. 1981. Permanent quadrats: an interface for theory and practice. – Vegetatio. 46–47: 1–10.

Baillie, I. C., Ashton, P. S., Court, M. N., Anderson, J. A. R., Fitzpatrick, E. A. & Tinsley, J. 1987. Site Characteristics and the Distribution of Tree Species in Mixed Dipterocarp Forest on Tertiary Sediments in Central Sarawak, Malaysia. – J Trop Ecol. 3: 201–220.

Barik, S. K., Pandey, H. N., Tripathi, R. S. & Rao. P. 1992. Microenvironmental Variability and Species-Diversity in Treefall Gaps in a Subtropical Broadleaved Forest. – Vegetatio. 103: 31–40.

Bates, J. W. 1994. Responses of the Mosses Brachythecium rutabulum and Pseudoscleropodium purum to a Mineral Nutrient Pulse. – Funct Ecol. 8: 686–693.

BeattY, S. W. & Sholes, D. D. V. 1988. Leaf litter effects on plant species composition of deciduous forest treefall pits. – Can J For Res. 18: 553–559.

Belbin, L. 1991. Semi-strong hybrid scaling: a new ordination algorithm. -J. Veg. Sci. 2: 491–496.

Belbin, L. 1993a. PATN Technical Reference Manual. – CSIRO Division of Wildlife and Ecology, pp. 234.

Belbin, L. 1993b. PATN User Manual. -CSIRO Division of Wildlife and Ecology, pp.78.

Benner, J. W., Conroy, S., Lunch, C. K., Toyoda, N. & Vitousek, P.M. 2007. Phosphorus Fertilization Increases the Abundance and Nitrogenase Activity of the Cyanolichen Pseudocyphellaria crocata in Hawaiian Montane Forests. – Biotropica 39: 400–405.

Bian, Y. M. & Yu, S. W. 1992. Forest Decline in Nanshan, China. Forest Ecol Manag. 51: 53–59.

Bragazza, L. & Gerdol, R. 2002. Are nutrient availability and acidity-alkalinity gradients related in Sphagnum-dominated peatlands? – J Veg Sci. 13: 473–482

Brown, M. J. & Parker, G. C. 1994. Canopy light transmittance in a chronosequence of mixed-species deciduous forests. – Can J Forest Res. 24: 1694–1703.

Brubaker, S. C., Jones, A. J., Lewis, D. T. & Frank, K. 1993. Soil properties associated with landscape

position. – Soil Sci Soc Am J. 57: 235–239.
Byrne, J, Shen, B. & Li, X. 1996. The Challenge of Sustainability: Balancing China's Energy, Economic and Environmental Goals. – Energy Policy. 24: 455–462.
Carson, W. P. & Peterson. C. J. 1990. The role of litter in an old-field community: impact of litter quantity in different seasons on plant species richness and abundance. – Oecologia 85: 8–13.
Chen, Z. S., Hsieh, C.F., Jiang, F. Y., Hsieh, T. H. & Sun, I. F. 1997. Relations of soil properties to topography and vegetation in a subtropical rain forest in southern Taiwan. – Plant Ecol. 132: 229–241.
Clark, D. B., Clark, D. A., Rich, P. M., Weiss, S. & Oberbauer, S. F. 1996. Landscape-scale analysis of forest structure and understory light environments in a neotropical lowland rain forest. – Can. J Forest Res. 26: 747–757.
Clarke, B. C., Foy, C. D., Fowden, L., Bradshaw, A. D., Wolfe, M. S., Epstein, E., Gressel, J., Hutchinson, T. C., Hartl, D. I., Sawicki, R. M., Wood, R. J. & Bell, E. A. 1984. Adaptation of Plants to Mineral Stress in Problem Soils – Discussion. – Ciba Found Symp. 102: 32–39.
Condit, R., Ashton, P. S., Baker, P., Bunyavejchewin, S., Gunatilleke, S., Gunatilleke, N., Hubbell, S. P., Foster, R. B., Itoh, A., LaFrankie, J. B., Lee, H. S., Losos, E., Manokaran, N., Sukumar, R. & Yamakura, T. 2000. Spatial patterns in distribution of tropical tree species. – Science. 288: 1414–1418.
Cook, J. G. & Irwin, L. L. 1992. Climate-vegetation Relationships between the Great Plains and Great Basin. – Am Midl Nat. 127: 316–326.
Crawley, M. J. 2002. Statistical Computing: An Introduction to Data Analysis using S-Plus. – John Wiley & Sons. pp.761.
Daniels, W. L., Zelazny, L. W. & Everett, C. J. 1987. Virgin hardwood forest soils of the southern Appalachian Mountains: II. Weathering, mineralogy and chemical properties. – Soil Sci Soc Am J. 51: 730–738.
De'ath, G. 1999. Extended dissimilarity: a method of robust estimation of ecological distances from high beta diversity data. – Plant Ecol. 144, 191–199.
Denslow J. S. & Guzman G. S. 2000. Variation in stand structure, light and seedling abundance across a tropical moist forest chronosequence, Panama. – J veg sci. 11: 201–212.
Dungan, J. L., Perry, J. N., Dale, M. R. T., Legendre, P., Citron-Pousty, S., Fortin, M. J., Jakomulska, A., Miriti, M. & Rosenberg, M. S. A balanced view of scale in spatial statistical analysis, – Ecography 25: 626–640.
Dwyer, L. M. & Merriam. G. 1981. Influence of topographic heterogeneity on deciduous litter decomposition. – Oikos. 37: 228–237.
Eilertsen, O., Økland, R. H., Økland. T. & Pedersen. O. 1990. Data manipulation and gradient length estimation in DCA ordination. – J veg sci. 1: 261–27.
Eldor, A. P. 2007. Soil Microbiology, Ecology and Biochemistry, ed. 3. – Academic Press, Colorado State University, Ft. Collins, U.S.A, pp. 552.
Enoki T. 2003. Micro-topography and distribution of canopy trees in a subtropical evergreen broad leaved forest in the northern part of Okinawa Island, Japan. – Ecol Res. 18: 103–113.
Enoki T., Kawaguhi, H. & Iwatsubo, G. 1997. Nutrient-uptake and nutrient-use efficiency of Pinus thunbergii Parl. along a topographical gradient of soil nutrient availability. – Ecol Res. 12: 191–199.
Enoki, T. & Abe, A. 2004. Saplings distribution in relation to topography and canopy openness in an evergreen broad-leave forest. – Plant Ecol. 173: 283–291.
Ewald, J. 2000. The Influence of Coniferous Canopies on Understorey Vegetation and Soils in Mountain Forests of the Northern Calcareous Alps. – Appl Veg Sci. 3: 123–134.
Faith, D. P., Minchin, P. R. & Belbin, L. 1987. Compositional dissimilarity as a robust measure of

ecological distance. – Vegetatio 69: 57–68.
Falkengren-Grerup, U. 1986. Soil acidification and vegetation changes in deciduous forest in southern Sweden. – Oecologia 70: 339–347.
FAO. 1998. World Reference Base for Soil Resources (WRB), Rome. http://www.fao.org.
Feldman, S. B., Zelazny, L. W. & Baker, J. C. 1991. High-elevation forest soils of the southern Appalachians: I. Distribution of parent materials and soil-landscape relationships. – Soil Sci Soc Am J. 55: 1629–1637.
Foster J. R. 1988. Disturbance history, community organization and vegetation dynamics of old-growth Pisgah Forest, southwestern New Hampshire, USA. – J. Ecol. 76: 105–134.
Foster, B. L. & Gross. K. L. 1997. Partitioning the effects of plant biomass and litter on Andropogon gerardi in oldfield vegetation. – Ecology 78: 2091–2104.
Foy, C. D. & Campbell, T. A. 1984. Differential Tolerances of Amaranthus Strains to High-Levels of Aluminum and Manganese in Acid Soils. – J Plant Nutr. 7: 1365–1388.
Fransson, S. 2003. Bryophyte vegetation on cliffs and screes in Western Värmland, Sweden. – Acta phytogeogr suec. 86: 1–95.
Futamura, C. W. & Wheelwright, N. T. 2000. The mosses of Kent island, New Brunswick. – Northeast Nat. 7: 277–288.
Gale N. 2000. The relationship between canopy gaps and topography in a western Ecuadorian rain forest. – Biotropica 32: 653–661.
Gao, Q. 1994. Flora Bryophytorum Sinicorum. – Chinese Science and Education Press, Beijing, China (Chinese Language).
Gartlan, J. S., Newbery, D. McC., Thomas, D. W. & Waterman, P. G. 1986. The influence of topography and soil phosphorous on the vegetation of Korup Forest Reserve, Cameroun. – Vegetatio 65: 131–148.
Gauch, H. G. & Stone, E. L. 1979. Vegetation and Soil Pattern in a Mesophytic Forest at Ithaca, New-York. – Am Midl Nat. 102: 332–345.
Gauch, H. G. & Whittaker, R. H. 1981. Hierarchical classification of community data. – J. Ecol. 69: 537–557.
Gauch, H. G. 1982. Multivariate analysis in community ecology. – Camb. Stud. Ecol. 1: 1–298.
Gleason, H. A. 1926. The individualistic concept of the plant association. – B Torrey Bot Club 53: 7–26.
Glenn, M., Eberhardt, R., Hall, B., Foster, D.R., Harrod, J. & MacDonald, D. 2002. Vegetation variation across Cape Cod, Massachusetts: environmental and historical determinants. – J Biog. 29: 1439–1454.
Golley, F. B., Richardson, T. & Clements, R. G. 1978. Elemental concentrations in tropical forests and soils of northwestern Colombia. – Biotropica 10: 144–151.
Graae, B. J., Økland, R. H., Petersen, P. M., Jensen, K. & Fritzbøger, B. 2004. Influence of historical, geographical and environmental variables on understorey composition and richness in Danish forests. – J Veg Sci. 15: 465–474
Grace, J. B. 2001a. Difficulties with estimating and interpreting species pools and the implications for understanding patterns of diversity. – Foli Geob. 36: 71–83.
Grace, J. B. 2001b. The roles of community biomass and species pools in the regulation of plant diversity. – Oikos 92: 193–207.
Green, R. N., Trowbridge, R. L. & Klinka, K. 1993. Towards a Taxonomic Classification of Humus Forms. – For Sci Monogr. 29: 1–49.
Grime, J. P. 1979. Plant strategies and vegetation processes. – John Wiley and Sons, Chichester, pp. 222.
Grime, J. P. 2001. Plant strategies, vegetation processes, and ecosystem properties. – John Wiley and

Sons, Chichester, New York, Toronto, pp. 417.
Guntenspergen, G. R. & Levenson, J. B. 1997. Understory plant species composition in remnant stands along an urban-to-rural land-use gradient. – Urban Ecos. 1: 155-169.
Haase, R. 1990. Community composition and soil properties in northern Bolivian savanna vegetation. – J Veg Sci. 1: 345–352.
Heikkinen, R. K. 1991. Multivariate analysis of esker vegetation in southern Häme, S Finland. – Annls Bot Fenn. 28: 201–224.
Heimstad, R. 2007. Understorey species compositional dynamics in a boreal coniferous forest in SE Norway: does past logging matter? Master of Science Thesis. – Botanical Museum, Natural History Museums and Botanical Garden, University of Oslo, pp. 97.
Hill, M. O. 1979. DECORANA – A FORTRAN program for detrended correspondence analysis and reciprocal averaging. Cornell University, Ithaca. New York, USA.
Hill, M.O. & Gauch, H.G.J. 1980. Detrended correspondence analysis: an improved ordination technique. – Vegetation 42: 47–58.
Honeycutt, C.W., Heil, R. D. & Cole, C. V. 1990. Climatic and topographic relations of three Great Plains soils: II. Carbon, nitrogen, and phosphorous. – Soil Sci Soc Am J. 54: 476–483.
Huddleston, J. H. & Riecken, F. F. 1973. Local soil-landscape relationships in western Iowa: I: Distribution of selected chemical and physical properties. – Soil Sci Soc Am Proc. 37: 264–270.
Hudson, B. 1994. Soil organic matter and available water capacity. – J Soil Water Cons. 49: 189–193.
Humboldt, A. von. & Bonpland, A. 1807. Essai sur la géographie des plantes. – Levrault, Schoell et Compagnie.
Hunter J. C. & Parker V. T. 1993. The disturbance regime of an old-growth forest in coastal California. – J. Veg. Sci. 4: 19–24.
Ito, S., Nakayama, R. & Buckley, G. P. 2004. Effects of previous land-use on plant species diversity in semi-natural and plantation forests in a warm-temperate region in southeastern Kyushu, Japan. – Forest Ecol Manag 196: 213–225.
Jans, L., Poorter, L., Vanrompaey, R. S. A. R. & Bongers, F. 1993. Gaps and Forest Zones in Tropical Moist Forest in Ivory-Coast. – Biotropica. 25: 258–269.
Kendall, M. G. 1938. A New Measure of Rank Correlation. – Biometrik 30: 81–93.
Kenkel, N. C. & Orloci, L. 1986. Applying metric and nonmetric multidimensional scaling to ecological studies: some new results. – Ecology 67: 919–928.
Kruskal, J.B. 1964. Multidimensional scaling by optimizing goodness of fit to a nonmetric hypothesis. – Psychometrika 29: l–27.
Kruskal, J.B., Young, F. W. & Seery, J. B. 1973. How to use KYST, a very flexible program to do multidimensional scaling and unfolding. – Bell Labs, Murray Hill, New Jersey, unpubl.
Larssen, T., Lydersen, E., Tang, D. G., He, Y., Gao, J. X., Liu, H.Y., Duan, L., Seip, H. M., Vogt, R. D., Mulder, J., Shao, M., Wang, Y. H., Shang, H., Zhang, X. S., Solberg, S., Aas, W., Økland, T., Eilertsen, O., Angell, V., Liu, Q. R., Zhao, D. W., Xiang, R. J., Xiao, J. S. & Luo, J. H. 2006. Acid Rain in China. – Environ Sci Technol. 40: 418–425.
Lawesson, J., Eilertsen, O., Diekmann, M., Reinikainen, A., Gunnlaugsdottir, E., Fosaa, A. M., Carøe, I., Skov, F., Groom, G., Økland, R. H., Økland, T., Andersen, P. N. & Bakkestuen, V. 2000. A concept for vegetation studies and monitoring in the Nordic countries. – Tema Nord. 517: 1–125.
Ledieu, J., De Ridder, P., De Clerck, P. & Dautrebande, S. 1986. A method of measuring soil moisture by time-domain reflectometry. – J. Hydrol. 88: 319–328.
Legendre, P. 1993. Spatial Autocorrelation – Trouble or New Paradigm. – Ecology. 74: 1659–

1673.
Lindgren, L. 1975. Beech forest vegetation and soil in Sweden. – In: Dierschke, H. (ed.), Vegetation und Substrat, Cramer, Vaduz, pp. 401–418.
Lindzen, R. 1992. Absence of scientific basis. – Nat Geogr Res. 9: 191–200.
Ma, Z. 1996. The historic changes of forest in China. – Chinese Forestry Press, Beijing, China (Chinese language).
Magura, T., Tóthmérész, B. & Elek, Z. 2005. Impacts of Leaf-litter Addition on Carabids in a Conifer Plantation. – Biodivers Conserv. 14: 475–491.
Marsh, D.M. & Pearman, P.B. 1997. Effects of Habitat Fragmentation on the Abundance of Two Species of Leptodactylid Frogs in an Andean Montane Forest. – Conserv Biol. 11: 1323–1328.
Masaki, T., Suzuki, W., Niiyama, N., Iida, S., Tanaka, H. & Nakashizuka, T. 1992. Community structure of species-rich temperate forest, Ogawa Forest Reserve, central Japan. – Vegetation 98: 97–111.
Mathiassen, G. & Økland, R. H. 2007. Relative importance of host tree species and environmental gradients for epiphytic species composition, exemplified by pyrenomycetes s. lat. (Ascomycota) on Salix in central north Scandinavia. – Ecography. 30: 251–263.
Matlack, G. 1994. Plant Demography, Land-Use History, and the Commercial Use of Forests. – Conserv Biol. 8: 298–299.
Matson, P. A., McDowell, W. H., Townsend, A. R. & Vitousek, P. M. 1999. The Globalization of N Deposition: Ecosystem Consequences in Tropical Environments. – Biogeochemistry 46: 67–83.
McEwan, R. W., Muller, R. N. & McCarthy, B. C. 2005. Vegetation-environment relationships among woody species in four canopy-layers in an old-growth mixed mesophytic forest. – Castanea 70: 32–46.
McLaughlin, S. B. & R. Wimmer. 1999. Tansley Review No. 104 Calcium physiology and terrestrial ecosystem processes. – New Phytol. 142: 373–417.
Mclaughlin, S. B. & Wimmer, R. 1999. Tansley Review No. 104 Calcium physiology and terrestrial ecosystem processes. – New Phytol. 142: 373–417.
Minchin, P. 1987. An evaluation of the relative robustness of techniques for ecological ordination. – Vegetatio. 69: 89–107.
Minchin, P. 1991. DECODA-Database for ecological community data. Notes on performing multidimensional scaling with DECODA and MDS. – Australian National University, Canberra. pp. 7.
Minchin, P.R. 1989. Montane vegetation of the Mt. Field massif, Tasmania: a test of some hypotheses about properties of community patterns. – Vegetatio, 83: 97–110.
Moen, A. 1998. National atlas for Norway: Vegetation. – Norwegian Mapping Authority, Hønefoss. pp. 200.
Munzbergova, Z. & Herben, T. 2005. Seed, dispersal, microsite, habitat and recruitment limitation: identification of terms and concepts in studies of limitations. – Oecologia, 145: 1–8.
Nekola, J. C. 2004. Terrestrial gastropod fauna of northeastern Wisconsin and the southern Upper Peninsula of Michigan. – Am Malacol Bull. 18: 21–44.
Nellemann, C. & Thomsen, M. G. 1994. Terrain ruggedness and caribou forage availability during snowmelt on the arctic coastal plain, Alaska. – Arctic 47: 361–367.
Nicotra A. B., Chazdon R. L. & Iriatre V. B. 1999. Spatial heterogeneity of light and woody seedling regeneration in tropical wet forests. – Ecology 80: 1908–1926.
Nieppola, J. 1992. Long-term vegetation changes in stands of Pinus sylvestris in southern Finland. – J Veg Sci. 3: 475–484.
Nilsen P. 2001. Fertilization Experiments on Forest Mineral Soils: A Review of the Norwegian Results.

– Scand J Forest Res. 16: 541–554.
Nomura, N. & Kikuzawa, K. 2003. Productive phenology of tropical montane forests: Fertilization experiments along a moisture gradient. – Ecol Res. 18: 573–586.
Noy-meir, I. & Van der maarel, E. 1987. Relations between Community Theory and Community Analysis in Vegetation Science – Some Historical Perspectives. – Vegetatio. 69: 5–15.
Nykvist, N. 1961. Leaching and decomposition of litter. IV. Experiments on leaf litter of Picea abies. – Oikos 12: 264–279.
O'Neill, R. V., Hunsaker, C. T., Timmins, S. P., Jackson, B. L., Jones, K. B., Riitters, K. H. & Wickham, J. D. 1996. Scale problems in reporting landscape pattern at the regional scale. – Landscape Ecol. 11: 169–180.
Oberbauer S. F., Clark D. B., Clark D.A. & Quesada M. 1988. Crown light environments of saplings of two species of rain forest emergent trees. – Oecologia 75: 207–212.
Økland, R. H. & Eilertsen, O. 1993. Vegetation-environment relationships of boreal coniferous forests in the Solhomfjell area, Gjerstad, S Norway. – Sommerfeltia 16: 1–254.
Økland, R. H. & Eilertsen, O. 1996. Dynamics of understory vegetation in an old-growth boreal coniferous forest, 1988–1993. – J Veg Sci. 7: 747–762.
Økland, R. H. 1986a. Rescaling of ecological gradients. I. Calculation of ecological distance between vegetation stands by means of their floristic composition. – Nord. J. Bot. 6: 651–660.
Økland, R. H. 1990.Vegetation ecology: theory, methods and applications with reference to Fennoscandia. – Sommerfeltia suppl. 1:1–233.
Økland, R. H. 1995a. Changes in the occurrence and abundance of plant species in a Norwegian boreal coniferous forest, 1988–1993. – Nord. J. Bot.15: 415–438.
Økland, R. H. 1995b. Population biology of the clonal moss *Hylocomium splendens* in Norwegian boreal spruce forests. I. Demography. – J. Ecol. 83: 697–712.
Økland, R. H. 2007. Wise use of statistical tools in ecological field studies. – Fol. Geobot. 42:123-140.
Økland, R. H., Økland, T. & Rydgren, K. 2001a. A Scandinavia perspective on ecological gradients in noth-west European mires: reply to Wheeler and Proctor. – J Ecol. 89: 481–486.
Økland, R. H., Økland, T. & Rydgren, K. 2001b. Vegetation-envrionmental relationships of boreal spruce swamp forests in Østmarka Nature Reserve, SE Norway. – Sommerfeltia. 29:1–190.
Økland, R. H., Rydgren, K. & Økland, T. 1999. Single-tree influence on understorey vegetation in a Norwegian boreal spruce forest. – Oikos, **87**: 488–498.
Økland, R.H. 1986b. Rescaling of ecological gradients. II. The effect of scale on symmetry of species response curves. – Nord. J. Bot. 6: 661–670.
Økland, R.H. 1996. Are ordination and constrained ordination alternative or complementary strategies in general ecological studies? – J Veg Sci. 7: 289–292.
Økland, R.H. 2000. Population biology of the clonal moss Hylocomium splendens in Norwegian boreal spruce forests. 5. Vertical dynamics of individual shoot segments. – Oikos 88: 449–469.
Økland, R.H., Eilertsen, O. & Økland, T. 1990. On the relationship between sample plot size and beta diversity in boreal coniferous forests. – Vegetatio. 87: 187–192.
Økland, R.H., Rydgren, K. & Økland, T. 1999. Single-tree influence on understorey vegetation in a Norwegian boreal spruce forest. – Oikos. 87: 488–498.
Økland, T. & Eilertsen, O. 2001. Manual for intensive monitoring of forest ground vegetation and environmental conditions in China. IMPACTS project; Integrated Monitoring Program on Acidification of Chinese Terrestrial Systems. 2001: 2: 1–28. http://www.niva.no/impacts/.
Økland, T. 1988. An ecological approach to the investigation of a beech forest in Vestfold, SE Norway. – Nord. J. Bot. 8: 375–407.
Økland, T. 1990. Vegetational and ecological monitoring of boreal forests in Norway. I. Rausjømarka

in Akershus County, SE Norway. – Sommerfeltia 10: 1–52.
Økland, T. 1996. Vegetation-environment relationships of boreal spruce forests in ten monitoring reference areas in Norway. – Sommerfeltia 22: 1–349.
Økland, T., Bakkestuen, V., Økland, R. H. & Eilertsen, E. 2004. Changes in forest understorey vegetation in Norway related to long-term soil acidification and climatic change. – J. Veg. Sci. 15: 437–448.
Økland, T., Økland R. H. & Steinnes, E. 1999 Element concentrations in the boreal forest moss Hylocomium splendens: variation related to gradients in vegetation and local environmental factors. – Plant Soil 209: 71–83.
Økland, T., Rydgren, K., Økland, R. H., Storaunet, K. O. & Rolstad, J. 2003. Variation in environmental conditions, understorey species number, abundance and composition among natural and managed Picea abies forest stands. – Forest Ecol Manag 177: 17–37.
Oksanen, J. 2007. Multivariate analysis of ecological communities in R: vegan tutorial, URL: http://cc.oulu.fi/~jarioksa/opetus/metodi/vegantutor.pdf, pp. 39.
Oksanen, J., Kindt, R., Legendre, P. & O'Hara, B. 2007. Package 'vegan' Version 1.9–13. URL: http://cc.oulu.fi/~jarioksa. -Univ.of Oulu, Oulu, Finland, pp.120.
Orndorff, K. A. & Lang, G. E. 1981. Leaf litter redistribution in a West Virginia hardwood forest. – J Ecol. 69: 225–235
Ostertag, R. 1998. Belowground effects of canopy gaps in a tropical wet forest. – Ecology 79: 1294–1304.
Palmer, M. 2000. Ordination methods for ecologists. http://www.okstate.edu/artsci/botany/ordinate.
Parker, A. J. 1989. Forest/environment relationships in Yosemite National Park, California, USA. – Vegetatio 82: 41–54.
Parker, C. 1996. Light Characteristics in Open-forest and Closed-forest Communities. http://people.hws.edu/mitchell/oz/papers/ParkerOz.html.
Partel, M. 2002. Local plant diversity patterns and evolutionary history at the regional scale. – Ecology 83: 2361–2366.
Pausas, J. G. 1994. Species Richness Patterns in the Understorey of Pyrenean Pinus-Sylvestris Forest. – J Veg Sci. 5: 517–524.
Pearson, K. 1901. On lines and planes of closest fit to systems of points in space. – Phil Mag. 2: 559–72.
Pianka, E. R. 1966. Convexity, desert lizards, and spatial heterogeneity. – Ecology 47: 1055–1059.
Pitkänen, S. 1997. Correlation between stand structure and ground vegetation: an analytical approach. – Plant Ecol. 131: 109–126.
Pitkänen, S. 2000. Classification of vegetational diversity in managed boreal forests in eastern Finland. – Plant Ecol. 146: 11–28.
Rambo, T.R. & Muir, P.S. 1998. Forest Floor Bryophytes of Pseudotsuga menziesii-Tsuga heterophylla Stands in Oregon: Influences of Substrate and Overstory. – Bryologist 101: 116–130.
Ren, H. B., Niu, S. K., Zhang, L. Y. & Ma, K. P. 2006. Distribution of vascular plant species richness along an elevational gradient in the Dongling Mountains, Beijing, China. – J Integr Plant Boil. 48: 153–160.
Rieley, J. O., Richards, P. W. & Bebbington, A. D. L. 1979. Ecological Role of Bryophytes in a North Wales Woodland. – J Ecol. 67: 497–527.
Rincon E. 1988. The effect of herbaceous litter on bryophyte growth. – J Bryol. 15:209–217.
Rincon, E. 1990. Growth responses of Brachythecium rutabulum to different litter arrangements. – J Bryol. 16: 120-122.
Robinson, T. S. 1966. Effects of canopy density and slope exposure on the subcanopy microenvironment

of a Northern hardwood forest. – Am Midl Nat. 75: 339–346.
Romell, L. G. 1935. Ecological problems of the humus layer in the forest. – Corn Univ agr Exp Stn Mem. 170:1–28.
Ruokolainen, L. & Salo. K. 2006. Differences in performance of four ordination methods on a complex vegetation dataset. – Ann. Bot. Fennici. 43: 269–275.
Rydgren, K. 1993. Herb-rich spruce forests in W Nordland, N Norway: an ecological and methodological study. – Nord. J. Bot. 13:667–690.
Rydgren, K., Økland, R. H. & Økland, T. 2003. Species response curves along environmental gradients. A case study from SE Norwegian swamp forests. – J. Veg. Sci. 14:869–880.
Saetre, P. 1999. Spatial Patterns of Ground Vegetation, Soil Microbial Biomass and Activity in a Mixed Spruce-Birch Stand. – Ecography. 22: 183–192.
Schimel, D., Stillwell, M.A. & Woodmansee, R.G. 1985. Biogeochemistry of C, N, and P in a soil catena of the shortgrass steppe. – Ecology 66: 276–282.
Scholes, R. J. & van Breemen, N. 1997. The effects of global change on tropical ecosytems. – Geoderma 79: 9–24.
Seip, H. M., Aagard, P., Angell, V., Eilertsen, O., Larssen, T., Lydersen, E., Mulder, J., Muniz, I. P., Semb, A., Tang, D., Vogt, R. D., Xiao, J., Xiong, J., Zhao, D. & Kong, G. 1999. Acidification in China: assessment based on studies at forested sites from Chongqing to Guangzhou. – Ambio 28: 522–528.
Shepard, R. N. 1974. The analysis of proximities: multidimensional scaling with an unknown distance function. – Psychometrika 39:373–421.
Sjors, H. & Gunnarsson, U. 2002. Calcium and pH in north and central Swedish mires. – J Ecol. 90: 650–657.
Sokal, R.R. & Rohlf, F.J. 1995. Biometry: the principles and practice of statistics in biological research. 3rd ed. – W.H. Freeman, New York, pp. 887.
Solangaarachchi, S. M. & Harper, J. L. 1987. The effect of canopy filtered light on the growth of white clover *Trifolium repens*. – Oecologia 72: 372–376.
Stott, G. H. 1981. What is animal stress and how is it measured. – J Animal Science 52:150–153.
Studlar, S. M. 1982. Host Specificity of Epiphytic Bryophytes near Mountain Lake, Virginia. – Bryologist 85: 37–50.
Sveinbjörnsson, B. & Oechel, W.C. 1992. Controls on growth and productivity of bryophytes: environmental limitations under current and anticipated conditions. Bryophytes and Lichens in a Changing Environment (eds J.W. Bates & A.M. Farmer), pp. 77–102. – Oxford University Press, Clarendon Press, Oxford, UK.
Svenning J. 1999. Microhabitat specialization in a species-rich palm community in Amazonian Ecuador. – J Ecol. 87: 55–65.
Swift, M. J., Heal, O. W. & Anderson, J. M. 1979. Decomposition in Terrestrial Ecosystems. Studies in Ecology, volume 5. – Oxford: Blackwell Scientific Publications.
Sydes, C. & Grime, J. P. 1981 Effects of tree leaf litter on herbaceous vegetation in deciduous woodland II. An experimental investigation. – J. Ecol. 69: 249–262.
Takyu, M., Aiba, S. & Kitayama, K. 2002. Effects of topography on tropical lower montane forests under different geological conditions on Mount Kinabalu, Borneo. – Plant Ecol. 159: 35–49.
Tamm, O. 1959. Stuclier over kliinatets huiniclitet i Sverige. – Kungl slrogshogsk slir. 32: 1-49
Tang, D., He, Y., Gao, J., Liu, H., Liu, Z., Liu, F., Zhang, X., Guo, J., Wang, Y., Shang, H., Yu, P., Zhu, J., Han, J., Yao, B., Hu, X., Zang, X., Shao, M., Zeng, L., Duan, L., Liu, Q., Zhao, D., Zhang, D., Chen, S., Xiang, R., Chang, Y., Zhang, J., Luo, J., Zhang, Z., Xiao, J., Peng, X., Vogt, R., Seip, H. M., Aas, W., Tørseth, K., Mulder, J., Sogn, T., Eilertsen, O., Økland, T., Bratli, H., Angell, V., Solberg, S., Myking, T. & Larssen, T. 2004. Integrated Monitoring

Program on Acidification of Chinese Terrestrial Systems-IMPACTS-Annual Report-Results 2003. – NIVA-report 4905, pp. 1–94.
Tang, Y., Kachi, N., Furukawa, A. & Awang, M. B. 1999. Hetrogeneity of light availbaility and its effects on simulated carbon gain of tree leaves in a small gap and the understory in a tropical rain forest. – Biotropica 31: 268–278.
Tarkhova, T. N. & Ipatov, V. S. 1975. Influence of illumination and litter-drop on the development of certain species of mosses. – Sov. J. Ecol. 6: 43–48.
Taylor, D. R., Aarssen, L.W. & Loehle, C. 1990. On the relationship between r/K selection and environmental carrying capacity: a new habitat templet for plant life history strategies. – Oikos 58: 239–250.
ter Braak, C. J. F. & I. C. Prentice. 1988. A theory of gradient analysis. – Adv. Ecol. Res. 18: 271–313.
Tooren, B. F. van. & During, H. J. 1988. Early succession of bryophytes communities on Dutch forest earth banks. – Lindbergia. 14: 40–46.
Tuomist, H., Ruokolainen, K., Kalliola R., Linna, A., Danjoy, W. & Rodriguez, Z. 1995. Dissecting Amazonian biodiversity. – Science 269: 63–66.
van den Burg, J. 1991. Results and experiences from fertilization experiments in The Netherlands. – Nutr Cycl Agroecosys. 27: 107–111.
van Pelt, R. & Franklin, J. 1999. Response of understory trees to experimental gaps in old-growth Douglas-fir forests. – Ecol Appl. 9: 504–512.
van Tooren, B.F., den Hertog, J. & Verhaar, J. 1988. Cover, biomass and nutrient content of bryophytes in Dutch chalk grasslands. – Lindbergia. 14: 47–54.
Vanhala, P., Fritze, H. & Neuvonen, S. 1996. Prolonged simulated acid rain treatment in the subarctic: Effect on the soil respiration rate and microbial biomass. – Biol Fert Soils. 23: 7–14.
Venables, W. & Ripley, B. 2002. Modern Applied Statistics with S-Plus. – Springer.
Wang, X. H., Yan, E. R. & Huang, J. J. 2004. Leaf litter decomposition of common trees in Tiantong. – Acta Phytoecologica Sinica. 28: 457–467.
Wang, Y., Solberg, S., Yu, P., Myking, T., Vogt, R.D. & Du, S. 2007. Assessments of tree crown condition of two Masson pine forests in the acid rain region in south China. – Forest Ecol Manag. 242: 530–540.
Wang, Z., Huang, M., He, D., Xu, H. & Zhou, L. 1997. Studies on transport of acid substance in China and East Asia Part I: 3-D Eulerian transport model for pollutants. – Sci Atmos Sin. 21: 366–378.
Weibull, H. 2001. Influence of tree species on the epilithic bryophyte flora in deciduous forests of Sweden. – J. Bryol. 23: 55–56.
Westman, W. E. & Roggers, R.V. 1977. Nutrient stocks in a subtropical eucalypt forest, North Stradbroke Island. – Austral Ecol. 2: 447–460.
Wheeler, B.D. & Giller, K.E. 1982. Species richness of herbaceous fen vegetation in Broadland, Norfolk in relation to the quantity of above-ground plant material. – J Ecol. 70: 179–200.
Whittaker, R. H. 1967. Gradient analysis of vegetation. – Biol Rev. 49: 207–264.
Whittaker, R. J., Willis, K. J. & Field, R. 2001. Scale and species richness: towards a general, hierarchical theory of species diversity. – J Biogeogr. 28: 453–470.
Wiens, 1989 J. A. Wiens, Spatial scaling in ecology. – Funct. Ecol. 3: 385–397.
Williamson, M.H. 1978. The ordination of incidencedata. – J. Ecol. 66:911–920.
Willig, M. R., Kaufman, D. M. & Stevens, R. D. 2003. Latitudinal gradients of biodiversity: pattern, process, scale and synthesis. – Annu RevEcol Evol S. 34: 273–309.
Wood, S. N. 2000. Modelling and smoothing parameter estimation with multiple quadratic penalties. – JRSSB 62: 413–428.

Woodward, F. I. 1987. Climate and plant distribution. – Cambridge University Press, Cambridge, London, England.
World Bank. 1999. China and the World Bank. – World Bank, Washington, DC.
Wright, D. H. 1983. Species-energy theory: an extension of species-area theory. – Oikos 41: 496–506.
Wright, S. J. 2002. Plant diversity in tropical forests: a review of mechanisms of species coexistence. – Oecologia 130: 1–14
Wu, C. C., Tsui, C. C., Hseih, C. F., Asio, V. B. & Chen, Z. S. 2006. Mineral nutrient status of tree species in relation to environmental factors in the subtropical rain forest of Taiwan. – Forest Ecol Manag. 239: 81–91.
Wu, P.C. 2000. Bryoflora of Hengduan Mts (Southwest China). – Chinese Science and Education Press, Beijing, China (Chinese Language).
Wu, Z.Y. 2000–2002. Flora Yunnanica. – Chinese Science and Education Press, Beijing, China (Chinese Language).
Wu, Z.Y., Lin, R., Chen, H.Y. & Chen, C.S. 1959–2005. Flora Reipublicae Popularis Sinica. – Chinese Science and Education Press, Beijing, China (Chinese Language).
Xiong, S. & Nilsson, C. 1999. The effects of plant litter accumulation on vegetation: a meta-analysis. – J. Ecol. 87: 984–994.
Yamada, T., Itoh, A., Kanzaki, M., Yamakura, T., Suzuki, E. & Ashton, P. S. 2000. Local and geographical distributions for a tropical 290 tree genus, Scaphium Sterculiaceae in the Far East. – Plant Ecol. 148: 23–30.
Yang H. X. & Lu Z.Y. 1981. The quantitative methods of plant ecology. – Chinese Scientific Press, Beijing, China (Chinese Language).
Yin, Z.Y., Ren, H., Zhang, Q. M., Peng, S. L., Guo, Q. F. & Zhou, G. Y. 2005. Species Abundance in a Forest Community in South China: A Case of Poisson Lognormal Distribution. – J Integ Plant Bio. 47: 801–810
Zak, D. R., Hairston, A. & Grigal, D. F. 1991. Topographic influences on nitrogen cycling within an upland pin oak ecosystem. – Forest Sci. 37: 45–53.
Zhang, J. T, 2002. A study on relations of vegetation, climate and soils in Sanxi province, China. – Plant Ecol. 162: 23–31.
Zhang, J. T. 1993, Fuzzy set ordination using multivariate environmental variables, A combination with DCA. – Abstracta Bot. 17: 133–139.
Zhao, D. & Sun, B. 1986. Air pollution and acid rain in China. – Ambio 15: 2–5.
Zhao D., Xiong J., Xu, Y. & Chan, W. H. 1988. Acid rain in southwestern China. – Atmos Environ. 22: 349–358.
Zhao, C. M., Chen, W. L., Tian, Z. Q. & Xie, Z, Q. 2005. Altitudinal pattern of plant species diversity in Shennongjia Mountains, central China. – J Integr Plant Biol. 47: 1431–1449.
Zobel, M. 1997. The relative role of species pools in determining plant species richness: an alternative explanation of species coexistence? – Trends Ecol Evol. 12: 266–269.

APPENDIX

Appendix 1. List of the species recorded in the 50 1-m^2 plots in TSP, LCG and LGS, in the 49 1-m^2 plots (plot number 5 omitted) in CJT, and in the 46 1-m^2 plots (plots number 38, 46, 47 and 48 omitted) in LXH.

Area	Species list		
TSP	*Aralia chinensis*	*Litsea mollis*	*Stenoloma chusanum*
	Ardisia pusilla	*Lophatherum gracile*	*Symplocos lancifolia*
	Camellia oleifera	*Loropetalum chinense*	*Symplocos sumuntia*
	Carex cruciata	*Lysimachia paridifomis*	*Syzygium buxifolium*
	Carex harlandii	*Maesa japonica*	*Thladiantha dubia*
	Cinnamomum camphora	*Millettia dielsiana*	*Trigonetis peduncularis*
	Cunninghamia lanceolata	*Miscanthus sinensis*	*Vaccinum sprengelii*
	Cyclosorus acuminatus	*Myrsine afriana*	*Viburnum setigerum*
	Dicranopteris pedata	*Oplismenus undulatifolius*	*Woodwardia japonica*
	Dryopteris erythrosora	*Parathelypteris glauduligera*	*Bazzania semiopaca*
	Dryopteris fuscipes	*Parathelypteris japonica*	*Calypogeia arguta*
	Elaeagnus bockii	*Phylostachis heteroclada*	*Calypogeia muelleriana*
	Embelia rudis	*Pinus massoniana*	*Calypogeia tosana*
	Eurya loquiana	*Podocarpus macrophyllus*	*Cephalozia macounii*
	Ficus gasparriniana	*Polygonum caesipitosum*	*Cephaloziella microphylla*
	Gardenia jasminoides	*Polygonum paetermissum*	*Dicranodontium denudatum*
	Heterosmilax chinensis	*Pteridium aquilinum*	*Heteroscyphus planus*
	Holboellia fargesii	*Quercus fabri*	*Hypnum plumaeforme*
	Ligustrum lianum	*Randia cochichinensis*	*Leucobryum bowringii*
	Ligustrum sinense	*Rubus corchorifolius*	*Pellia epiphylla*
	Lindera glauca	*Setaria palmifolia*	*Taxiphyllum subarcuatum*
	Liquidambar fomosana	*Smilax china*	
LCG	*Ardisia japonica*	*Lysimachia trientaloides*	*Viburnum setigerum*
	Athyrium epirachis	*Miscanthus sinensis*	*Bazzania semiopaea*
	Camellia brevistyla	*Oplismenus compositus*	*Brotherella fauriei*
	Carex fillicina	*Parathelypteris japonica*	*Brotherella henonii*
	Carex henryi	*Parthenocissus himalayana*	*Brotherella nictans*
	Castanea sequinii	*Pinus massoniama*	*Calypogeia arguta*
	Cayratia japonica	*Plagiogyria euphlebia*	*Calypogeia muelleriana*
	Cunninghamia lanceolata	*Pseudocyclosorus esquirolii*	*Cephalozia macounii*
	Deyeuxia effusiflora	*Pteridium aquilinum* var. *latiusculum*	*Cephaloziella microphylla*
	Dicranopteris pedata	*Quercus fabri*	*Dicranodontium denudatum*
	Dioscorea japonica	*Rhapis excelsa*	*Dicranum japonicum*
	Diospyros kaki	*Rhododendron simsii*	*Ditrichum pallidum*
	Dryopteris erythrosora	*Rubus buergeri*	*Ectropothecium zollingeri*
	Eurya semiserrata	*Rubus corchorifolius*	*Fissidens areolatus*
	Ficus gasparriniana	*Schefflera delavayi*	*Hypnum plumaeforme*
	Gaultheria leuocarpa var. *crenulata*	*Smilax china*	*Leucobryum bowringii*
	Hydrangea davidii	*Smilax glabra*	*Leucobryum chlorophyllosum*
	Hydrangea paniculata	*Smilax davidiana*	*Chiloscyphus minor*
	Litsea cubeba	*Symplocos lancifolia*	*Pellia epiphylla*
	Litsea pungens	*Symplocos stellaris*	*Sematophyllum caespitosum*
	Liriope spicata	*Toxicodendron vernicifluum*	*Taxiphyllum subarcuatum*
	Lophatherum gracile	*Woodwardia japonica*	
	Lyonia ovalifolia	*Vaccinium fragile*	

Appendix 1 (continued). List of the species recorded in the 50 1-m^2 plots in TSP, LCG and LGS, in the 49 1-m^2 plots (plot number 5 omitted) in CJT, and in the 46 1-m^2 plots (plots number 38, 46, 47 and 48 omitted) in LXH.

Area	Species list		
LGS	*Acer davidii*	*Metathelypteris hattori*	*Symplocos sumuntia*
	Acer palmatum	*Microtropis obliquinervis*	*Toxicodendron succedaneum*
	Achyranthes longifolia	*Miscanthus floridulus*	*Viburnum satigerum*
	Actinidia fortunatii	*Nothosmyrnium japonicum*	*Viola pricipis*
	Amphicarpaca edgeworthii	*Oenanthe dielsii*	*Barbella compressiramea*
	Antenoron filiforme	*Ophiopogon japonicus*	*Brachythecium pulchellum*
	Aster ageratoides	*Ophiorrhiza japonica*	*Brachythecium plumosum*
	Betula luminifera	*Osmunda japonica*	*Brachythecium kuroishium*
	Boehmaria gracilis	*Oplismenus compositus*	*Brotherella fauriei*
	Boehmaria tricuspis	*Oxalis griffithii*	*Clastobryella cuculligera*
	Carex cruciata	*Panicum psilopodium*	*Dicranodentium denudatum*
	Carex glossostigma	*Paraprenanthes heptantha*	*Entodon challengeri*
	Carex thibetica	*Paraprenanthes sororia*	*Eurhynchium eustegium*
	Celastrus vaniotii	*Parathelypteris beddomei*	*Herzogiella perrobusta*
	Circaea mollis	*Parathelypteris glanduligera*	*Hypnum plumaeforme*
	Clematis urophylla	*Pilea japonica*	*Homomallium connexum*
	Clinopodium gracile	*Pimpinella coriacea*	*Homaliodendron scalpellifolium*
	Commelina triquetra	*Pittosporum glabratum* var. *neri.*	*Isopterygium albescens*
	Cornus controversa	*Pternopetalum heterophyllum*	*Leucobryum juniperoideum*
	Custuta japonica	*Polygonatum cyrtonema*	*Plagiominum acutum*
	Cypripedium henryi	*Polygonum campanulatum*	*Plagiothecium cavifolium*
	Dennstaetia pilosella	*Polygonum thunbergii*	*Plagiothecium euryphyllum*
	Deyeuxia arundinacea	*Polystichum tsus-simense*	*Ptychanthus striatus*
	Dioscorea japonica	*Prunus glandulosa*	*Rhyncostegium pallidifolium*
	Dryopteris scottii	*Pyrrosia martinii*	*Rhyncostegium contractum*
	Fagus lucida	*Rubia cordifolia*	*Thuidium kanedae*
	Galium aparine	*Rubus caudifolius*	*Ulota crispa*
	Galium asperuloides	*Rubus columellaris*	*Apometzgeria pubescens*
	Glechoma longituba	*Rubus irenaeus*	*Calypogeia sphagnicola*
	Goodyera schlechtendaliana	*Rubus limbertanus*	*Chiloscyphus heterophyllus*
	Gynostemma pentaphyllum	*Rubus malifolius*	*Chiloscyphus latifolius*
	Hedera nepalensis	*Rubus pirifolius*	*Cyanthoporella intermedium*
	Hydrangea davidii	*Rubus swinhoei*	*Frullania hamatiloba*
	Hydrangea paniculata	*Rubus tsangii*	*Frullania moniliana*
	Impatiens cyanantha	*Rumex nepalensis*	*Frullania parvistipula*
	Impatiens dicentra	*Sabia emaryinata*	*Heteroscyfus zollingeri*
	Impatiens dolichoceras	*Sabia parviflora*	*Lejeuna flava*
	Impatiens stenosepala	*Sabia swinhoei*	*Metzgeria conjugata*
	Isedom amethystoides	*Scepteridium ternatum*	*Metzgeria darjeelingensis*
	Laportea bulbifera	*Schefflera bodinieri*	*Metzgeria furcata*
	Lepidogrammitis rostrata	*Selaginella remotifolia*	*Metzgeria temperata*
	Lepisorus thunbergianus	*Smilax glabra*	*Porella caespitans*
	Ligularia intermedia	*Stellaria chinensis*	*Plagiochila elegans*
	Litsea cubeba	*Strobilanthes triflorus*	*Plagiochila subtropica*
	Lonicera acuminata	*Symplocos lucida*	*Radula cavifolia*
	Lyonia villosa	*Symplocos lancifolia*	

Appendix 1 (continued). List of the species recorded in the 50 1-m^2 plots in TSP, LCG and LGS, in the 49 1-m^2 plots (plot number 5 omitted) in CJT, and in the 46 1-m^2 plots (plots number 38, 46, 47 and 48 omitted) in LXH.

Area	Species list		
CJT	*Akebia trifoliata*	*Loropetalum chinense*	*Symplocos ernestii*
	Alangium chinense	*Lygodium japonicum*	*Symplocos paniculata*
	Ampelopsis sinica	*Miscanthus floridulus*	*Symplocos sumuntia*
	Aster ageratoides	*Miscanthus sinensis*	*Trachycarpus fortunei*
	Betula luminifera	*Oplismenus undulatifolius*	*Vibernum betulifolium*
	Camellia oleifera	*Paliurus ramossissimus*	*Vibernum dilatatum*
	Camellia sinensis	*Parathelypteris glanduligera*	*Woodwardia japonica*
	Carex bodinieri	*Photinia parvifolia*	*Zanthoxylum schinifolium*
	Carex brunnea	*Polygonatum cyrtonema*	*Diphyscium foliosum*
	Castanea sequinii	*Polygonum aubertii*	*Ditrichum pallidum*
	Clerodendrum cyrtophyllum	*Premna microphylla*	*Fissidens taxifolius*
	Cunninghamia lanceolata	*Pteridium aquilinum*	*Hypnum plumaeforme*
	Dalbergia hupeana	*Pteris henryi*	*Isopterygium albescens*
	Desmodium caudatum	*Pteris multifida*	*Isopterygium fauriei*
	Deyeuxia arundinacea	*Pteris nervosa*	*Leucobryum juniperoideum*
	Dryopteris fuscipes	*Quercus aliana*	*Plagiomnium acutum*
	Eurya alata	*Quercus chenii*	*Pseudotaxiphyllum pohliaecarpum*
	Gardneria multiflora	*Quercus fabrii*	*Taxiphyllum subarcuatum*
	Ilex aculeolata	*Rhododendron molle*	*Trachycystis microphylla*
	Kalopanax septemlobus	*Rhododendron simsii*	*Bazzania tridens*
	Lespedeza bicolor	*Rosa cymosa*	*Calypogeia muellerana*
	Lespedeza davidii	*Rubus corchorifolius*	*Cephaloziella microphylla*
	Lindera glauca	*Rubus lambertianus*	*Chiloscyphus minor*
	Liquidambar formosana	*Selaginella delicatula*	*Conocephalum japonicum*
	Liriope spicata	*Serissa serissoides*	
	Lophatherum gracile	*Smilax china*	

Appendix 1 (continued). List of the species recorded in the 50 1-m^2 plots in TSP, LCG and LGS, in the 49 1-m^2 plots (plot number 5 omitted) in CJT, and in the 46 1-m^2 plots (plots number 38, 46, 47 and 48 omitted) in LXH.

Area	Species list		
LXH	*Abacopteris simplex*	*Eurya nitida*	*Rubus leucanthus*
	Acer tutcheri	*Ficus hirta*	*Sabia limoniacea*
	Adina pilulifera	*Ficus pumila*	*Sapium discolor*
	Adiantum flabellulatum	*Ficus variolosa*	*Schima superba*
	Albizia corniculata	*Fissistigma oldhamii*	*Scleria hebecarpa*
	Allantodia metteniana	*Gahnia tristis*	*Selaginella doederleinii*
	Alpinia chinensis	*Gardenia jasminoides*	*Selaginella heterostachys*
	Alyxia vulgaris	*Gnetum montanum*	*Smilax lanceifolia*
	Ampelopsis grossedenta	*Gnetum parvifolium*	*Sonerila cantonensis*
	Angiopteris fokinensis	*Gomphostemma chinense*	*Stauntonia chinensis*
	Anoectochilus roxburghii	*Hypolytrum nemorum*	*Strobilanthes tetraspermus*
	Aristolochia tagala	*Ilex asprella*	*Symplocos adenopus*
	Ardisia crenata var. bicolor	*Ilex memecylifolia*	*Symplocos lancifolia*
	Ardisia punctata	*Indocalamus longiauritus*	*Syzygium buxifolium*
	Ardisia mamillata	*Ilex pubescens*	*Syzygium hancei*
	Ardisia quinquegona	*Itea chinensis*	*Tarenna mollissima*
	Arthraxon hispidus	*Jasminum lanceolarium*	*Tutcheria spectabilis*
	Artocarpus styracifolius	*Kadsura coccinea*	*Viburnum fordiae*
	Bambusa textilis	*Ligustrum sinense*	*Wikstroemia nutans*
	Bauhinia purpurea	*Liriope spicata*	*Woodwardia japonica*
	Blastus cochinchinensis	*Lithocarpus glader*	*Xylosma japonicum*
	Blechnum orientale	*Litsea acutivena*	*Bazzania japonica*
	Calamus rhabdocladus	*Litsea rotundifolia* var.*oblongifolia*	*Calypogeia arguta*
	Camellia ptilopylla	*Lonicera confusa*	*Calypogeia fissa*
	Capparis contoniensis	*Lonicera rhytidophylla*	*Calypogeia tosana*
	Carex filicina	*Lophatherum gracile*	*Calypogeia muellerana*
	Carex maculata	*Machilus breviflora*	*Cephaloziella microphylla*
	Castanopsis carlesii	*Machilus chinensis*	*Claopodium aciculm*
	Castanopsis fissa	*Machilus velutina*	*Cololejeunea* sp.
	Castanopsis fordii	*Maesa japonica*	*Dicranodotium denudatum*
	Cibotium barometz	*Maesa perlarius*	*Ectropothecium obtusulum*
	Cinnamomum parthenoxylon	*Melastrum candidum*	*Ectropothecium* sp.
	Coptossapelta diffusa	*Meliosma fordii*	*Fissidens zippelianus*
	Cratoxylon ligustrinum	*Melodinus suaveoleus*	*Fissidens taxifolius*
	Croton lachnocarpus	*Microtropis gracilipes*	*Heteroscyphus argutus*
	Cyclobalanopsis myrsinaefolia	*Millettia dielsiana*	*Heteroscyphus coalitus*
	Dalbergia millettii	*Millettia reticulata*	*Isopterygium pohliaecarpum*
	Daphne championii	*Miscanthus sinensis*	*Kurzia gonyotricha*
	Dendronpanax proteus	*Mussaenda pubescens*	*Lejeunea borneensis*
	Dicranopteris pedata	*Neolitsea chuii*	*Leptocolea goebelii*
	Diospyros tsangii	*Ophiorrhiza pumila*	*Matzgeria conjugata*
	Dryopteris podophylla	*Parthenocissus heterophylla*	*Pallavicinia subciliata*
	Dryopteris cycadina	*Pericampylus glaucus*	*Radula japonica*
	Elaeocarpus sylvestris	*Pittosporum glabratum.*	*Radula kojana*
	Embelia longifolia	*Pothos chinensis*	*Riccardia* sp.
	Embelia rudis	*Premna fordii*	*Taxiphyllum taxirameum*
	Engelhardtia fenzelii	*Psychotria rubra*	*Thuidium pristocalyx*
	Eriobotrya fragrans	*Psychotria serpens*	*Trichosteleum mammosum*
	Euonymus laxiflorus	*Pteris insignis*	*Trichosteleum* sp.
	Eurya chinensis	*Rapanea neriifolia*	*Tricholejeunea sandvicensis*
	Eurya loquaiana	*Raphiolepis indica*	*Leucobryum bowringii*
	Eurya muricata	*Rhododendron henryi*	

Appendix 2. Tie Shan Ping: DCA, LNMDS and GNMDS ordination of 50 meso plots. Meso plot umbers are plotted onto the sample plot positions. Scaling of axes in S.D. units. The correlation between corresponding axes (DCA 1 - LNMDS 2 - GNMDS 2, DCA 2 - LNMDS 1 - GNMDS 1, DCA 3 - LNMDS 3 - GNMDS 3) of DCA, LNMDS and GNMDS was very strong ($|\tau| > 0.51$, Tab. 5).

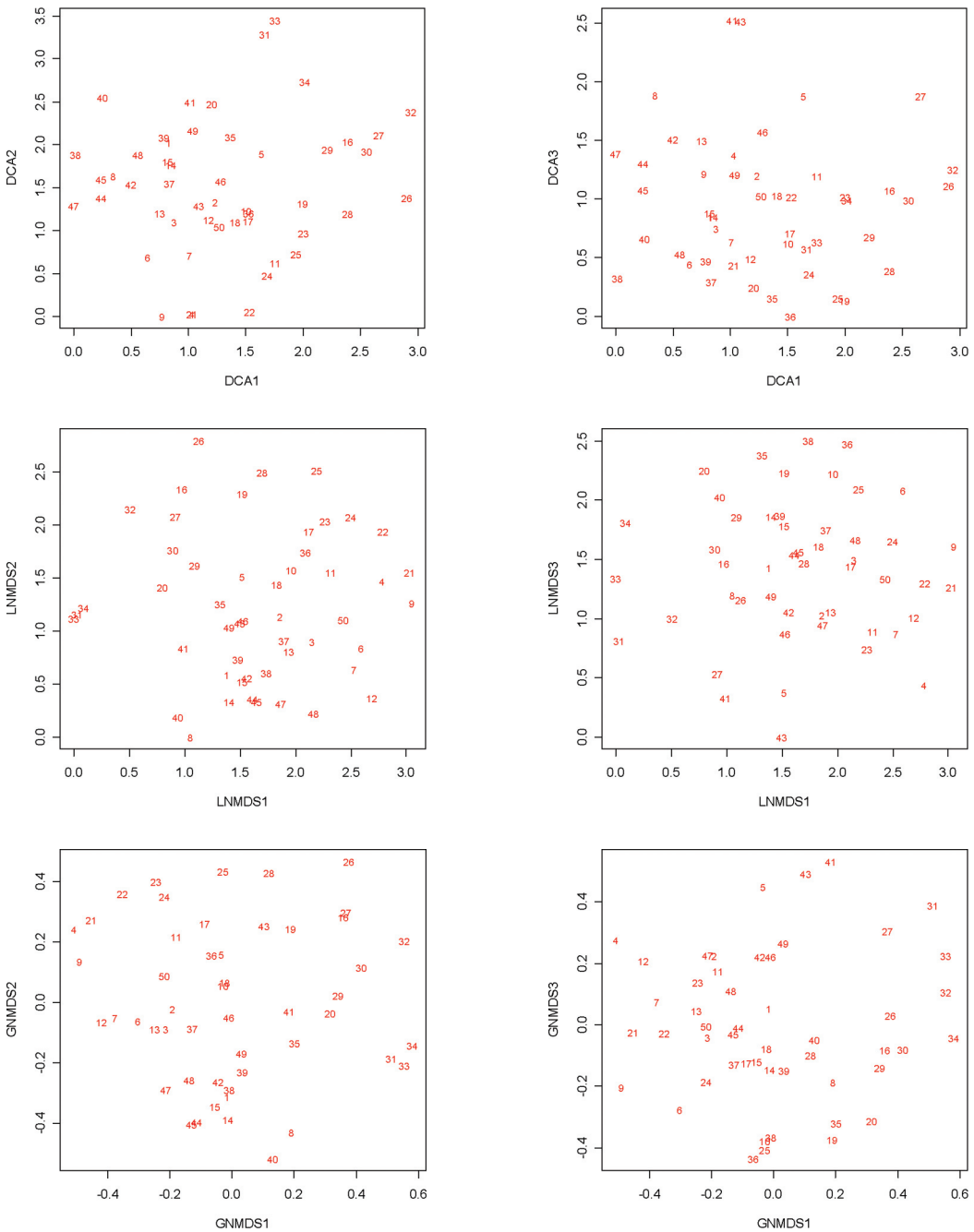

Appendix 3. Liu Chong Guan: DCA, LNMDS and GNMDS ordination of 50 meso plots. Meso plot umbers are plotted onto the sample plot positions. Scaling of axes in S.D. units. The correlation between corresponding axes (DCA 1-LNMDS 1-GNMDS 1, DCA 2-LNMDS 2-GNMDS 2) of DCA, LNMDS and GNMDS was very strong ($|\tau| > 0.53$, Tab. 5).

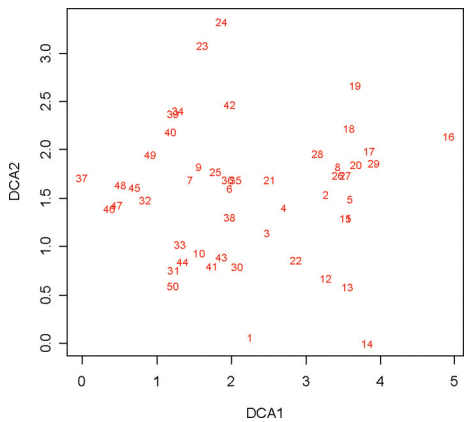

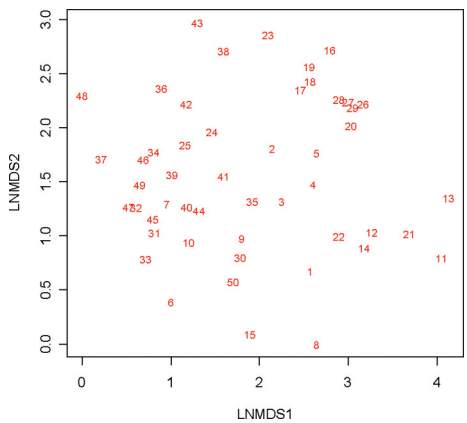

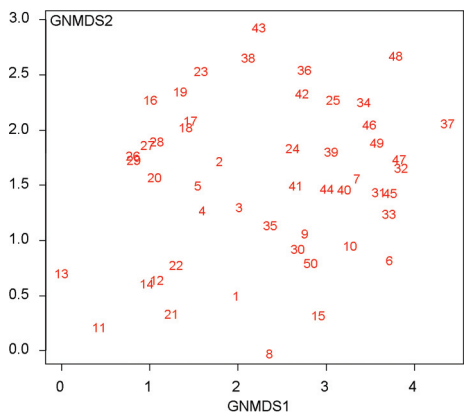

Appendix 4. Lei Gong Shan: DCA, LNMDS and GNMDS ordination of 50 meso plots. Meso plot umbers are plotted onto the sample plot positions. Scaling of axes in S.D. units. The correlation between corresponding axes (DCA 1-LNMDS 1-GNMDS 1, DCA 2-LNMDS 2-GNMDS 2) of DCA, LNMDS and GNMDS was very strong ($|\tau| > 0.63$, Tab. 5).

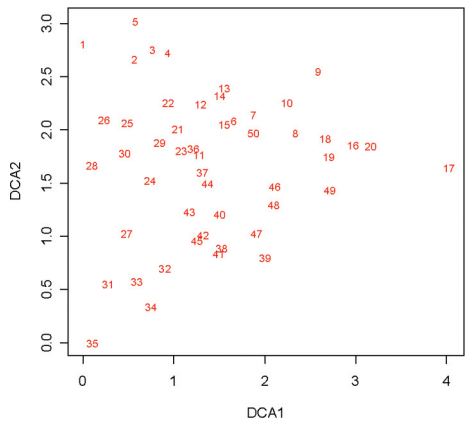

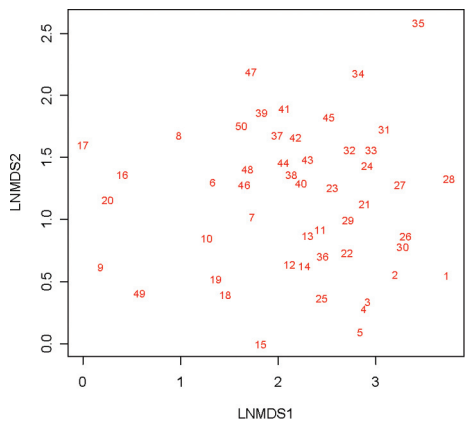

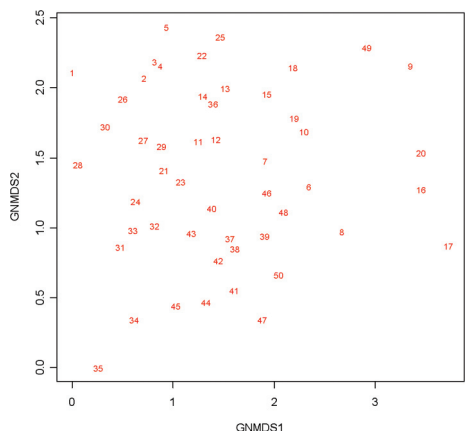

Appendix 5. Cai Jia Tang: DCA, LNMDS and GNMDS ordination of 50 meso plots. Meso plot umbers are plotted onto the sample plot positions. Scaling of axes in S.D. units. The correlation between corresponding axes (DCA 1-LNMDS 1-GNMDS 1, DCA 3-LNMDS 2-GNMDS 2) of DCA, LNMDS and GNMDS was very strong ($|\tau| > 0.39$, Tab. 5).

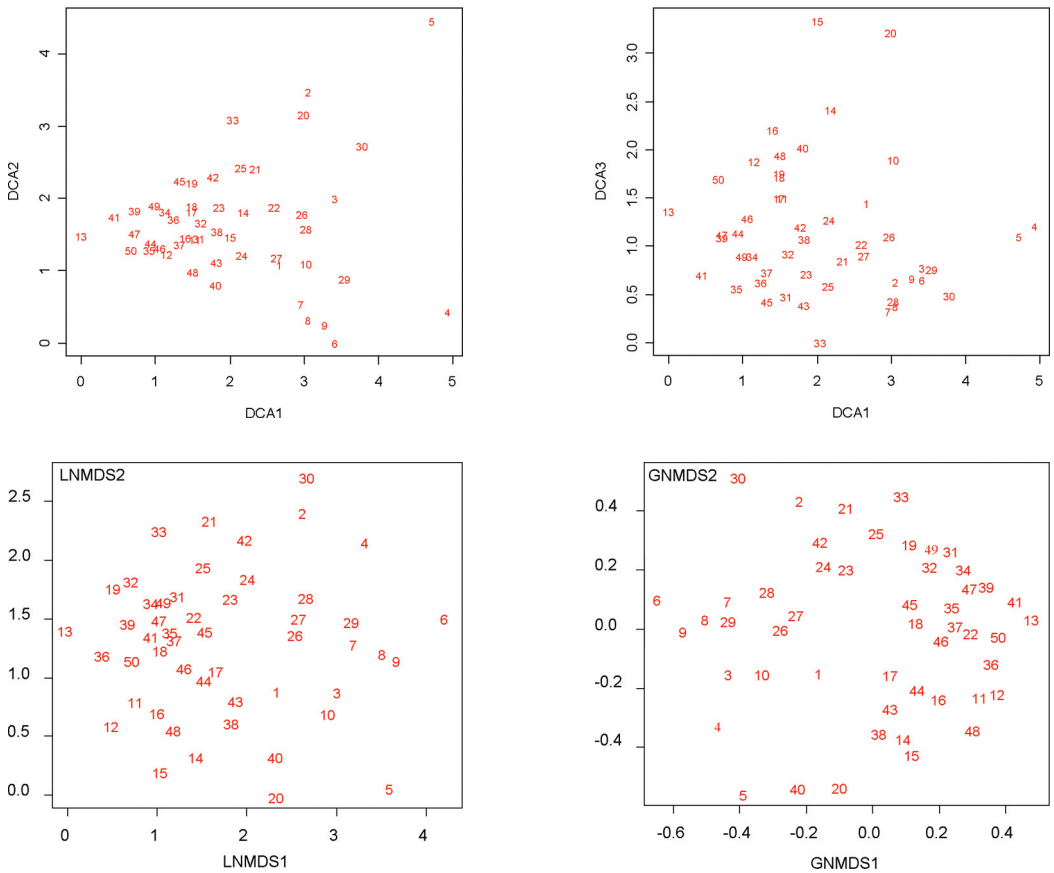

Appendix 6. Cai Jia Tang: DCA, LNMDS and GNMDS ordination of 49 meso plots (plot number 5 omitted). Meso plot umbers are plotted onto the sample plot positions. Scaling of axes in S.D. units. The correlation between corresponding axes (DCA 1-LNMDS 1-GNMDS 1, DCA 3-LNMDS 2-GNMDS 2) of DCA, LNMDS and GNMDS was very strong ($|\tau| > 0.39$, Tab. 5).

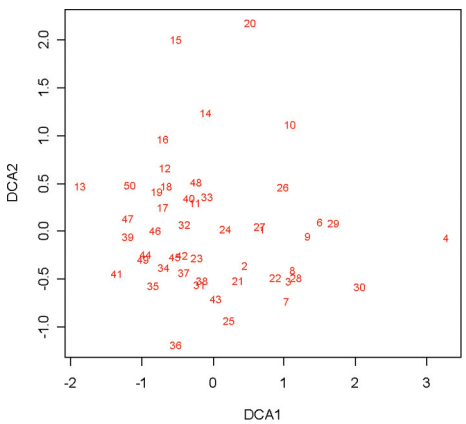

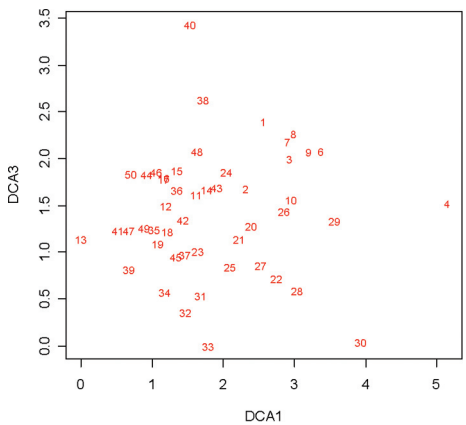

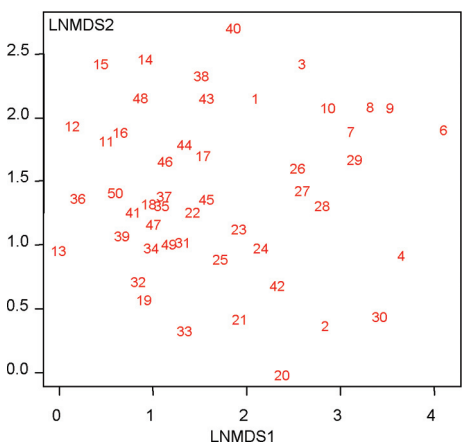

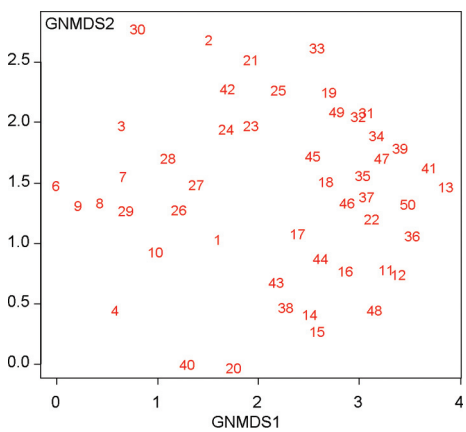

Appendix 7. Liu Xi He: DCA, LNMDS and GNMDS ordination of 50 meso plots. Meso plot umbers are plotted onto the sample plot positions. Scaling of axes in S.D. units. The correlation between corresponding axes (DCA 1-LNMDS 1-GNMDS 1, DCA 3-LNMDS 3-GNMDS 2, DCA 2- LNMDS 2-GNMDS 3) of DCA, LNMDS and GNMDS was very strong ($|\tau| > 0.22$, Tab. 5).

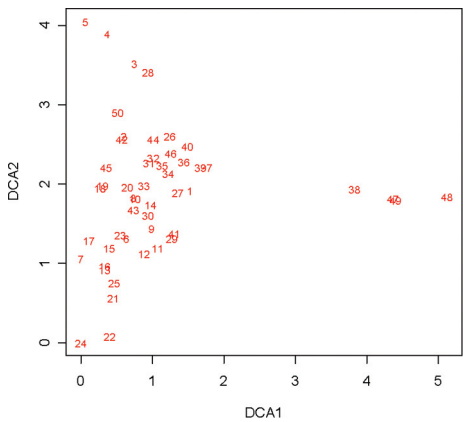

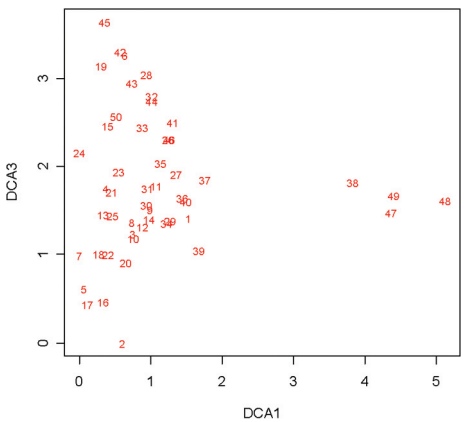

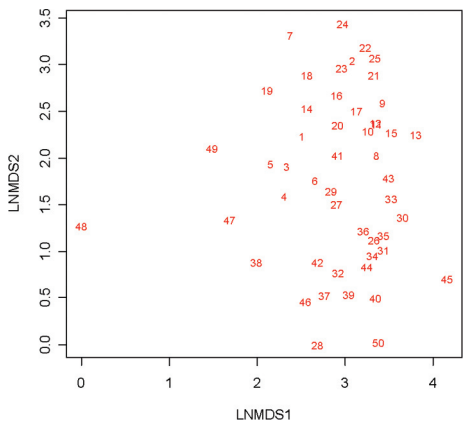

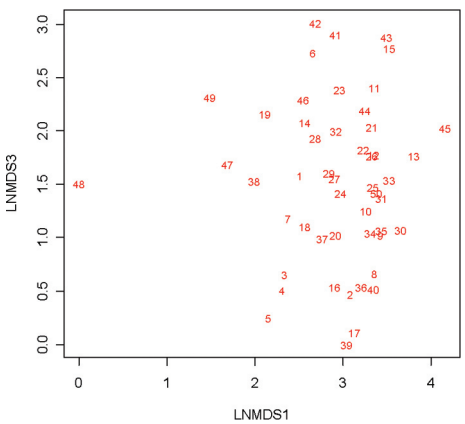

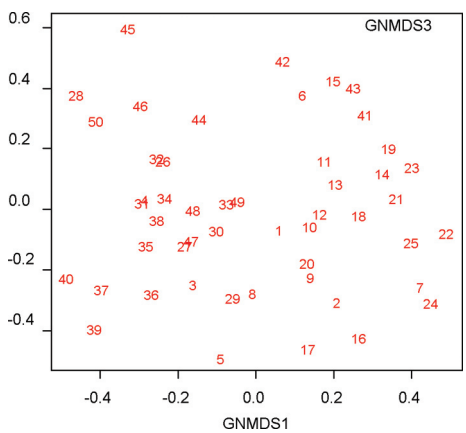

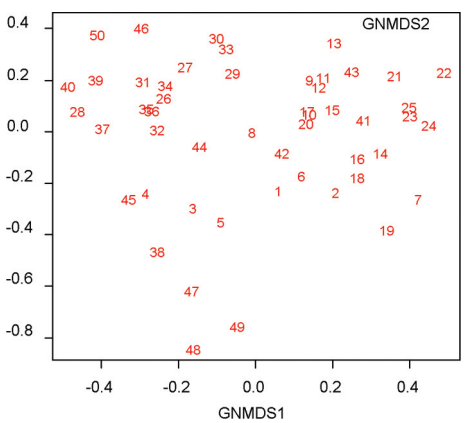

Appendix 8. Liu Xi He: DCA, LNMDS and GNMDS ordination of 46 meso plots (plots number 38, 47, 48 and 49 omitted). Meso plot umbers are plotted onto the sample plot positions. Scaling of axes in S.D. units. The correlation between corresponding axes (DCA 1-LNMDS 1-GNMDS 1, DCA 3-LNMDS 3-GNMDS 2, DCA 2- LNMDS 2-GNMDS 3) of DCA, LNMDS and GNMDS was very strong ($|\tau| > 0.22$, Tab. 5).

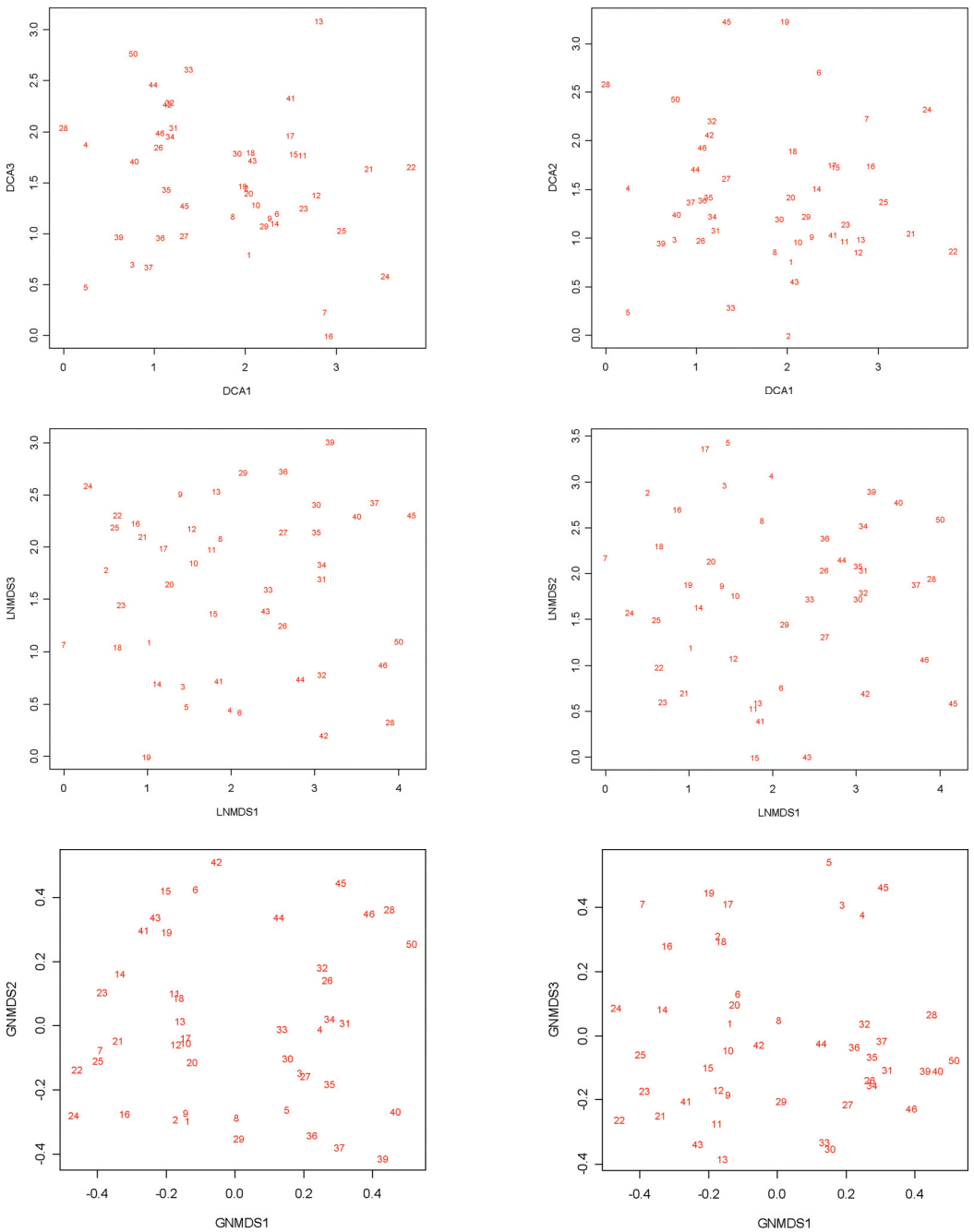

SOMMERFELTIA AND SOMMERFELTIA SUPPLEMENT

Vol. 1. A. Hansen & P. Sunding: Flora of Macaronesia. Checklist of vascular plants. 3. revised edition. 167 pp. NOK 140. (Jan. 1985; out of stock).

Vol. 2. R.H. Økland & E. Bendiksen: The vegetation of the forest-alpine transition in Grunningsdalen, S. Norway. 224 pp. NOK 170. (Nov. 1985).

Vol. 3. T. Halvorsen & L. Borgen: The perennial Macaronesian species of *Bubonium* (Compositae-Inuleae). 103 pp. NOK 90. (Feb. 1986).

Vol. 4. H.B. Gjærum & P. Sunding: Flora of Macaronesia. Checklist of rust fungi (Uredinales). 42 pp. NOK 50. (Dec. 1986).

Vol. 5. J. Middelborg & J. Mattsson: Crustaceous lichenized species of the Caliciales in Norway. 71 pp. NOK 70. (May 1987).

Vol. 6. L.N. Derrick, A.C. Jermy & A.C. Paul: Checklist of European Pteridophytes. xx + 94 pp. NOK 95. (Jun. 1987).

Vol. 7. L. Malme: Distribution of bryophytes on Fuerteventura and Lanzarote, the Canary Islands. 54 pp. NOK 60. (Mar. 1988).

Vol. 8. R.H. Økland: A phytoecological study of the mire Northern Kisselbergmosen, SE. Norway. I. Introduction, flora, vegetation, and ecological conditions. 172 pp. NOK 140. (Oct. 1989).

Vol. 9. G. Mathiassen: Some corticolous and lignicolous Pyrenomycetes s. lat. (Ascomycetes) on *Salix* in Troms, N Norway. 100 pp. NOK 85. (Oct. 1989).

Vol. 10. T. Økland: Vegetational and ecological monitoring of boreal forests in Norway. I. Rausjømarka in Akershus county, SE Norway. 52 pp. NOK 55. (June 1990).

Vol. 11. R.H. Økland (ed.): Evolution in higher plants: patterns and processes. Papers and posters presented on a symposium arranged on occasion of the 175th anniversary of the Botanical Garden in Oslo, June 5-8, 1989. 183 pp. NOK 150. (Dec. 1990).

Vol. 12. O. Eilertsen: Vegetation patterns and structuring processes in coastal shell-beds at Akerøya, Hvaler, SE Norway. 90 pp. NOK 85. (June 1991).

Vol. 13. G. Gulden & E.W. Hanssen: Distribution and ecology of stipitate hydnaceous fungi in Norway, with special reference to the question of decline. 58 pp. NOK 110. (Feb. 1992).

Vol. 14. T. Tønsberg: The sorediate and isidiate, corticolous, crustose lichens in Norway. 300 pp. NOK 330. (May 1992).

Vol. 15. J. Holtan-Hartwig: The lichen genus *Peltigera*, exclusive of the *P. canina* group, in Norway. 77 pp. NOK 90. (March 1993).

Vol. 16. R.H. Økland & O. Eilertsen: Vegetation-environment relationships of boreal coniferous forests in the Solhomfjell area, Gjerstad, S Norway. 254 pp. NOK 170. (March 1993).

Vol. 17. A. Hansen & P. Sunding: Flora of Macaronesia. Checklist of vascular plants. 4. revised edition. 295 pp. NOK 250. (May 1993).

Vol. 18. J.F. Ardévol Gonzáles, L. Borgen & P.L. Péres de Paz: Checklist of chromosome numbers counted in Canarian vascular plants. 59 pp. NOK 80. (Sept. 1993).

Vol. 19. E. Bendiksen, K. Bendiksen & T.E. Brandrud: *Cortinarius* subgenus *Myxacium* section *Colliniti* (Agaricales) in Fennoscandia, with special emphasis on the Arctic-alpine zones. 37 pp. NOK 55. (Nov. 1993).

Vol. 20. G. Mathiassen: Corticolous and lignicolous Pyrenomycetes s.lat. (Ascomycetes) on *Salix* along a mid-Scandinavian transect. 180 pp. NOK 180. (Nov. 1993).

Vol. 21. K. Rydgren: Low-alpine vegetation in Gutulia National Park, Engerdal, Hedmark, Norway, and its relation to the environment. 47 pp. NOK 65. (May 1994).

Vol. 22. T. Økland: Vegetation-environment relationships of boreal spruce forests in ten monitoring reference areas in Norway. 349 pp. NOK 230. (May 1996).

Vol. 23. T. Tønsberg, Y. Gauslaa, R. Haugan, H. Holien & E. Timdal: The threatened macrolichens of Norway - 1995. 258 pp. NOK 220. (June 1996).

Vol. 24. C. Brochmann, Ø.H. Rustan, W. Lobin & N. Kilian: The endemic vascular plants of the Cape Verde islands, W Africa. 356 pp. NOK 230. (Dec. 1997).

Vol. 25. A. Skrindo & R.H. Økland: Fertilization effects and vegetation-environment relationships in a boreal pine forest in Åmli, S Norway. 90 pp. NOK 90. (Dec. 1998).

Vol. 26. A. Granmo: Morphotaxonomy and chorology of the genus *Hypoxylon* (Xylariaceae) in Norway. 81 pp. NOK 120. (Sept. 1999).

Vol. 27. A. Granmo, T. Læssøe & T. Schumacher: The genus *Nemania* s.l. (Xylariaceae) in Norden. 96 pp. NOK 135 (Sept. 1999).

Vol. 28. H. Krog: Corticolous macrolichens of low montane rainforests and moist woodlands of eastern Tanzania. 75 pp. NOK 135 (July 2000).

Vol. 29. R.H. Økland, T. Økland & K. Rydgren: Vegetation-environment relationships of boreal spruce swamp forests in Østmarka Nature Reserve, SE Norway. 190 pp. NOK 155 (Sept. 2001).

Vol. 30. E. Bendiksen, R.H. Økland, K. Høiland, O. Eilertsen & V. Bakkestuen: Relationships between macrofungi, plants and environmental factors in boreal coniferous forests in the Solhomfjell area, Gjerstad, S Norway. 125 pp. NOK 140. (Oct. 2004).

Vol. 31. K. Høiland & R.H. Økland (eds): Arctic and alpine mycology VII. 211 pp. NOK 240. (Feb. 2008).

Vol. 32. H.Y. Liu, T. Økland, R. Halvorsen, J.X. Gao, Q.R. Liu, O. Eilertsen & H. Bratli: Gradient analyses of forests ground vegetation and its relationships to environmental variables in five subtropical forest areas, S and SW China. 196 pp. NOK 275. (Nov 2008).

Supplement Vol. 1. R.H. Økland: Vegetation ecology: theory, methods and applications with reference to Fennoscandia. 233 pp. NOK 180. (Mar. 1990).

Supplement Vol. 2. R.H. Økland: Studies in SE Fennoscandian mires, with special regard to the use of multivariate techniques and the scaling of ecological gradients. (Dissertation summary). 22 pp. NOK 35. (Dec. 1990).

Supplement Vol. 3. G. Hestmark: To sex, or not to sex... Structures and strategies of reproduction in the family Umbilicariaceae (Lecanorales, Ascomycetes). (Dissertation summary). 47 pp. NOK 55. (Dec. 1991).

Supplement Vol. 4. C. Brochmann: Polyploid evolution in arctic-alpine *Draba* (Brassicaceae). 37 pp. NOK 60. (Nov. 1992).

Supplement Vol. 5. A. Hansen & P. Sunding: Botanical bibliography of the Canary Islands. 116 pp. NOK 130. (May 1994).

Supplement Vol. 6. R.H. Økland: Boreal coniferous forest vegetation in the Solhomfjell area, S Norway: structure, dynamics and change, with particular reference to effects of long distance airborne pollution. 33 pp. NOK 43. (May 1995).

Supplement Vol. 7. K. Rydgren: Fine-scale disturbance in an old-growth boreal forest – patterns and processes. 25 pp. NOK 40. (May 1997).